

Simulation and analysis in electromyography.

**Thesis submitted for the degree of
Doctor of Philosophy
at the University of Leicester**

by

**Gary James Small
Department of Engineering
University of Leicester.**

September 1998

UMI Number: U106315

All rights reserved

INFORMATION TO ALL USERS

The quality of this reproduction is dependent upon the quality of the copy submitted.

In the unlikely event that the author did not send a complete manuscript and there are missing pages, these will be noted. Also, if material had to be removed, a note will indicate the deletion.



UMI U106315

Published by ProQuest LLC 2013. Copyright in the Dissertation held by the Author.
Microform Edition © ProQuest LLC.

All rights reserved. This work is protected against
unauthorized copying under Title 17, United States Code.



ProQuest LLC
789 East Eisenhower Parkway
P.O. Box 1346
Ann Arbor, MI 48106-1346

Il y a malgre vous quelque chose,
Que j'emporte, ce soir, quand j'entrerai chez Dieu,
Mon salut balaiera largement le seuil bleu,
Quelque chose que sans un pli, sans un tache,
J'emporte malgre vous...et c'est...Mon panache!

Edmond Rostand, 1897

Simulation and analysis in electromyography.

by

Gary James Small

Declaration of Originality:

A thesis submitted in fulfilment of the requirements for the degree of Doctor of Philosophy in the Department of Engineering, University of Leicester, UK. All work presented in this thesis is original unless otherwise acknowledged in the text or by references. No part of it has been submitted for any other degree, either to the University of Leicester or to any other university.

A handwritten signature in black ink, appearing to read 'Gary J. Small', written in a cursive style.

Gary J. Small

September 1998

Acknowledgments

Firstly, I would like to thank Professor Barrie Jones for his support and encouragement during the three years of my research, and for encouraging me to embark on the course that has lead to this thesis.

I would like to thank Dr. John Fothergill and the other academics within the Biomedical, Transducers and Signal Processing research group for their assistance and constructive criticism over the years and for keeping me on my toes.

My thanks also go to the friends that I made during my three years in the research group, for making the time pass more pleasantly and enjoyably than it otherwise may have.

Finally my thanks are due to my family and fiancé, for the support they gave me and for the belief they had that I could reach this stage, even when I did not believe it myself.

Contents.

Abstract

Glossary

Chapter 1-	Introduction.	1
1.1	The motivation for this research.	1
1.2	Objectives.	1
1.3	Medical decision support systems.	2
1.4	The blackboard system.	2
1.5	Application to Neurophysiological diagnosis.	4
1.6	Electromyography.	4
1.6.1	The Motor Unit (MU).	5
1.6.2	The Electromyogram, (EMG).	7
1.6.3	The Motor Unit Action Potential, (MUAP).	7
1.6.4	The Motor Unit Action Potential Train, (MUAPT).	9
1.6.5	Force generation.	10
1.6.6	The EMG of Myopathy.	11
1.6.7	The EMG of the Neurogenic Lesion.	13
1.6.8	Spontaneous activity.	16
1.6.8.1	Insertion activity.	16
1.6.8.2	Fibrillation and fibrillation potentials.	16
1.6.8.3	Positive sharp waves.	17
1.6.8.4	End-plate potentials.	17
1.6.8.5	Fasciculation and fasciculation potentials.	18

1.7	Investigations in Electromyography.	18
1.7.1	The Electrode.	18
1.7.1.1	The Surface Electrode.	19
1.7.1.2	The Needle Electrode.	19
1.7.1.3	The EMG Amplifier.	20
1.7.2	Physical tests.	21
1.7.2.1	Nerve conduction velocity studies.	21
1.7.2.2	Blood Creatine Phosphokinase content.	23
1.7.3	Low force electrophysiological tests.	24
1.7.4	High force electrophysiological tests.	25
1.7.4.1	Single database principal component analysis.	26
1.7.4.2	Triple database principal component analysis.	27
1.7.4.3	Turns Analysis.	27
1.8	The type of system.	29
1.9	Summary.	29
Chapter 2 -	A simulated patient.	31
2.1	Introduction.	31
2.2	Why create a simulated patient?	31
2.3	The simulated knowledge sources.	32
2.4	Operation of Simulated Knowledge sources.	33
2.5	Physical test knowledge source simulations.	36
2.5.1	Nerve Conduction Velocity.	36
2.5.2	Blood Creatine Phosphokinase level.	38
2.6	Low force electrophysiological assessments.	40
2.6.1	Low/medium force EMG tests.	40
2.6.2	Very low force EMG tests.	43
2.6.3	Zero force EMG tests.	44

2.7	High force electrophysiological assessments.	47
2.7.1	Single database principal component analysis.	47
2.7.2	Triple database principal component analysis.	49
2.7.3	Turns analysis.	50
2.8	Discussion.	53
2.9	Summary.	53
Chapter 3 - The dynamics of the EMG.		55
3.1	Introduction.	55
3.2	What is Chaos?	56
3.3	Methods of Identifying Chaos in a time series.	56
3.3.1	Construction of Phase Planes/Portraits.	56
3.3.2	Correlation Dimension Analysis.	57
3.3.3	Calculation of Lyapunov exponents.	62
3.4	Is the clinical Electromyogram Chaotic?	65
3.4.1	Chaos in Biomedical Systems.	65
3.4.2	EMG Simulation.	66
3.4.3	Models of the membrane.	67
3.4.4	A Chaotic EMG Simulator?	68
3.5	Attempted identification of Chaos in the EMG.	69
3.5.1	EMG Phase Portraits.	69
3.5.2	The behaviour of the correlation dimension.	70
3.5.3	Lyapunov exponents of the EMG.	77
3.6	Summary.	79
Chapter 4 - The EMG simulation knowledge source.		80
4.1	Introduction.	80
4.2	The importance of spontaneous activity.	80
4.3	Some characteristics of spontaneous activity.	82

4.3.1	Fibrillation Potentials.	82
4.3.2	Fasciculation potentials.	82
4.3.3	End-Plate potentials.	83
4.3.4	Positive sharp waves.	83
4.3.5	Bizarre high frequency potentials.	83
4.4	The inclusion of spontaneous activity in a simulation program.	83
4.5	Models for EMG simulation.	85
4.6	Characteristics of volitional activity.	87
4.7	Simulation of volitional activity.	88
4.8	Simulation in a medical decision support system.	97
4.9	Summary.	98
Chapter 5 -	The decomposition knowledge source.	99
5.1	Introduction.	99
5.2	Decomposition as a knowledge source.	99
5.3	The decomposition problem.	100
5.4	An overview of techniques.	102
5.5	The method of interest.	102
5.5.1	Classification of non-overlapping MUAPs.	103
5.5.2	Resolution of superimposed waveforms.	104
5.5.3	Discussion.	104
5.6	Summary.	105
Chapter 6 -	MUAP clustering using artificial neural networks.	106
6.1	Introduction.	106
6.2	Neural networks and the MUAP clustering problem.	106
6.3	The neural network.	107
6.3.1	The neuron.	108
6.3.1.1	The activation function.	108
6.3.2	The perceptron.	109

6.3.2.1	Gradient descent: perceptron learning.	110
6.3.3	The multilayer perceptron.	111
6.3.3.1	The backpropagation learning rule.	112
6.3.4	Self organisation: competitive networks and self organising feature maps.	113
6.3.4.1	Competitive learning.	115
6.3.5	Learning vector quantisation networks.	115
6.4	Application of neural networks to the problem.	116
6.4.1	Describing features as network inputs.	116
6.4.1.1	The multilayer perceptron.	118
6.4.1.2	The competitive network.	119
6.4.1.3	The learning vector quantization network.	123
6.4.2	Discussion	126
6.4.3	Orthogonal factors as network inputs.	127
6.4.3.1	The generation of orthogonal features.	129
6.4.3.2	The multilayer perceptron with orthogonal inputs.	131
6.4.3.3	The LVQ network with orthogonal inputs.	131
6.4.3.4	Testing the LVQ networks.	140
6.4.3.4.1	MUAPs in white noise.	140
6.4.3.4.2	MUAPs in band limited noise.	145
6.4.3.4.3	Identification of overlapping MUAPs.	148
6.4.3.5	Discussion.	152
6.5	Summary.	155
Chapter 7-	Alternative applications in decomposition.	156
7.1	Introduction.	156
7.2	Multiple database principal component analysis.	156
7.2.1	The classification of different MUAP shapes.	158
7.2.2	The classification of similar MUAP shapes.	160
7.2.2.1	The classification of MUAP types in noise.	160

7.2.2.2	The classification of MUAP types with amplitude variation.	163
7.2.2.3	The classification of MUAP types with time dilation variation.	168
7.2.3	Tests with real data.	171
7.2.4	Discussion.	175
7.3	Resolution of overlapping data.	176
7.3.1	Method 1.	176
7.3.2	Method 2.	177
7.3.3	Processing time requirements.	178
7.3.4	Discussion.	180
7.4	Summary.	181
Chapter 8 -	Conclusions and future work.	182
8.1	Conclusions.	182
8.2	Future Work.	185

References

Appendices

Appendix 1	Principal component analysis.
Appendix 2	Diagonal factor analysis.
Appendix 3	Band pass filter construction.
Appendix 4	Time intensive overlap resolution, calculations.
Appendix 5	Simulation of the clinical electromyogram.
Appendix 6	Chaos as a possible model of myoelectric activity.
Appendix 7	The use of neural networks in the automatic extraction of firing time statistics in electromyography.

Abstract.

This thesis deals with the construction of a medical decision support system, and more specifically with the knowledge sources within the system that facilitate its operation. Simulations of some results from a proportion of these knowledge sources are created, the results correspond to the physical and electrophysiological tests carried out on a patient during neuromuscular diagnosis, and various methods of processing the acquired data for interpretation.

Chaos as a method of modelling myoelectric activity is assessed for the purpose of creating an EMG simulation knowledge source and for differentiating between disorder types. The construction of phase portraits, correlation dimension analysis and calculation of Lyapunov exponents are all used to attempt to establish the presence of chaotic behaviour in the myoelectric signal. However, it is proven that the dynamics of the EMG are not chaotic in nature, thus a more suitable model for EMG simulation is chosen.

The second knowledge source looked at in detail is that of EMG decomposition. Two methods of clustering MUAPs into their classes are assessed. Firstly the use of a neural network to cluster action potentials represented by correlated features and then non correlated factors. The method proves most effective when non-correlated factors are used. The second method looked at is that of multiple database principal component analysis. This method proves capable of clustering MUAP classes in the presence of noise and MUAP variation. The method is tested on real data and, within the limits of the study, the results are confirmed.

A study of time requirements is made for resolution of overlapping action potentials. Two methods are considered a fast and a more thorough one. It is established that it would be appropriate for these methods to be used in complement with one and other, in a method for automatic decomposition that includes both clustering methods discussed along with various other appropriate techniques such as firing time analysis.

Glossary of terms.

AP -	Action Potential.
CPK -	Creatine Phosphokinase.
CNE -	Concentric Needle Electrode.
Dc -	Correlation Dimension.
ECG -	Electrocardiogram.
EEG -	Electroencephalogram.
EMG -	Electromyogram.
FLOPS -	Floating Point Operations per Second.
IEMG -	Interference Electromyogram.
IPI -	Inter Pulse Intervals.
LGMD -	Limb Girdle Muscular Dystrophy.
LVQ -	Learning Vector Quantization.
MC -	Myotonia Congenita.
MDSS -	Medical Decision Support System.
MND -	Motor Neuron Disease.
MU -	Motor Unit.
MUAP -	Motor Unit Action Potential.
MUAPT -	Motor Unit Action Potential Train.
NCV -	Nerve Conduction Velocity.
PCA -	Principal Component Analysis.

Chapter 1- Introduction.

1.1 The motivation for this research.

The problem of diagnosing disorders of the neuromuscular system is a complex one. It involves the invocation of various types of testing and the ability to interpret disparate forms of information. The overall process, most notably the electrophysiological assessment, can be quite time consuming. Electrophysiological assessment of a patient is a frequently used test during diagnosis. It is hampered by the limitations imposed upon the force, generated within the observed muscle, by manual identification of its content. The relatively low forces involved increase the number of tests required to achieve a diagnosis. In this case an automatic routine would reduce the cost in time by allowing a fuller (higher force) signal to be analysed, and improve the diagnostic procedure by allowing analysis of higher force activity.

The creation of a medical decision support system applied to neuromuscular diagnosis would make the diagnostic procedure less time consuming and more efficient. As may be seen from the example above, there is a need to improve the procedure of neuromuscular diagnosis for the benefit of clinicians and to reduce patient discomfort. This forms the motivation for the research presented within this thesis.

1.2 Objectives

The objectives of this research are as follows:

1. To enable development and testing of a blackboard based medical decision support system, for use in neuromuscular diagnosis, by creating simulations of required but unavailable sources of knowledge;
2. To investigate the hypothesis that the dynamics underlying the interference electromyogram are chaotic in nature;

3. To create a knowledge source capable of simulating the EMG signal and of contributing to a simulated patient for use within the medical decision support system;
4. To investigate methods of clustering motor unit action potentials into both their classes and their trains, for use within an automatic decomposition knowledge source. This knowledge source is to be applied within the medical decision support system; and
5. To assess the feasibility, with respect to required processor time, of two methods of resolving superimposed motor unit action potential complexes, to be utilised within the same automatic decomposition routine.

1.3 Medical decision support systems.

Medical decision support systems (MDSS) are specially designed computer programs which perform not only ordinary numerical analysis, but also knowledge intensive operations (Wang, 1995). Knowledge based systems use the information stored in their own knowledge base in order to solve the problem with which they are presented. Medical decision support systems fall within this category.

MDSS are systems which will aid and complement the formation of a diagnosis by a clinician. They are in no way intended to replace the doctor. An MDSS may be considered to be another test that may be ignored by the diagnostician if, for example, the yielded results are contrary to the results of other tests employed in the diagnostic procedure.

1.4 - The blackboard system.

The blackboard approach was designed to cope with ill-defined, complex applications in decision making. The original metaphor upon which today's systems are based is as follows:

“Imagine a group of human experts seated next to a large blackboard. The specialists are working co-operatively to solve a problem. Problem solving begins when the problem and initial data are written on the blackboard. The specialists look for an opportunity to apply their expertise to the developing solution. When a specialist finds sufficient information to make a contribution, the contribution is recorded on the blackboard, which lets other specialists apply their expertise. This process of adding contributions to the blackboard continues until the problem is solved.” (Corkhill, 1991).

As a system implemented in software the metaphor is translated into various groups. These consist of the blackboard itself, the repository of knowledge of all kinds relevant to the problem, knowledge sources, distinct modules representative of the metaphor’s experts and the scheduler which acts as the chairman of the meeting of experts.

An important feature of the blackboard system is that it may deal with information in diverse formats. Each knowledge source is distinct and interacts with the blackboard only, thus many data types may be accommodated within the system.

The tasks to which blackboard systems are applied, all share common characteristics, (Nii, 1994):

1. The problems are complex and ill-structured, with large solution spaces.
2. The solutions require situation dependant or opportunistic invocation of diverse sources of knowledge.

3. The problems require both synthetic and analytic processes.

1.5 - Application to Neurophysiological diagnosis.

The diagnosis of neuromuscular disorders is based on the results of different tests. These tests may be of procedural form, i.e. they may depend upon numerical techniques to present information in a form useable by the clinician, or they may mix procedural and knowledge based methods. The data produced by each of these methods must necessarily be of diverse form, consisting of numeric and symbolic forms, etc.

The problem of forming a diagnosis from these diverse inputs is not an easy one, it takes a great deal of experience for a doctor to be able to do so. This is because the information is drawn from complex signals and procedures that require a great deal of understanding in order to be interpreted. The blackboard system has been fairly widely accepted today as a pertinent scheme for biomedical applications (Suranammi, 1993). It provides an opportunistic problem solving environment calling on multiple knowledge sources to reach a co-operative solution to a complex task (Jones, Sehmi & Kabay, 1992). Both data and goal driven strategies may be used and these are necessary for neurophysiological diagnosis. The blackboard system is thus suitable for application to the creation of medical decision support systems.

1.6 - Electromyography.

“*Electromyography* is the study of muscle function through the inquiry of the electrical signal the muscles emanate.” (Basmajian & De Luca, 1985).

1.6.1 - The Motor Unit (MU).

The structural unit within the muscle that undergoes contraction is the muscle cell or muscle fibre. This muscle fibre, which consists of a very fine thread, has a length that may vary from approximately a few millimetres to 30 centimetres and a diameter in the region of 10 to 100 micrometers. When subjected to contraction, each individual muscle fibre can reduce in length by up to approximately 43%

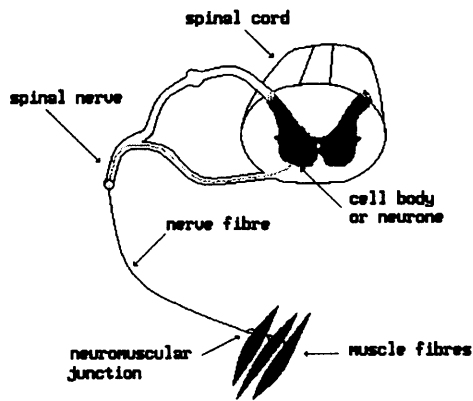
In order for a muscle fibre to sustain a contraction, it must undergo reactivation continuously, and as such is subject to rapid contraction and relaxation for the duration of the muscle contraction.

When looking at normal mammalian skeletal muscles, muscle fibres tend to be activated in groups rather than on an individual basis. All the muscle fibres contained within these groups are supplied by the terminal branches of a single neurone or axon, the body of which is contained in the anterior horn of the spinal grey matter.

Thus it may be seen that the motor unit consists of:

1. The nerve cell body.
2. The long axon running down the motor nerve.
3. Its terminal branches.
4. The muscle Fibres.

Figure 1.6.1.1 - An illustration of a motor unit.



It is now clear that the MU is the functional unit of striated muscle, because the impulse which travels along the motor neurone causes all constituent muscle fibres of the motor unit to contract almost simultaneously.

However, there are two factors which prevent the simultaneous contraction of the muscle fibres, these being;

- The variation in time which is a consequence of the different lengths and diameters of the axon branches activating the muscle fibres. This is, however, a constant time delay.
- The delay in time caused by random emission of Acetylcholine packets, from each neuromuscular junction.

The second of these two factors is believed to be a random process and as such, the excitation of each muscle fibre in a MU also appears to be random in time.

The actual size of MUs is variable, muscles controlling fine movements, such as those in the ear and eye, contain relatively few muscle fibres (less than 20) whilst those in, for example the leg or any other limb will have large MUs containing many muscle fibres (up to and over 1000), (Lenman & Ritchie, 1977).

The motor units in a muscle are arranged in a hierarchy based on size. The MUs containing a small no. of fibres are activated by the smaller alpha motoneurons and are excited in the earlier stages of a contraction requiring an increasing level of force. The larger MUs are activated, as would be expected, by larger alpha motoneurons, and at progressively greater levels of force.

1.6.2 - The Electromyogram, (EMG).

The EMG is the electrical manifestation of the neuromuscular activation associated with the contraction of a muscle. It is a very complex signal which, although extremely noise like in appearance, is highly structured.

The EMG signal is affected by several different factors, these being anatomical and physical properties of the muscle under observation, the control scheme of the peripheral nervous system, and the characteristics of the instrumentation used to detect and observe it.

The main component of the EMG is :

1.6.3 - The Motor Unit Action Potential, (MUAP).

Under normal conditions, an action potential propagating down a motoneuron activates all of the branches of that motoneuron. These in turn activate all the muscle fibres in that MU.

When the post synaptic membrane of a muscle fibre is depolarised, the depolarisation travels in both directions along the fibre. The depolarisation of the membrane is accompanied by a movement of ions. These together generate an electromagnetic field in the vicinity of the muscle fibres.

If an electrode is located within this field, it will detect the potential or voltage whose time excursion is the action potential of that MU.

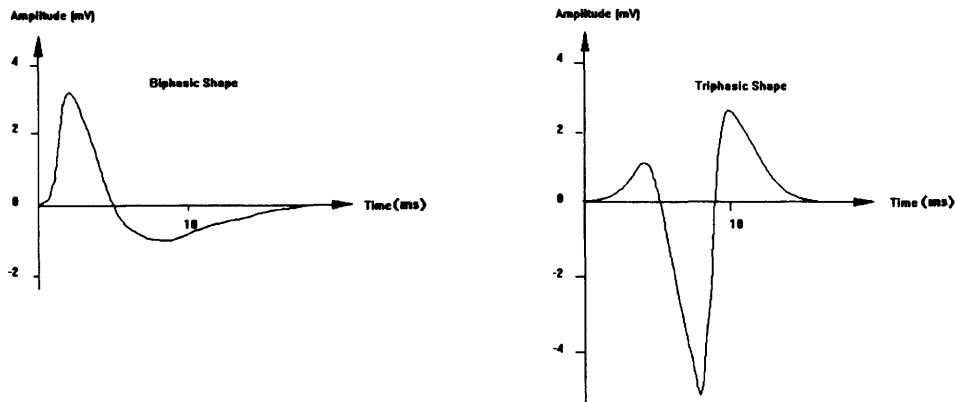
The signal seen at the site of detection will, in actual fact, be a superposition in both time and space, of the individual MU components contributed from each muscle fibre in the MU, and of other nearby, active MUs. This is because the depolarisation of the individual muscle fibres of one MU overlap in time.

The shape and amplitude of a MUAP depend upon the geometric arrangement, with respect to the electrode's location, of the active muscle fibres in the MU. If there are fibres in the detection site which belong to other MU and which are excited these too will be detected. They will, however, be recognisable from one and other because their shape will vary: this is an effect of the geometric arrangement previously mentioned. The differences in the arrangement of fibres between MU, relative to the electrode, alter the size and shape of their action potentials.

It is true, however, that MUAPs from different MU may have similar amplitude and shape. This occurs when the fibres of MU in the detectable area of the electrode have similar spatial arrangement. The geometric arrangement of the fibres in a MU is very sensitive to disruption. Even slight movements of the penetrative electrode will significantly alter the geometric arrangement of the fibres, and thus, the amplitude and shape of the corresponding MUAP also.

When the factors which effect MUAP shape are taken into account, it comes as no surprise at all that variations are found in the amplitude, number of phases and duration of MUAPs detected by the same electrode, and especially in MUAPs detected by different electrodes.

Figure 1.6.3.1 - Normal Action Potential Shapes .



1.6.4 - The Motor Unit Action Potential Train, (MUAPT).

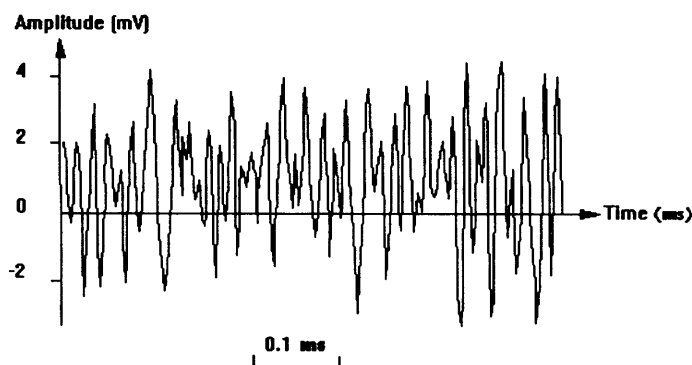
The occurrence of a MUAP is accompanied by a twitch of the muscle fibres contained within that MU. For a contraction of the muscle to be sustained, it is necessary for the MU within it to be continuously reactivated. The waveform produced by one MU is then known as the Motor Unit Action Potential Train (MUAPT).

The waveform of the MUAP will remain constant in the MUAPT if the geometric relationship between the active muscle fibres in the muscle, and the electrode recording the electrical activity within the muscle, remains constant. Other factors requiring constancy are the properties of the recording electrode and the biochemical set-up of the muscle tissue.

It is known that, in humans, the muscle fibres of any one particular MU are scattered randomly within a section of the normal muscle, also that they are intermingled with constituent fibres of other MUs. The Cross Sectional Area of a MU, in fact, ranges from 10 to 30 times that of the muscle fibres within it. This implies that the muscle may contain fibres belonging to between 20 and 50 MU. It is thus clear that a single MUAPT is observed only when the muscle fibres from one MU are active, and that this will only occur under very low levels of contraction.

As the force output of the muscle increases, the MU with fibres in the pickup area of the electrode become activated causing simultaneous detection of several MUAPTs. This is the case, even for highly selective electrodes. As the number of simultaneously detected MUAPTs increases, it becomes more difficult to determine which MUAPT a certain MUAP comes from, and thus to group together the MUAPs which form a MUAPT. This is due to the increase in the probability that MUAPs from different MUAPTs will overlap, that is associated with the increase in force output of the muscle and the increase in simultaneously detected MUAPTs. As the MUAPTs present in the EMG overlap, the Interference Electromyogram (IEMG) is formed. This is a superposition of MUAPTs in time.

Figure 1.6.4.1 - An Example of the Interference EMG



1.6.5 - Force generation.

When a healthy, normal muscle is at rest, with the exception of occasional nerve potentials and endplate potentials, it is electrically silent. Any electrical activity that may be detected due to the insertion or relocation of the electrode will be of minimal duration.

When such a muscle as the one described above is subjected to a weak voluntary contraction, a few MUAPs within it begin to fire asynchronously. This is typically at a rate of between 5 and 40 per second. As the required force output of the muscle becomes

greater, it is necessary for more force to be generated. This is achieved via two separate mechanisms:

1. Recruitment of Motor Units.
2. Alteration of Motor Unit Firing / Discharge rates.

When the force output of a muscle becomes greater, there is a transient increase in the firing rate of the MUs already active within the muscle. This is closely followed by recruitment, and an associated decrease in the firing rate. This is the case until all of the MU within the muscle are active.

For recruitment, firstly the small MU within the muscle fire. These are followed by the larger MUs, thus the contraction of a muscle is known as a 'Production of Graded Muscular Tension.' It is usual for MU that have been recruited to remain active throughout the period of the contraction, and when all the MU available have been recruited, the second mechanism for increasing the force output of a muscle, by increasing the frequency at which the individual MUs fire, is resorted to.

As the required force output of the muscle decreases, the last MU to be recruited is the first to be released from work. The release of MUs continues in this first in, last out manner, until the last MU is deactivated. At this point an iso-electric baseline is restored.

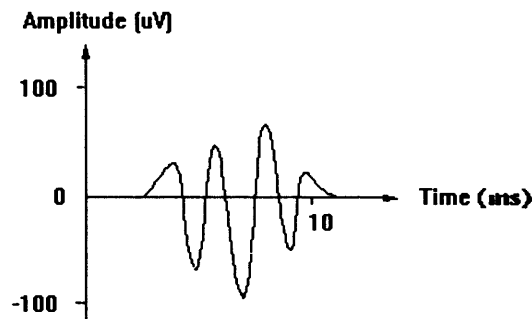
1.6.6 - The EMG of Myopathy.

The changes in the appearance of the EMG, due to muscular diseases, depict firstly, the pathological changes in a muscle which result in a loss of fibres. The signal consists of a main spike potential and others following it. These other spike potentials are due to activity in muscle fibres not within the immediate recording vicinity of the electrode. The spikes arise because the electrode is recording near to a MU which has lost some of its fibres. Thus within that MU, the muscle fibre membranes and the motor end plates are not functioning properly. This produces a scatter of time delays in the elements

of the MU. These different delays cause the firings of the remaining fibres within the MU to be out of phase with one and other, thus they appear in the EMG as individual spikes.

When observing the EMG of a muscle suffering with a myopathic disorder, the electrode will pick up signals from nearby muscle fibres, but those fibres belonging to the MU that are some distance away are lost. This affects the appearance of the signal, therefore the action potential of a myopathic MU will be of low amplitude, short duration, and will be polyphasic during voluntary contraction

Figure 1.6.6.1 - The Myopathic Action Potential.



So, the reduction in the dimensions of MUAPs, and the fragmentation of normal bi- and Triphasic potentials into polyphasic potentials, result from the loss of functioning muscle fibres within MU. However, the most interesting aspect of voluntary contraction in a myopathic muscle, is the occurrence of a full interference pattern during contractions of only weak force.

The increase in the interference pattern at low levels of contraction within myopathic muscles, in comparison with the level of interference observed in a normal muscle, may be explained as a 'Reduction in the Mechanical Output' of the diseased muscle. This is characterised by fewer muscle fibres being available within the MU to produce an output of force. Each muscle fibre as a single entity is very weak, and as there are fewer within the MU, to produce the desired output, the muscle fibres that are available are recruited at a rate greater than that demonstrated by a normal muscle, and at a higher firing rate, at relatively lower force level, in order to produce a comparable

output to that of the norm. This relative increase in the firing rate, at low force levels, contributes more action potentials than may be normally expected, thus creating an interference pattern. It follows that a full interference pattern will be observed, at a lower proportion of maximum voluntary contraction than in normal muscles.

In general, when a muscle is host to a myopathic disorder, the motor and sensory conduction velocities remain normal.

1.6.7 - The EMG of the Neurogenic Lesion.

There are three types of trauma from which a nerve may suffer:

1. Neurapraxia: this is a temporary failure of nerve conduction without loss of axonal continuity between the neurone and its end organ;
2. Axonotmesis: this describes severance or damage to the axon with subsequent wallerian degeneration distal to the axonal lesion, but without damage to the basement membrane and connective tissue of the nerve bundle. Axonal regeneration occurs after this lesion at a rate of 1-2mm/day.
3. Neurotmesis: this describes more serious cases of axonotmesis, where damage to the basement membrane and connective tissue occurs. The perineurium may also sustain damage. In the most severe cases the nerve may be severed. Regeneration is less effective than for axonotmesis, because of the damage sustained by the basement membrane or connective tissue sheaths of the nerves, therefore making functional recovery of the muscle less complete.

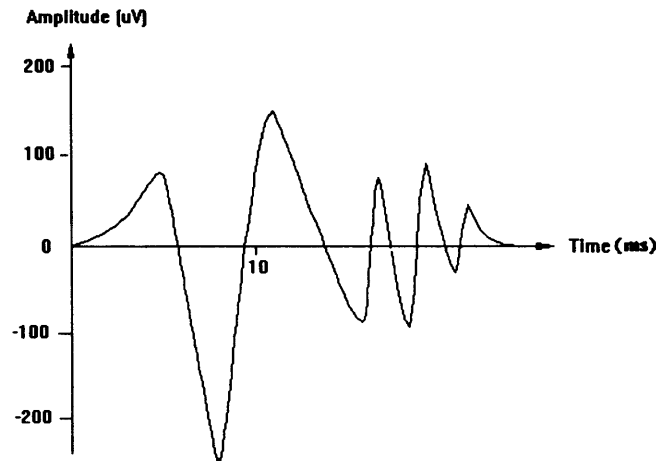
There are two types of pathology that can occur in a neuropathic disorder:

1. **Demyelination:** damage to the Myelin sheath which covers the nerve fibre. This type of disorder results in an overall slowing of the Nerve Conduction Velocity, (NCV). It is usually observed to be less than one half of the expected value. There is a second potential that is sometimes recorded in NCV test: this is known as the F wave. The F wave is formed from the evoked impulse travelling proximally along the nerve to the anterior horn cell, before travelling distally to innervate the muscle. In a neuropathic disorder of this type, the F wave is seen to be of reduced amplitude, prolonged duration and exhibiting polyphasicity.
2. **Axonal Lesion:** When there are lesions on the anterior horn cell or the peripheral nerve, there results a partial injury to the motor nerve, (i.e. the alpha motoneuron). The effect of this is that some of the muscle fibres within an MU will no longer be activated when the muscle contracts. This may be viewed as a break in the interface between the nervous system and individual muscle fibres. To cope with this, the surrounding MU, providing of course that there are some still in a normal state, will grow out to encompass the muscle fibres which are no longer connected to the nerve of their MU, thus connecting them with a new nerve, and re-innervating them. This obviously results in a change in the geometric arrangement of fibres within the MU. There are groups of several muscle fibres, all belonging to the same MU, present within the pick-up area of the electrode.

When observing the action potentials of a muscle suffering from neurogenic lesions, it is possible that those due to the MU recruited early on in the contraction may appear as normal, though it is likely that some will be polyphasic. It is more likely that these early action potentials will be polyphasic in chronic (i.e. those of a long period) lesions than in acute (i.e. short and severe) lesions. Generally, a neurogenic EMG signal will contain spontaneous activity such as fibrillation potentials, which are potentials due

to a local involuntary contraction of muscle resulting from the spontaneous activation of a single muscle fibre whose nerve supply has been damaged or cut off, even at rest.

Figure 1.6.7.1 - The Neurogenic Action Potential.



As the force of the contraction increases, and more MU are recruited, the action potentials increase in magnitude. The later recruited units are significantly larger than those first recruited. The increase in size is due to recruitment of those MUs re-innervated, by the axons of surviving MU. The increased percentage of polyphasic MUAPs is due to the larger spatial distribution of muscle fibres, (Ludin, 1980). These action potentials are known as “Giant Potentials”, if their magnitude is greater than approximately 10mV.

A neuropathic disorder may be “Sensory” or “Motor”, or a combination of both. Sensory Neuropathy is usually caused by damage to the nerve fibres connected to the skin surface. In this case there is no effect in the EMG, but the NCV tests show abnormal results. Motor Neuropathy is caused by damage to the nerve fibres connected to the muscle. In this case, abnormal affects are observed in the EMG, but mainly in the NCV tests.

It has been observed that the most characteristic factor of the EMG of neuropathy, is the reduction in the degree of interference pattern at maximum voluntary contraction,

during all stages of the disorder. This is an indication of the loss of functioning MUAPs within a muscle, and the respective interference pattern is seen to consist of a reduced number of large amplitude, fast firing MUAPs.

When a muscle is severely affected in the way described above, only a single MUAP may be recorded during maximum contraction. This differs from severe cases of muscle fibre lesion, where the full interference pattern may be seen, even at relatively low force levels.

1.6.8 - Spontaneous activity.

Unlike the voluntary activity of a muscle, the spontaneous activity is studied whilst the muscle is at rest. It is studied like this because at rest there is little or no voluntary content in the signal being observed, thus making the spontaneous activity recognisable.

Spontaneous activity may be grouped as follows: insertion activity; fibrillation potentials; positive sharp waves; bizarre high frequency potentials; end-plate potentials; and fasciculation potentials.

1.6.8.1 - Insertion activity.

This is the electrical activity caused by either the insertion or the movement of a needle electrode. It consists of a very brief burst of potentials lasting less than 500ms (Swash & Schwarz, 1981). The potentials caused by insertion are of shorter duration and smaller amplitude than the action potentials caused by the firing of a motor unit.

1.6.8.2 - Fibrillation and fibrillation potentials.

Fibrillation is the spontaneous contraction of a single muscle fibre. The fibrillation potential is the electrical activity associated with that fibrillation. The

potentials may fire spontaneously, or in a similar fashion to insertion activity, may be provoked by movement of the recording electrode. The potentials usually fire at a constant rate, although a small proportion fire irregularly (DeLisa *et al*, 1994). The firing rate often decreases just prior to the cessation of the discharge. These potentials rarely occur in normal muscle, they are associated with denervation.

1.6.8.3 - Positive sharp waves.

The positive sharp wave is caused by insertion or movement of the needle electrode. It is characterised by a fast rise time and relatively short positive phase, and a slower negative phase of smaller amplitude. It is considered to originate from a damaged region of muscle fibres, (Richardson & Barwick, 1969) (Lenman & Ritchie, 1977).

Positive sharp waves may be recorded from fibrillating muscle fibres when the potential arises from an area immediately adjacent to the needle electrode, (DeLisa *et al*, 1994). Both positive sharp waves and fibrillation potentials occur more commonly in peripheral nerve disorders than in lesions near or on the anterior horn cells.

1.6.8.4 - End-plate potentials.

The end plate potential may be defined as the graded, non-propagated membrane potential induced in the postsynaptic membrane of the muscle fibre by the action of acetylcholine released in response to an action potential in the postsynaptic axon terminal, (DeLisa *et al*, 1994).

These potentials may be confused with fibrillation potentials. The major difference is that a slight movement of the needle will cause the end-plate potential to disappear.

1.6.8.5 - Fasciculation and fasciculation potentials.

A fasciculation is the spontaneous firing of a group of muscle fibres or a motor unit, it is accompanied by visible movement of the skin (limb), mucous membrane (tongue), or digits, (DeLisa *et al*, 1994).

The fasciculation potential has the configuration of a motor unit action potential, but it occurs spontaneously. They most often occur sporadically, but sometimes occur as a grouped discharge, (DeLisa *et al*, 1994).

Fasciculation potentials are usually found in spinal cord lesions and in motor root lesions, (Swash & Schwarz, 1981). They do occur in normal muscles, however, their discharge rate is significantly different. In normal subjects they occur at a rate of approximately 1/s, but in anterior horn cell disorders their frequency is slower: one every 3 to 4s, (Trojaberg & Buchthal, 1965).

1.7 - Investigations in Electromyography.

Various investigations are carried out during neurophysiological examinations. A large proportion of these fall into the category of electrophysiological tests and as such require the use of electrodes.

1.7.1 - The Electrode.

The electrical activity in a muscle is monitored using electrodes. The main constraint of these electrodes is that they must be relatively harmless to the patient and at the same time must be brought close enough to the muscle under observation to detect the current created by the ionic movement within it.

There are several different types of electrode used in the study of muscle function, the first of these being:

1.7.1.1 - The Surface Electrode.

The surface electrode comes in two general formats, either the passive electrode or the active electrode. Both are very similar in that they consist of a detection surface which monitors the current on the patient's skin, via the electrode-skin interface. i.e. the area of contact between the skin and the detection surface. The major difference between the two occurs in the active configuration. Here, the input impedance of the electrode is increased greatly. This reduces the effects of both the impedance and the quality of the electrode-skin interface. Both of these formats are required.

This electrode type may be used to detect those EMG signals that contain the contributions from many individual MUs within the pickup area of the electrodes detection surface. They may also be used to detect motor unit action potential trains during low level contractions of the muscle. However, the concentric needle or EMG electrode, is mostly used for these purposes, in practice, whilst the surface electrode is used for nerve conduction velocity testing.

1.7.1.2 - The Needle Electrode.

The most common electrode is a penetrative electrode, inserted into the muscle, i.e. the needle electrode. The needle electrode is available in many forms, but the most widely used in electromyography is the concentric needle electrode (CNE).

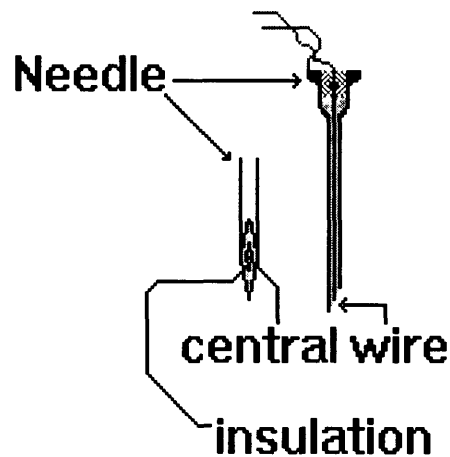
The CNE is used in both clinical and research environments, and comes in different formats. The monopolar configuration contains a single insulated wire in the cannular of the needle, the tip of that wire being bared to act as the electrodes detection surface, whilst the bipolar configuration contains two insulated wires in the cannular, thus providing the electrode with two detection surfaces.

The CNE has two significant advantages over other electrode types: its relatively small detection surface enables the electrode to detect MUAPs individually. This is especially so at low levels of contraction, and the electrode may easily be repositioned

within the muscle, without reinsertion, to improve the signal quality or to view signals from surrounding areas

It is also possible to obtain electrodes specifically designed to study certain characteristics of the MU.

Figure 1.7.1.2.1 - The Concentric Needle Electrode.



1.7.1.3 - The EMG Amplifier.

The basic electrical characteristics of the EMG signal may be seen from figure 1.5.1.3.1 to be as follows: in frequency, the EMG ranges from approximately 25Hz to several kilohertz; in amplitude it varies from 100uV to 90mV, and the DC potential is small in magnitude.

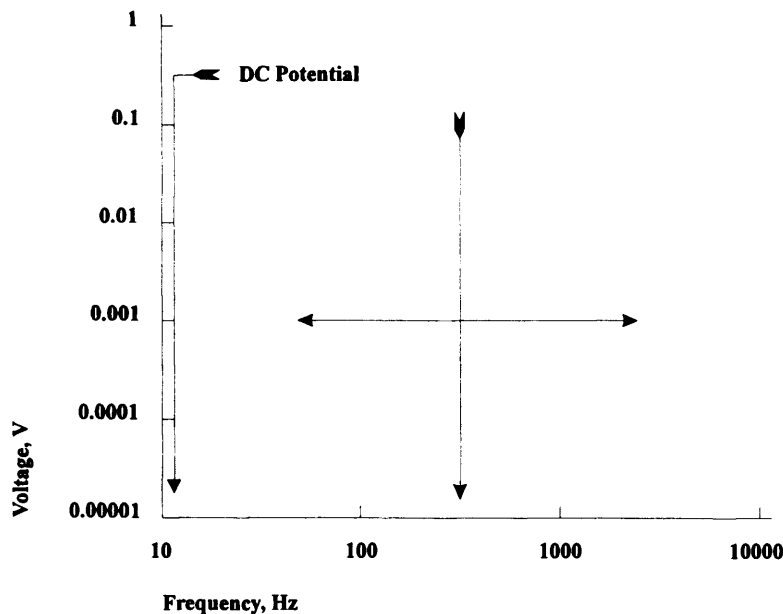
This indicates that amplifiers to be used in the observation and recording of the EMG must have a wide frequency response. It is beneficial, however, that the amplifier need not cover the very low frequencies, i.e. less than approximately 25Hz, because motion of the body consists mostly of low frequencies. Thus motion may easily be filtered out of the EMG, without having adverse affects on the quality of the signal.

The type of electrode used affects the amplifier characteristics. Surface electrodes reduce the level of the signal, so that amplitudes vary from approximately 0.1 to 1mV.

The electrode impedance is low, ranging from about 200 to 5000 Ω . This increases the required gain of the amplifier. If an intramuscular electrode is used, the signal may be an order of magnitude greater than that observed using the surface electrode, thus the gain required is an order of magnitude less.

Another factor affecting the amplifier, is the surface area of the electrode. This area is small, so the electrodes source impedance will be relatively high. In order to obtain a good quality signal reproduction, it is necessary to have a reasonably high amplifier input impedance.

Figure 1.7.1.3.1 - The electrical characteristics of the EMG.



1.7.2 - Physical tests.

1.7.2.1 - Nerve conduction velocity studies.

Nerve conduction studies are technical procedures used to assess objectively the functional states of the peripheral neuromuscular system, (DeLisa *et al*, 1994).

The velocity with which a stimulus propagates along a peripheral nerve is a useful indicator of the state of the muscle - nervous system interface. However, this is not the only thing of interest, various other observations, both motor and sensory, are made on the peripheral nerves to aid in diagnosis.

The apparatus required to perform nerve conduction studies consists of various electrodes for stimulating the nerve, recording from the nerve and for grounding it. These electrodes are all surface electrodes and are arranged into different configurations for different types of observation.

The main observations are those of the motor and sensory nerve responses (latencies) and hence the motor and sensory nerve conduction velocities. It should be routine practice to measure sensory and motor nerve conduction velocities in at least one nerve in all patients, because some patients, especially those with proximal weakness, may thus be shown to have a neuropathy rather than other myopathic or neurogenic disorders, (DeLisa *et al*, 1994).

Various levels of stimulation may be used, though for motor nerve conduction studies, supramaximal stimuli must be used, (Swash & Schwarz, 1981). Supramaximal stimulation uses a stimulus 20% stronger in voltage or current than that which is required for maximal stimulation. Maximal stimulation is the stimulus intensity after which a further increase in the stimulus intensity causes no increase in the amplitude of the evoked potential in the nerve under investigation, (DeLisa *et al*, 1994)

Measurements of the applied stimulus current give a measure of the stimulus threshold of the nerve and these are sometimes useful in detecting slight abnormalities, particularly when comparison is made between sensory thresholds in opposite limbs, (Swash & Schwarz, 1981).

The motor latency is the time from the time of stimulation of the nerve to the initial deflection of the response from the isoelectric baseline; whilst its sensory counterpart may be measured from the time of stimulation of the nerve to, either the peak of the negative phase, or the initial positive dip of the response.

From these latencies, the appropriate conduction velocities may be calculated. This is done by stimulating the nerve at two separate locations and relating the stimulus propagation time difference to the separation of stimulation sites, as follows:

$$\text{Conduction Velocity} = \text{Stimulus Separation} / (\text{Proximal Latency} - \text{Distal Latency})$$

Proximal latency being the latency recorded from the location of stimulation most proximal to the nerve, and likewise for the distal latency.

It is accepted that the maximal nerve conduction velocity usually exceeds 50 m/s in the arms and 40 m/s in the legs. In more proximal parts of the nerve, the conduction is usually slightly faster, (Swash & Schwarz, 1981).

When stimulating a mixed nerve (i.e. a motor and sensory nerve), a nerve action potential is propagated and may be recorded at another point along the nerve. and its conduction velocity calculated. This technique is useful in the assessment of entrapment syndromes, when it may give information about local slowing of nerve conduction and loss of nerve fibre, (Swash & Schwarz, 1981).

So, NCV studies are useful in distinguishing between different types of disorder, and in diagnosing the presence and whereabouts of nerve entrapment syndromes, both using the propagation of nerve action potentials and the comparison between limbs of velocities through possible entrapment sites.

1.7.2.2 - Blood Creatine Phosphokinase content.

Creatine Phosphokinase is an enzyme which is present within human muscles in large quantities. Upon the occurrence of muscle fibre damage, this enzyme leaks from the muscle and causes a raised level in the blood.

The most valuable test in patients with neuromuscular disorders is measurement of the blood creatine phosphokinase (CPK) levels (Swash & Schwarz, 1981).

The level of CPK in the blood varies in relation to muscular activity, and even normal subjects may show slight elevations after exercise in which muscular trauma is

sustained, (Swash & Schwarz, 1981). Even the trauma of the EMG electrode or muscle biopsy will cause a raise in CPK levels.

The major factor to be considered in the analysis of CPK is a high content in the blood. Muscular disorders may be identified from unusual increases in CPK level. The CPK is raised in most myopathies, the highest values being found in Duchenne muscular dystrophy. In some indolent myopathies the CPK may be normal. It is also normal in peripheral neuropathies and other neurogenic disorders. However, in some severe chronic neurogenic disorders, the CPK may be moderately raised, (Swash & Schwarz, 1981).

In general though, most myopathies have a raised CPK level whilst most neuropathies have a normal or slightly raised CPK level. So the CPK level is a useful indicator of the state of the fibres within muscles. CPK level may also be used to monitor the progress of myopathic disorders within their hosts. The level of CPK within the blood is ascertained by analysis of a patients blood sample.

1.7.3 - Low force electrophysiological tests.

Low force electrophysiological assessment of the muscle consists of observation of the activity within the muscle, whilst no force is being exerted, and observation of the activity in the muscle whilst it is generating a low to medium force output, i.e. prior to the development of the interference signal. Voluntary activation is studied in a graded manner so that individual units may be studied, (Swash & Schwarz, 1981).

At zero force, after insertion activity has died away and its parameters been recorded, the other forms of spontaneous activity are looked for. These consist of fasciculation and fibrillation potentials, end-plate potentials, positive sharp waves and bizarre high frequency potentials. The presence or absence of such activity can be highly indicative of certain disorders, thus negating others and facilitating diagnosis.

The important parameters which are required to be identified from volitional activity are as follows: action potential amplitude; action potential duration; number of phases; firing rate. This information, most notably the number of phases, will differentiate between normal and disordered muscle, and myopathic and neuropathic

muscle. Combined with the information about spontaneous activity present within the signal and physical test results, along with further information about the patient, a diagnosis may be possible. However, other investigations may be required to isolate the disorder present.

These observations are made using the CNE described previously, attached to the relevant amplifiers and displays. The needle should be placed in one of the most affected muscles. It is important that there is a standard for measuring the parameter dimensions. Thus, the amplitude is measured as the maximum peak to peak amplitude. This is affected by: the diameter of the muscle fibres; the number of fibres; the temporal distribution of the action potential closest to the recording electrode; the leading off area of the electrode, (DeLisa *et al*, 1994). The number of phases in an action potential is the number of baseline crossings plus one. A phase is seen to be the area between two adjacent baseline crossings.

In a clinical environment, all of these observations are generally made by the clinician using his or her eye. There has been much interest over the years in the automation of this process. Various methods of decomposition have been presented, demonstrating differing levels of success. However, the traditional doctor's eye is, at present, the more effective method.

1.7.4 - High force electrophysiological tests.

At high force levels, the electrical activity recorded from the muscle is much harder to analyse. The EMG shows an interference pattern in many cases and it is difficult to discover any useful information, simply using visual observation. Various techniques have been devised for gleaning useful information from high force/interference EMG signals. Some of these are described.

1.7.4.1- Single database principal component analysis.

It has been shown that different types of spectra derived from signals typical of normal, myopathic and neurogenic subjects, can be classified successfully using the method of principal component analysis, (Jones *et al*, 1990).

Principal component analysis is a multivariate statistical technique which is capable of representing a set of data variables by a completely new, orthogonal, set of data variables, reduced in number from the original. It is an effective way of classifying the spectra of the turning point process of interference EMGs and its application to interference EMGs has allowed successful separation of normals and cases of neurogenic and myopathic disorders.

The use of two principal component coefficients, to classify each interference EMG, can give adequate discrimination between cases. If extra information is available to separate neurogenic disorders from early myopathic disorders, whilst the use of three coefficients provides enhancement to discrimination in difficult cases, (Jones *et al*, 1990).

These results are presented in more detail by Jones *et al*, who state that mixtures of normal and myopathic EMG's with more than 10% and fewer than 40% abnormal units are classified as neurogenic in two dimensional analysis. EMG's with fewer than 10% abnormal units are classified as normal and those with more than 40% myopathic units are classified as myopathic.

Mixtures of normal and neurogenic EMGs with more than 10% abnormal units are correctly classified as neurogenic in two dimensional analysis, EMGs with fewer than 10% abnormal units are classified as normal

The addition of a third principal component coefficient into the procedure allows the correct classification of all mixtures of normal and myopathic units when there are more than 20% abnormal units present, (Jones *et al*, 1990).

1.7.4.2- Triple database principal component analysis.

It is apparent that the principal component analysis algorithm (single database) is capable of taking in a recorded high force (interference) EMG signal, resolving it into its principal components, representing it using the first three, and forming a comparison of this representation with the clusters ascribed to the different disorder types.

The triple database principal component analysis knowledge source is very similar to its single database counterpart. The major difference being that the database from which the principal components and their associated weights are calculated, in the single database method, consists of the turning point spectra of interfering EMG signals representative of normal, myopathic and neurogenic signals, whilst in the triple database method there is an individual database for each disorder type.

The method of muscle condition determination consists of generating the principal component representation of a new signal using each database concurrently to see which set of principal components fits its turning point spectrum most closely. Closeness being measured in terms of the size and whiteness of the residual. The residual is defined as the difference between the actual spectrum, and the least squares approximation using weighted sums of the principal component spectra from the particular class being considered, (Jones *et al*, 1987).

1.7.4.3 - Turns Analysis.

Willison's method uses two parameters to characterise the EMG:

- The number of potential reversals (turns) per unit time.
- The mean amplitude between turns.

A comparison is made between the amplitude of the potential deflection and a pre-set threshold level. Only those phase changes that exceed this threshold are registered

as significant turns. The threshold uses a point of change in phase of potential as its reference.

It has been shown by different investigators that this method will successfully discriminate between healthy, myopathic and neurogenic muscle. Myopathic muscle shows an increased turns count per unit time and a mean amplitude between turns that tends to fall below the normal range. Neurogenic muscles show grossly increased mean amplitude between turns, (Willison, 1964) (Rose & Willison, 1967) (Colston & Fearnley, 1967) (Hayward & Willison, 1973 & 1977).

Hayward and Willison also showed that the increase in mean amplitude between turns in progressive neurogenic disorders, such as Motor Neurone Disease, may be followed from within the normal range to within the clearly abnormal, (Hayward & Willison, 1973).

Fuglsang-Frederikson *et al* reported that the number of patients identified as having neurogenic or myopathic disorders by turns analysis and by inspection of MUAP waveforms were very nearly the same, (Fuglsang-Frederikson *et al*, 1976 & 1977)

The turns count in an IEMG has been shown to correlate with the percentage of polyphasic MUAPs measured from individual motor units.

The main requirement for the correct operation of the algorithm is that the contraction force is accurately controlled. This requirement prevents the method being used successfully on children and on uncooperative patients. It also limits the number of muscles that may be studied.

It is important to note that the mean amplitude between turns, and the number of turns per unit time are directly related to the number of MU present within a contraction, and as such, correct classification of a muscles state will only occur if enough MU are present within the contraction. It was found that for myopathic, neurogenic and semi-neurogenic disorders correct classification is made for signals containing 10 or more potential trains, but for semi-myopathic disorders, 10 normal and 10 myopathic potential trains are required for correct classification, (Parekh, 1986).

Myopathic disorders are classified correctly for signals containing above 30% myopathic potential trains, and Neurogenic disorders are also classified correctly for signals containing above 30% Neurogenic potential trains.

1.8 - The type of system

It may be appreciated from the details of those tests carried out in neurophysiological examination, that the results are diverse in form and inference. Not all tests bear the same relevance to different disorders, in fact some tests may not be required to form the diagnosis. Thus for an MDSS to be successful in this area it must be able to deal with the diversity of information present and the degree of relevance that the data has to the problem. The blackboard system is well suited to this type of situation.

Each of the different tests outlined may be viewed as a distinct source of knowledge to the blackboard. No one knowledge source requires interaction with another, this is only required with the blackboard. As such, the blackboard system will be able to deduce the validity of suggested hypotheses, making it a support device rather than a diagnostic replacement for the clinician.

1.9 - Summary.

This chapter has introduced the idea of medical decision support systems and the architecture and operation of the blackboard system, highlighting reasons for its suitability for application to the problematic field of neuromuscular diagnosis.

Background information on the subject of neurophysiology has been presented, including descriptions of the components that make up the electromyogram in both healthy and abnormal conditions. The methods of force generation have been outlined along with the behaviour of certain elements of the muscle and its associated EMG under various conditions of disorder. Spontaneous activity has been summarised and its occurrence presented. Types of electrode used in electromyography have been discussed and some characteristics of the required signal amplification have been outlined.

Simulation and analysis in electromyography.

The tests that may be carried out during neurophysiological investigations have been presented briefly. These included physical tests, low force electrophysiological tests and high force physiological tests.

Chapter 2 - A simulated patient.

2.1 - Introduction.

This chapter is concerned with the creation of a simulated patient for interaction with a medical decision support system, and as a source of clinical reference. The MDSS interacted with is that created and tested in EPSRC Rep GR/J47064. Initially the reasons for creating such a simulated patient are addressed. In section 2.3 the components required for creating the simulated patient are outlined. Section 2.4 introduces the basic concepts of these components and isolates what form the simulations will take. This section also discusses the method of data representation used and the method by which the simulations operate within the simulated patient. Section 2.5 presents the data produced by the simulation of physical tests; section 2.6 presents the data produced by simulation of low force electrophysiological tests, and section 2.7 presents the data produced by simulation of high force electrophysiological tests. The usefulness of these simulations is discussed in section 2.8 and summarised in section 2.9.

2.2- Why create a simulated patient?

There are two main reasons for creating a simulated patient. The first reason is to provide appropriate results for the validation and modification of the neuropsychological MDSS. The second is to create the ability to provide training in comparative diagnosis of neuromuscular disorders. Both of these reasons are important and will be dealt with separately.

How can the creation of a simulated patient facilitate validation of an MDSS? To create an MDSS and ensure its correct operation, in the case of a blackboard based system, it is necessary to have operative knowledge sources to provide the information requisite to making a decision, or proving/disproving an hypothesis. There are two reasons at this stage for using simulations of knowledge sources. Either the real

knowledge source is not available, or it is advisable to use data, the characteristics of which are known, in order to test whether the system is making the required decisions correctly.

So, simulations of the knowledge source may enable the system to operate in the absence of various knowledge sources necessary to diagnosis, during development. It may also allow the validity of the system's decision making abilities to be assessed, by providing data to the system where the corresponding diagnosis is already known, and checking that the system agrees.

How does the creation of a simulated patient help with comparative diagnosis training? Many disorders of the muscle and nerve are not commonly seen and as such, they have characteristics that may not have been seen by clinicians. The creation of a reference, via simulations, of rare conditions and also of commonly occurring ones, provides a valuable source of comparison. The simulations may be used as a primary source of training for doctors approaching practice, or they may simply be used as a source of comparison during diagnosis.

In this capacity, simulations of knowledge sources which create a simulated patient are useful in a clinical environment.

The test results which create the simulated patient all herald from those knowledge sources which are a part of the neurophysiological MDSS. It is important to appreciate that these results are necessary to the diagnostic decision making process.

2.3 - The simulated knowledge sources.

The knowledge sources that are simulated fall into three distinct categories: knowledge sources dealing with the results of physical tests performed on patients (these are the knowledge sources most pertinent to comparative diagnosis); knowledge sources representing the results of low to medium force electrophysiological assessment of patients and their associated post processing; and knowledge sources representing the results of high force electrophysiological assessment of patients and their associated post processing. These knowledge sources are listed below.

Physical tests: Nerve conduction velocity tests;
 Blood Creatine Phosphokinase level tests.

Low force Electrophysiological assessments:

 Low/medium force EMG tests;
 Very low force EMG tests;
 Zero force EMG tests.

High force Electrophysiological assessments:

 Single database principal component analysis of high force EMGs;
 Triple database principal component analysis of high force EMGs;
 Turns analysis (Willisons Method).

2.4 - Operation of Simulated Knowledge sources.

Two exclusive types of knowledge source have been isolated in the MDSS (Small *et al*, 1997a). These may be described as follows:

Firstly, the disease knowledge source. This is a module that contains details of diseases and disorders, the tests necessary to diagnose such diseases and finally the appropriate results from the specified tests to identify the relevant disorder.

Secondly, there is the test knowledge source. This type of knowledge source takes information and processes it, yielding useful results. It may also prompt for observations made of the patient under investigation and return more appropriate and useful information generated from these. So, in effect, the test knowledge sources contain numerical algorithms to take in collected data and return useful diagnostic information to the blackboard.

Simulations occur primarily of the latter type of knowledge source. These are important modules because they provide the system with information that may be used to

form the diagnosis. Without the results returned by these knowledge sources, there would be no grounds upon which to base a decision and the MDSS would not function.

The results obtained from the numerical algorithms within some knowledge sources are not in themselves of great use to the blackboard system's decision engine. A more useful form of information is how the result of each knowledge source compares with what is accepted to be normal within the field of neurophysiology. For example, MUAP Amplitude may be one of either, normal, small or large. However, there is no clear-cut boundary between the end of one class and the beginning of the next. Normal logic is unable to represent the unclear boundaries presented here.

It is convenient to use set theory to discuss the application of logic to this problem. Kosko & Isaka (1993) explain that, in standard set theory, an object either does or does not belong to a set: there is no middle ground. In such bivalent sets, the object may not belong to both a set and its complement set, nor to neither of the two sets. This is a demonstration of standard logic, and was termed "the law of the excluded middle" by Aristotle.

Fuzzy logic is a variation on standard logic that enables us to deal with uncertainties such as the unclear boundary between classes shown above. It may be looked upon as a fuzzification of the boundaries between sets. Sets that are fuzzy or multivalent break the law of the excluded middle to some extent. Items belong only partially to a fuzzy set, and they may also belong to more than one set.

It is important to appreciate that fuzzy degrees are not the same as probability percentages. Probability measures the likelihood of something occurring, whilst fuzziness measures the degree to which something occurs, or some condition exists.

The only constraint on fuzzy logic is that an object's degrees of membership in complementary groups must sum to unity, so the law of the excluded middle holds, merely as a special case in fuzzy logic. (Kosko & Isaka, 1993).

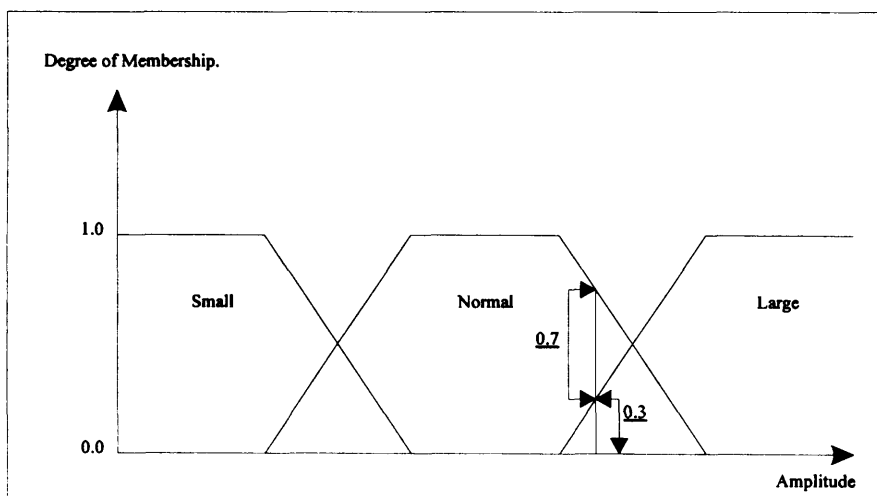
It is thus apparent that a fuzzy logic representation of the results of knowledge sources in comparison to what is normal would suit the ill defined boundaries between classes, allowing levels of confidence to be applied to the results returned to the blackboard.

i.e. The amplitude is Small (0.0) so we have an amplitude that is normal with
Normal(0.7)
Large (0.3)

70% certainty but that may be larger than normal (with 30% certainty) i.e. the result falls somewhere in the boundary between the two, figure 2.4.1.

The method by which useful information is provided to the blackboard is as follows: whilst the system is working to either prove or disprove a hypothesis of disease classification, the knowledge sources will provide their information to aid in the decision making process. In general, the characteristics displayed by myopathic and neurogenic muscles do not resemble one another. So, where necessary, an inhibitory clause that will prevent unsuitable results from being returned is intrinsic in the simulations.

Figure 2.4.1 - Graphical representation of Degree of Membership.



However, as a means of testing the systems ability to handle spurious information in the diagnosis, the knowledge source will not always return the result corresponding to the disorder suspected. This brings an element of reality to the procedure. It is operated using a Gaussian distribution with the correct result situated at the mean location of the distribution. Various other results are located at sites less likely to occur.

It was preliminarily decided that a set of five neuromuscular conditions would be provided within each simulation. Those five conditions are as follows: Limb Girdle Muscular Dystrophy (LGMD), a myopathy, but by no means characteristic of the entire myopathy family; Motor Neurone disease (MND), a neuropathy; of the other three cases, two are completely normal and one is representative of Thomsens myotonia congenita (MC), a type of myotonia.

2.5- Physical test knowledge source simulations.

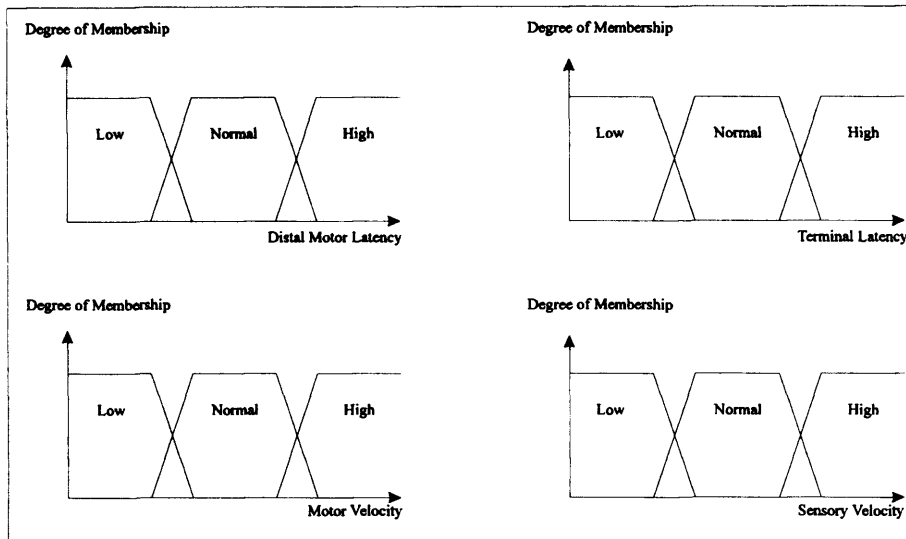
2.5.1- Nerve Conduction Velocity.

In this simulation, location of the site of recording is of the utmost importance. For example, the required values from this knowledge source are velocities, both motor and sensory, and latencies from all the relevant nerves. In order to calculate these, the exact sites of recording and stimulation, and their separations, are required. Here, the motor NCV from the Ulnar nerve is provided along with the Distal Motor Latency and the sensory NCV from the Median nerve along with the Terminal Latency is also provided. Both of these sets of recordings are performed in the arms and hands.

For completeness, and the provision of the facility to carry out comparisons between the upper and lower body, the addition of velocities and latencies from the Sural, Peroneal, Posterior and Tibial nerves should be carried out.

The types of result returned to the blackboard from this simulation may be viewed diagrammatically in figure 2.5.1.1, and their specific values may be justified by the following clinical findings:

Figure 2.5.1.1 - NCV simulation outputs.



Motor Neurone Disease - motor nerve conduction may be abnormal; in particular an increased distal motor latency (Lambert, 1962) and a slightly slowed motor nerve conduction velocity may be found (Argyropoulos *et al*, 1978). Sensory nerve conduction is normal. (Swash & Schwarz, 1981).

Limb Girdle Muscular Dystrophy - Nerve conduction studies are normal (Swash & Schwarz, 1981). This is due to LGMD being a myopathy, a disorder of the muscle fibre, thus there is no impediment to transmission along the motoneurone.

Thomsens Myotonia Congenita - The motor NCV is normal (Swash & Schwarz, 1981). This is the only part of the NCV studies likely to be affected because myotonia is “ a persistent contraction of a muscle, or group of fibres in a muscle, observed after the cessation of voluntary contraction.” (Swash & Schwarz, 1981).

The numerical results for this knowledge source may be viewed in table 2.5.1.1;

Table 2.5.1.1 - NCV simulation outputs, numerical.

	Motor Velocity	CF	Distal Motor Latency	CF	Sensory Velocity	CF	Terminal Latency	CF	Location
1 (MND)	Low	0	Low	0	Low	0	Low	0.1	Ulnar &
	Normal	0.8	Normal	0.3	Normal	0.7	Normal	0.9	Median
	High	0.2	High	0.7	High	0.3	High	0	Nerves
2 (LGMD)	Low	0.6	Low	0.2	Low	0.2	Low	0.1	Ulnar &
	Normal	0.4	Normal	0.8	Normal	0.8	Normal	0.9	Median
	High	0	High	0	High	0	High	0	Nerves
3 (MC)	Low	0	Low	0.3	Low	0.1	Low	0.2	Ulnar &
	Normal	0.7	Normal	0.7	Normal	0.9	Normal	0.8	Median
	High	0.3	High	0	High	0	High	0	Nerves
4 (NORM)	Low	0.2	Low	0.1	Low	0.2	Low	0	Ulnar &
	Normal	0.8	Normal	0.9	Normal	0.8	Normal	0.9	Median
	High	0	High	0	High	0	High	0.1	Nerves
5 (NORM)	Low	0	Low	0.1	Low	0	Low	0.3	Ulnar &
	Normal	0.7	Normal	0.9	Normal	0.6	Normal	0.7	Median
	High	0.3	High	0	High	0.4	High	0	Nerves

These numbers are representative of the medically accepted results for the chosen disorders when in the form of fuzzy triplets.

2.5.2- Blood Creatine Phosphokinase level.

Simulation of the CPK levels characteristic to different disorders is fundamental to the diagnostic procedure of the MDSS. This knowledge source is of great use in differentiating between myopathic and neurogenic disorders.

Only one result is returned from this simulation to the blackboard, this is in the fuzzy format previously used. Fuzzification of CPK is the first step towards an integrated fuzzy approach, (Zimmerman, 1990). The outputs of the simulation may be viewed diagrammatically in figure 2.5.2.1. The numerical results for this simulation may be seen in table 2.5.2.1 and their specific values may be justified by the following clinical findings:

Motor Neurone Disease - The CPK level is increased in more than half the patients, it may be increased to 2 or 3 times the normal range (Williams & Bruford,

1970). The higher levels are found in patients whose muscle biopsies show secondary myopathic changes, (Achari & Anderson, 1974)(Schwartz *et al*, 1976).

Figure 2.5.2.1 - Fuzzy output, graphical, for Biochemistry simulation.

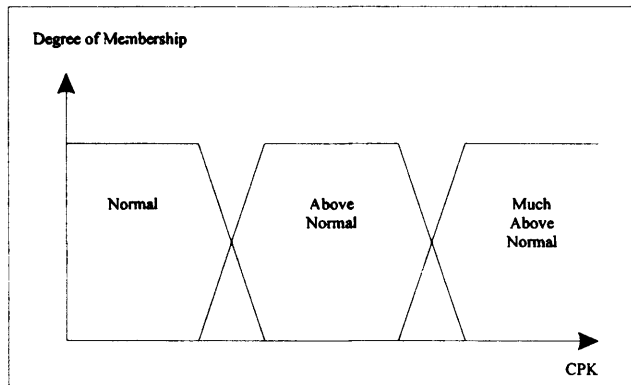


Table 2.5.2.1 - Biochemistry simulation outputs, numerical.

	% of CPK	CF
1 (MND)	Normal	0.4
	Above	0.6
	Much above	0
2 (LGMD)	Normal	0
	Above	0.5
	Much above	0.5
3 (MC)	Normal	0.7
	Above	0.3
	Much above	0
4 (NORM)	Normal	0.8
	Above	0.2
	Much above	0
5 (NORM)	Normal	0.1
	Above	0.9
	Much above	0
6 (Myositis)	Normal	0
	Above	0.2
	Much above	0.8

These numbers are representative of the medically accepted results for the chosen disorders when in the form of fuzzy triplets.

Limb Girdle Muscular Dystrophy - The CPK level is moderately increased; it is rarely as high as 10 times the normal range. (Swash & Schwartz, 1981).

Thomsens Myotonia Congenita - The CPK may be slightly raised in some patients, presumably those with the recessive form of the disease in whom distal weakness and atrophy is developing, but this has not been carefully evaluated.

The raised CPK level apparent in one normal case may be attributed to recent vigorous exercise or electromyographic investigations, whilst the presence of a sixth disorder here, a general myocitis, is to enable the system to differentiate between myopathy and myocitis.

2.6 - Low force electrophysiological assessments.

2.6.1 - Low/medium force EMG tests.

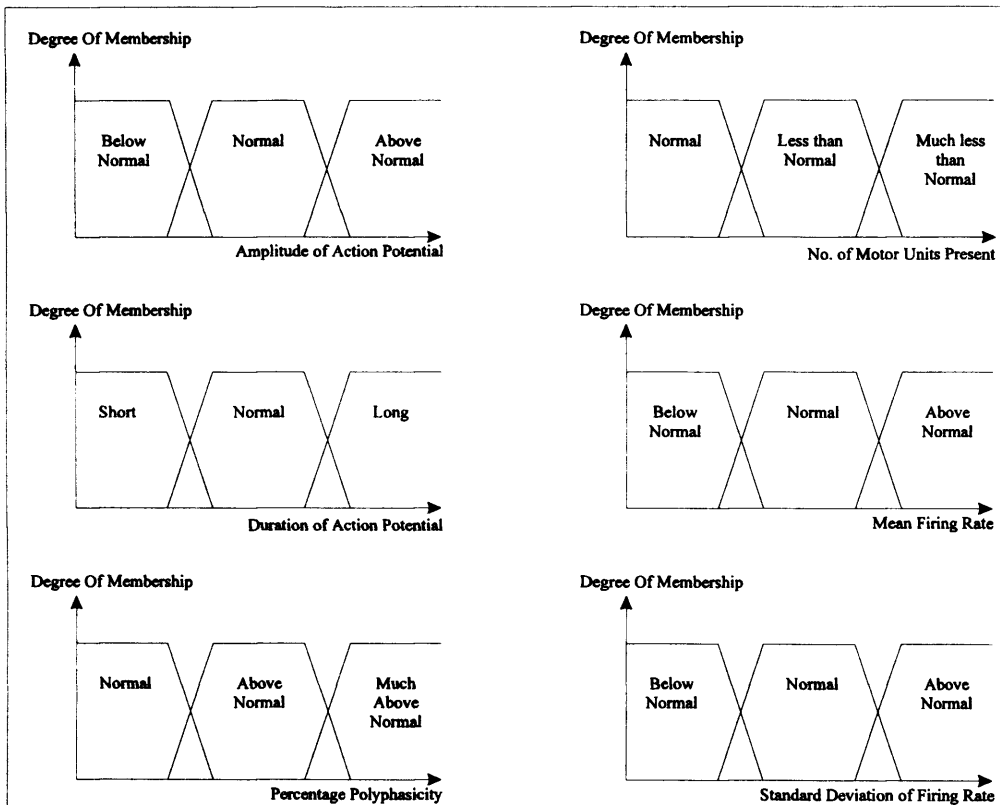
This simulation provides the results that may be produced by a decomposition algorithm, the purpose of which is to take in a signal of low to medium force, and from that signal, determine certain MUAP characteristics, and certain features of the signal as a whole.

The Characteristics observed by the decomposition algorithm, and as such those simulated here are:

- Action Potential Amplitude.
- Action Potential Duration.
- Percentage Polyphasicity
- Number of Motor Units Present.
- Mean Firing Rate.
- Standard Deviation of the Firing Rate.

The outputs of the simulation may be viewed diagrammatically and numerically below, and their specific values may be justified by the following clinical findings. They are represented using the method considered most suitable, fuzzy triplets.

Figure 2.6.1.1 - Fuzzy outputs, Graphical, for Lowmed simulation.



Motor Neurone Disease - On volition, The MUAPs are typical of a neurogenic disorder, they are increased amplitude, long duration and polyphasic, (Swash & Schwarz, 1981).

Thus for Motor Neurone Disease, amplitude, duration and polyphasicity are all increased. It follows that if the duration of the action potential is increased, then the number of firings in a set time is reduced, so the number of units present is reduced. In order to combat this and present a comparatively normal force output, the firing rate must be increased. So firing rate is above normally acceptable parameters.

Limb Girdle Muscular Dystrophy - Concentric Needle EMG reveals typical myopathic, short duration, polyphasic MUAPs of low amplitude, often with a full interference pattern, (Swash & Schwarz, 1981).

The characteristics are standard for a myopathic disorder. The interference at relatively low levels of force indicates an increase in firing rate.

Thomsens Myotonia Congenita - In the dominant form of Thomsens Myotonia Congenita, the EMG Shows Myotonia, but is usually otherwise normal, (Swash & Schwarz, 1981).

For both normal cases, the parameters fall within normal bounds for each individual characteristic.

Table 2.6.1.1- The Lowmed simulated results, numerical.

	Amplitude	CF	Duration	CF	%Poly	CF	No. of Units	CF	Mean FR	CF	S.D. FR	
1 (MND)	Below	0	Short	0	Normal	0	Normal	0	Below	0	Below	0.4
	Normal	0.2	Normal	0.3	Above	0.2	Less	0.5	Normal	0.3	Normal	0.6
	above	0.8	Long	0.7	Much Abv	0.8	Much Less	0.5	Above	0.7	Above	0
2 (LGMD)	Below	0.7	Short	0.8	Normal	0	Normal	0.6	Below	0	Below	0.4
	Normal	0.3	Normal	0.2	Above	0.4	Less	0.4	Normal	0.2	Normal	0.6
	above	0	Long	0	Much Abv	0.6	Much Less	0	Above	0.8	Above	0
3 (MC)	Below	0.6	Short	0.6	Normal	0.3	Normal	0.9	Below	0	Below	0.3
	Normal	0.4	Normal	0.4	Above	0.7	Less	0.1	Normal	0.3	Normal	0.7
	above	0	Long	0	Much Abv	0	Much Less	0	Above	0.7	Above	0
4 (NORM)	Below	0	Short	0	Normal	0.9	Normal	0.7	Below	0	Below	0.1
	Normal	0.8	Normal	0.8	Above	0.1	Less	0.3	Normal	0.7	Normal	0.9
	above	0.2	Long	0.2	Much Abv	0	Much Less	0	Above	0.3	Above	0
5 (NORM)	Below	0.2	Short	0.3	Normal	0.9	Normal	0.9	Below	0.2	Below	0
	Normal	0.8	Normal	0.7	Above	0.1	Less	0.1	Normal	0.8	Normal	0.7
	above	0	Long	0	Much Abv	0	Much Less	0	Above	0	Above	0.3

These numbers are representative of the medically accepted results for the chosen disorders when in the form of fuzzy triplets.

2.6.2 - Very low force EMG tests.

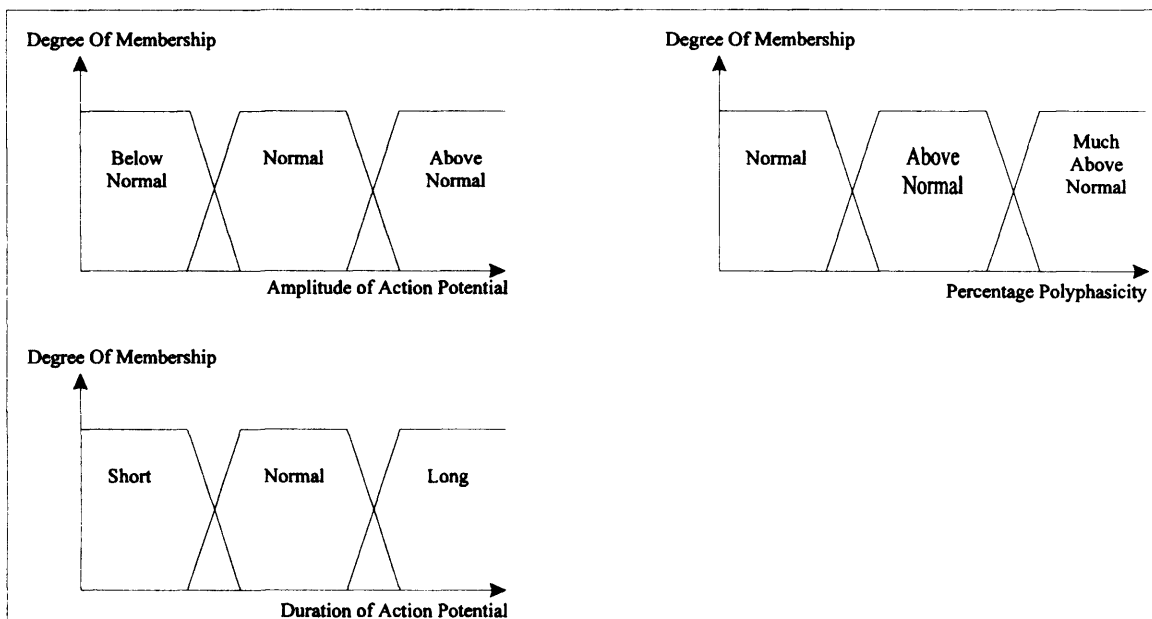
This simulation is similar in some respects to the previous one. It observes some of the characteristics that are observed by the decomposition algorithm, but, as the name would suggest, it does not deal with such high force levels. This simulation accounts for manual observation of the EMG signal, at levels of force where the identification of parameters is readily possible.

The Characteristics observed in this simulation are:

- Action Potential Amplitude.
- Action Potential Duration.
- Percentage Polyphasicity

The types of result, once again in the preferred fuzzy format, returned to the blackboard from this simulation may be viewed diagrammatically below, and their specific values may be justified by the following clinical findings.

Figure 2.6.2.1 - Fuzzy output, graphical, for Vlow simulation.



Motor Neurone Disease - On volition, The MUAPs are typical of a neurogenic disorder, they are increased amplitude, long duration and polyphasic, (Swash & Schwarz, 1981).

Limb Girdle Muscular Dystrophy - Concentric Needle EMG reveals typical myopathic, short duration, polyphasic MUAPs of low amplitude, often with a full interference pattern, (Swash & Schwarz, 1981).

Myotonia Congenita - In the dominant form of Thomsens Myotonia Congenita, the EMG Shows Myotonia, but is usually otherwise normal, (Swash & Schwarz, 1981).

As would be expected, for both normal cases, the amplitude, duration and percentage polyphasicity of the observed voluntary activity fall within normal bounds.

Table 2.6.2.1 -Vlow EMG simulation results, numerical.

	Amplitude	CF	Duration	CF	%Poly	CF
1 (MND)	Below	0	Short	0	Normal	0
	Normal	0.3	Normal	0.4	Above	0.2
	above	0.7	Long	0.6	Much Abv	0.8
2 (LGMD)	Below	0.8	Short	0.8	Normal	0
	Normal	0.2	Normal	0.2	Above	0.3
	above	0	Long	0	Much Abv	0.7
3 (MC)	Below	0.6	Short	0.5	Normal	0.3
	Normal	0.4	Normal	0.5	Above	0.7
	above	0	Long	0	Much Abv	0
4 (NORM)	Below	0	Short	0	Normal	0.8
	Normal	0.8	Normal	0.7	Above	0.2
	above	0.2	Long	0.3	Much Abv	0
5 (NORM)	Below	0.4	Short	0.3	Normal	0.9
	Normal	0.6	Normal	0.7	Above	0.1
	above	0	Long	0	Much Abv	0

2.6.3 - Zero force EMG tests.

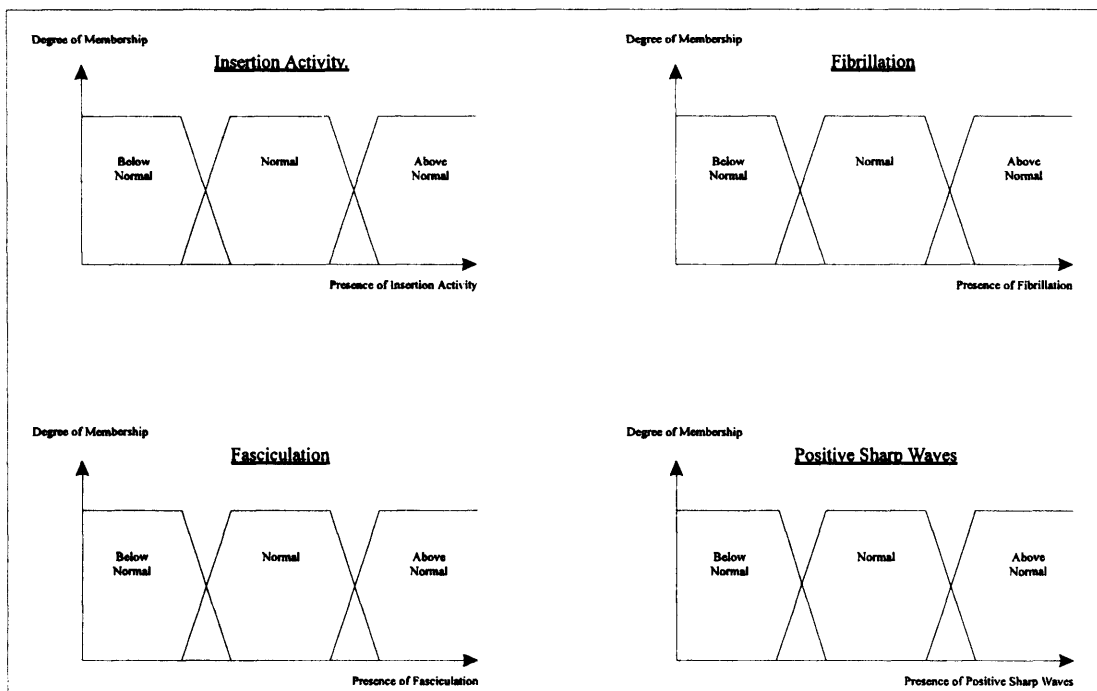
The zero force EMG simulation is concerned with spontaneous activity. That is, electric activity recorded from muscle or nerve at rest, after insertion activity has subsided and when there is no voluntary contraction or external stimulus, also with insertion activity.

The types of activity dealt with in this simulation are:

- Insertion Activity;
 - Fibrillations;
 - Fasciculations;
 - Positive Sharp Waves;
- and may be expanded to accommodate;
- Endplate Activity;
 - Bizarre High Frequency Activity.

The types of result returned from the blackboard from this simulation may be viewed diagrammatically below, and the specific values, displayed in table 2.6.3.1, may be justified by the following clinical findings.

Figure 2.6.3.1 - Fuzzy output, graphical, for zero force EMG simulation.



Motor Neurone Disease - There is increased insertional activity, fibrillation potentials and positive sharp waves are not prominent but are almost invariably found, particularly in atrophic muscles. Fibrillations tend to become more prominent in the later stages of the disease (Goodgold & Eberstein, 1977). Fasciculation potentials are often found, they may be very polyphasic,(Swash & Schwartz, 1981).

Limb Girdle Muscular Dystrophy - Bizarre high frequency potentials may be present, but myotonia is absent and fibrillation potentials are rare, (Swash & Schwartz, 1981).

Myotonia Congenita - In the dominant form of Thomsens myotonia congenita, the EMG shows myotonia but is usually otherwise normal, (Swash & Schwartz, 1981).

The normal cases will exhibit normal amounts of spontaneous activity.

Table 2.6.3.1 - Zero force EMG KS results, numerical.

	Insertion Activity	DM	Fasciculation	DM	Fibrillation	DM	PSW	DM
1 (MND)	Below	0	Below	0	Below	0	Below	0
	Normal	0.4	Normal	0.5	Normal	0.2	Normal	0.6
	Above	0.6	Above	0.5	Above	0.8	Above	0.4
2 (LGMD)	Below	0.1	Absent	0.9	Absent	0.9	Absent	0.9
	Normal	0.9	Present	0.1	Present	0.1	Present	0.1
	Above	0						
3 (MC)	Below	0	Below	0	Below	0	Below	0
	Normal	0.6	Normal	0.7	Normal	0.8	Normal	0.7
	Above	0.4	Above	0.3	Above	0.2	Above	0.3
4 (NORM)	Below	0	Below	0	Below	0	Below	0
	Normal	0.7	Normal	0.8	Normal	0.8	Normal	0.7
	Above	0.3	Above	0.2	Above	0.2	Above	0.3
5 (NORM)	Below	0.1	Below	0	Below	0	Below	0
	Normal	0.9	Normal	0.7	Normal	0.7	Normal	0.6
	Above	0	Above	0.3	Above	0.3	Above	0.4

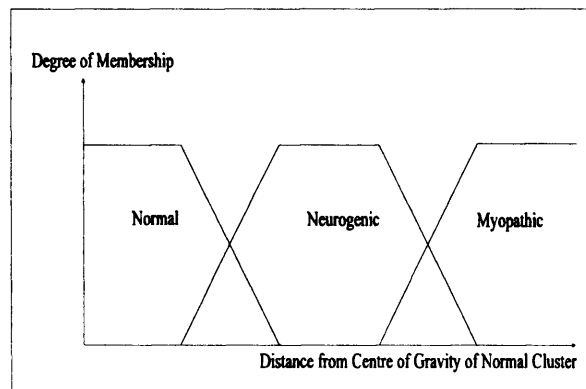
2.7 - High force electrophysiological assessments.

2.7.1 - Single database principal component analysis.

The principal component analysis algorithm (single database) which is at the heart of this procedure is capable of taking a high force EMG and representing it in such a way, that when compared to normal and disordered representations, it is possible to determine which group it belongs to.

The data returned to the blackboard from this simulation is less than that from low force analysis. This test merely distinguishes between the classes normal, myopathic and neurogenic. The result of this process of identification is presented in a fuzzy format shown in figure 2.7.1.1.

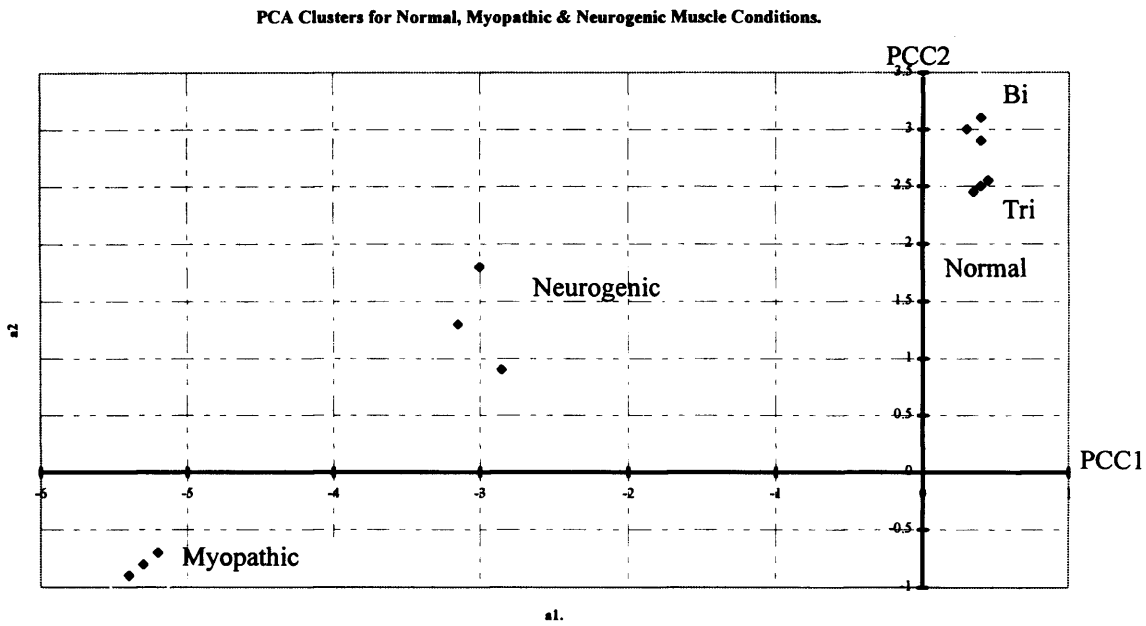
Figure 2.7.1.1 - Fuzzy output, graphical, for Single database PCA simulation.



The membership of each class is calculated using a measure of distance between the representation of the EMG being analysed in 3-D space and the centre of the normal cluster, see figure 2.7.1.2, of principal component coefficients.

Due to the fact that this method is not in common use in the clinical environment, there are no clinical examples of the results of this test when performed on specific disorders. As such, the results for this simulation assume that the routine will correctly classify both the myopathic and neurogenic disorders, whilst the normal and myotonic muscle conditions will be classified as normal. Investigations made by Jones *et al* suggest that this would be the case, (Jones *et al*, 1990)

Figure 2.7.1.2 - Principal Component cluster positions in 2D.



The numerical results returned to the blackboard may be seen in table 2.7.1.1.

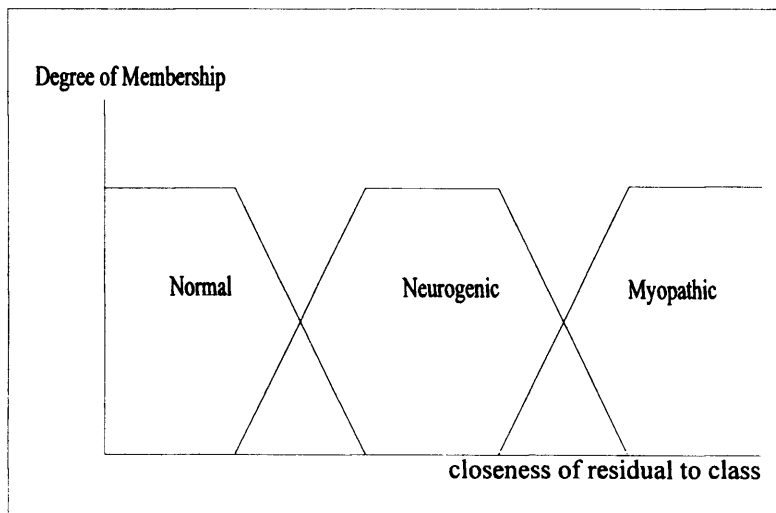
Table 2.7.1.1 - Single database PCA simulation results, numerical.

	Muscle Condition	CF
1 (MND)	Myopathic	0
	Neuropathic	0.6
	Normal	0.4
2 (LGMD)	Myopathic	0.7
	Neuropathic	0.3
	Normal	0
3 (MC)	Myopathic	0
	Neuropathic	0.4
	Normal	0.6
4 (NORM)	Myopathic	0
	Neuropathic	0.7
	Normal	0.3
5 (NORM)	Myopathic	0
	Normal	0.5
	Neuropathic	0.5

2.7.2 - Triple database principal component analysis.

The results of the triple database principal component analysis algorithm simulation are presented below. The method for determining the degrees of membership for each of the fuzzy classes, shown in figure 2.7.2.1, differs from that of the single database method in that it is not necessary to establish the proximity in 3-D space to predetermined disorder clusters. This similarity to a disorder class is determined by isolating the smallest residual and whitest residual spectrum for the principal component spectra calculated using the different disorder databases.

Figure 2.7.2.1 - Fuzzy output, graphical, from triple database PCA simulation.



The results should be very similar to those of the single database method, but as before there are no clinical standard results. The numerical results are shown in table 2.7.2.1, these are returned upon request to the blackboard.

Table 2.7.2.1 - Triple database PCA simulation results, numerical.

	Muscle Condition	CF
1 (MND)	Myopathic	0
	Neuropathic	0.6
	Normal	0.4
2 (LGMD)	Myopathic	0.7
	Neuropathic	0.3
	Normal	0
3 (MC)	Myopathic	0
	Neuropathic	0.4
	Normal	0.6
4 (NORM)	Myopathic	0
	Neuropathic	0.7
	Normal	0.3
5 (NORM)	Myopathic	0
	Normal	0.5
	Neuropathic	0.5

2.7.3 - Turns analysis.

The method of determining class allegiance in this algorithm is by a simple set of rules. For a 5 second signal:

If Count Rate < 3101 per 5s ***Then*** Muscle Condition = Normal

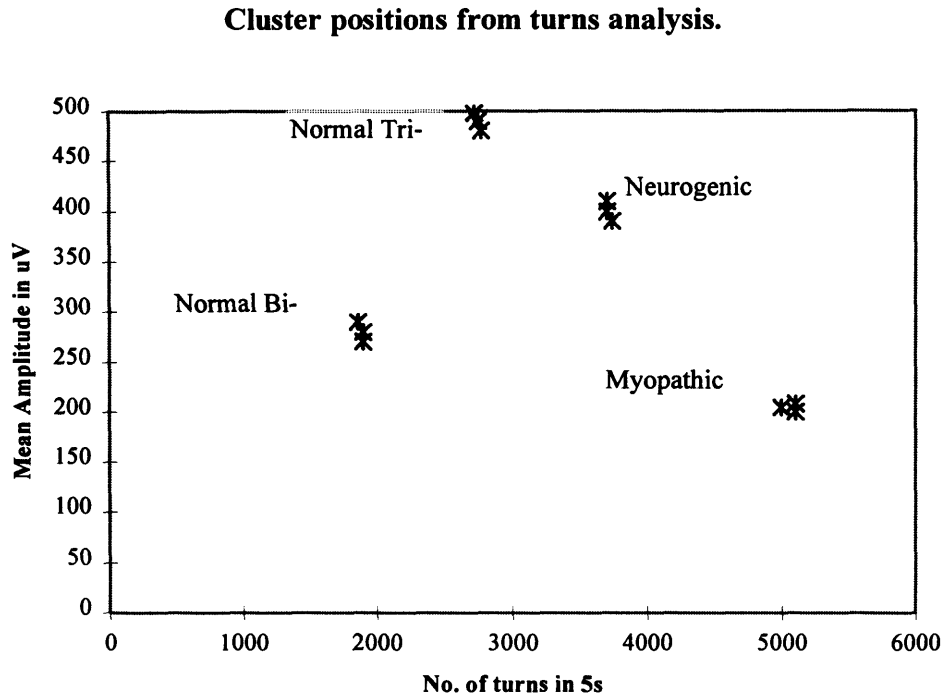
If Count Rate > 3101 per 5s ***and*** mean amplitude < 289mV ***Then*** Muscle Condition = Myopathic

If Count Rate > 3101 per 5s ***and*** mean amplitude > 289mV ***Then*** Muscle Condition = Neurogenic

(Willison, 1964) (Parekh, 1986).

This may be seen in figure 2.7.3.2.

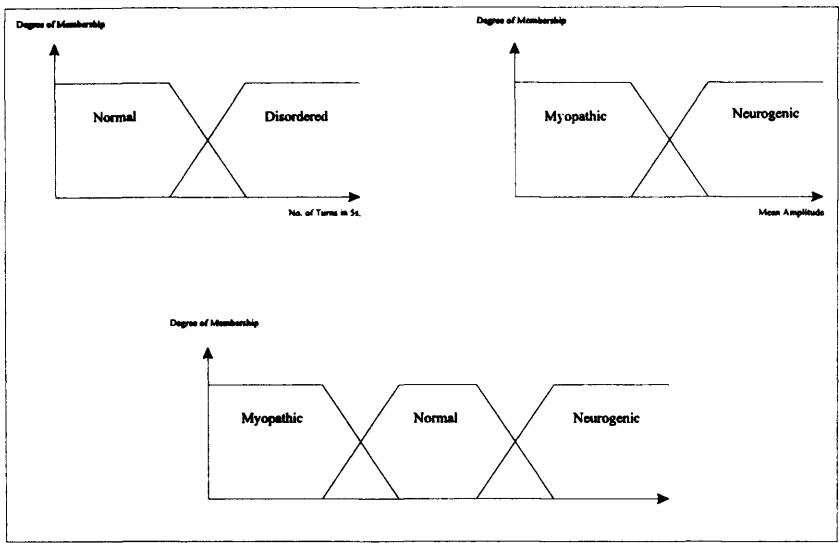
Figure 2.7.3.2 - Disorder class cluster positions



This result is returned to the blackboard system in the form of a fuzzy triplet representing the state of the muscle according to Willison's algorithm. The fuzzy triplet is a standardised combination of two fuzzy pairs. These are representations of the rules presented above, the first pair containing the information on confidence of the signal being analysed falling in the normal class or disordered class, and the second pair containing the confidence information on whether the signal being analysed is myopathic or neurogenic in nature. The three degrees of membership taken from our two fuzzy pairs are forced to yield a sum of 1.0 in order to satisfy the requirements of fuzzy logic. The fuzzy relationship diagrams may be seen below.

Simulation and analysis in electromyography.

Figure 2.7.3.3 - Fuzzy output, graphical, from Turns Analysis simulation.



The third relationship diagram seen in the figure above is a forced combination of the two fuzzy pairs depicted, as such it is not representative of a set of measurements itself, rather it is a combination of the measurements required to form the fuzzy pairs.

The results for this knowledge source assume that the routine will correctly classify both the myopathic and neurogenic disorder, whilst the normal and myotonic conditions are represented as normal. The results are as follows:

Table 2.7.3.2 - Turns analysis simulated results, numerical.

	Muscle Condition	DM
1 (MND)	Normal	0
	Myopathic	0.1
	Neuropathic	0.9
2 (LGMD)	Normal	0
	Myopathic	0.7
	Neuropathic	0.3
3 (MC)	Normal	0.4
	Myopathic	0.4
	Neuropathic	0.2
4 (NORM)	Normal	0.4
	Myopathic	0.3
	Neuropathic	0.3
5 (NORM)	Normal	0.5
	Myopathic	0.2
	Neuropathic	0.3

2.8 - Discussion

The reasons, stated initially, for creating a simulated patient were to enable testing and development of an MDSS and to aid in comparative diagnosis training. The interaction of some or all of the simulations, outlined in the previous pages, with the central blackboard in the MDSS facilitates operation of that system in situations where some or all of the actual knowledge sources are unavailable. This is only for the purpose of development: they would not be utilised in the actual diagnostic procedure.

These simulations may be used to validate the decision making process of the MDSS. They will form a set of test results for certain disorders that are known to be characteristic of that disorder. When the MDSS is used to form a suggested diagnosis upon these test results, its performance may be monitored, and the diagnosis checked against the known diagnosis for the test results being utilised. Thus, the level of performance may be quantified

The two simulations of most interest to the creation of a synthetic patient for comparative diagnosis are the physical test result simulations. These give nerve conduction velocity readings, both motor and sensory, with latencies, for various nerves in the human body, and an indication of the blood creatine phosphokinase level respectively.

At present, these two simulations are able to provide, results representative of the five disorder classes mentioned earlier, with the possibility of extending to include many more. In order to create a realistic simulation of a patient it is necessary to have records of the myoelectric activity associated with the CPK and NCV test results. The inclusion of this data would allow a diagnosis to be made through analysis of all the data available. It is thus necessary to create a realistic simulation of myoelectric activity.

2.9 - Summary.

This chapter introduced the requirement for a simulated patient and discussed the uses to which it would be put. It highlighted the operation and construction of the

components within such a simulated patient. Each individual simulation of a relevant component was detailed, and the content was justified.

The use of the simulations went a long way towards creating a synthetic patient for use in conjunction with the MDSS, enabling rigorous testing of the MDSS, and aiding clinicians in diagnosing both rare and common disorders.

In order to make a more complete simulation of a patient, it is necessary to be able to simulate the electrical activity of the muscle. This, in conjunction with those simulations outlined in this chapter, will go even further towards creating a simulated patient for the purposes outlined.

Chapter 3 - The dynamics of the EMG.

3.1 Introduction

The main thrust of this research is to provide knowledge sources for use in an MDSS applied to neuromuscular disease diagnosis. One important area requiring further development is the difficult issue of characterising the EMG generated during high force contractions. Previous methods, such as principal component analysis and Willison's method, are promising but it seems likely that a more fundamental approach to parametrising the interference EMG may be a more powerful discriminator. Thus may the EMG be characterised by a chaotic model?

This chapter seeks to introduce and explain the existence of chaotic dynamics, especially in biomedical systems. A brief description of Chaos and the observable behaviour both causing and characterising it is given. Section 2.3 introduces and explains in detail some methods of identifying the presence of chaos in experimental and real time series, giving insight as to how results should be interpreted. In the next section, evidence of the occurrence of chaos in biomedical systems is given, and along with details of pitfalls in current techniques for simulating electromyograms, used to form the hypothesis that the dynamics underlying the firing of MUAPs may be chaotic in nature, and as such, that a model based upon chaotic dynamics would be better suited to the purpose of EMG simulation than current techniques. Section 2.5. presents the results of application of the outlined methods of identifying chaos, and discusses their implications.

3.2 What is Chaos?

Chaos may be defined as a deterministic dynamical system in which there is a long term unpredictability arising from sensitive dependence on initial conditions.

Deterministic chaos is a natural occurrence in many non-linear systems, that 'until recent years has been believed to be totally unpredictable', (Kearney & Stark,1992).

Chaotic systems are deterministic, although their output may be random in appearance. They are characterised by a high sensitivity to initial conditions.

Thus, in a chaotic system, any small differences in initial conditions grow exponentially with time, rather than decrease or grow linearly. It is therefore impossible to predict the long term behaviour of such systems, in spite of their being deterministic. However the short term behaviour of the system may be predicted successfully.

Chaotic behaviour is characterised by the divergence of nearby trajectories in state space. As a function of time, the separation between two initially close trajectories increases in an exponential way, at least for periods of short duration. The short duration is a necessary factor because in chaotic systems the trajectories remain within some bounded region by intertwining and wrapping around each other without intersecting and without repeating exactly. This forms a complex strange attractor in phase space, (Hilborn, 1994). The presence of a strange attractor in the phase space of a system is usually a positive sign of chaos, although some non-chaotic strange attractors do exist.

3.3 Methods of Identifying Chaos in a time series.

There are several different ways in which chaos may be identified in a time series. These include qualitative methods such as the construction of phase portraits. There are also quantitative methods such as correlation dimension analysis, and calculation of Lyapunov exponents. These three methods are employed in this investigation, and are described in this section.

3.3.1 Construction of Phase Planes/Portraits.

The phase plane or portrait is a representation of the state of a dynamical system in phase space. The instantaneous system state is represented by a point in this space. As time evolves, the system state changes forming a trajectory in the phase space, the ensemble of these forms the phase portrait (Casaleggio *et al*, 1988)(Babloyantz & Destexhe, 1988). See figure 3.3.1.1.

Phase portraits are constructed from a single measured system variable. A time delay is introduced between the variables used to describe the system in m -dimensional phase space, leading to an m -dimensional vector;

$$X(t) = x(t), x(t + \tau), x(t + 2\tau), \dots, x(t + (m - 1)\tau) \quad (1)$$

The phase space spanned by the new variables, $x(t), \dots, x(t + (m - 1)\tau)$, has topological properties identical to the original phase portrait. (Takens, 1980)(Broomhead & King, 1986a)(Broomhead & King, 1986b).

Two or three dimensional views of the phase portrait may be observed, these offer information about the dynamics of the system from which they are constructed. Stable systems have trajectories that approach a single point in phase space, an attractor, by describing a straight line or spiral. An example of chaotic behaviour, for the EEG, the trajectories are much more complex because they attempt to approach a strange attractor, a sign of chaos. (Babloyantz & Destexhe, 1988)

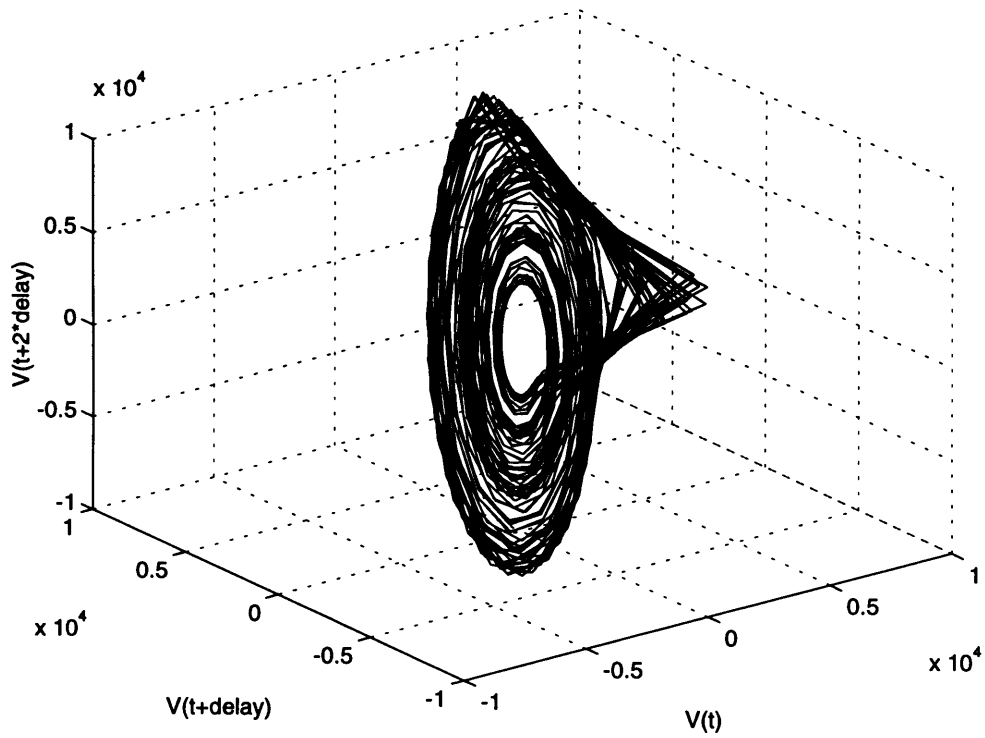
3.3.2 Correlation Dimension Analysis.

This quantitative method is based upon Takens Embedding Theorem, (Takens, 1981), which states that for all typical time series obtained from a finite degree of freedom dynamical system, there is some integer m and a function G such that:

$$x_{n+1} = G(x_n, x_{n-1}, \dots, x_{n-m+1}) \quad (2)$$

where m is the embedding dimension, and $m \leq 2d + 1$, where d is the number of degrees of freedom of the underlying dynamical system.

Figure 3.3.1.1 - A phase portrait constructed from the Rossler time series, a known Chaotic time series.



The method of identification of chaos employed here requires the calculation of the Correlation dimension for increasing values of m (Kearney & Stark, 1992). The correlation dimension seeks to measure the dimension of a finite data set extracted from a time series, in m -dimensional space, on which the points of the embedded data set lie. It is therefore a measure of the number of variables that are necessary to describe that data set.

Application of this theorem requires the creation, of a vector series $\{v_n\}$, from the scalar series $\{x_n\}$, where:

$$v_n = (x_n, x_{n-1}, \dots, x_{n-m+1}) \quad (3)$$

An advantage of this process is that the co-ordinate independent properties of $\{v_n\}$, such as the Lyapunov exponent (λ , Lambda) which is a dynamical measure of the sensitive dependence on initial conditions and correlation dimension (Dc), are the same as those of the system which created the original $\{x_n\}$.

It is possible for both λ and Dc to be calculated from $\{v_n\}$. Dc is a measure of the number of variables that are necessary to describe a set, and is determined using a finite data set, $\{v_1, v_2, \dots, v_N\}$. N samples are used, and the Euclidean distance ($r_{ij} = |v_i - v_j|$) is found between the N^2 possible pairs (v_i, v_j) of these points.

The calculation of Dc may be performed using the original series $\{x_n\}$ rather than $\{v_n\}$, removing the need for manual embedding, as follows:

Firstly the Euclidean Distance, r_{ij} is calculated:

$$r_{ij} = \left[\sum_{k=0}^{m-1} (x_{i-k} - x_{j-k})^2 \right]^{1/2} \quad (4)$$

Now for a given separation E , let $N(E)$ be the number of pairs such that $r_{ij} \leq E$. $C(E)$ is the proportion of pairs that are within a distance E of each other, and is found as follows:

$$C(E) = \frac{N(E) - N}{N^2 - N} \quad (5)$$

The correlation dimension itself, may now be defined as:

$$Dc = \lim_{E \rightarrow 0} \left\{ \frac{\log C(E)}{\log E} \right\} \quad (6)$$

that is, the gradient of the plot of $\log C(E)$ against $\log E$ as E , the separation of pairs of points, approaches zero.

As the correct embedding dimension for a system is unknown and may not be calculated, a trial and error procedure must be followed to determine whether or not the system under scrutiny is chaotic. The Correlation dimension must be calculated for increasing values of m , and the way in which the correlation dimension behaves determines the nature of the system.

The behaviour of the correlation dimension is controlled by the values contained in the finite data set. For example:

- When all the samples in the data set are constant, the correlation dimension will equal 0.
- If the samples in the data set lie upon a curve, the correlation dimension will equal 1.
- If the samples in the data set fill a plane, the correlation dimension will equal 2.
- If the samples in the data set completely fill the m -dimensional space in which they lie, the correlation dimension will equal the embedding dimension (m).

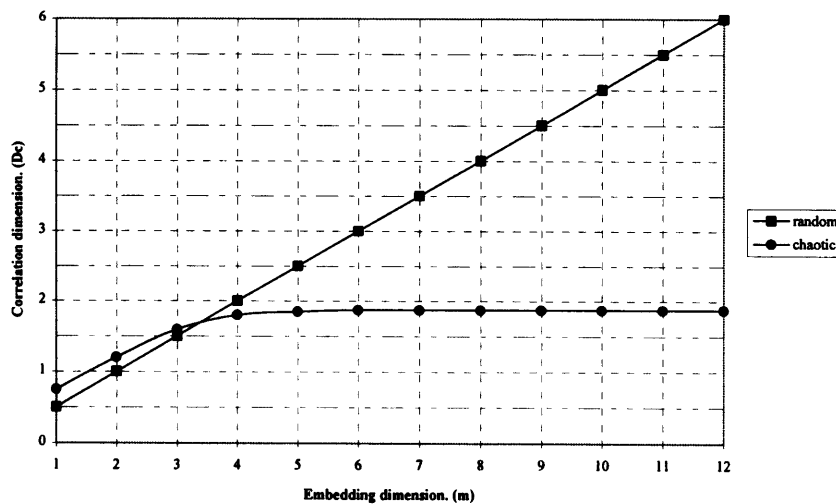
The way in which the correlation dimension behaves, as the embedding dimension increases, determines the nature of the system. If $Dc=0$ we have a regular periodic time series; if Dc continues to increase with m , then the series was generated by a truly random process, i.e. for white noise $Dc=\infty$; if however, the correlation dimension should stabilise at a non-integer value, then the system is said to contain a 'strange attractor'. This is usually a sign of chaos, although strange non-chaotic systems do occur.

Figure 3.3.2.1 shows the expected behaviour of the correlation dimension of a random and a chaotic time series, with increasing embedding dimension.

The behaviour of the correlation dimension of a chaotic system is demonstrated by the Henon map, a two dimensional chaotic system, whose correlation dimension varies with m as follows: $Dc(1) \cong 1$, $Dc(2) \cong 1.21$, $Dc(3) \cong Dc(4) \cong Dc(5) \cong 1.21$, [5].

There are certain factors effecting the computational accuracy of correlation dimension analysis, of which the two most pertinent are described. If insufficient data points are used in the analysis, a hard limit is set on the upper value of the correlation dimension, thus causing possible prevention of a true result being reached, should the actual value of correlation dimension exceed the enforced upper limit. A second effect of too few points is that, at higher levels of embedding the density of points in phase space is too low to yield useful information. The points appear to spread out in phase space giving the appearance that they herald from a system dominated by random dynamics, and no correlation dimension will be settled upon.

Figure 3.3.2.1 - The Ideal Behaviour of the correlation dimension for chaotic and random time series.



Noise in the signal being analysed may effect accurate calculation of the correlation dimension. Whilst the average magnitude of the noise in the signal is greater than the separation of point pairs generated from the signal the noise will dominate the structure of the attractor and as such, the correlation dimension. (Hilborn, 1994).

These two factors have opposite effects. Whilst the limited number of data points used in the analysis will tend to reduce the calculated value of correlation dimension, at least at lower levels of embedding, the presence of noise will increase it if the above condition is true. It is possible that fortuitous cancelling may occur between the two, producing an artificial region for calculation of the correlation dimension.

3.3.3 Calculation of Lyapunov exponents.

The second quantitative method addressed here is accepted to be a more conclusive test for the presence of chaos within a system, and involves the calculation of Lyapunov exponents.

The spectrum of Lyapunov exponents has proven to be the most useful dynamical diagnostic tool for chaotic systems. (Wolf *et al*, 1985). Lyapunov exponents are a measure of the average exponential rates of either divergence or convergence of nearby trajectories in phase space. There are as many Lyapunov exponents as there are dimensions in the state space, however the largest or dominant Lyapunov exponent is considered to be of most interest.

Since nearby orbits in the system correspond to nearly identical states, exponential orbital divergence means that systems whose initial differences were irresolvable, will soon behave quite differently. (Wolf *et al*, 1985). The dominant Lyapunov exponent is then, the time averaged logarithmic growth rate of the difference between two orbits.

Negative Lyapunov exponents are indicative of converging trajectories, positive exponents are indicative of diverging trajectories whilst zero exponents indicate the temporary stable nature of a system. It is the presence of at least one positive Lyapunov exponent that indicates chaotic behaviour in a system. A positive exponent indicates that

motion within the attractor is locally unstable and exhibits sensitive dependence to initial conditions. (Broomhead & King, 1986a.) (Broomhead & King, 1986b.)

The magnitudes of Lyapunov exponents determine the length of time for which a chaotic system may be effectively predicted. (Wolf *et al*, 1985) The exponents measure the rate at which system processes create or destroy information about that system, and are expressed as bits/sec. Hence, if a system has a positive exponent of 3 bits/sec and the recorded system variable is digitised to 16 bits precision, the predicted instantaneous values of the system will cease to be reliable after $16/3 = 5.33$ seconds. Predicted values would still be available but would be useless because all information about the system will have been lost.

The Lyapunov exponents may be defined as follows; (Grassberger *et al*, 1992) Grassberger *et al* said let B_ε be an ε -ball around the vector \vec{x} . If ε is infinitesimal, then this ball will be transformed after a time t into an ellipsoid with semi-axes ε_i . They assumed that these were ordered by magnitude, i.e. $\varepsilon_1 \geq \varepsilon_2 \geq \dots$. Thus λ_i is given by:

$$\lambda_i = \lim_{t \rightarrow \infty} \left\{ \frac{1}{t} \log \varepsilon_i \right\} \quad (7)$$

In other words, the λ_i 's measure the geometric growth of vectors in tangent space. This method requires use of the tangent map which governs divergence of nearby trajectories in phase space.

An alternative way of defining the Lyapunov exponent is presented by Hilborn. If two nearby trajectories on a chaotic attractor initially with separation d_0 at time $t = 0$ diverge so that their separation becomes $d(t)$ at time t ,

$$d(t) = d_0 e^{\lambda t} \quad (8)$$

then λ is the Lyapunov exponent for the trajectories.

The method used here, for preliminary experimentation, does not use tangent maps explicitly, although their explicit use in exponent estimation has been shown to make the procedure more systematic. (Eckman *et al*, 1986)(Sano & Sawada, 1985). Any more involved investigations should compare the results of different estimation algorithms.

The method of phase space reconstruction based upon the embedding theorem described in section 2.3.2 provides a reconstructed attractor with the identical co-ordinate independent properties, such as Lyapunov exponent, as the system that created the original time series.

The employed approach to estimating Lyapunov exponents from experimental data requires the long term evolution of a single pair of nearby orbits to be monitored. This technique is useful when the starting point is a time series rather than describing equations. Two data points may be considered to define the early state of the 1st principal axis of the n-ellipsoid as long as their separation is small (Wolf *et al*, 1985).

When the evolved separation of the two points becomes too large, the non-fiducial data point is replaced with a point more closely representing the fiducial data point, also in the same direction as the original vector. One limitation of using a finite data set for calculation of dominant Lyapunov exponent is that the point inserted by replacement will be an approximation to the fiducial point because not enough data will be present to ensure the exact point, this would require infinite data.

Each replacement is evolved until another becomes necessary, or until the entire data set has been traversed, when an estimate of λ will be made.

The use of finite data prevents probing of the desired infinitesimal length scales of the attractor, Noise is also capable of this, although the method employed estimates the dominant exponent in signals containing a degree of noise. (Wolf *et al*, 1985)(Wolf & Bessior, 1991).

3.4 Is the clinical Electromyogram Chaotic?

3.4.1 Chaos in Biomedical Systems.

Evidence of chaotic behaviour has been found in biological signals, such as the Electrocardiogram (ECG). The ECG exhibits quasi-periodic behaviour, but with many irregularities in the record. Babloyantz & Destexhe found that the correlation dimension of recorded ECGs settled at values ranging from 3.6 ± 0.1 to 5.2 ± 0.1 (Babloyantz & Destexhe, 1988). These values suggested that the normal cardiac oscillations follow deterministic dynamics of a chaotic nature, characterised by an unusually high dimension. Babloyantz & Destexhe also suggested that any mathematical model for the description of cardiac activity must contain at least five dimensions, to encompass the majority of the dimension range, and must show deterministic chaos in its output. These results were supported by Bortolan & Casallegio, who found that at rest, normal ECG had a correlation dimension value usually below 3, whilst for arrhythmic patients, the values were as large as 4.5. (Bortolan & Casallegio, 1995). For the cardiac attractor, the largest Lyapunov exponent was found to be $\lambda = 0.38 \pm 0.08$ (Babloyantz & Destexhe, 1988). This is a clear positive exponent and implies that the ECG exhibits chaotic dynamics.

Similar results have been obtained for the Electroencephalogram (EEG), where although the EEG dimensionality varies according to the cognitive state, and also with some pathological brain conditions such as epileptic seizures (Rapp *et al*, 1989). Researchers have found that the EEGs correlation dimension falls within the range 3 to 8 (Principe & Reid, 1990).

It has been reported (Ogo & Nakagawa, 1995), that the maximum Lyapunov index is positive for most of the EEG frequency components, for almost all subjects in the study. In other words, it is estimated that the EEG is composed of a large number of frequency components with chaotic properties.

All of this is evidence that Chaos exists within the human body, and allows that it may be present, though undiscovered, in other biomedical systems such as the electromyogram.

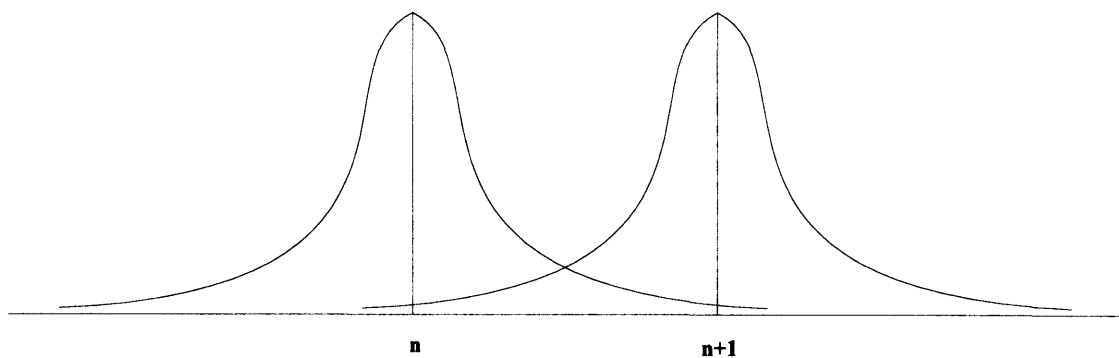
3.4.2 EMG Simulation.

The model upon which EMG simulation is currently based consists of banks of filters whose impulse responses are equivalent to individual MUAP templates, and trains of pulses determining the firing of each motor unit, thus determining the inter pulse interval (IPI) between each MUAP. The Model is derived conceptually from that presented by Parker & Scott, (Parker & Scott, 1973) and others.

The model employs a Gaussian renewal process to determine the occurrence of the next firing. This method has been found to be the most suitable to date, (Jones & Lago, 1977) (Jones et al, 1987).

Despite the success of the Gaussian distribution in modelling some key features of the EMG, it is deficient in determining the occurrence of each successive MU firing. The Gaussian distribution falls short of ideal because beyond a few standard deviations of the distribution, the probability of a firing occurring, although small, is not zero.

Figure 3.4.2.2 - The problem with Gaussian distributed Inter Pulse Intervals.



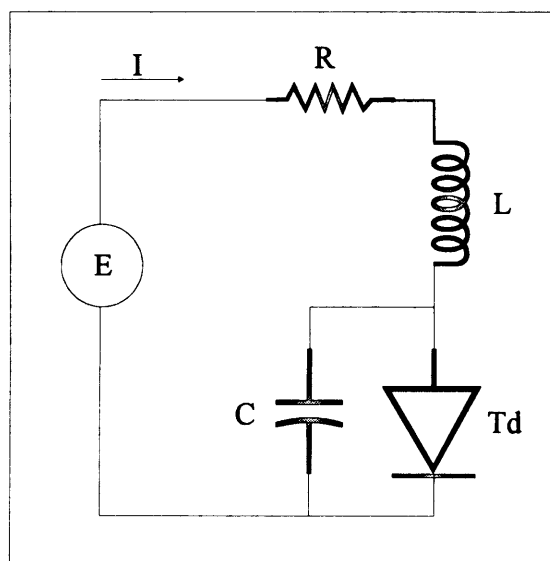
This cannot be ignored because a model of motor unit firing based upon the Gaussian distribution could fire pulse $n+1$, see figure 3.4.2.2, at the same time as, or before pulse n , the previous pulse in the series of pulses making up the firing times of a MUAPT. It is thus necessary to search for new methods of modelling the firing of MUs within human muscle, which will predict firing time accurately and without ambiguity.

3.4.3 Models of the membrane.

The Hodgkin-Huxley membrane model is the analog circuit studied most in neurophysiology. Simplifications such as that by Fitzhugh & Nagumo, and others such as the Bonhoeffer-Van der Pol model show that there are non-linear and positive and negative feedback processes in operation during neural discharge. These processes are prerequisite for the occurrence of chaos, thus further grounds for hypothesising that chaos is present in the neurophysiological system are evident.

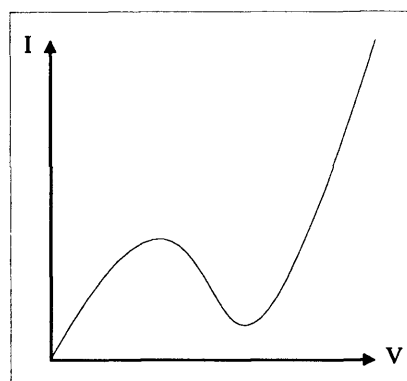
Non-linearity may be observed in the current voltage characteristics of the tunnel diode, an element of the Fitzhugh-Nagumo simplification of the Hodgkin-Huxley membrane model. see figure 3.4.3.1.

Figure 3.4.3.1 - The Fitzhugh-Nagumo Analogue Circuit.



The current-voltage (I-V) characteristics of the Tunnel diode (Td) may be observed in figure 3.4.3.2. They are clearly non-linear.

Figure 3.4.3.2 - I-V characteristics of the Tunnel diode.



3.4.4 A Chaotic EMG Simulator?

It may be stated that the EMG is neither wholly stochastic nor deterministic. It is a highly structured signal, made up from a collection of signals that have elements of variation within them, and the contributions of other spontaneous factors. The fact that there are elements of variation within the signal, and that the firing of MUs appears to be difficult to predict, supports the suggestion that the EMG, at medium to high levels of force, may be better described by a chaotic model than by a model based on a random procedure such as Gaussian Renewal.

Other factors supporting this are the problems inherent in the use of Gaussian renewal, the most suited statistical distribution, to determine the next firing of a MU, the presence of non-linear and positive and negative feedback processes in neural discharge, and the presence of chaotic dynamics in other biomedical systems, namely the heart and the brain, inferring that chaos is present in the human body, so it may be present in the muscle system.

A further reason for attempting to establish whether the EMG is chaotic or not is the use of the analysis as a discriminator. If a chaotic model for the EMG is established as being appropriate, it is possible that the number of parameters describing certain muscle states or conditions, determined by the chaotic analysis, could be used to discriminate between those muscle conditions. This could form the basis of a discriminatory knowledge source for the MDSS.

3.5 Attempted identification of Chaos in the EMG.

The three methods of identifying chaos, previously outlined in this chapter are employed to determine whether the dynamics of MUAP firing exhibit any signs of chaotic behaviour. Authentic EMG signals, recorded using the TEAC R81 analogue recorder and digitised using an AT&T DSP32C 16Bit DSP board are analysed. The data was sampled at a rate of 8kHz.

3.5.1 EMG Phase Portraits.

Phase portraits were constructed for EMG signals recorded from muscles considered to be in a normal condition, and for signals recorded from muscles in various states of disorder. Different delays (τ) were employed, using signals of approximately 40000 samples. Figure 3.5.1.1. displays this.

The phase portraits observed appear to consist of trajectories that loop as time passes and the state of the system driving MUAP firing changes. It is clear that the behaviour of the EMG is not periodic, periodicity being represented by a single closed curve. However the phase portraits of the EMG in no way infer that the underlying dynamics are Chaotic. It is, in fact, not possible to extract any useful information from these plots.

3.5.2 The Behaviour of Dc.

Real signals of approximately 9000 samples, recorded from both normal and disordered muscle groups, were analysed using this technique.

The correlation dimension was calculated for successive levels of embedding, 1 through 10, in order that the behaviour of Dc may be observed over the length of the progression.

The gradient of the $\log C(E)/\log E$ plot is the correlation dimension, and this is calculated by the program "CORDIM" using regression analysis, with a 65% confidence level in the gradient of each regression line. This gives an indication of how accurate the estimate of the correlation dimension is. See figure 3.5.2.1. This figure depicts seemingly random behaviour of a normal EMG signal and the levels of confidence given to correlation dimension estimate at each level of embedding.

Figure 3.5.2.1 - Correlation dimension progression for a normal signal (male subject) exhibiting 65% Error boundaries.

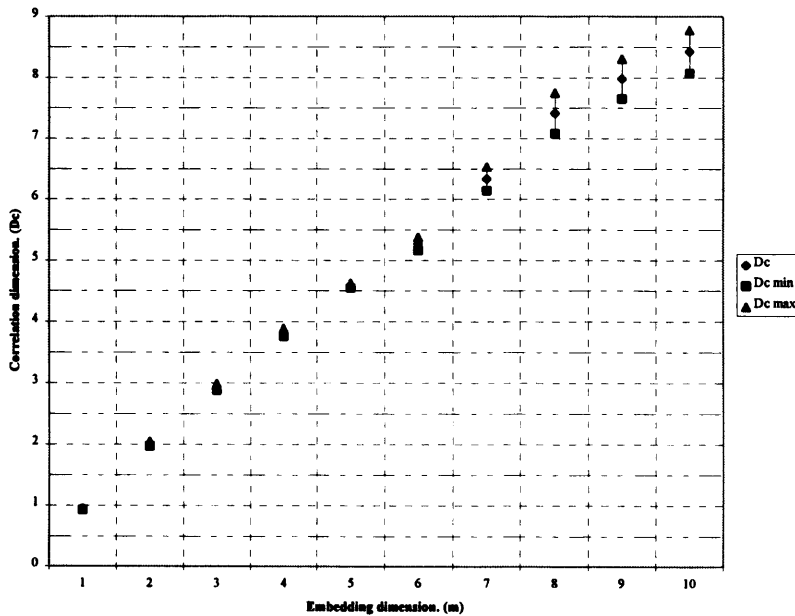
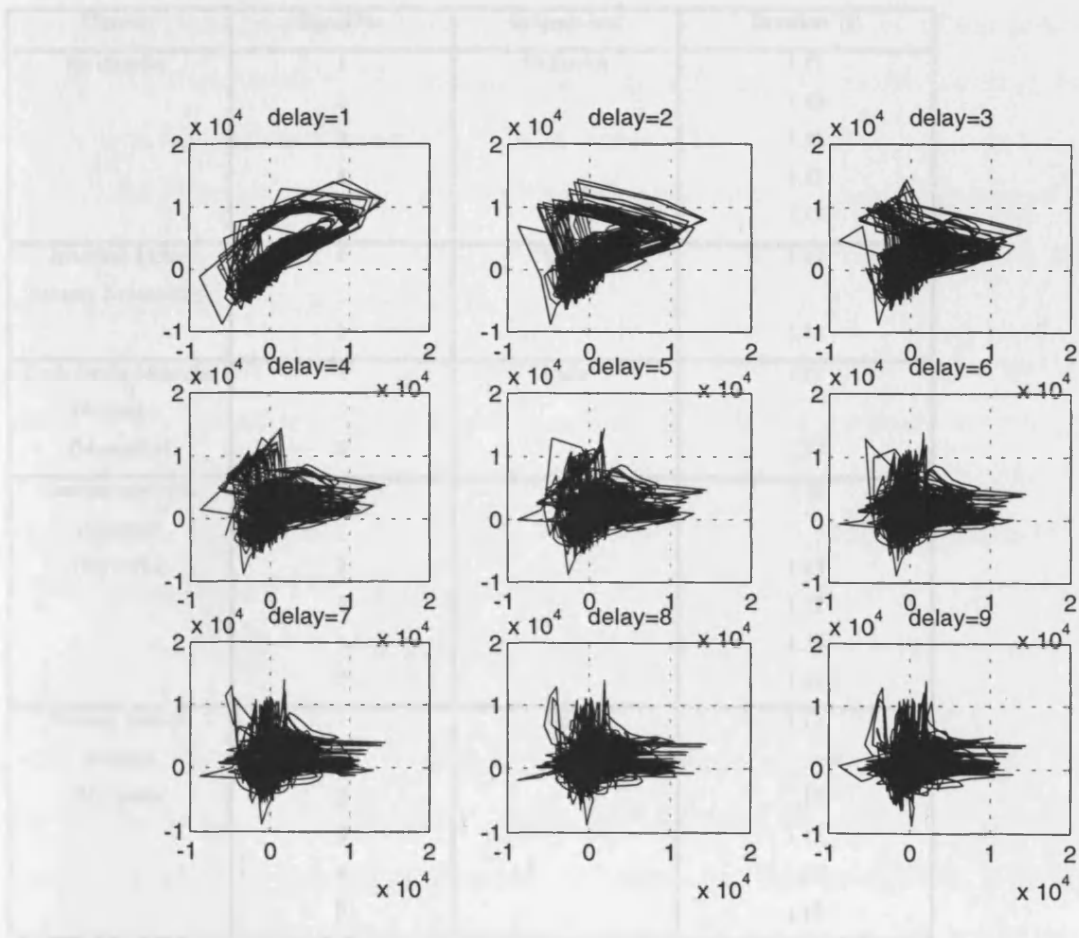


Figure 3.5.1.1 - Phase portraits of a normal EMG signal, for delay (τ)=1 to 9.

Table 3.5.1.1 - The signals upon which characteristic dimension analysis was performed. (Sampling frequency = 1000 Hz)



The progression of the trajectories with increasing embedding dimension is shown in Figure 3.5.1.2. It is clear that the trajectories become more complex and dense as the embedding dimension increases, which is consistent with the results of the phase portraits shown in Figure 3.5.1.1.

Correlation dimension progressions were constructed for sets of signals exhibiting certain disorders, see table 3.5.2.1, and their behaviour was observed. See figures 3.5.2.2 to 3.5.2.6.

Table 3.5.2.1 - The signals upon which correlation dimension analysis was performed, (Sampling Frequency = 8000Hz)

Disorder	Signal No.	Subjects sex.	Duration. (s)
No disorder.	1	Unknown	1.12
	2		1.12
	3		1.12
	4		1.12
	5		1.12
Inherited Motor Sensory Neuropathy.	1	Male	1.12
	2		1.12
Limb Girdle Muscular Dystrophy. (Myopathy)	1	Male	1.12
	2		1.12
Dermatomyocytis (Chronic). (Myocytis)	1	Male	1.12
	2		1.12
	3		1.12
	4		1.12
	5		1.12
Primary Muscle Atrophy. (Myopathy)	1	Male	1.12
	2		1.12
	3		1.12
	4		1.12
	5		1.12

The progression of the correlation dimension with increasing embedding dimension, for EMGs with no disorder, as seen in figure 3.5.2.2, indicates, in agreement to a certain extent with the results displayed by the construction of phase portraits that the hypothesis of chaotic dynamics determining MUAP firing is not a valid one.

It may be seen that the correlation dimension values, for all five signals in this class, continue to rise in an almost linear fashion. This does not match the standard behaviour for the correlation dimension of a chaotic system which will taper off and settle around some non-integer value. The non-integer value where the correlation dimension settles is an indication of chaos in this analysis, and the next integer above the correlation dimension is the minimum number of variables required to describe the system. If the value settled at was an integer, the system would not be chaotic. The non integer correlation dimension on its own, is not however, conclusive proof of the presence of chaos in a time system. To obtain a definite affirmative, further testing, such as calculation of Lyapunov exponents, must be carried out.

The behaviour of Dc seen in figure 3.5.2.2, does not give any indication of chaotic behaviour. The continuous increase in numerical value is more consistent with that of a system governed by random dynamics than by chaotic dynamics.

The progressions shown in figure 3.5.2.3, for signals recorded from a muscle with an inherited motor sensory neuropathy, although limited in number by the lack of available data, also have a prevailing tendency to increase almost linearly. This furthers the argument that the underlying dynamics of the human muscular system, unlike those of the human heart (ECG), or the human brain (EEG), are not driven by a chaotic process.

Figure 3.5.2.4 introduces some results which provide evidence against this argument. The two progressions, in this case, for a muscle undergoing a severe form of myopathy, display a correlation dimension which appears to settle at values of 5.7 ± 0.3 in the case of signal one, and at 3.02 ± 0.1 in the case of signal two. However, the number of data points used for correlation dimension calculation, in this case ~ 9000 , is insufficient for accurate calculation at high levels of embedding. The number of data points necessary for accurate calculation of the correlation dimension is in the range 5^n to 10^n , where n is the embedding dimension. The number of points used here allows confidence in levels of embedding up to between 3 and 5. Thus, not much confidence can be placed in these apparent non-integer correlation dimensions, because they do not settle until the seventh or eighth level of embedding. It is also possible that this indication of chaotic behaviour

is totally case specific. It does not, in itself, negate the general thesis that chaos theory will not provide an appropriate method for modelling the clinical electromyogram.

Figure 3.5.2.5 shows a set of progressions that add weight to our argument. The correlation dimension, once again increases with embedding dimension in a manner more indicative of random than chaotic dynamics.

Figure 3.5.2.6 shows results that are similar to those of figure 3.5.2.4, the main difference being that the correlation dimension does not actually settle, but continues to increase at a much decreased rate after the sixth level of embedding. This could however be attributed to a hard upper limit being set upon the magnitude of the correlation dimension by a limited number of input data points. Again great confidence cannot be placed in these results, because the correlation dimension does not actually settle at a non-integer value within the 10 levels of embedding used, although it remains within the range 5.5 to 7.5.

Figure 3.5.2.2 - Summary of the correlation dimension progressions with increasing embedding dimension, for signals recorded from a muscle with no disorder.

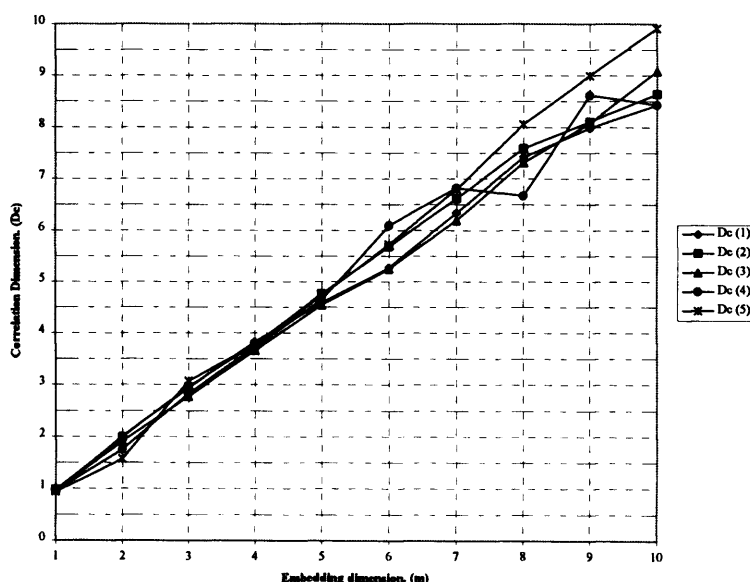


Figure 3.5.2.3 - Summary of the correlation dimension progressions with increasing embedding dimension, for signals recorded from a muscle with inherited sensory motor neuropathy.

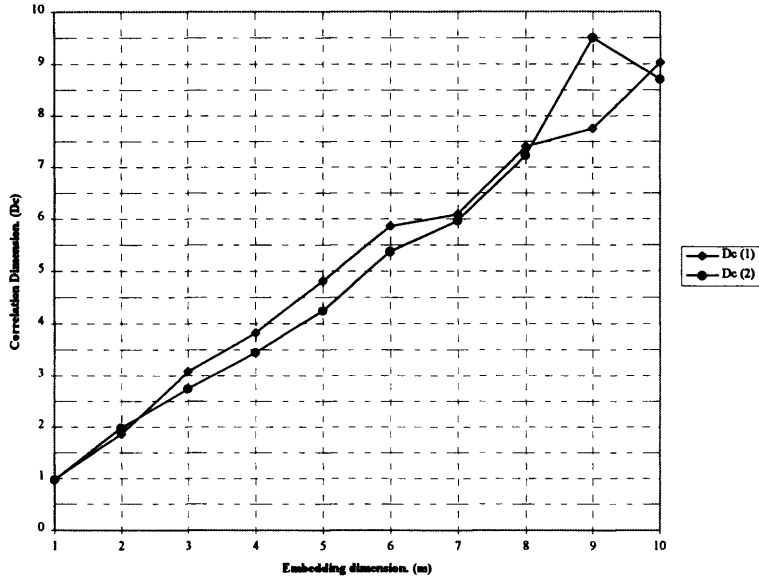


Figure 3.5.2.4 - Summary of the correlation dimension progressions with increasing embedding dimension, for signals recorded from a muscle with limb girdle muscular dystrophy.

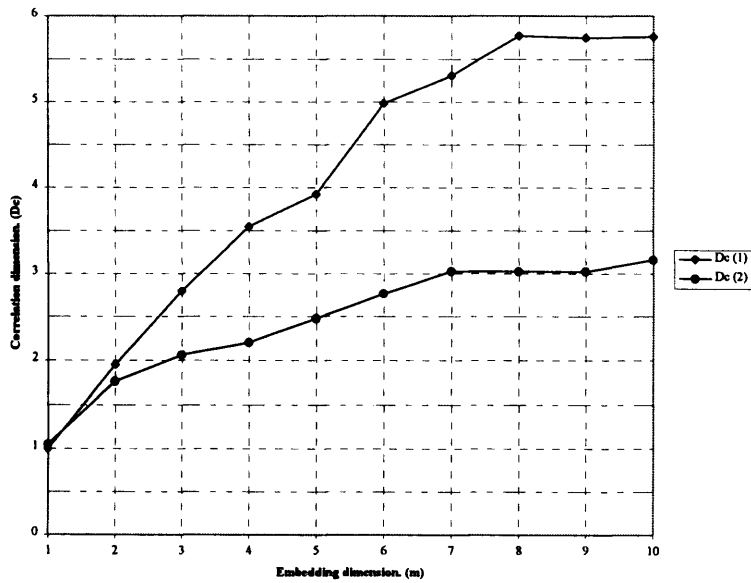


Figure 3.5.2.5 - Summary of the correlation dimension progressions with increasing embedding dimension, for signals recorded from a muscle with chronic dermatomyocytis.

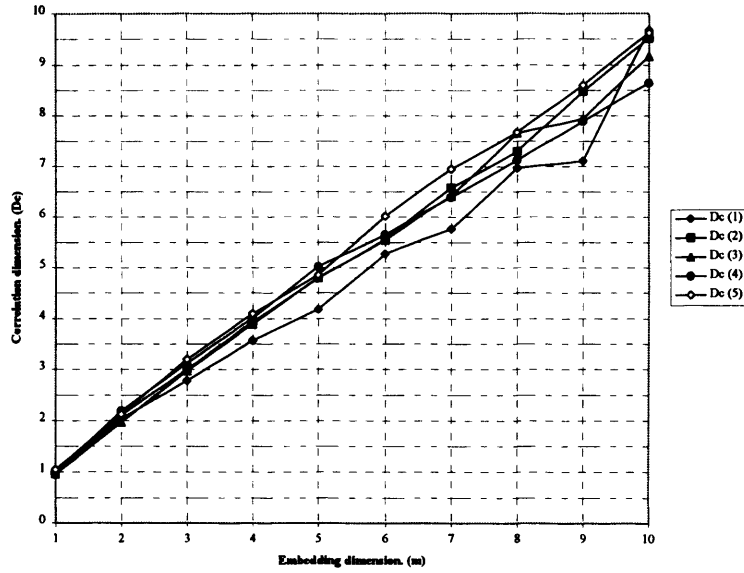
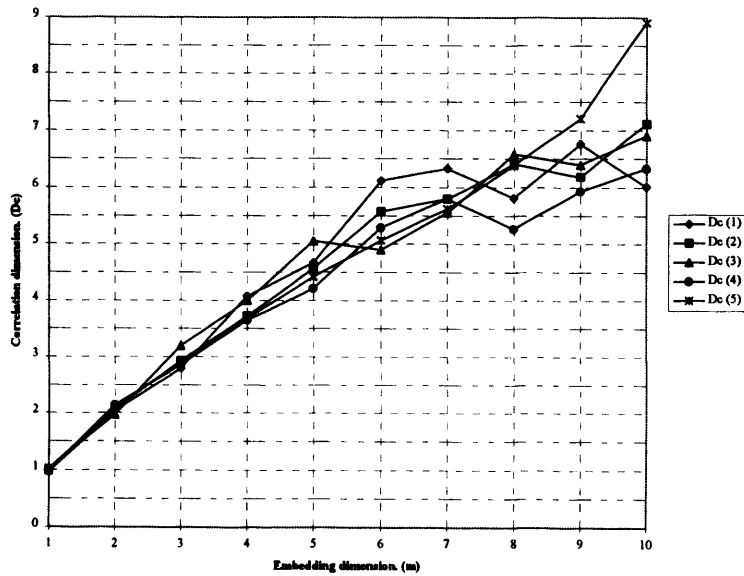


Figure 3.5.2.6- Summary of the correlation dimension progressions with increasing embedding dimension, for signals recorded from a muscle with primary muscle atrophy.



3.5.3 Lyapunov exponents of the EMG.

Lyapunov exponents were estimated using the method previously described. The data upon which the analysis was performed, was the same data used for correlation dimension analysis, the sole difference being that the number of points used was raised from approximately 9000 to 32000.

In order to verify the stability of the resulting estimated dominant Lyapunov exponent it is necessary to repeat the calculation for varied embedding dimensions and evolution times etc.

The estimated values calculated for differing EMG signals varied in magnitude, but the amplitude was of the order of approximately 200 to 350 bits/second. This order of magnitude was estimated for varied inputs to the estimation algorithm.

An exponent falling within this range would lead one to believe that the data of interest was being drowned out by noise. There are two reasons for this not being so.

The analysis algorithm has been tested on data known to be chaotic in nature and in these instances has yielded the expected results. The algorithm is known to deal with some noise and the data being analysed has a very low noise content.

The second reason for believing that the unusually high exponent is not indicative of noise is more involved. A comparison between the yielded dominant exponents from real EMG signals and from synthetic signals comprising MUAP templates firing randomly was made. The results for both types of signal were similar in that they exhibited exponents with amplitudes in the same order of magnitude, but more importantly numerically close to one another.

The dominant Lyapunov exponent estimated for a truly random time series whose dynamics were based upon the normal distribution, was an order of magnitude larger than those calculated for both the real EMG and synthetic signals.

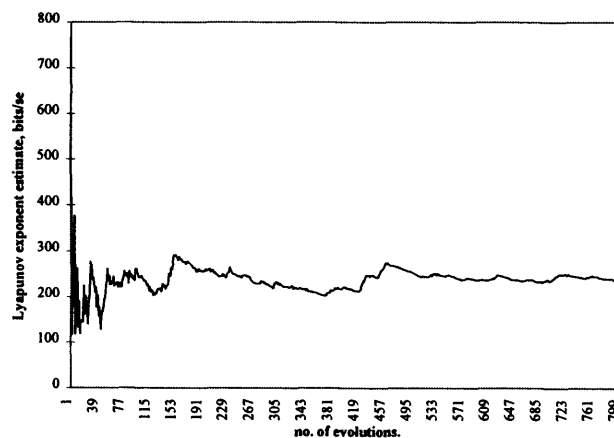
The exponent then, leads us to believe that the dynamics displayed by our real signals are random. This is because the dominant exponent is large, suggesting noiselike random behaviour, but is not as large as that for a true random signal, also because the

exponent is comparable with that of signals that do not contain a large proportion of noise, and whose dynamics are known.

These results, and their meaning, are in accordance with the information gained from correlation dimension analysis of real EMG signals. Thus within the scope of this investigation it is reasonable to believe that the dynamics behind the clinical electromyogram may be better described by a random procedure than a chaotic one.

An example of the progression of dominant exponent estimation may be seen in figure 3.5.3.1.

figure 3.5.3.1 - Dominant Lyapunov exponent estimation for a normal signal.



In general, a chaotic model for the firing of MUAPs within the EMG would seem inappropriate. A better suited model for simulation of the EMG remains banks of filters whose impulse responses are representative of various Action Potential templates, triggered by trains of pulses, whose firing is determined by statistical methods i.e. Gaussian renewal, summed to provide a synthetic EMG.

3.6 Summary.

There is a requirement to parametrise the interference EMG and to see if these parameters are disease sensitive. A novel way of attempting this was investigated here, the use of a chaotic model.

In this chapter, chaotic deterministic dynamics and some of their characteristics have been introduced along with various techniques, both qualitative and quantitative, for identifying the possible presence and the actual presence of chaotic dynamics in a time series.

It has been suggested that the driving dynamics for motor unit firing in the clinical electromyogram, at medium to high levels of force, may be chaotic. Investigations to establish the truth of this have been carried out and the results presented and interpreted.

Finally, it is concluded that the hypothesis of a chaotic model for EMG simulation must be put to one side in favour of a statistical model. It may not be wholly discarded however, due to the difficulty of extracting final proof of non-chaotic behaviour from the EMG.

Chapter 4 - The EMG simulation knowledge source.

4.1 Introduction

The importance of spontaneous muscular activity to neuromuscular diagnosis is discussed, with reference to disorders of the muscle and nerve. The conclusions drawn from this discussion are then used to confirm the necessity of including spontaneous activity in myoelectric activity simulation routines if they are to produce realistic results.

Methods for simulating spontaneous activity as a part of an overall myoelectric activity simulation routine are outlined and discussed.

Different techniques used for the simulation of the electromyogram are considered along with the results of the previous chapter. The most appropriate methods for modelling the EMG are selected.

A simulation routine based upon these methods is described. The routine is capable of producing synthetic signals representative of both voluntary and spontaneous activity. The voluntary activity may comprise amplitude and duration variation. The simulator also contains a noise generator.

4.2 The importance of spontaneous activity.

Spontaneous activity is the electrical activity recorded from muscle or nerve at rest after insertion activity has subsided and where there is no voluntary contraction or external stimulus, (DeLisa et al, 1994).

There are various types of spontaneous activity, which have been described in chapter 1. Insertion activity may be viewed as an involuntary activity, this is comparable with spontaneous activity, the difference being that it is the result of an applied stimulus i.e. insertion or movement of the recording electrode with relation to the muscle fibres.

It is helpful to consider one or two disorders of the muscle or nerve in order to demonstrate the importance of the presence and degree of severity of spontaneous activity in forming a useful and accurate diagnosis.

A presenting feature of Motor Neurone disease is Fasciculation. These potentials are usually repeated at a rate of approximately one every three or four seconds, (Trojaborg & Buchthal, 1965). Fasciculations are most commonly observed in the arms but any muscle may be affected: it is particularly important to examine the tongue carefully since fasciculations are easily detected in this muscle, (Swash & Schwarz, 1981)

In electrophysiological assessment of this disorder, the insertional activity is increased. Fibrillation potentials and positive sharp waves are not prominent but are invariably found, particularly in atrophic muscles, (Swash & Schwarz, 1981). Fibrillations tend to become more prominent in the later stages of the disease, (Goodgold & Eberstein, 1977).

For a second example of a disorder and its associated spontaneous activity, Duchenne muscular dystrophy is used. In this disorder, spontaneous activity is present as follows: on insertion of the electrode there is increased activity. Fibrillation potentials are frequently recorded, (Buchthal & Rosenfalck, 1963). Fibrillation potentials were found in 7 out of 8 patients with this disorder, (Desmedt and Borenstein, 1976). Positive sharp waves are usually only seen in the weakest muscles, (Swash & Schwarz, 1981).

From the preceding two examples, it is clear to see that the types of spontaneous activity and their prevalence in disorders of different kinds vary considerably. In the two examples given, the first has a great deal of fasciculations, whilst there is a greater degree of fibrillation potentials present in the second. After insertion activity has died away, it would be expected that a normal muscle would provide an electrically silent record for observation.

These two observations lead to the statement that if any spontaneous activity is present within the signal observed from a muscle at rest after any insertion activity has died away, then the state of that muscle or its nerve supply is not normal. The length of time required for the insertion activity to completely die away can be indicative of disorder. Insertion activity tends to be prolonged in denervated muscles and muscles

affected by certain muscular disorders such as polymyositis, (Lenman & Ritchie, 1977). In conditions of acute inexcitability of muscle fibres, there is a noticeable reduction in the insertion activity, (Richardson & Barwick, 1969). The degree to which it is present is also an indicator of the state of the muscle or nerve, for example, in both of the example disorders there is increased insertion activity.

Secondly, the type of spontaneous activity and the strength of its presence are major indicators of the nature of the disorder. In fact, this information may be instrumental in differentiating between otherwise similarly characterised disorders.

We may thus see that any attempt to simulate myoelectric activity, if it is to produce realistic results, must provide the ability to include spontaneous activity. Where this is not the case, realistic simulations may only be produced for muscle conditions that contain no spontaneous activity, effectively excluding many disorders.

4.3 Some characteristics of spontaneous activity.

4.3.1 Fibrillation Potentials.

Nature	- Biphasic spike of short duration.
Duration	- <5ms.
Pk - Pk Amplitude	- <1mV (Typically 20-300uV).
Firing Rate	- 1 -50 Hz, (10 common).
Sound	- High Pitched and Regular (Rain on a tin roof).

4.3.2 Fasciculation potentials.

Nature	- A Potential with the configuration of a bi or triphasic MUAP.
Duration	- As MUAP.
Pk - Pk Amplitude	- As MUAP.
Firing Rate	- 1/s normal, 1 per 3 or 4s for anterior horn cell disorders.
Sound	- Plunk, Plunk, Plunk.

4.3.3 End-Plate potentials.

Nature	- Biphasic potentials with an initial negative phase.
Duration	- <2ms
Pk - Pk Amplitude	- up to 200 uV.
Firing Rate	- 2-30/s
Sound	- Sharp, high pitched.

4.3.4 Positive sharp waves.

Nature	- Biphasic, positive negative action potential.
Duration	- Positive phase <5ms - Negative phase 10 - 100 ms
Pk - Pk Amplitude	- up to 1mV
Firing Rate	- 1 -50 Hz, (10 common).
Sound	- Sharp click to thud.

4.3.5 Bizarre high frequency potentials.

Nature	- Polyphasic action potentials.
Duration	-
Pk - Pk Amplitude	- 100uV to 1mV
Firing Rate	- 5 - 100Hz
Sound	-

4.4 The inclusion of spontaneous activity in a simulation program.

The types of spontaneous activity to be included in the myoelectric activity simulation program are positive sharp waves, motor end-plate potentials, fibrillation potentials and fasciculation potentials. The simulation program itself will be detailed later in this chapter. Examples of these potentials may be observed in figures 4.4.1 to 4.4.3.

Figure 4.4.1 - The fibrillation potential template.

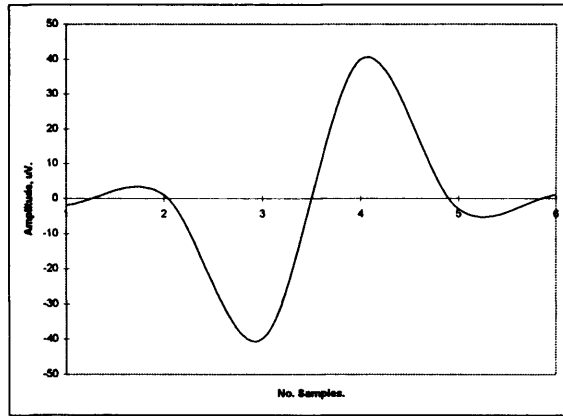


Figure 4.4.2 - The motor end-plate potential template.

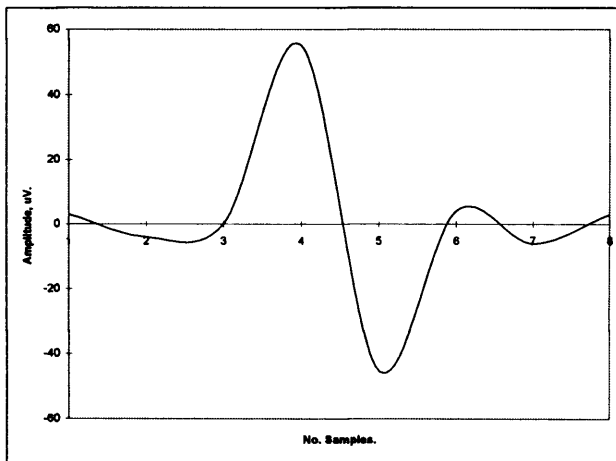
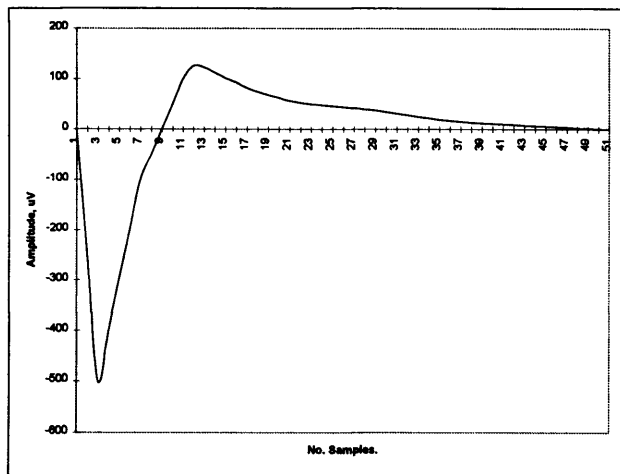


Figure 4.4.3 - The positive sharp wave template.



The manner in which these potentials are incorporated into an EMG simulator is outlined. For both Fibrillation potentials and positive sharp waves, whose firing frequency is reported to vary between 1 and 50Hz (Swash & Schwarz, 1981) and 2 and 30 per second (Echternach, 1997), the most common firing frequency observed is 10Hz (Echternach, 1997). It is stated in Swash & Schwartz that positive sharp waves recur in a uniform and regular pattern (Swash & Schwartz, 1981) whilst Delisa et al say that fibrillation potentials usually fire at a constant rate, although a small proportion fire irregularly, (Delisa et al, 1994).

As such, in order to determine the firing frequency of all the included types of spontaneous activity, with the exception of fasciculation potentials, a Gaussian distribution is employed. In order to provide the most realistic range for fibrillation potentials and positive sharp waves, the mean of the distribution is set at 10Hz, the typical value. The distribution is set to vary around the mean value by ± 8 Hz. This provides a range of frequency from 2 to 18Hz that may occasionally be exceeded. Although this method does not encompass the whole range of occurrences of these activities, it will cater for a large proportion, i.e. the most common occurrences.

Echternach states that motor end plate potentials have an irregular discharge pattern, and fire at a rate of 2 to 30 per second, (Echternach, 1997). In order to accommodate these characteristics a Gaussian distribution is used with the mean set to 16 so that it causes firing rate to vary between 2 and 30 Hz.

In the case of fasciculation potentials, firing frequency is determined by ascertaining whether the fasciculations occurring are the product of a normal or a disordered muscle. If the fasciculations are in a muscle in a normal state, the firing rate is set to 1 per second, whilst in disordered muscle it is varied Gaussianly between 1 firing every 3 to 4 seconds. The potentials used for fasciculation are those of a normal biphasic or normal triphasic action potential, and may be seen in section 4.7

4.5 Models for EMG simulation.

There has been much thought on the subject of determining the occurrence of motor unit firing and hence modelling myoelectric activity. The most controversial properties of human single motor unit activity are the inter pulse interval and the

correlation structure between successive intervals, (Lago, 1979). Various researchers found no evidence of significant correlation between adjacent inter pulse intervals, (Clamann, 1969) (DeLuca & Forrest, 1973) (Shiavi & Negin, 1975), whilst others produced contradictory results, (Person & Kudina, 1972).

In 1979 DeLuca stated that only minimal (if any) dependence exists among the inter pulse intervals of a particular MUAP train. Therefore the MUAPT may be represented as a renewal pulse process, one in which each IPI is independent of all other inter pulse intervals, (DeLuca, 1979).

This was supported by Jones *et al* in 1987. They reported that works carried out on different muscles had produced conflicting conclusions on the suitability of renewal procedures for modelling muscular behaviour. It was then suggested that the process of firing is almost certainly of the non-renewal type, based on the biophysics of membrane recovery after firing. However, they concluded that the non-renewal characteristics exhibited were muscle dependant, and of less importance than the distributions associated with the firings, (Jones *et al*, 1987).

Despite some speculation about the applicability of the renewal process to the firing statistics of a single motor unit in human muscle, it has been adopted in the majority of attempts to model these statistics.

Various distributions have been advocated for determining the next firing in a train of pulses. The Gaussian distribution was suggested to be appropriate, (Rosenfalck, 1954) (Clamann, 1969). This was agreed upon by Person & Kudina, with the limiting condition of the firing frequency exceeding 10.5 pulses per second, (Person & Kudina, 1972). The Gamma distribution, (Shiavi & Negin, 1975), the Poisson distribution, (Brody & Scott, 1974) and the Weibul distribution, (DeLuca & Forest, 1973)(Maranzana *et al*, 1981) were also proposed.

The Gamma, Weibul or Poisson distributions, however, would not predict a peak in the EMG power spectrum at the appropriate firing frequencies, which is in fact often observed (Jones & Lago, 1982). The use of a renewal process utilising Gaussianly distributed inter pulse intervals fits the data published by Clamann for the human brachii biceps muscle very well (Clamann, 1969). It has been shown by Lago and Jones to predict the local peak in the EMG power spectrum, (Jones and Lago, 1977) (Jones *et al*, 1987).

In the previous chapter, reasons for the Gaussian distribution being less than ideal for determining motor unit firing time information were presented. The basis for hypothesising that firing times may be determined by a chaos driven model were laid out. It has, however, been shown that a chaotic model is inappropriate, (Small et al, 1997b) (Small et al, 1998).

Taking all of these findings into consideration, the Gaussian distribution, though not deemed wholly suitable for the purpose intended, appears to be the best.

4.6 Characteristics of volitional activity.

All measurable parameters vary from muscle to muscle because the number of muscle fibres in the individual motor unit varies from muscle to muscle. The parameters also change with age. In addition, they are strongly affected by the type of needle used, (Liveson & Ma, 1992).

Despite all of these limiting factors, some usual (expected) characteristics for the potentials observed during voluntary activation, are shown below.

Normal Muscle:

Amplitude; 100 μ V to 4 - 5mV (assessed at MVC).

Duration; 2 - 17 ms (most 8 - 12 ms).

Phases; 1 to 4.

Myopathic potentials:

Amplitude; Less than 1 mV is abnormally low.

Duration; Majority are very short, (i.e. less than 5 ms).

Phases; Polyphasic.

Neurogenic Potentials:

Amplitude; Greater than 5mV.

Duration; Increased (by definition).

Phases; Polyphasic.

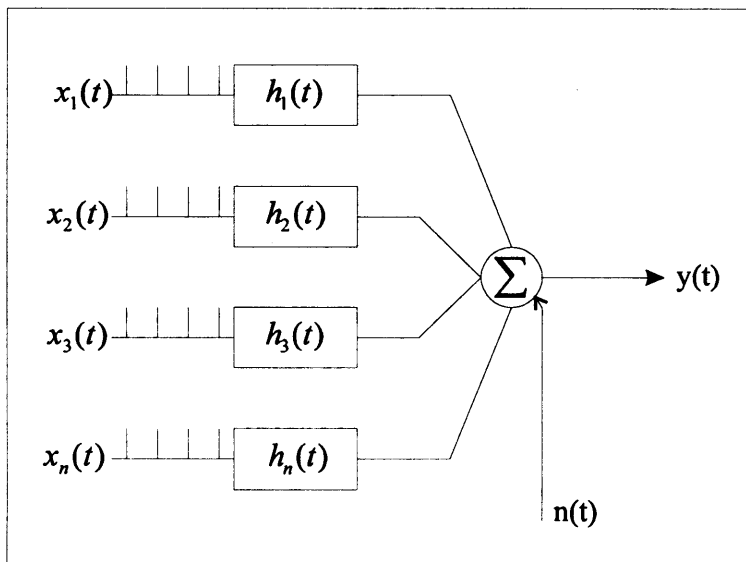
An extra characteristic feature of neurogenic motor units is that the number of potentials issuing from that unit will be reduced.

4.7 Simulation of volitional activity.

The model upon which volitional activity is based comes from that of Parker & Scott, (Parker & Scott, 1973). It is based upon the work of Lago, (Lago, 1979).

It has been stated previously that the model consists of a bank of filters, the impulse responses of which are representative of motor unit action potential templates. These filters are driven by trains of pulses, each train determining the firing times of one filter in the bank. The model may be seen diagrammatically in figure 4.7.1.

Figure 4.7.1 - The model for myoelectric activity.



Twelve different action potential shapes are used as templates. These consist of three of each of the following types: *normal biphasic*, *normal triphasic*, *myopathic* and *neurogenic*. These templates span the width of typical duration for their

respective classes, and fall within expected ranges for amplitude. The waveforms may be seen in figures 4.7.2 to 4.7.5.

It is known that motor unit firing time statistics are not deterministic in nature. Previous sections have established that the most appropriate way of modelling motor unit firing is by use of the Gaussian renewal process. The firing times of a single motor unit may be viewed as being characterised by a random variation around a set inter pulse interval. Different coefficients of variation for inter pulse interval have been reported. These have varied from 0.08 to 0.2 (Person & Kudina, 1972) to 0.7 to 0.9 (DeLuca & Forrest, 1973).

Determination of firing time in the case of simulation operates upon the generation of a random firing occurrence, based upon a range of inter pulse interval specified by the user. This method allows the user's choice of inter pulse interval and coefficient of variation to be created in the signal.

Other elements of variation within the routine are variation in template amplitude and variation in template duration. Addition of random noise to the signal is also a feature. The levels of noise within the signal are set by the user.

There are two mechanisms for variation in duration. As shown in figures 4.7.2 to 4.7.5, different duration templates are available for each action potential type. Variation in duration between signals may be achieved by using these different templates. The same affect, and that of variation between action potential trains, may be attained by varying the duration of a single template. Variation in template duration is performed by interpolation between sample points in the original template. This mechanism allows the user to specify the duration of action potentials. It also allows the introduction of random variation in duration between successive firings of the same motor unit. Such variation occurs between limits set by the user.

The number and type of units active within the synthetic signal is user defined. The resulting signal is sampled at 4096 Hz.

No account has been taken of recruitment of motor units or synchronisation between motor units during a contraction.

Examples of synthetic signals produced, both low and high force voluntary activity, and spontaneous activity may be seen in Figures 4.7.6, 4.7.7 & 4.7.8

Figure 4.7.2 - The biphasic templates.

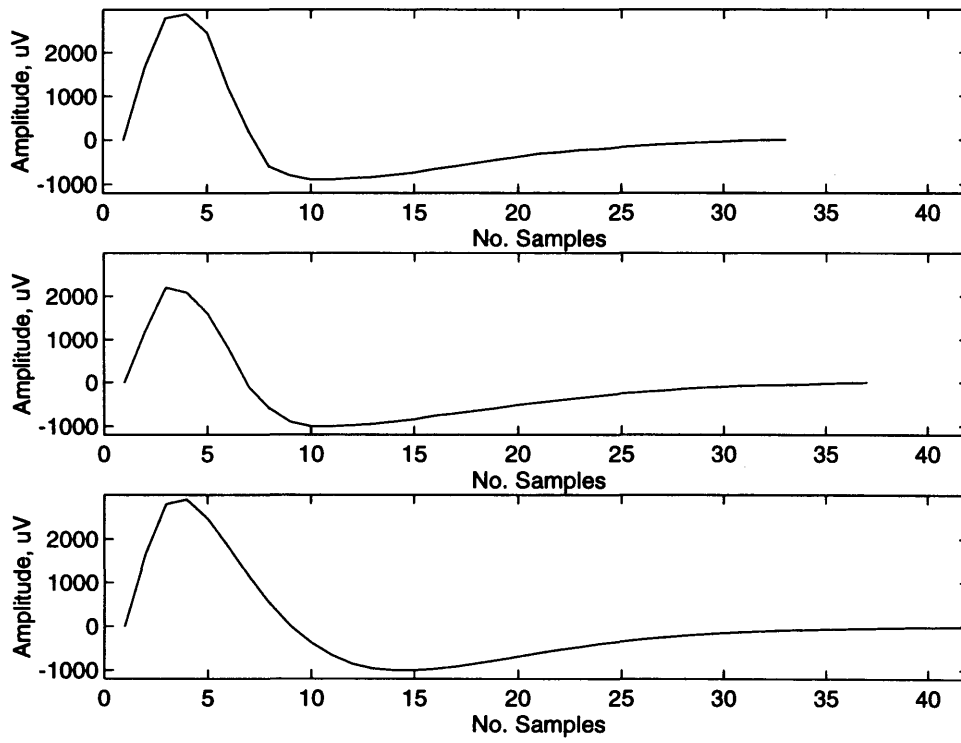


Figure 4.7.3 - The triphasic templates.

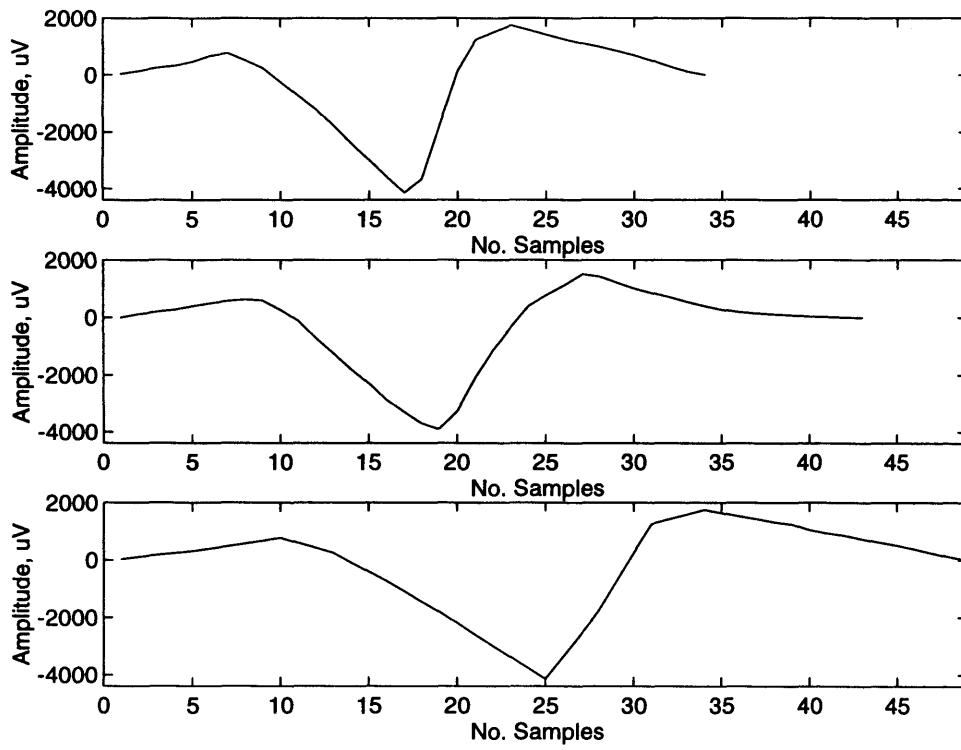


Figure 4.7.4 - The myopathic templates.

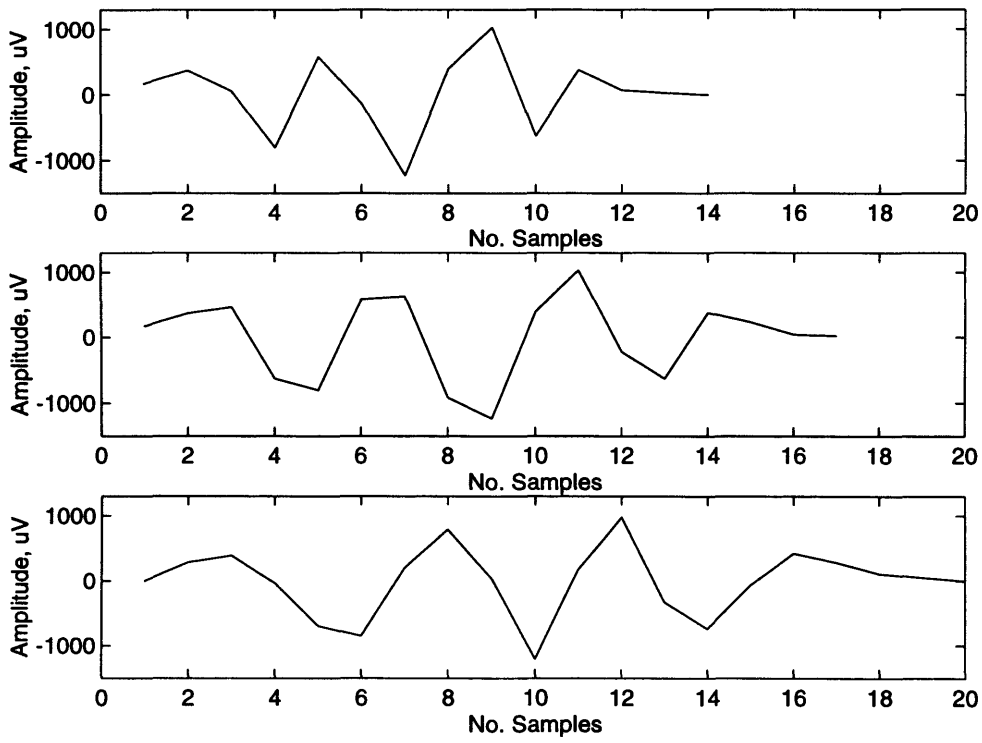


Figure 4.7.5 - The neurogenic templates.

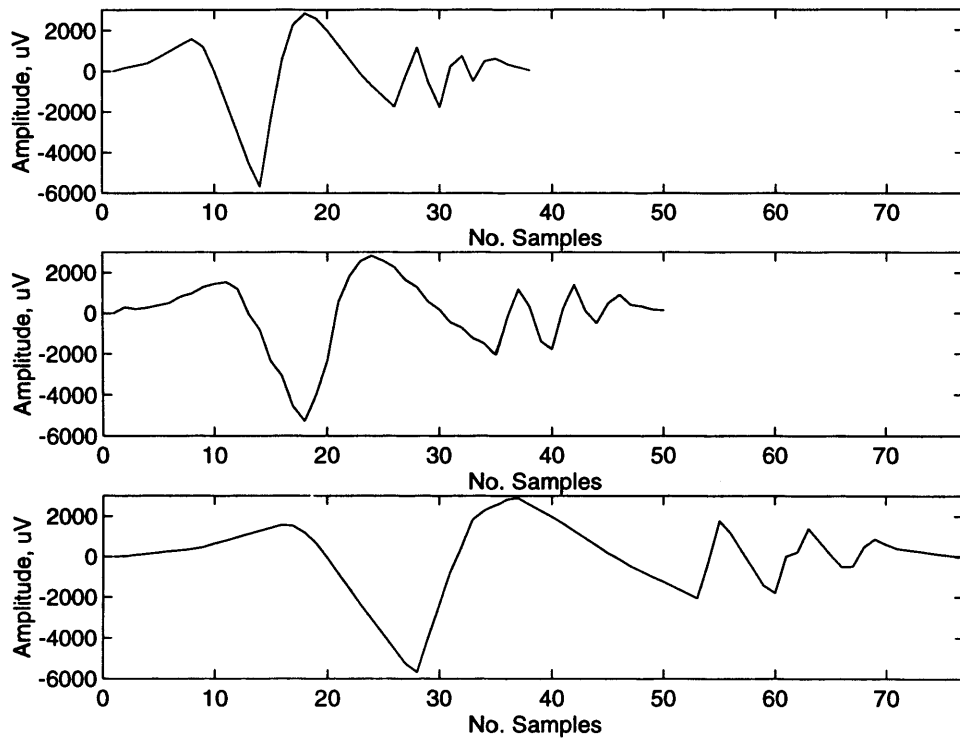


Figure 4.7.6 - A simulated low force EMG, containing 3 normal MUAPTs.

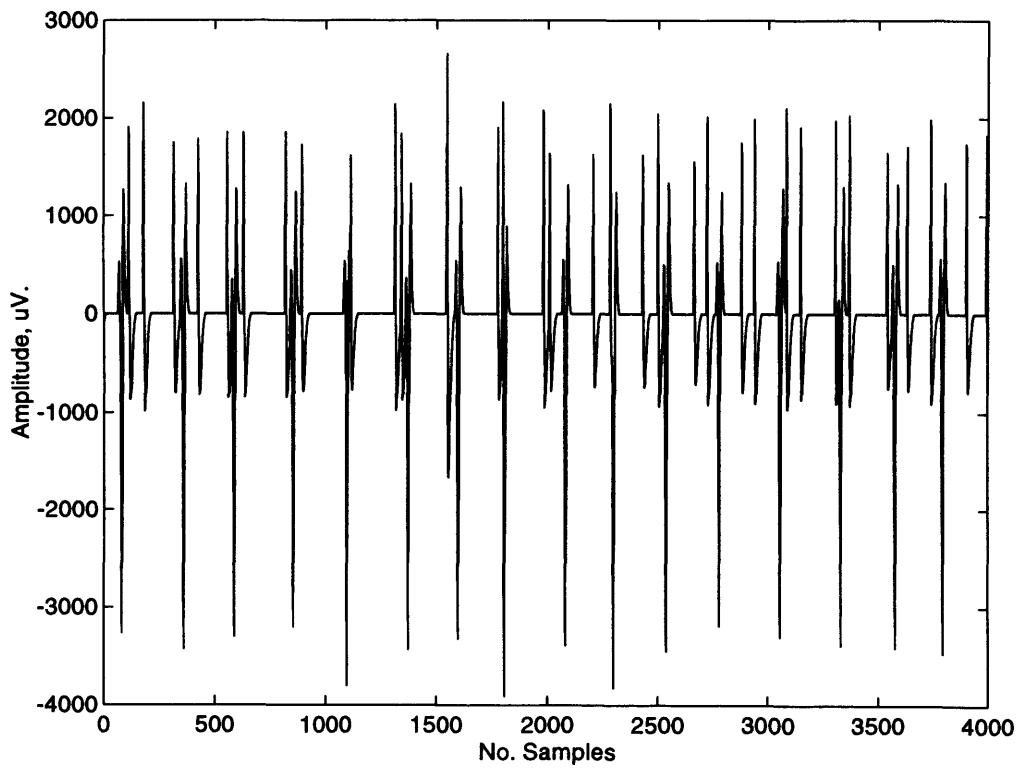


Figure 4.7.7 - A simulated high force EMG containing 15 normal MUAPTs.

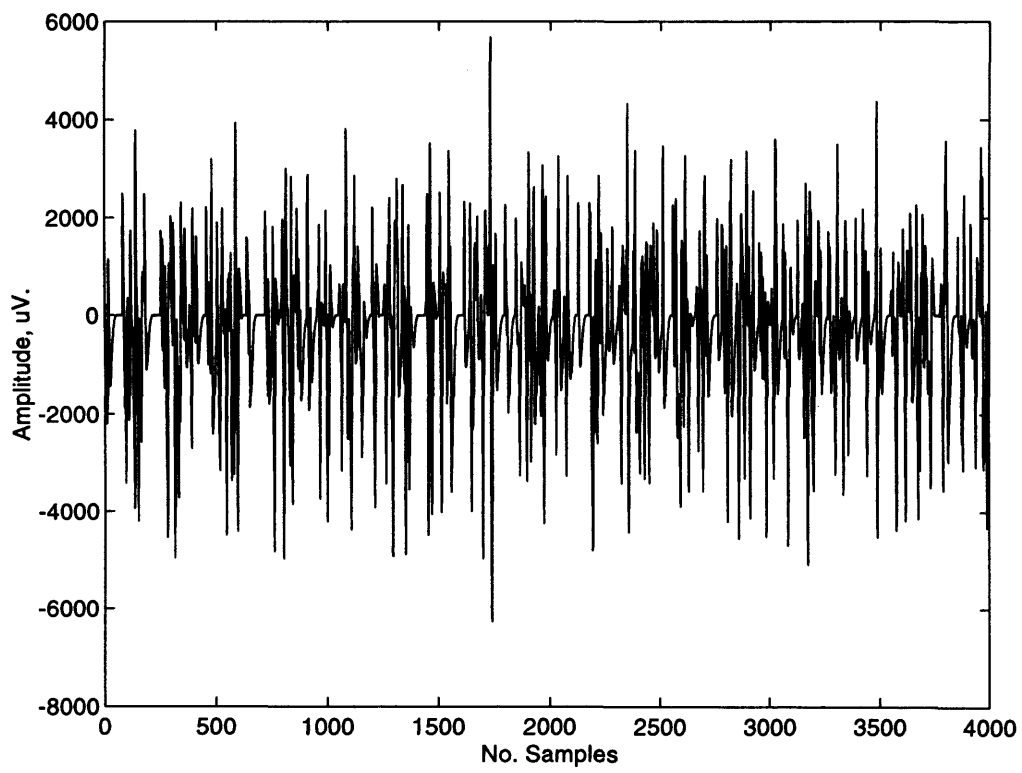
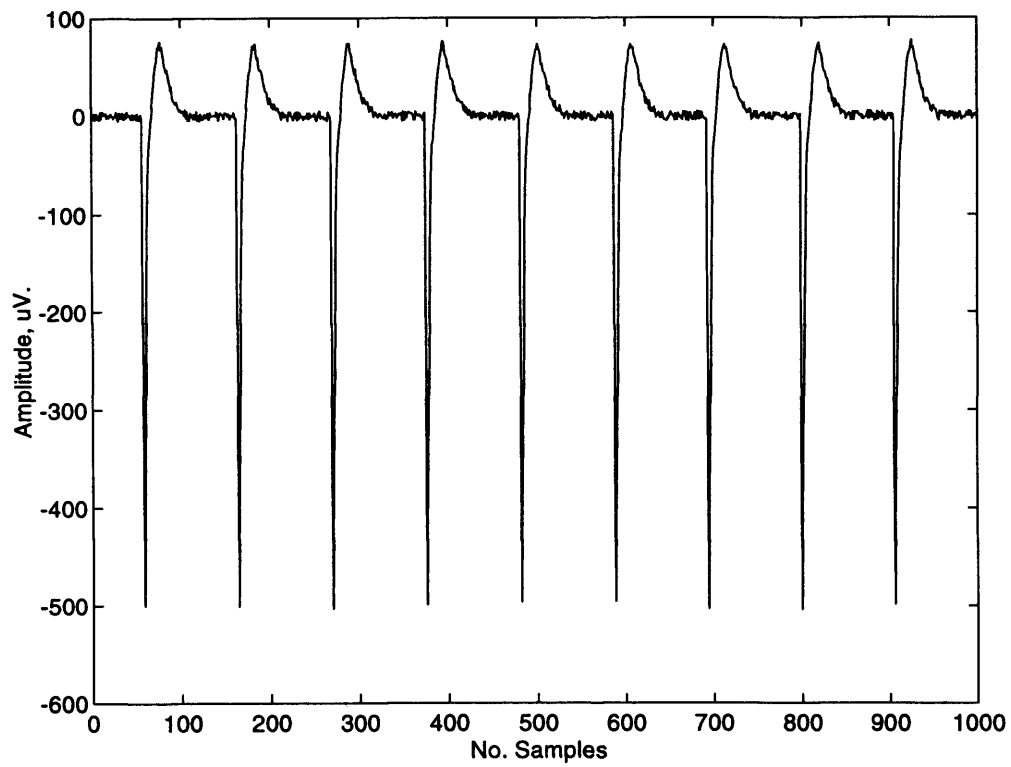


Figure 4.7.8 - A simulated train of positive sharp waves.



4.8 Simulation in a medical decision support system.

Earlier in this chapter, the relevance of spontaneous activity to neuromuscular diagnosis was discussed. This is part of a larger picture. A large proportion of neuromuscular diagnostic information is gained from analysis of the electromyogram of the patient being investigated. The electromyogram will be measured at different force levels depending upon which investigations are being carried out. Zero voluntary force for investigation of spontaneous activity, etc.

An EMG simulation routine may be used as a knowledge source for interaction with a decision support system used in neurophysiological diagnosis in a number of ways. Simulated data may be used when a clinician is learning the use of the decision support system. It may also be used when a clinician is being trained. The use of a simulator in this respect will provide access to a large source of signals for observation and experimentation. Many of the signals that will be available through simulation are representative of rare disorders. Signals such as these are not often encountered in clinical situations, where the disorder most often observed is carpal tunnel syndrome.

A second use of a similar nature would be for preparation. In a situation where a patient has been referred to a neurophysiologist with a suspected disorder of a rare nature, simulation would be of use. Observation of a signal representative of the disorder would be beneficial in familiarising him/herself with the characteristics of the disorder before identification is attempted. A simulator would be able to provide such an example. In this instance a simulation knowledge source as a part of the MDSS would complement the use of medical and laboratory texts in disorder characteristic determination, by providing readily available visual examples.

Simulations of EMG signals are made up from known elements. They have characteristics that are known by the user. Such simulations may be used to test the performance of signal processing algorithms, (Jones et al, 1987). This idea may be expanded to encompass whole systems rather than just single algorithms. The use of simulated signals in the MDSS will allow its correct operation to be established, a known input should give the correct output. An example signal may be analysed using the system. The corresponding outputs and recommendations may be compared with

those gained from analysing a real signal that is suspected to be from the same disorder. This procedure of comparison may be an aid to diagnosis.

Finally, the incorporation of a myoelectric activity simulator in the MDSS will add to the work reported in chapter 2. The simulator, when combined with simulations of the results of other tests in the diagnostic procedure, especially those highlighted in chapter 2, will be instrumental in the generation of a readily available source of reference for neurophysiology, i.e. a simulated patient. This source of reference will contain not only characteristic information and test results for disorders, but the ability to produce examples of their associated activity too. This will be of great use in comparative diagnosis training.

4.9 Summary.

In this chapter the importance of the inclusion of spontaneous activity in any realistic simulation package has been presented. Typical characteristics of spontaneous activity have been introduced and the inclusion of this activity in a myoelectric activity simulator has been discussed and outlined.

Various models for the simulation of voluntary myoelectric activity were presented and their suitability to the task were discussed. The most appropriate was selected and reasons for this selection given. Typical characteristics of voluntary activity have been presented and their inclusion in a simulation package outlined.

The use of myoelectric simulations with medical decision support systems was discussed.

Chapter 5 - The decomposition knowledge source.

5.1 Introduction.

This chapter is concerned with the process of decomposition and its use as a knowledge source within a blackboard based MDSS. Section 5.2 discusses the merits of using this procedure as a knowledge source. Section 5.3 addresses the problem of decomposition. A description of what the process is intended to achieve is presented, and its usefulness is outlined. Comparisons are made with the techniques currently employed in clinical practice.

In section 5.4 highlights of various methods presented over the years by different researchers are outlined and some of their inappropriate features are explained. In section 5.5 a detailed description of one method of particular interest is offered. Problems and possible additions are discussed.

5.2 Decomposition as a knowledge source.

When developing an MDSS for application to the problem of neurophysiological diagnosis, it is vital that all of the knowledge and data necessary to accurate decision making is available. Should this not be the case, system suggested diagnoses will be of little value and may be misleading.

Decomposition (or low force electrophysiological assessment) is a vital component of the diagnostic procedure. There are circumstances when these tests and the knowledge they will supply are not needed. An example of this is the occurrence of carpal tunnel syndrome, a nerve entrapment disorder. Nerve conduction studies and the patients physical symptoms will be sufficient to make the diagnosis. Electrophysiological assessment would be unnecessary. The blackboard system has the ability to choose which sources of knowledge it utilises, thus catering for this situation and the next.

The diagnosis of many disorders is not as simple as that of a nerve entrapment. Observations of MUAP shape, amplitude, duration and firing frequency are required

for the discovery of the state of a muscle that is host to an unknown disorder. It is electrophysiological assessment of the muscle in question, at low to medium levels of contraction, that will provide this information. In a computer based system, it is the task of a decomposition routine to analyse the EMG signal and provide this information.

It is thus necessary to incorporate into any computer based neurophysiological diagnostic system, whether it be for decision support or for decision making, the ability to process low to medium force EMG signals and utilise the extracted information in the diagnostic procedure. Without this ability the system would be incapable of making accurate or realistic diagnoses in the majority of cases. As such, a decomposition knowledge source is a prerequisite for a blackboard based MDSS applied to neurophysiological diagnosis.

5.3 The decomposition problem.

As was described in chapter one, the EMG signal is a summation in time of the contributions of active motor units. Each motor unit produces a train of action potentials which, when superimposed upon one another, form the electromyogram.

Decomposition of such signals involves determining from which motor unit each action potential came. The extraction and grouping of action potentials supplies a lot of information.

In current medical practice, electromyographic diagnosis is based on visual and auditory assessment of EMG signals, (Coatrieux et al, 1985). Visual analysis is obviously a difficult task. It necessitates a great deal of training. The doctor is required to perform manual thresholding in order to separate the motor unit activity from the disparate forms of background activity that may be present. The most significant constraint imposed upon investigations by visual analysis is the necessity for a low force of contraction. As we know, the greater the force of contraction, the more motor units there are contributing to it (until they have all been recruited). Consequently, the degree of overlap prevalent within the EMG signal increases too. There is an escalating degree of difficulty in making accurate visual identifications in

these circumstances. As a result of this, it is necessary for visual analysis of the EMG to be performed at low force levels.

There are detrimental effects caused by this constraint. Firstly, in a muscle, the activation threshold of motor units ranges from low to high. The higher activation threshold units will not become active during these tests. It is quite possible that these units would display signs of disorder. Thus diagnosis may be made all the more difficult by the imposition of the low force contraction constraint.

A second undesirable effect of this constraint is that the number of requisite tests for diagnosis is increased. In order to gain information about an adequate number of motor units within the muscle suspected of being disordered, multiple tests must be carried out, (Loudon, 1991). Even so, the most useful data will not necessarily be gained.

All of this causes the analysis to be time consuming, which is undesirable. Not least because of the discomfort caused to the patient by insertion, reinsertion and movement of the penetrative needle electrodes used. The major problem with totally visual procedures is the tremendous amount of time required to make the MUAP identifications and precise firing time measurements, (LeFever & DeLuca, 1982).

The feature of the EMG of most use diagnostically is MUAP shape. The shapes of the MUAP waveforms in an EMG signal are an important source of information used in the diagnosis of neuromuscular disorders. The problem is that it is difficult for the doctor to extract the MUAP information from an EMG signal, (Bhullar et al, 1990).

It has been made apparent that an automated decomposition procedure would be beneficial in several ways. Firstly, it would reduce the number of tests required during analysis, thus reducing diagnosis time and patient discomfort. Secondly, it would allow analysis of higher threshold motor units, thus providing access to much more information of diagnostic use. As such, a reliable and effective automatic decomposition routine would be a useful tool for the neurophysiologist.

5.4 An overview of techniques.

The obvious usefulness of automatic decomposition, highlighted in the previous section, has lead many researchers to attempt to find solutions to the problem.

Different approaches have been tried. These have included supervised, unsupervised and partially supervised methods making either single or multiple passes through the data. (Stashuk & Paoli, 1998). Many routines have utilised shape based classification, examples of these are LeFever & DeLuca and Loudon et al,(LeFever & Deluca, 1982)(Loudon et al, 1992). Firing statistics have also been incorporated into the discriminatory process, for example, the methods of McGill et al and Loudon et al, (McGill et al, 1985)(Loudon et al, 1992).

The success of the existing routines has been variable. The method of LeFever & Deluca achieves decomposition at force levels of up to 100% of maximum voluntary contraction, containing up to eight MUAPs. However, to acquire the data it takes a considerable amount of time to run, requires interaction with a highly skilled operator and utilises a special electrode that is not in common use. Other methods such as those of McGill et al, and recently, Stashuk & Paoli (Stashuk & Paoli, 1998) do not consider superimposed activity. No method has yet been widely accepted.

5.5 The method of interest.

The method of most interest in this study is that presented by Loudon et al, (Loudon et al 1992). The procedure for decomposing an EMG signal is divided into two parts: one for the classification of non-overlapping action potentials and the other for the resolution of superimposed waveforms.

5.5.1 Classification of non-overlapping MUAPs.

The initial stage involves splitting the EMG signal into active segments (segments containing significant activity) and non-active segments. Only the active segments are retained. The rest of the signal is discarded.

Next, each active segment is described by a set of eight features. These form a feature vector, a simpler and more useful representation of the activity. The problem of correlation between features is overcome at this stage by orthogonalisation. Orthogonalisation of the features produces a new set of characterising vectors of reduced dimension. This is achieved using diagonal factor analysis.

The final stage in the routine dealing with non-overlapping data is that of classification. Classification is performed in a number of steps. The first is the formation of a network connecting all active segments; the second is clustering of non-overlapping MUAPs and the third is the application of MU statistical analysis.

The active segment network is formed so that vectors which are most similar are joined together. The measure of closeness used is the Euclidean distance between vector pairs. The network distance, i.e. the distance between adjacent segments in the network, is a normalised Euclidean distance.

Clustering of active segments within the network is achieved by cutting the network where there is an increase in network distance above the average distance of the next four segments. Superpositions are discarded at this point. It is stated that clusters due to superpositions will have less than five members.

Finally the firing statistics are calculated for the classified motor units. The mean and standard deviation are calculated for each cluster. The criterion used to group together firing period values of an MU is that the periods are within $\pm 20\%$ of one another. Groups of similar periods form within each MU, the mean and standard deviation is calculated for each of these groups and the smallest mean firing period is used to represent the true firing of the MU.

5.5.2 Resolution of superimposed waveforms.

This is performed using both procedural analysis, in the form of a net area study followed by template matching, and knowledge based analysis.

The net area study reduces the possible number of MUAP combinations that could be the constituents of the overlapping complex. This is achieved by the use of a thresholding procedure based upon the theory that the sum of MUAP areas forming a complex will be equal to the area of the actual complex. This suggests the most likely combinations of MUAPs to make up the complex.

The template matching procedure uses these suggested combinations. The maximum peak of each MUAP in a combination is aligned with that of the complex, and subtracted. This is done for each MUAP in the combination, consecutively. It is repeated for every possible combination of MUAP order within the specific combination of MUAPs. This process is repeated for all the combinations suggested by the net area study. The combinations yielding the smallest residuals below a set threshold are selected.

The final discrimination is made during the knowledge based analysis. This assesses whether or not the MUAP combinations suggested fit in with the previously calculated MU firing statistics. The most appropriate combination is selected at this stage.

5.5.3 Discussion

Whilst this routine has been shown, in the past, to work well on both simulated and real data, testing, by various parties, has revealed that it does not always perform as well as may be expected.

It is hypothesised that an improvement in the MUAP classification section of the routine would improve the overall operation of the non-overlapping classification part of the routine.

With regard to resolution of superimposed waveforms, an improvement of the method is advisable. Should the existing method not find a combination that has the minimum residual and that falls below the predetermined threshold, every possible

time registration for the selected combinations should be compared with the complex in question. This method, although more time consuming, is more likely to produce an appropriate solution than the more subtle methods recommended by Loudon & Jones.

5.6 Summary.

In this chapter the importance of decomposition as an element of the MDSS has been established. The problem of decomposition and some reasons for the need for an automatic routine have been discussed.

An overview of previously attempted methods of automatically decomposing EMG signals has been presented. Several different methods have been commented on and their shortcomings highlighted.

The method upon which future work is to be based has been described in some detail, and areas where improvement may be possible have been pointed out.

Chapter 6 - MUAP clustering using artificial neural networks.

6.1 Introduction.

In this chapter it is suggested that neural networks may be suitable for application to the problem of action potential clustering, i.e., discriminating between normal, myopathic and neurogenic classes, providing that appropriate inputs are chosen. The problem is addressed using simulated data, as a study in the feasibility of the approach. In section 6.3, various neural networks and the methods in which they are trained are described. Section 6.4 describes the application of various networks and data representations to the task of clustering. It also portrays the testing and performance of these networks in the presence of noise, both white and band limited, and in the presence of overlapping data. The performance of the networks in correctly clustering normal, noisy and overlapping data is discussed and the implications highlighted.

6.2 Neural networks and the MUAP clustering problem.

It may be seen from the last chapter that the clustering of MUAPs into groups containing MUs from the same MUAPT is a problem in pattern recognition. However one chooses to represent an action potential, other potentials from the same train (assuming they are similar in shape and duration, etc.) will be characterised by similar representations. The formation of clusters will consist of recognising similar representations of MUAPs and labelling them as such. Thus, the task is pattern recognition.

Pattern recognition is a task which has received much attention in the world of artificial intelligence (AI). Many problems have been addressed using neural networks and suitable solutions have been found. One example of interest is the method of zip code recognition devised by Le Cun et al. This method uses a multilayer perceptron to recognise hand written digits.

The use of neural networks to cluster MUAPs may well provide an improvement upon the performance of the algorithm presented in chapter 5. Important

factors to the operation of this method are the type of artificial neural network (ANN) used and the method used to classify each segment of activity from the EMG signal.

6.3 The neural network.

The material in this section is based to some extent upon the books of Haykin and Gurney respectively, (Haykin 1994)(Gurney, 1997).

The neural network may be best described by the presentation of definitions:

“A neural network is an interconnected assembly of simple processing, units or nodes, whose functionality is loosely based upon that of the animal neuron. The processing ability of the network is stored in the inter-unit connection strengths or weights, obtained by a process of adaptation to, or learning from, a set of training patterns.” (Gurney, 1997)

An alternative definition is given by Haykin:

“A neural network is a massively parallel distributed processor that has a natural propensity for storing experiential knowledge and making it available for use.

It resembles the brain in two respects:

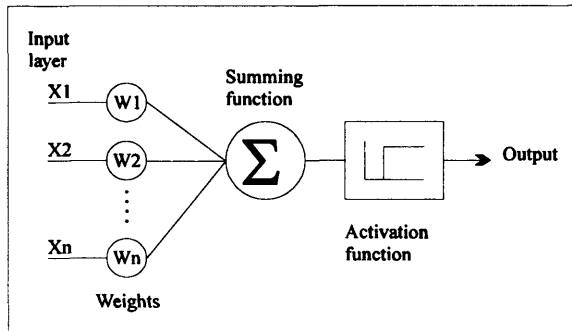
1. Knowledge is acquired by the network through a learning process.
2. Interneuron connection strengths known as synaptic weights are used to store the knowledge.” (Haykin, 1994)

In order to understand the operation of such networks, it is important that the basic element of operation within the network, the node or neuron, be understood.

6.3.1 The neuron

The artificial neuron was originally proposed by *McCulloch & Pitts*, (McCulloch & Pitts, 1943). Figure 6.3.1.

Figure 6.3.1 The artificial neuron model.



The model consists of synapses with their corresponding weights, a summation element and an activation function. In the case of the original model, the activation function was a hard limit or step function. Other terms that may be incorporated within the neuron model are those of threshold and bias. The threshold has the effect of lowering the net input to the activation function, whilst the bias raises it.

6.3.1.1 The activation function.

The activation function defines the output of a neuron in terms of the activity level at its input, (Haykin, 1994). It limits the output amplitude of a neuron.

Two examples of activation function are shown below: figure 6.3.1.1.1 shows the hard limit function and figure 6.3.1.1.2 shows the sigmoid or soft limit function.

The sigmoid function is a softened step function. Its use allows non-binary numbers to be output from the neuron. This ability may be of great use in some applications.

Figure 6.3.1.1.1 The hard limit activation function.

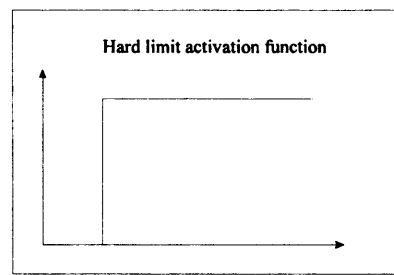
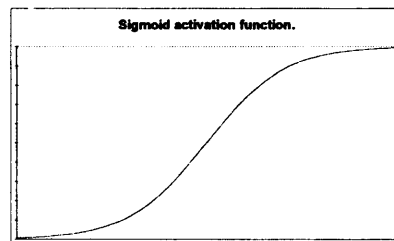


Figure 6.3.1.1.2 The sigmoid (soft limit) activation function.



6.3.2 The perceptron

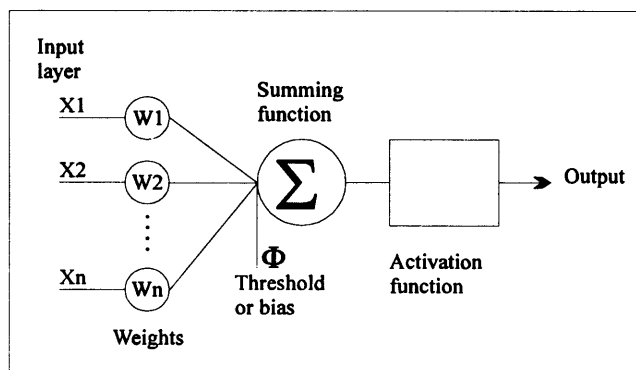
The perceptron is the simplest form of neural network. It is used to classify patterns that are linearly separable, (Haykin, 1994). The perceptron is also used as an element within a layer of perceptrons. The use of single and multiple layers of perceptrons will be dealt with later.

A single perceptron is capable of classifying its inputs into one of only two classes. This explains the requirement for linear separability of inputs. Further explanation is drawn from the way in which a neuron works in classifying inputs. Classification is achieved via the formation of what is termed a “hyperplane” between the two linearly separable sets of input data. All data falling on one side of the plane will be classified as a member of one group and all data falling on the other side will be classified as a member of the second group. It is thus clear that if the two sets of data are linearly inseparable, the neuron will misclassify some input patterns.

If an input data set consists of more than two linearly separable groups, the introduction of a single hyperplane will not correctly separate them. As this is the case, a single neuron will not correctly classify the inputs. The use of more than one neuron, i.e. a layer of neurons, will introduce more hyperplanes to separate the input space. As long as all the clusters of inputs within the input space are linearly separable, a layer of neurons containing enough neurons will be able to solve the problem

A schematic diagram of the perceptron may be seen in figure 6.3.2.1. It may also be seen, from this figure, how the perceptron is derived from the *McCulloch-Pitts* neuron model of section 6.3.1. This derivation was made by Rosenblatt, (Rosenblatt, 1962).

Figure 6.3.2.1 The perceptron model.



6.3.2.1 Gradient descent: perceptron learning.

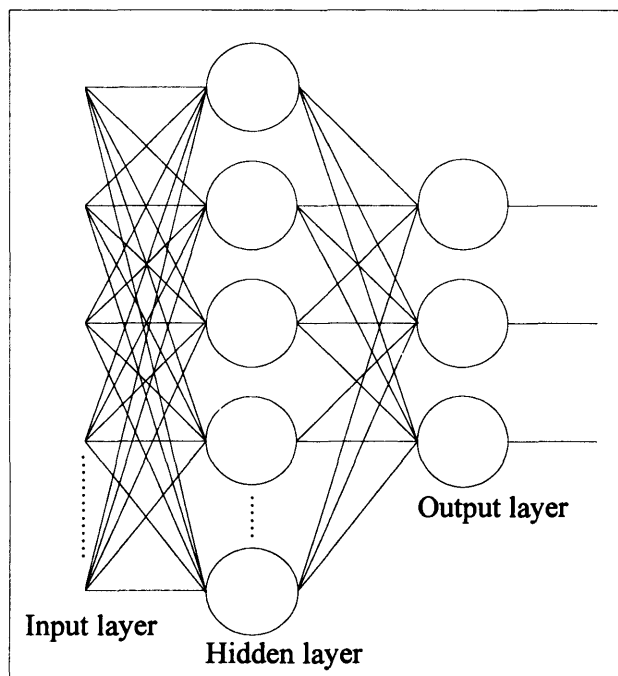
Gradient descent is the term given to an iterative procedure used to find the minimum of a function. Gradient descent may be used to train a single neuron or layers of neurons. The method consists of calculating an error, the difference between a neuron's actual output and its target output, and performing gradient descent upon the error as a function of the neuron's input weights. Thus the weights giving the minimum error are found. The squared sum difference between output and target is

the usual measure of error for a neuron. For neuron layers, the sum of squared errors is used.

6.3.3 The multilayer perceptron.

The multilayer perceptron, as its name suggests, consists of more than one layer of neurons. For the sake of simplicity, a two layer network using a small number of neurons in each layer will be used to illustrate the entire set of networks, figure 6.3.3.1. The value of a multiple layer network is evident when the input data requiring classification is not linearly separable. The use of multiple layers allows the decision surface (the hyperplane in the case of a single neuron) to have a shape appropriate to solving the specified problem.

Figure 6.3.3.1 The multilayer perceptron network.



As may be seen from figure 6.3.3.1, multilayer networks consist of at least one hidden layer and a single output layer. The hidden layer is so named because it is not a part of either the input or output to the network. Inputs to the network progress through it in a layer-by-layer fashion. Nodes within the network may be either fully

connected, as they are in figure 6.3.3.1, or they may be only partially connected. If a network is partially connected, not all nodes in the network will be connected to all nodes in the surrounding layers.

There are problems with the use of multiple layers of neurons. One of these is the possible use of too many hidden neurons to classify inputs into their desired groups. If there are too many neurons, the decision surface created upon presentation of the training data may provide good classification of the training data, but may fail to generalise when similar data is presented. Generalisation is the ability of a trained network to correctly classify data that is a part of the target set, but that was not included in the training set. The network is able to generalise its solution to include new data.

A second problem is the occurrence of local minima in the error function. When these are present, the method of gradient descent (backpropagation for multiple layers, see section 6.3.3.1) may well find a local minimum, rather than the function's global minimum. Should this occur, the solution settled upon will not be the best one; it may not even be an acceptable solution.

6.3.3.1 The backpropagation learning rule.

The error backpropagation method of network training is based upon gradient descent. It is specifically for use with multilayer networks. The method consists of making two passes through the network. Initially an input is presented to the network. This propagates through the network layers producing an output. The output error is calculated in the same way as for pure gradient descent. This error is propagated backwards through the network. During the backward pass, the synaptic weights of the network are adjusted, using gradient descent, to reduce the error. It is only during the backward pass that the weights are altered, during the forward pass they remain fixed, (Haykin, 1994).

The training of a network by this method consists of presentation of input vectors to the net until an acceptable sum of squared errors is reached. The speed with which this occurs is controlled in part by the *learning rate*. The learning rate is quite a sensitive term. Too large a learning rate may cause the learning process to become

oscillatory around the error minimum, thus never reaching a solution. Too small a learning rate may cause the learning process to take far too long a time. There is an obvious trade off between the speed of learning and the ability to reach an acceptable solution.

The oscillatory effect introduced by too high a learning rate may be combated by the introduction of momentum to the backpropagation method. Momentum ensures that any change in synaptic weight is not dramatically different from the previous change. This is achieved by including a proportion of the last weight change in the current weight change. This has a tendency to smooth out small fluctuations in the error-weight space, (Gurney, 1997). So the addition of momentum allows the learning rate to be increased by suppressing oscillatory behaviour.

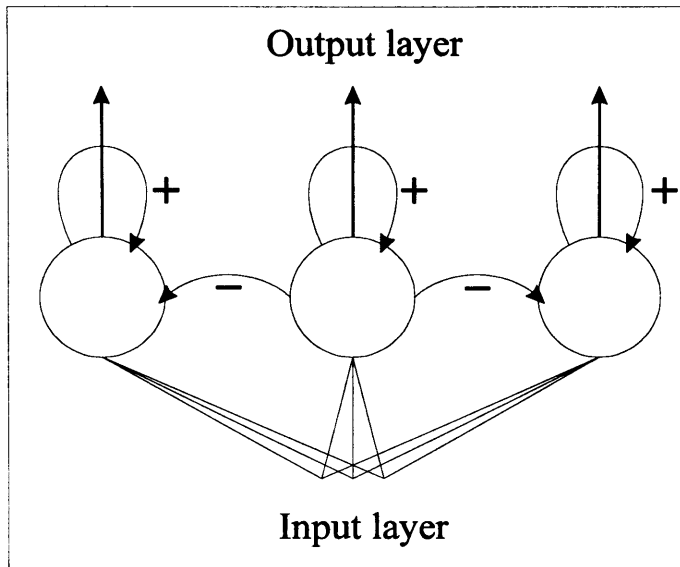
6.3.4 Self organisation: competitive networks and self organising feature maps.

Self-organising networks can learn to detect regularities and correlations in their input and adapt their responses to that input accordingly, (Demuth & Beale, 1994). We shall look at competitive networks and self organising feature maps. Both of these are based upon competitive learning.

If a network can learn a weight vector configuration without being told explicitly of the existence of clusters at the input, then it is said to undergo a process of self-organised or unsupervised learning, (Gurney, 1997) Competitive learning, section 6.3.4.1, allows behaviour such as this.

In a self-organising feature map, the neurons are placed at the nodes of a lattice that is usually one or two dimensional, (Haykin, 1994). When training is undergone, these neurons distribute themselves to recognise the presented input data and to represent its topography. Self organising networks are based upon the competitive network, they are competitive networks in the lattice formation. Understanding is enhanced by the presentation of the competitive network architecture, figure 6.3.4.1.

Figure 6.3.4.1 The competitive architecture.



The inputs presented to the network are seen by all the neurons within it. There are intralayer, or lateral, connections such that each node is connected to itself via an excitatory (positive) weight, and inhibits all other nodes in the layer with negative weights, (Gurney, 1997). The latter connections are seen only for the central node in the above figure.

After training of the network has taken place, presentation of an input will result in all neurons in the network giving a result. The maximum result will be given by the neuron, or neurons, associated with the cluster of inputs in which the currently presented input falls. A more specific example of this type of behaviour is given by the *winner takes all* network. This network behaves in exactly the same way as that previously described, but it only outputs ones and zeros. The winning neuron will output a one whilst all others output a zero.

A competitive network learns to categorise the input vectors presented to it, it also learns the distribution of inputs by dedicating more neurons to classifying parts of the input space with higher densities of input, (Demuth & Beale, 1994). Self organising feature maps map the topological characteristics of the inputs to the network. They operate similarly to competitive networks, but smooth the transition between inputs by presenting a neighbourhood of neuron firings. The maximum firing in the neighbourhood represents the winner of the competition and the other firings

represent those that came close. This allows the progression of the input transition to be mapped and observed as the winning neuron changes.

6.3.4.1 Competitive learning.

For the net to encode the training set, the weight vectors must become aligned with any clusters present in this set and each cluster must be represented by at least one node, (Gurney, 1997).

In order to do this, training input data must be presented to the network. Learning occurs as follows: an input vector is presented to the network and a sum of weighted inputs is calculated for each neuron. The initial synaptic weights for each neuron will differ. The neuron with the highest sum of weighted inputs has won the competition between all neurons. Only the winning neuron has its weights adjusted.

The weights of the winning neuron are updated so that the weight vector moves closer in space to the current input vector. This alteration of weight ensures that the winning neuron is more likely to fire again when a vector similar to the current input is presented to the network, and less likely when a dissimilar vector is presented.

This procedure is repeated for the whole training set, many times over, in order that each input, single or cluster, be characterised. As long as there are enough neurons present within the network, each cluster of inputs should contain at least one neuron.

A problem with competitive learning is that of *dead neurons*. If too many neurons are present, some may never win the competition, and thus never take part in characterising the input data set.

6.3.5 Learning vector quantisation networks.

To achieve the best results for pattern classification, the use of the feature map should be accompanied by a supervised learning scheme, (Kangas et al, 1990).

Learning vector quantisation is a pattern classification method in which each output unit represents a particular class or category, (Fausett, 1994). Learning vector

quantisation networks can classify any set of input vectors, not just linearly separable sets of input vectors, (Demuth & Beale, 1994).

This method of supervised learning is based upon two techniques: that of competitive networks and that of vector quantisation. The first technique has already been covered, however, vector quantisation is explained below.

In vector quantisation, the input space is divided into distinct sections. These sections are based upon the inputs. For each section a characteristic weight vector is assigned.

Learning vector quantisation is a supervised learning technique that uses class information to move the weight vectors slightly, so as to improve the quality of the classifiers decision regions, (Haykin, 1994).

Initially, the competitive section of the network forms clusters. This is followed by learning vector quantisation. The essence of the method is that input vectors are selected randomly from the input space and the similarity between the input's class and the class of each region's characteristic weight vector is assessed. The weight vectors that are similar to the selected input are moved towards it and those that are not similar are moved away.

After several passes through the input data, the weight vectors would typically converge, and the training is complete.

6.4 Application of neural networks to the problem.

6.4.1 Describing features as network inputs.

The initial consideration when trying to group data sets into distinct classes using neural networks, is how best to represent the data. Any representation must contain the majority of the information available about the data entry, or at least enough of this information to allow discrimination between similar but different entries. This is important because the distribution of inputs in the input space of the neural network determines the number of input units in the network and the ease of classification. It is obvious that the fewer inputs there are describing a single data entry, the easier classification will be (this is relative to the ease of classification of

the problem itself). This is due to a lower dimension input space requiring less complex decision surfaces.

In the case of identifying individual action potentials and grouping them appropriately, samples of the signal are inappropriate. This is so because, depending upon the sampling frequency employed during the digitisation process, a single MUAP will necessitate a large number of inputs to the neural network. Another problem apparent with this type of input is that the number of samples in different action potentials will vary, thus the number of required input nodes to the network will vary too. The most direct solution to this problem is the use of null input nodes. This, however, is not ideal because the APs are altered and thus the accuracy of classification will be altered too. It is also possible that an AP with more samples than there are input nodes will still occur.

A more suitable representation of data for input to neural networks, based upon that of Loudon (Loudon, 1991), is outlined. The method consists of representing each input to the network by a set of eight features. These features are characteristic of certain aspects of action potentials that will vary between different MUAPTs. The features are listed below:

1. *The maximum peak to peak amplitude feature.*
2. *The maximum positive amplitude feature.*
3. *The positive area feature.*
4. *The negative area feature.*
5. *The maximum positive gradient feature.*
6. *The maximum negative gradient feature.*
7. *The number of turns feature.*
8. *The number of samples feature.*

In the following investigations, these features will be used to create the input vectors presented to each neural network. The data used both for training and testing the neural networks is simulated and at this stage consists wholly of non-overlapping data. Each action potential within a data set is represented by its features for presentation to the neural networks.

6.4.1.1 The multilayer perceptron.

It is clear that where the inputs to be classified consist of vectors in eight dimensions, the problem requires the decision surface to be quite complex within the input space. We know that a single perceptron is capable of differentiating between only two linearly separable clusters, a single layer of perceptrons is capable of differentiating between more than two linearly separable clusters (the number determined by the number of neurons within the layer) and a multilayer perceptron is capable of differentiating between clusters that are not linearly separable.

An eight dimensional representation of a MUAP may not be visualised by the human eye. The most that may be seen is a three dimensional slice of such a representation. As such it is not possible to assess visually, whether our problem consists of linearly separable groups of input data or not. In order to deal with this uncertainty both single and multilayer networks were utilised in the attempt to solve the problem.

The set of data used for training the networks consisted of normal biphasic, normal triphasic myopathic and neurogenic simulated action potentials. Within each of the four classes the duration of an action potential was fixed at five standards (those standards being different for each class, and representative of the limits of expectation for real data). For each class the amplitudes varied randomly. The training set consisted of five examples of each standard for each class. All data was simulated, noise free, and consisted solely of non-overlapping action potentials.

Various networks, both single and multilayer, were trained using this data set. It was attempted firstly to train these networks to classify the input data into 20 groups (one group representing each MU), and secondly into 4 groups (one group representing each class of MU). The number of neurons in the hidden layers and the learning rate and training times were altered in the attempt to achieve the optimal learning procedure. The momentum term was included in learning to prevent the networks settling at local minima.

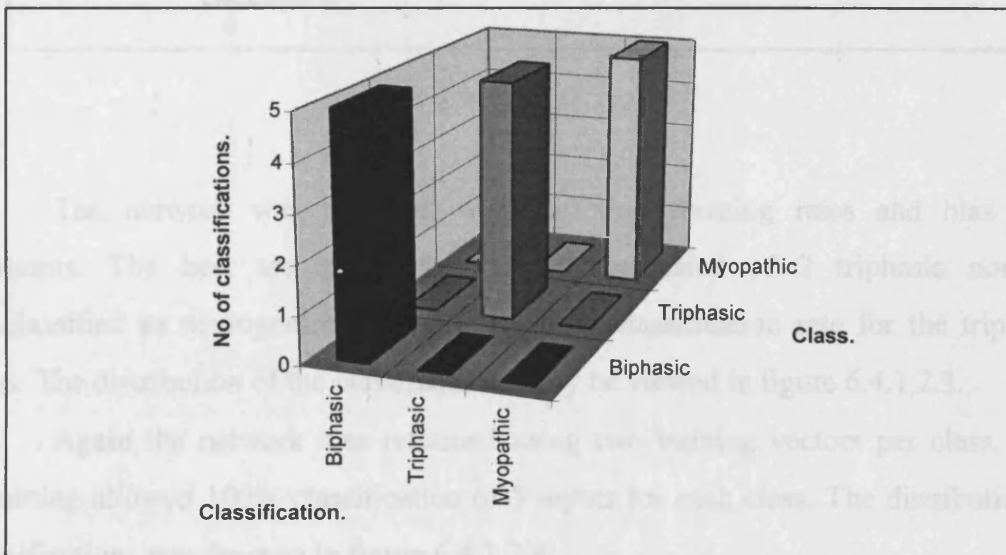
In all cases it was found that the sum of squared errors failed to reach an acceptable level. In fact, the levels at which the sum of squared errors settled far exceeded acceptable levels for single, double, and triple layer networks. This was in

spite of the addition of neurons to different layers, and in spite of variation in learning rate and of momentum. The sum of squared errors always settled at values too large for the resulting network to have been of any use in classification. Thus, a suitable solution to our problem was not found using perceptron networks.

6.4.1.2 The competitive network.

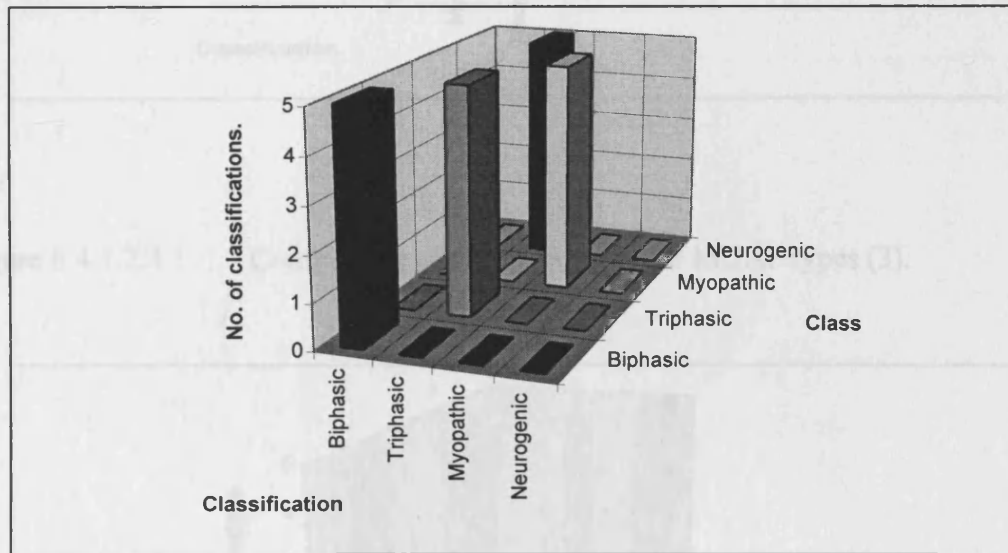
Various competitive networks were trained to address the problem. Initially the networks were used to classify between 2 (biphasic normal and triphasic normal) and 3 (biphasic normal, triphasic normal and myopathic) classes of action potential. The results of the three class operation may be seen below. A network consisting of three competitive neurons (the minimum possible amount for this operation) was used. It was trained using a single example of each class and used to identify five example of each class (including the training example). The number of training cycles was 1000. 100% accuracy of classification was achieved. The distribution of classifications may be seen in figure 6.4.1.2.1.

Figure 6.4.1.2.1 Competitive classification of three MUAP types.



A separate network was trained in a similar way. This network utilised four neurons to distinguish between four action potential classes (biphasic normal, triphasic normal, myopathic and neurogenic). It was trained with one example of each class for 1000 cycles. The distribution of classifications between the four classes may be seen in figure 6.4.1.2.2. It is evident that all the neurogenic action potentials are wrongly classified as triphasic normals.

Figure 6.4.1.2.2 Competitive classification of four MUAP types (1).



The network was retrained with differing learning rates and bias time constants. The best set of results obtained consisted of 2 triphasic normals misclassified as neurogenics. This is a 40% misclassification rate for the triphasic class. The distribution of the classifications may be viewed in figure 6.4.1.2.3.

Again the network was retrained using two training vectors per class. This retraining allowed 100% classification of 5 inputs for each class. The distribution of classifications may be seen in figure 6.4.1.2.4.

Figure 6.4.1.2.3 Competitive classification of four MUAP types (2).

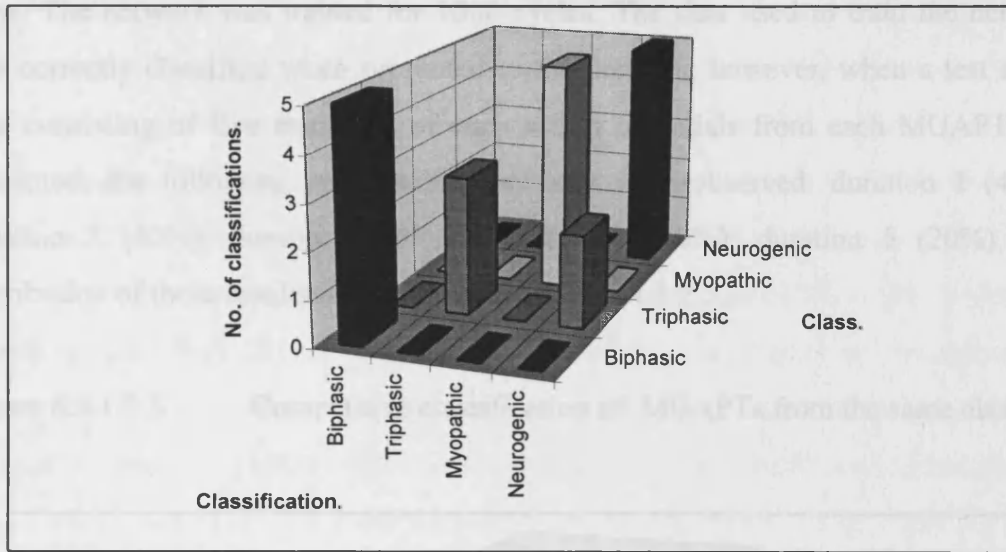
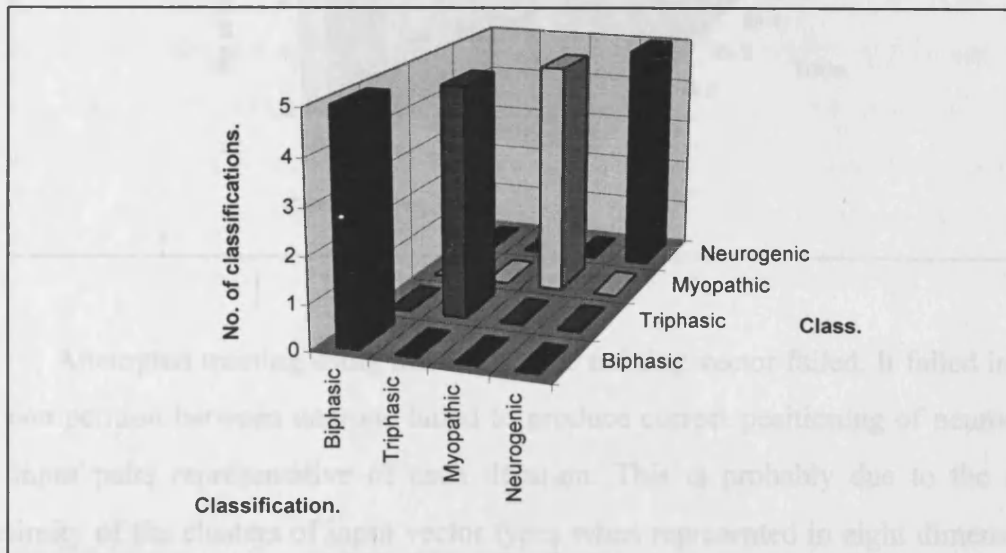


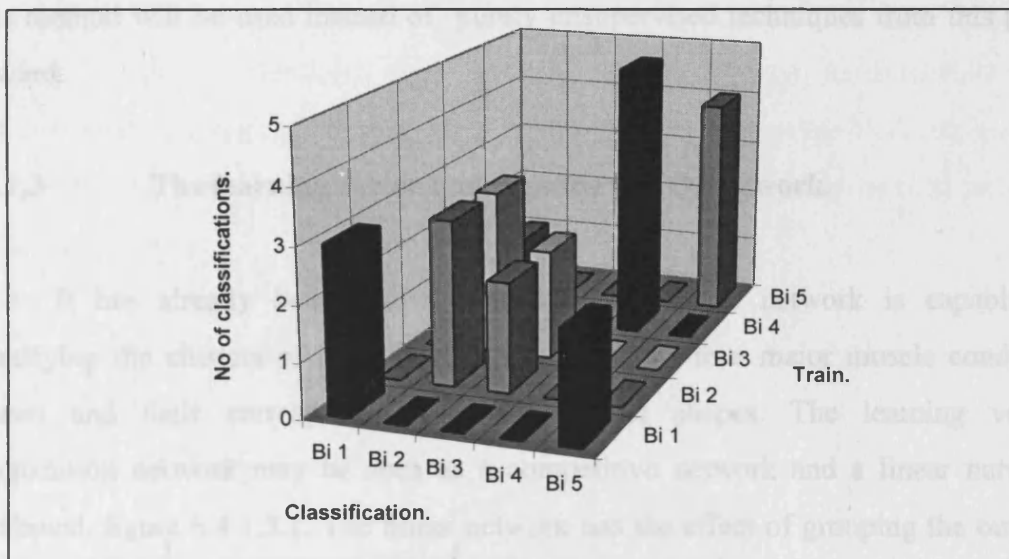
Figure 6.4.1.2.4 Competitive classification of four MUAP types (3).



All of the previous tests in this section use only a single MUAP train per class. In order that this network be tested more thoroughly, more MUAPTs must be represented. A good test is the ability of the network to differentiate between action potentials from trains within the same class.

A network was trained for this purpose. The training data consisted of one action potential from each of five different standard durations within the biphasic class. The network was trained for 1000 cycles. The data used to train the network was correctly classified when presented to the network, however, when a test set of data consisting of five examples of each action potentials from each MUAPT was presented, the following misclassification rates were observed: duration 1 (40%); duration 2 (60%); duration 3 (0%); duration 4 (40%); duration 5 (20%). The distribution of these results may be seen in figure 6.4.1.2.5.

Figure 6.4.1.2.5 Competitive classification of MUAPTs from the same class.



Attempted training using more than one training vector failed. It failed in that the competition between neurons failed to produce correct positioning of neurons in the input pairs representative of each duration. This is probably due to the close proximity of the clusters of input vector types when represented in eight dimensions. Moving the analysis into three dimensions by employing self organising maps may help to alleviate this somewhat.

However, the purpose of the self organising map is to trace the progress of the inputs in a multidimensional space. This is achieved by a neighbourhood of neurons

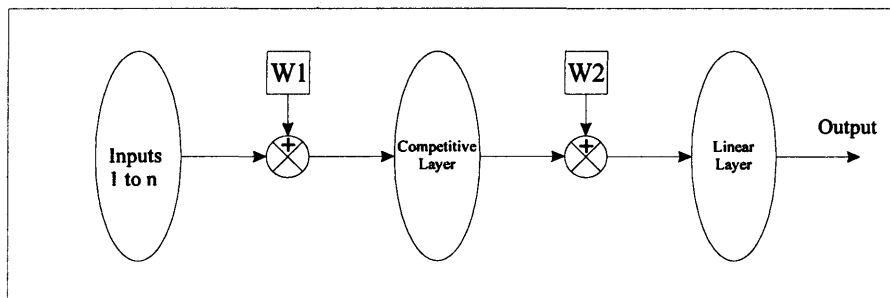
firing around the responsive neuron, but with less strength. This allows the progress of firing neurons to be traced as different inputs are presented to the network.

The purpose of the self organising map is to map the topological characteristics of a system or set of inputs. The map will identify any naturally occurring groups of input and classify them as such. The self organising map or network will not necessarily classify the data in the way intended for differentiation purposes. It is stated by Fausett (Fausett, 1994) that non-supervised (i.e. self organising) techniques should not be used for pattern recognition for the above reason. Instead they should be used in conjunction with supervised techniques to ensure the clusters formed are those desired. Learning vector quantization is an example of such a combination of unsupervised and supervised learning techniques. This method will be used instead of purely unsupervised techniques from this point forward.

6.4.1.3 The learning vector quantization (LVQ) network.

It has already been shown that the competitive network is capable of identifying the clusters of inputs representative of the four major muscle condition classes and their corresponding action potential shapes. The learning vector quantization network may be seen as a competitive network and a linear network combined, figure 6.4.1.3.1. The linear network has the effect of grouping the outputs of the competitive network as specified by the user. This is the supervised element of the otherwise unsupervised network.

Figure 6.4.1.3.1 - The LVQ network architecture.

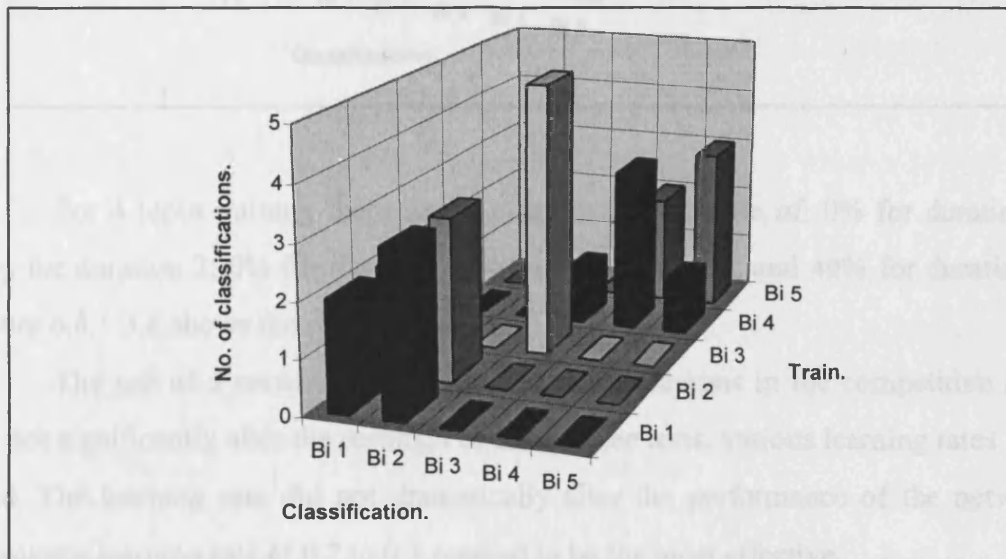


The effect of this is that more neurons may be used to classify the input data than the number of output classes. All outputs are grouped into the desired output classes by the linear layer.

In order to test the learning vector quantization network's performance the problem of differentiating between MUAPs from different trains in the same class was addressed. A learning vector quantization network consisting of 5 competitive neurons (one per standard MUAP duration) and 5 linear neurons was trained for 1000 cycles. The training data consisted of 10 example simulated biphasic action potentials, 2 each from each of the five duration standards.

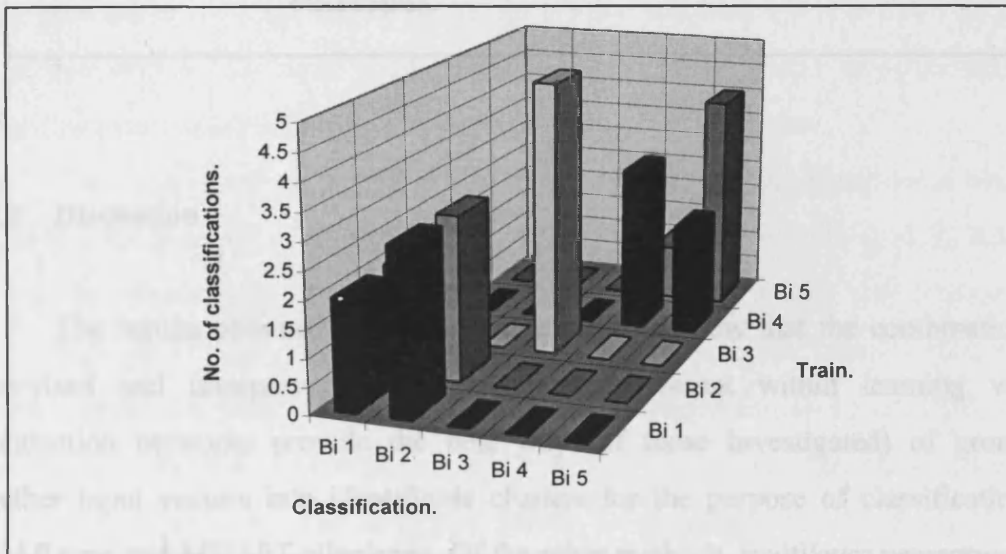
Upon completion of the training a test set of data comprised of five examples of each duration of biphasic action potential was presented to the network for classification. The results obtained were as follows: for duration 1 there was 60% misclassification; for duration 2 there was 40% misclassification; for duration 3 there was 0% misclassification; for duration 4 there was 40% misclassification; and for duration 5 there was 40% misclassification. These distributions may be seen in figure 6.4.1.3.2.

Figure 6.4.1.3.2 LVQ discrimination between MUAPTs from the same class (1).



The same test was repeated, retraining the network with first three, then four input vectors per duration of MUAP. For 3 input training: duration 1 had a misclassification rate of 40%; duration 2 had a misclassification rate of 0%; duration 3 had a misclassification rate of 0%; duration 4 had a misclassification rate of 40%; and duration 5 had a misclassification rate of 40%. These results may be seen in figure 6.4.1.3.3.

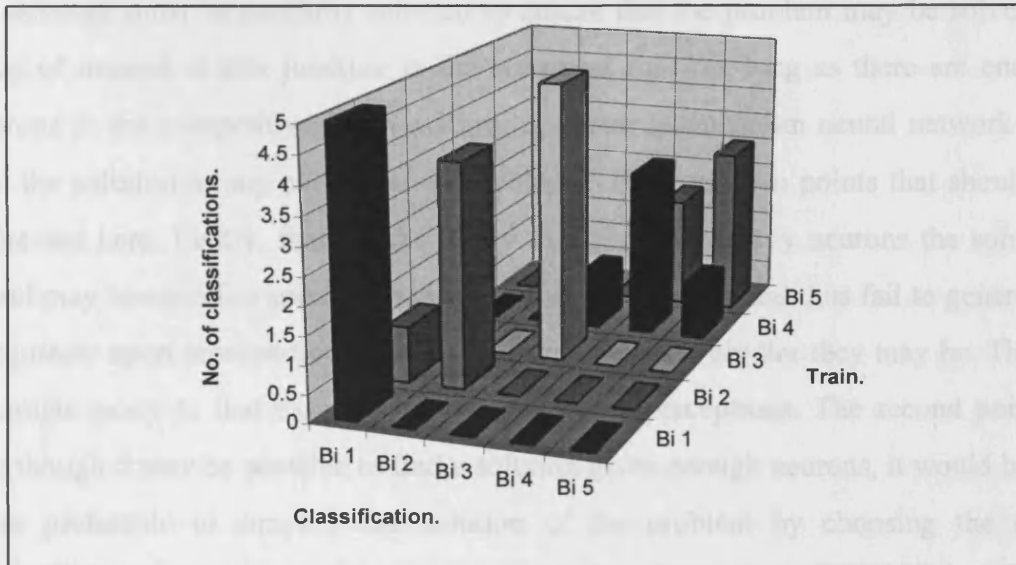
Figure 6.4.1.3.3 LVQ discrimination between MUAPTs from the same class (2).



For 4 input training there was a misclassification rate of: 0% for duration 1; 20% for duration 2; 0% for duration 3; 40% for duration 4; and 40% for duration 5. Figure 6.4.1.3.4 shows the results.

The use of a network containing 10 and 15 neurons in the competitive layer did not significantly alter the results. For all of these tests, various learning rates were used. The learning rate did not dramatically alter the performance of the network, however a learning rate of 0.2 to 0.3 seemed to be the most effective.

Figure 6.4.1.3.4 LVQ discrimination between MUAPTs from the same class (3).



6.4.2 Discussion

The results obtained in the last three sections show that the combination of supervised and unsupervised learning methods present within learning vector quantization networks provide the best way (of those investigated) of grouping together input vectors into identifiable clusters for the purpose of classification of MUAP type and MUAPT allegiance. Of the other methods, multilayer perceptrons do not work well at all, and though competitive networks work reasonably there are limitations with them. The main limitation is that of the number of competitive neurons. The number of classes is determined to a large extent by the input data, but also by the number of neurons present in the competitive layer. The clusters formed will not necessarily be those desired by the user: they will be naturally occurring ones. It is likely that if more neurons than the number of required classes are used, more than the required classes will be isolated, though null neurons may occur. This problem is overcome by the LVQ network, thus the LVQ is more suited to pattern recognition.

The results also indicate that a neural network is not capable of classifying any set of inputs in the way that the user would want them classified. Thus, the inputs to the network must be carefully selected to ensure that the problem may be solved. A point of interest at this juncture is the statement that “as long as there are enough neurons in the competitive layer, a learning vector quantization neural network will find the solution to any classification problem”. There are two points that should be addressed here. Firstly, there is the worry that given too many neurons the solution found may become too specific to the data used for training and thus fail to generalise adequately upon presentation of other data sets, however similar they may be. This is a similar worry to that expressed about multilayer perceptrons. The second point is that though it may be possible to find a solution given enough neurons, it would be far more preferable to simplify the solution of the problem by choosing the most appropriate inputs. Doing so will minimise the learning time and the network dimensions, and make the problem more straightforward in general.

The inputs used up to this point have consisted of eight dimensional vectors. Vectors that consist of a lower dimension are easier to deal with. The eight features used to describe a segment of MUAP activity are correlated with one another to a certain extent. It is desirable that the number of inputs to the neural networks be reduced whilst the maximum possible amount of information about each MUAP is retained. One method of achieving this aim is to remove correlated information, i.e. information repeated in more than one feature, by replacing the describing features with orthogonal (uncorrelated) factors calculated from the features themselves. This will have the effect of reducing the number of dimensions of our input vectors, whilst retaining a maximum amount of useful information from the describing features.

6.4.3 Orthogonal factors as network inputs.

Two ways of creating orthogonal factors from correlated features are diagonal factor analysis and principal component analysis respectively. There are characteristics of these methods which reflect upon their suitability for the application in mind: these are discussed below.

In their method for automatic decomposition of the EMG of 1991, Loudon & Jones applied the method of diagonal factor analysis (Appendix 1) to the problem of producing uncorrelated factors from correlated features. The method produces a number of factors less than the original number of features. The new factors consist of appropriately weighted features and their number, their choice and their order are dictated by the data being orthogonalised.

Preference was given to the above method by Loudon & Jones because it required a relatively small amount of processor time in comparison with principal component analysis. This is no longer an important consideration. At the time that the method was devised, the speed of CPUs was considerably slower. Today's technology ensures that the processor time required to perform principal component analysis is negligible as a constituent part of an analysis algorithm. It is now more important to apply the most appropriate method. Time considerations are not so weighty, but they do still occur in some cases.

Diagonal factor analysis and PCA both reduce the number of describing factors by creating an approximation to the original data. The question is, which method is most suited to our application?

The main problem with diagonal factor analysis is that the number of orthogonal factors generated from each orthogonalised set of inputs will not necessarily be the same. This will cause problems in neural network classification, should a network be trained using five dimensional inputs, i.e. each MUAP is represented by the first five diagonal factors and their associated weights, and be presented with a set of MUAPs for classification where each MUAP is represented in six dimensions, the network would be unable to operate with the data. The dimension of the input vectors must remain the same for the trained network to accurately classify the data. A second problem with diagonal factor analysis is that whilst the number of factors generated is less than the original number of describing features, it is only just so. There are eight describing features, and these are often reduced to five or six diagonal factors. It is desirable that the reduction in dimension of input be greater than two or three dimensions.

Principal component analysis (Appendix 2) is more suited because the majority of variance in the inputs is accounted for in the 1st component and the

majority of the remainder occurs within the earlier components, hence fewer are required to account for most of the information available. This addresses the last problem apparent in diagonal factor analysis, a small number of components may be used to describe each MUAP, whilst retaining the majority of the information portrayed by the eight describing features.

A further important fault with the method of diagonal factor analysis is that the features chosen as factors may not always be the same. This will depend upon the data set being orthogonalised. A change in the chosen features will represent a change in the distribution of inputs within the input space of the network. Should this occur, once again the trained network will be unable to classify the data because the inputs for classification will be representative of a different task or problem.

This problem will not occur when using PCA. Overall the PCA method is more suited to the orthogonalisation of features for use with neural networks, than is the diagonal factor analysis method.

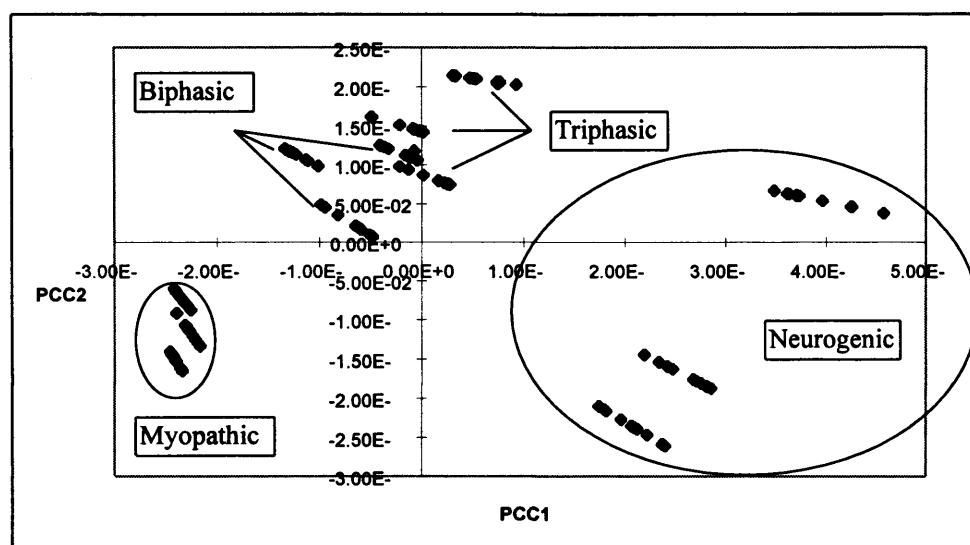
6.4.3.1 The generation of orthogonal features.

As was stated previously the method for orthogonalising the input data deemed most suitable is principal component analysis. The mathematics behind the method may be seen in Appendix 2, whilst its application is described here.

Principal component analysis was carried out on each set of inputs. In order that the distribution of inputs was related from set to set the same database was used to calculate the components from. The standard database contained 120 action potentials consisting of normal biphasics, normal triphasics, myopathics and neurogenics, all of typical clinical characteristics. As before, these classes were subdivided into MUAPs with different duration templates, this time three different durations per class were present. Simulated non-overlapping, noise-free data was used. Initially the standard database was used alone; subsequently more inputs were added for the purpose of different investigations.

This standard database was used to train and test the different neural networks. Two dimensional representations of the new orthogonal inputs may be seen below. The whole data set is shown in figure 6.4.3.1.1

Figure 6.4.3.1.1 - PCA representation of the standard database, in 2D.



It is clear to see that the different types of action potentials form separate clusters. These are clearly marked in figure 6.4.3.1.1. The behaviour of the clusters may be remarked upon as follows: the appearance of the clusters in straight lines is due to the lack of variation in duration in each class. This affects two of the original eight features directly. However, there is a difference in position within each class for the three chosen durations: any further variation around these durations would cause the phenomenon observed within the clusters to disappear. The variation in position observed within the clusters is due to the members of each cluster differing in amplitude. The variation in position is as follows: the point representing the smallest action potential resides at the top left of the cluster, whilst the point representing the largest action potential in the cluster is the bottom right point. The position of other MUAPs in the class varies between these points linearly.

It may be seen that factors orthogonalised in this way present good inputs to neural networks because they are lower in dimension and consist of well separated clusters. It was found that the first three principal components accounted for approximately 96% of the variance between inputs. Further principal components added very little information, but would increase the complexity of the problem. It was decided to use three principal components to represent the data, thus providing three dimensional inputs to the neural networks. The method of representation is as

follows: each input is reconstructed by the sum of the products of the principal components and its associated principal component coefficients, thus each individual input may be represented by its own principal component coefficients, numbering three in this case.

6.4.3.2 The multilayer perceptron with orthogonal inputs.

Multilayer and single layer perceptron networks of varying dimension were trained to attempt a solution to the problem. As before, no matter how many neurons or layers were used, the sum of squared errors failed to reach anywhere near an acceptable level, thus no solution was found. This was the case irrespective of learning rate, momentum and training time. It is thus apparent that the application of multilayer perceptrons to the problem, in this way, will not yield a solution.

6.4.3.3 The LVQ network with orthogonal inputs.

The data used in the following three tests is that contained within the standard database of four classes of action potential, after orthogonalisation. The database was split into two halves equal in content. One of the two sets was used for network training, the other for testing the trained network.

Test 1 - Classifying data into MUAP classes.

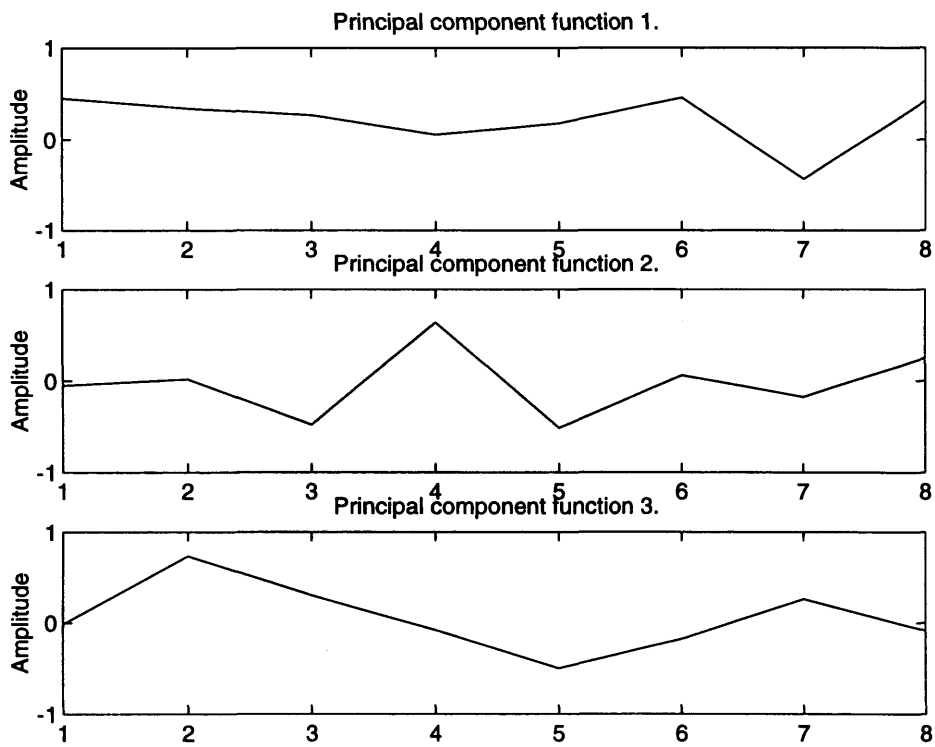
A learning vector quantization neural network consisting of 3 input nodes, 4 competitive neurons and 4 linear output neurons was trained using the data shown in table 6.4.3.3.1, for the purpose of differentiating between the four MUAP classes (normal biphasic, normal triphasic, myopathic and neurogenic). The principal component functions associated with both the training and test data are shown in figure 6.4.3.3.1. The functions consist of eight values each because they are calculated from the eight features used to represent each MUAP.

Table 6.4.3.3.1

The training data.

MUAPT	PCC1	PCC2	PCC3
biphasic	-4.89E-02	8.33E-03	1.72E-01
duration 1	-8.16E-02	3.50E-02	1.40E-01
	-9.42E-02	4.52E-02	1.27E-01
	-5.06E-02	9.71E-03	1.71E-01
	-4.80E-02	7.62E-03	1.73E-01
biphasic	-1.25E-01	1.15E-01	5.62E-02
duration 2	-1.29E-01	1.17E-01	5.32E-02
	-1.33E-01	1.21E-01	4.90E-02
	-1.11E-01	1.05E-01	6.88E-02
	-1.22E-01	1.13E-01	5.88E-02
biphasic	-3.20E-02	1.21E-01	1.22E-01
duration 3	-3.58E-02	1.23E-01	1.19E-01
	-3.90E-03	1.06E-01	1.47E-01
	-9.91E-03	1.09E-01	1.42E-01
	-3.89E-02	1.24E-01	1.16E-01
triphasic	-2.12E-02	9.78E-02	-8.82E-03
duration 1	2.26E-02	7.69E-02	1.20E-02
	2.25E-02	7.69E-02	1.19E-02
	1.67E-02	7.97E-02	9.18E-03
	2.62E-02	7.52E-02	1.37E-02
triphasic	-4.79E-02	1.61E-01	-6.66E-02
duration 2	-4.88E-02	1.61E-01	-6.69E-02
	-2.09E-02	1.51E-01	-5.66E-02
	1.29E-03	1.43E-01	-4.85E-02
	-5.81E-03	1.45E-01	-5.11E-02
triphasic	7.41E-02	2.04E-01	-6.88E-02
duration 3	3.08E-02	2.14E-01	-8.27E-02
	5.11E-02	2.11E-01	-7.73E-02
	5.29E-02	2.10E-01	-7.68E-02
	5.34E-02	2.10E-01	-7.66E-02
myopathic	-2.46E-01	-1.41E-01	-5.48E-02
duration 1	-2.43E-01	-1.46E-01	-5.20E-02
	-2.41E-01	-1.51E-01	-4.93E-02
	-2.44E-01	-1.44E-01	-5.30E-02
	-2.36E-01	-1.63E-01	-4.29E-02
myopathic	-2.39E-01	-9.19E-02	-7.85E-02
duration 2	-2.17E-01	-1.34E-01	-5.44E-02
	-2.30E-01	-1.09E-01	-6.87E-02
	-2.28E-01	-1.12E-01	-6.71E-02
	-2.31E-01	-1.07E-01	-6.98E-02
myopathic	-2.37E-01	-6.85E-02	-8.37E-02
duration 3	-2.41E-01	-6.25E-02	-8.73E-02
	-2.29E-01	-8.23E-02	-7.54E-02
	-2.31E-01	-7.82E-02	-7.79E-02
	-2.32E-01	-7.65E-02	-7.89E-02
neurogenic	1.96E-01	-2.28E-01	5.70E-02
duration 1	1.82E-01	-2.16E-01	4.77E-02
	1.79E-01	-2.15E-01	4.64E-02
	2.40E-01	-2.61E-01	8.48E-02
	2.37E-01	-2.59E-01	8.29E-02
neurogenic	2.75E-01	-1.81E-01	1.90E-02
duration 2	2.42E-01	-1.60E-01	1.74E-03
	2.19E-01	-1.45E-01	-1.01E-02
	2.81E-01	-1.85E-01	2.17E-02
	2.68E-01	-1.77E-01	1.53E-02
neurogenic	3.61E-01	6.31E-02	-1.09E-01
duration 3	4.25E-01	4.60E-02	-8.93E-02
	3.48E-01	6.66E-02	-1.13E-01
	3.73E-01	5.99E-02	-1.05E-01
	3.97E-01	5.37E-02	-9.80E-02

Figure 6.4.3.3.1 The 3 associated principal component functions.

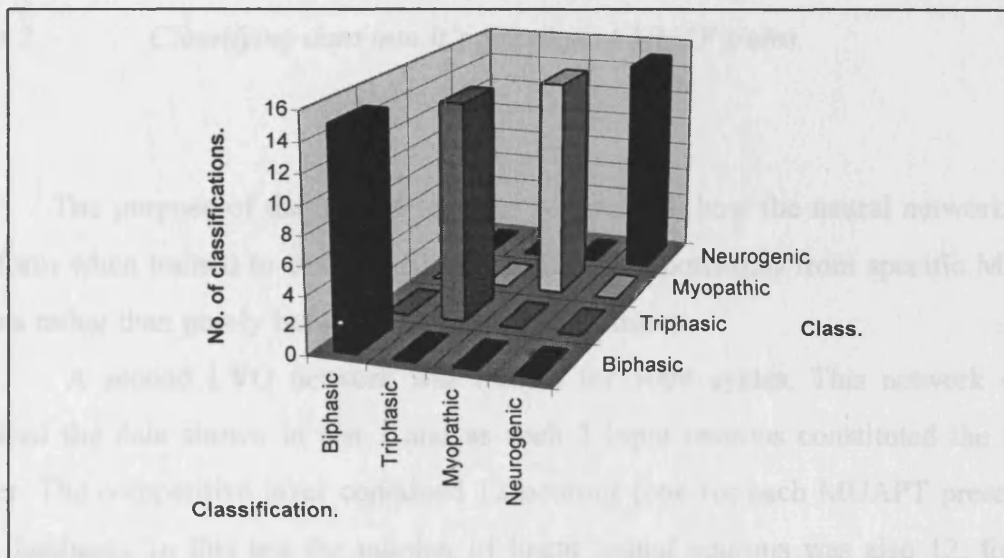


The data consists of the first 3 principal component coefficients for the database used previously. The network was trained for 5000 cycles.

The purpose of this test was to attempt to train the network to distinguish between the four classes of action potential present within the database. The network was provided with a set of ranges within which all its inputs would fall, and a set of target vectors corresponding to the correct class of each input vector.

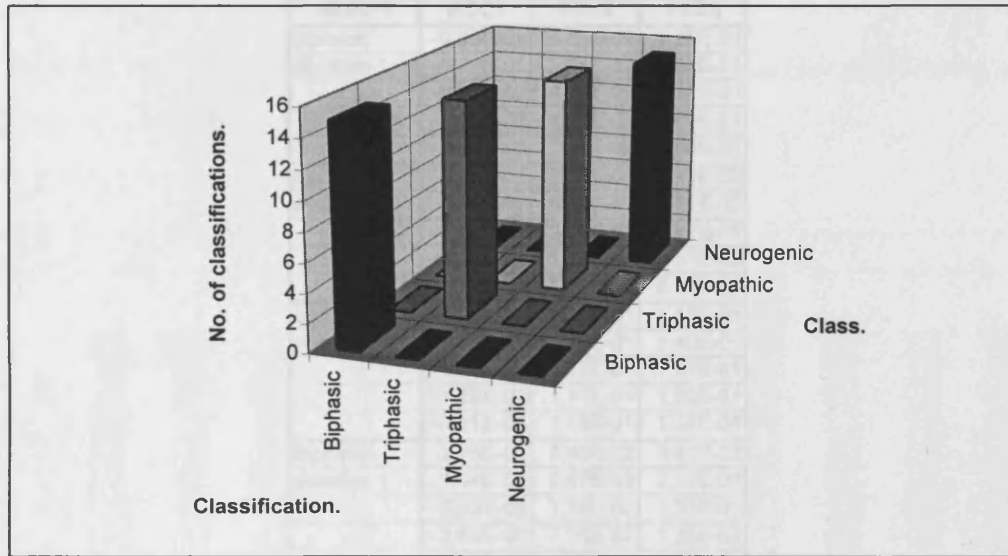
A solution was found prior to the completion of the training period. Upon presentation of the training data to the trained network for classification, 100% accuracy was achieved, see figure 6.4.3.3.2. Again, learning rates between 0.2 and 0.3 were found to be most effective.

Figure 6.4.3.3.2 LVQ identification of class of noiseless simulated training data.



Upon presentation of the test data set (the second set from the standard database) shown in table 6.4.3.3.2, 100% accuracy was achieved also, see figure 6.4.3.3.3.

Figure 6.4.3.3.3 LVQ identification of class of noiseless simulated training data.



Test 2 - Classifying data into it's constituent MUAP trains.

The purpose of the second test was to establish how the neural network will perform when trained to discriminate between action potentials from specific MUAP trains rather than purely between action potential classes.

A second LVQ network was trained for 5000 cycles. This network again utilised the data shown in test 1 and as such 3 input neurons constituted the input layer. The competitive layer contained 12 neurons (one for each MUAPT present in the database). In this test the number of linear output neurons was also 12, for the same reason as was given for the number of competitive neurons present.

After training the data set used to train the network was presented for the purpose of classification. The results gained showed a 98.3% success rate. There was only one misclassification present, see figure 6.4.3.3.4, and that was only a misclassification with respect to MUAP allegiance, not class allegiance. This problem could be overcome by the use of more neurons in the competitive layer.

Table 6.4.3.3.2

The test data.

MUAPT	PCC1	PCC2	PCC3
biphasic	-9.82E-02	4.85E-02	1.23E-01
duration 1	-6.46E-02	2.11E-02	1.57E-01
	-9.78E-02	4.82E-02	1.23E-01
	-6.18E-02	1.89E-02	1.59E-01
	-5.90E-02	1.66E-02	1.62E-01
biphasic	-1.13E-01	1.07E-01	6.71E-02
duration 2	-1.29E-01	1.17E-01	5.32E-02
	-1.01E-01	9.84E-02	7.77E-02
	-1.26E-01	1.16E-01	5.57E-02
	-1.32E-01	1.19E-01	5.06E-02
biphasic	-4.02E-02	1.25E-01	1.15E-01
duration 3	-1.25E-02	1.10E-01	1.40E-01
	-1.56E-02	1.12E-01	1.37E-01
	-1.28E-02	1.11E-01	1.39E-01
	-6.81E-03	1.18E-01	1.34E-01
triphasic	2.75E-02	7.46E-02	1.43E-02
duration 1	1.94E-03	8.67E-02	2.17E-03
	2.53E-02	7.56E-02	1.33E-02
	2.65E-02	7.50E-02	1.38E-02
	-1.25E-02	9.36E-02	-4.67E-03
triphasic	-2.46E-03	1.44E-01	-4.99E-02
duration 2	-7.36E-03	1.46E-01	-5.17E-02
	-8.34E-03	1.46E-01	-5.20E-02
	2.11E-03	1.42E-01	-4.82E-02
	-9.69E-05	1.43E-01	-4.90E-02
triphasic	7.64E-02	2.06E-01	-7.05E-02
duration 3	7.37E-02	2.06E-01	-7.12E-02
	9.25E-02	2.03E-01	-6.62E-02
	4.69E-02	2.11E-01	-7.84E-02
	3.34E-02	2.14E-01	-8.20E-02
myopathic	-2.42E-01	-1.48E-01	-5.10E-02
duration 1	-2.34E-01	-1.66E-01	-4.12E-02
	-2.45E-01	-1.44E-01	-5.35E-02
	-2.36E-01	-1.62E-01	-4.33E-02
	-2.40E-01	-1.53E-01	-4.80E-02
myopathic	-2.19E-01	-1.30E-01	-5.69E-02
duration 2	-2.27E-01	-1.15E-01	-6.53E-02
	-2.24E-01	-1.21E-01	-6.21E-02
	-2.21E-01	-1.25E-01	-5.94E-02
	-2.21E-01	-1.25E-01	-5.94E-02
myopathic	-2.31E-01	-7.86E-02	-7.76E-02
duration 3	-2.42E-01	-6.07E-02	-8.84E-02
	-2.26E-01	-8.82E-02	-7.18E-02
	-2.39E-01	-6.45E-02	-8.61E-02
	-2.35E-01	-7.26E-02	-8.12E-02
neurogenic	2.07E-01	-2.36E-01	6.36E-02
duration 1	2.09E-01	-2.38E-01	6.53E-02
	2.12E-01	-2.40E-01	6.72E-02
	1.74E-01	-2.11E-01	4.32E-02
	2.22E-01	-2.47E-01	7.33E-02
neurogenic	2.82E-01	-1.86E-01	2.26E-02
duration 2	2.71E-01	-1.78E-01	1.66E-02
	2.34E-01	-1.55E-01	-2.52E-03
	2.47E-01	-1.63E-01	4.50E-03
	2.86E-01	-1.88E-01	2.43E-02
neurogenic	4.58E-01	3.74E-02	-7.95E-02
duration 3	4.26E-01	4.57E-02	-8.89E-02
	3.71E-01	6.05E-02	-1.06E-01
	3.70E-01	6.07E-02	-1.06E-01
	3.63E-01	6.27E-02	-1.08E-01

The proportion of inputs from the test data set that were correctly classified was 100%, see figure 6.4.3.3.5. This was a good result.

Figure 6.4.3.3.4 LVQ identification of MUAPT of noiseless simulated training data.

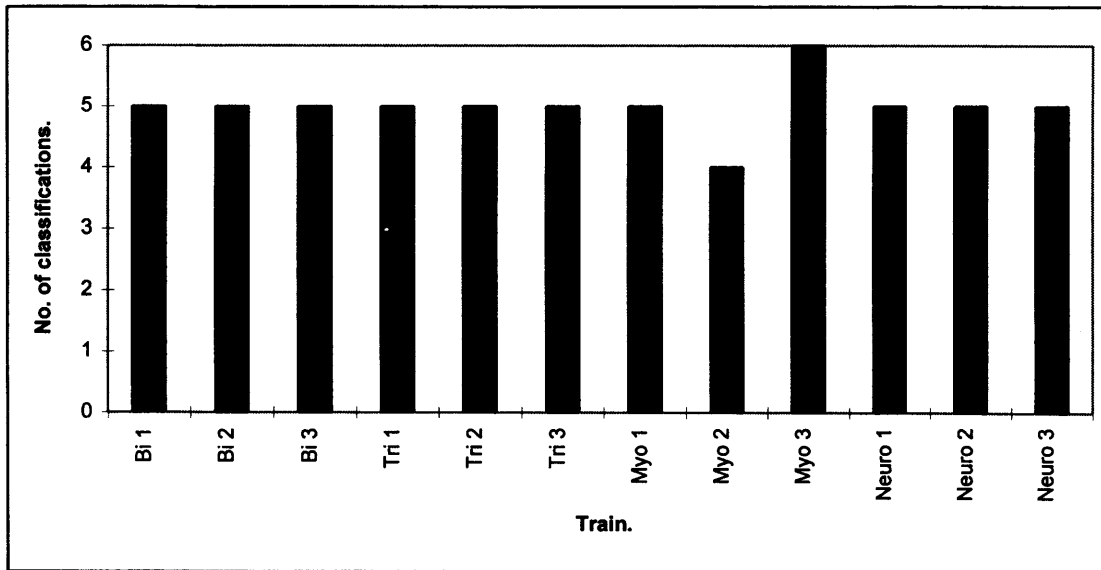
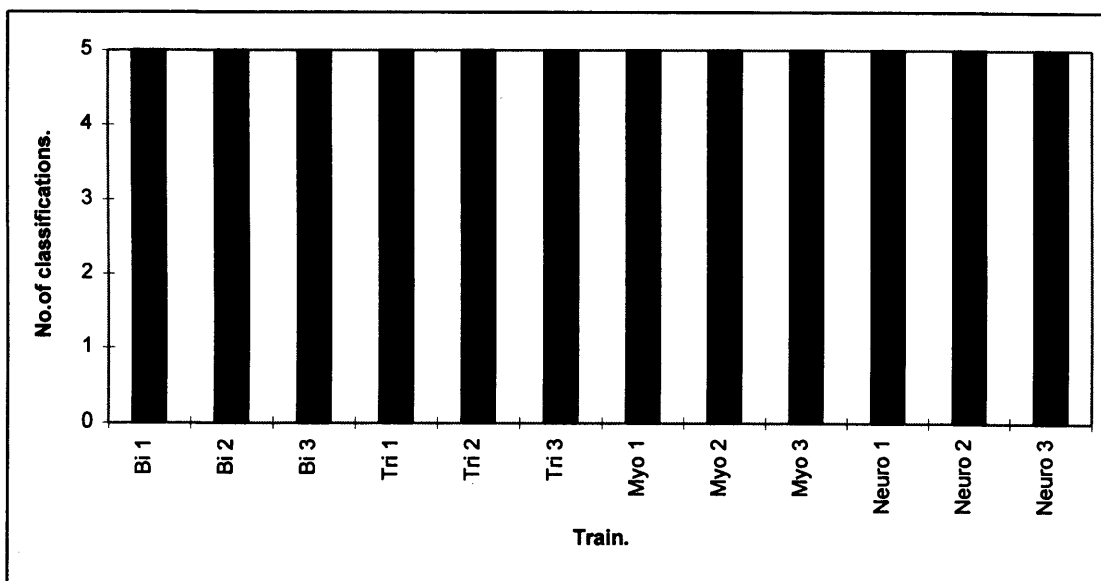


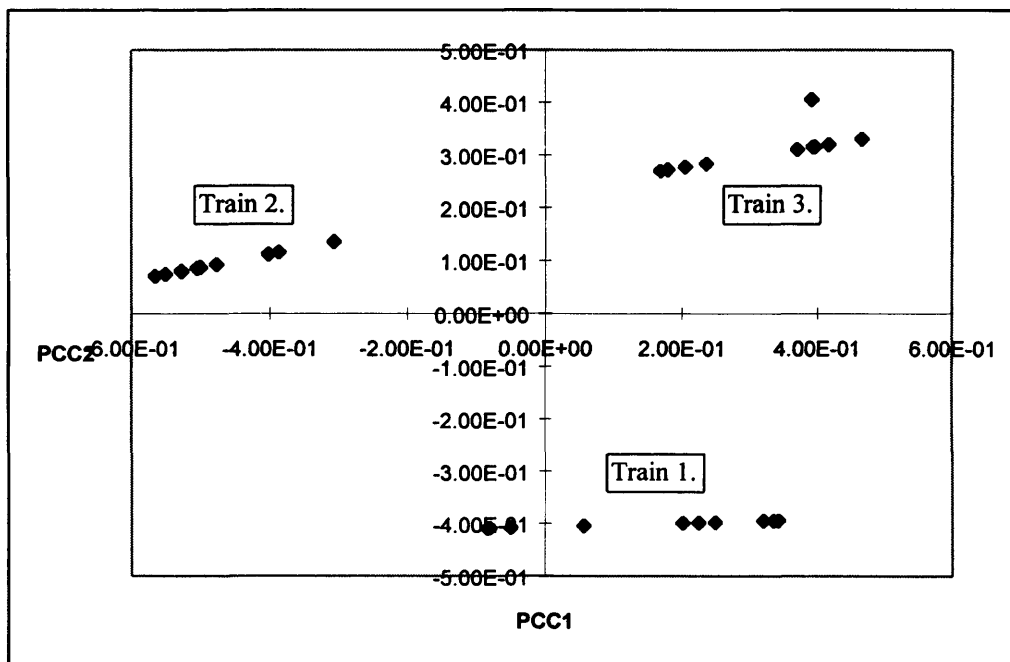
Figure 6.4.3.3.5 LVQ identification of MUAPT of noiseless simulated test data.



Test 3 - *Classifying three different Biphasic MUAPs*

It is easy to see that when the principal component coefficients for one class, in this case normal biphasic, are calculated alone, i.e. without the presence of the other classes held within the standard database, the clusters are easily separable. This may be seen for the biphasic class in figure 6.4.3.3.6.

Figure 6.4.3.3.6 Biphasic principal component clusters.



The object of test 3 was to observe this and to demonstrate that given an input data set, an LVQ network could differentiate between MUAPs from different MUAPTs. A network consisting of 3 input neurons, 3 competitive neurons and 3 linear output neurons was trained for 5000 cycles. The data used for training was the biphasic content of the training data set used in tests 1 & 2. This consisted of 15 examples, five each of 3 different durations. A similar set taken from the test data set of tests 1 & 2 was used to assess the performance of the network after training was completed.

Presentation of the training data to the trained network yielded a correct classification rate of 100%, the same was apparent for the test data set, see figures 6.4.3.3.7 and 6.4.3.3.8.

Figure 6.4.3.3.7 Differentiation between three biphasic trains, training data.

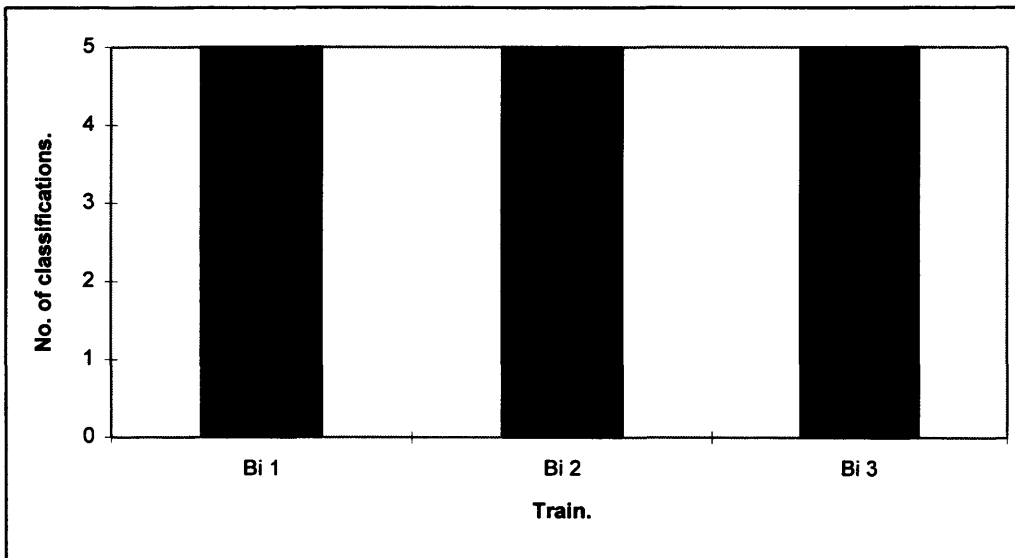
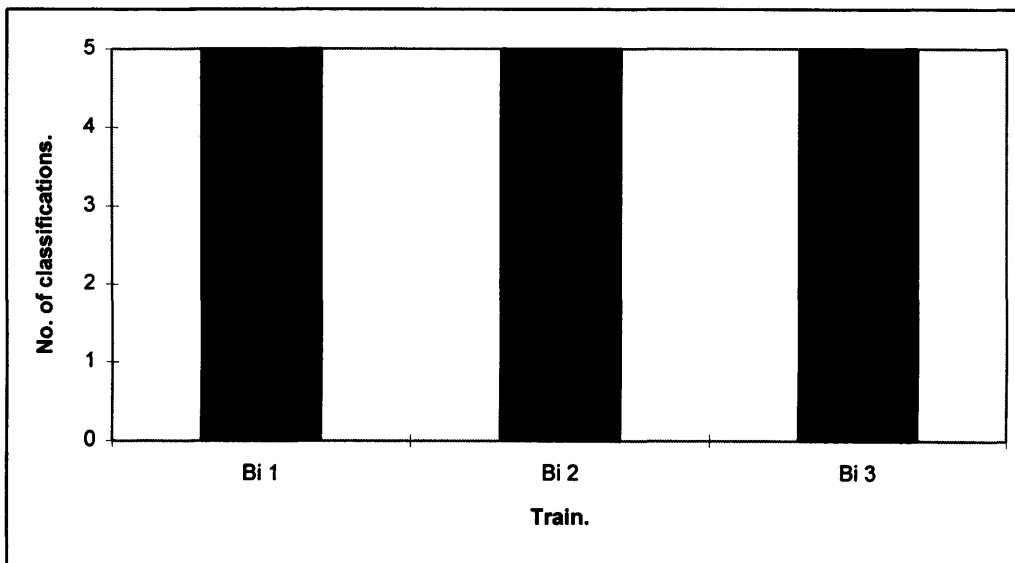


Figure 6.4.3.3.8 Differentiation between three biphasic trains, test data.



6.4.3.4 Testing the LVQ networks.

Real EMG signals are often polluted by the presence of noise and the potentials within them often obscure one another. What is seen by the clinician is the superposition of all such components. It is thus important to test the successful neural networks from section 6.4.3.3, to see how they will cope with noise and overlapping data.

6.4.3.4.1 MUAPs in white noise.

Test 1 - The Identification of noisy data.

The equipment used today to monitor and record EMG information is very sophisticated. As a result of this, the amount of noise present in the recorded signals is of a very low level.

Five different levels of noise were used to investigate the effect of noise upon the neural networks trained to classify clean simulated data. These noise levels are shown in table 6.4.3.4.1.1.

Table 6.4.3.4.1.1 Noise levels for simulated data.

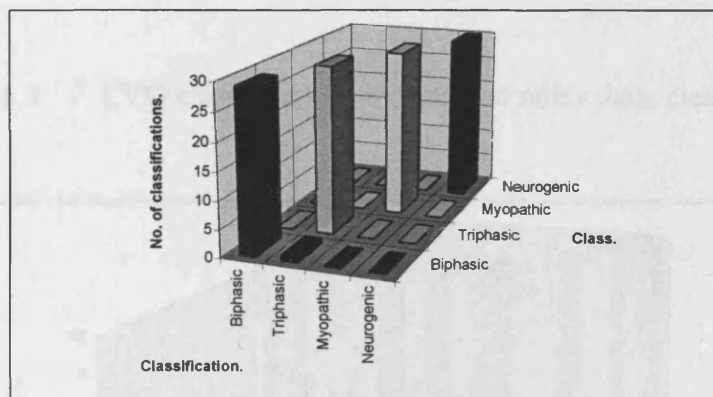
Level	Range (μV)
1	± 5
2	± 10
3	± 20
4	± 30
5	± 40

One EMG signal containing a single train of biphasic action potentials was simulated at each noise level. This was repeated for each standard duration of biphasic template present within the standard database used previously. The number of signals was 15. Action potentials were manually extracted, ten from each signal, and added to the general database. The database was then re-analysed using principal

component analysis and the first three coefficients were again used to represent each data entry.

The purpose of this test was to assess the performance of the neural network trained to identify MU classes, in classifying action potential in the presence of white noise. The entire database was presented to the network and the following results were obtained: for the unpolluted data, 1 misclassification was recorded from the 120 presented inputs; for the noisy data, 10 misclassifications (5, 1, 3, 0, 1, for levels 1 to 5 respectively) were recorded for 150 presented inputs. Thus the misclassification rates were 0.83% and 6.67% respectively. These results are presented in figures 6.4.3.4.1.1 and 6.4.3.4.1.2.

Figure 6.4.3.4.1.1 LVQ class determination in the presence of white noise, clean data.



Test 2 - Classification of MUAPs into MUAPTs in white noise.

The same simulated database as was used in test 1 was utilised in test 2. In this case, the neural network trained in section 6.4.3.3 (Test 2) was presented with the database as its inputs in order to assess its performance in the presence of white noise. The results obtained may be seen in figures 6.4.3.4.1.3 and 6.4.3.4.1.4. For the noise free data, a misclassification rate of 28.3 % was observed, whilst for the noisy data, the overall misclassification rate was 67%. Individual misclassification rates were 73%, 60%, 63%, 67% and 70% for noise levels 1 to 5 respectively.

Figure 6.4.3.4.1.2 LVQ class determination in the presence of white noise, noisy data.

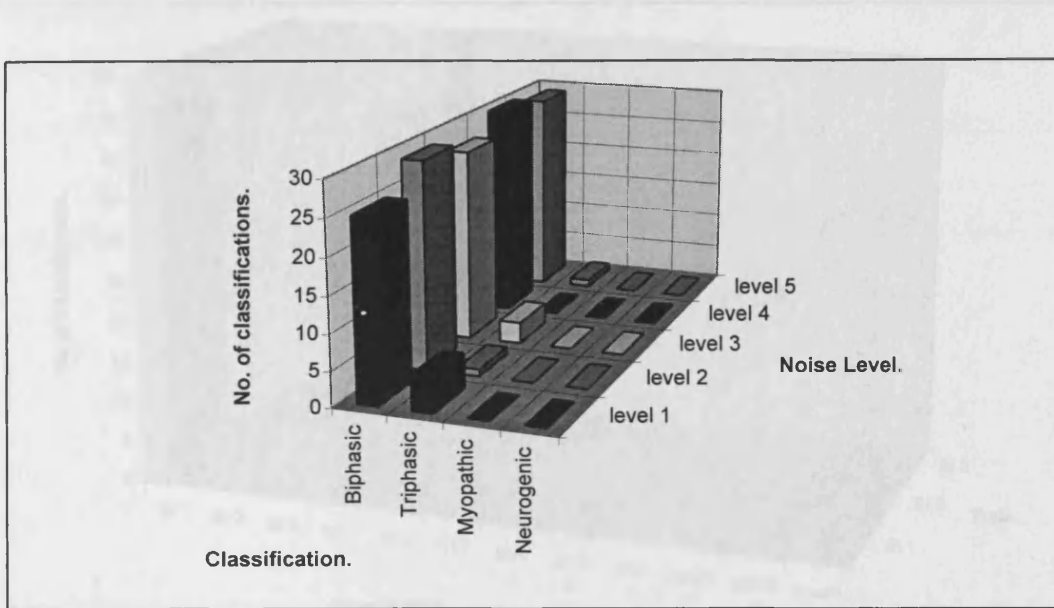


Figure 6.4.3.4.1.3 LVQ classification of clean and noisy data, clean results.

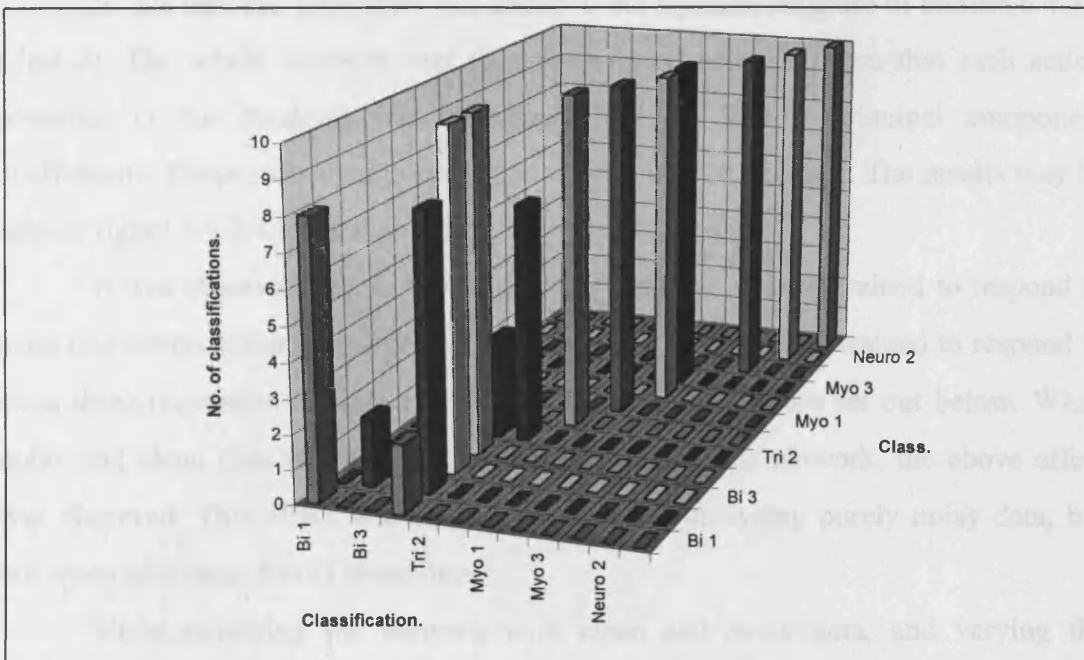
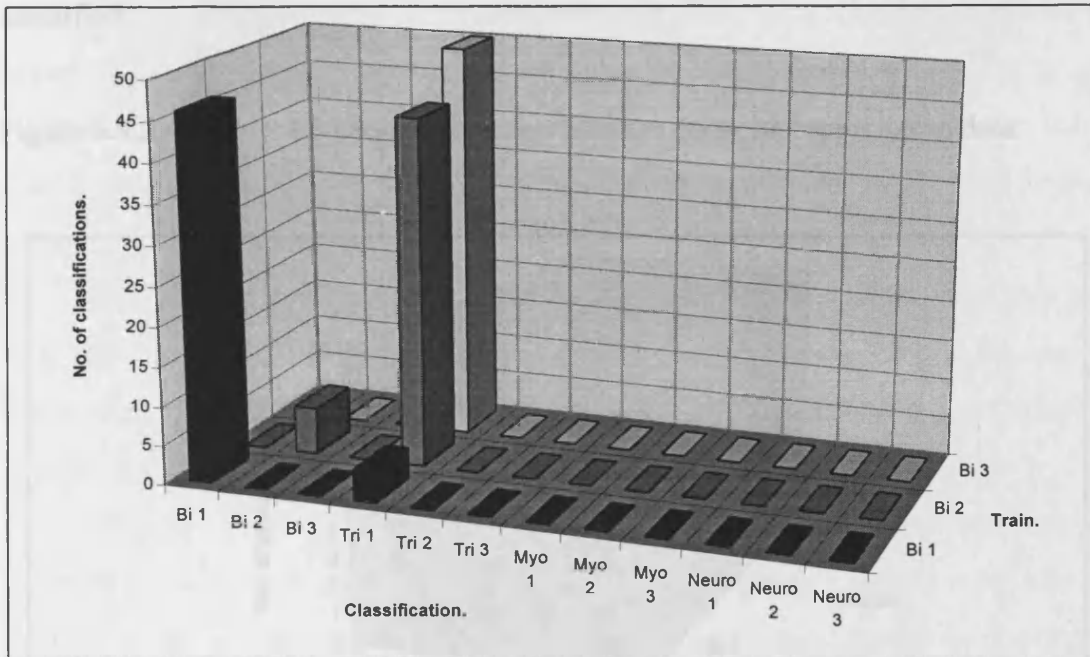


Figure 6.4.3.4.1.4 LVQ classification of clean and noisy data, noisy results.



Test 3 - *Classifying different Biphasic MUAPs.*

In this test, the noisy data was added to the biphasic database of section 6.4.3.3 (Test 3). The whole database was then re-analysed using PCA so that each action potential in the database was represented by its first 3 principal component coefficients. These were then presented to the pre-trained network. The results may be seen in figure 6.4.3.4.1.5 and 6.4.3.4.1.6.

It was observed that in classifying this data the neurons trained to respond to class one action potentials responded to class three, whilst those trained to respond to class three responded to class one. The conditions for this are set out below. When noisy and clean data was analysed simultaneously by the network, the above effect was observed. This effect was also observed when analysing purely noisy data, but not when analysing purely clean data.

Upon retraining the network with clean and noisy data, and varying the number of neurons in the competitive layer of the network, the effect was still observed to some extent. When classifying clean and noisy data, or noisy data alone, the correct groupings were observed. However, when classifying normal data alone,

the effect was observed. It was noticed, however, that the clusters formed contained all MUAPs from the appropriate train, whether or not the trains were correctly identified.

Figure 6.4.3.4.1.5 LVQ differentiation between noisy biphasics, clean data.

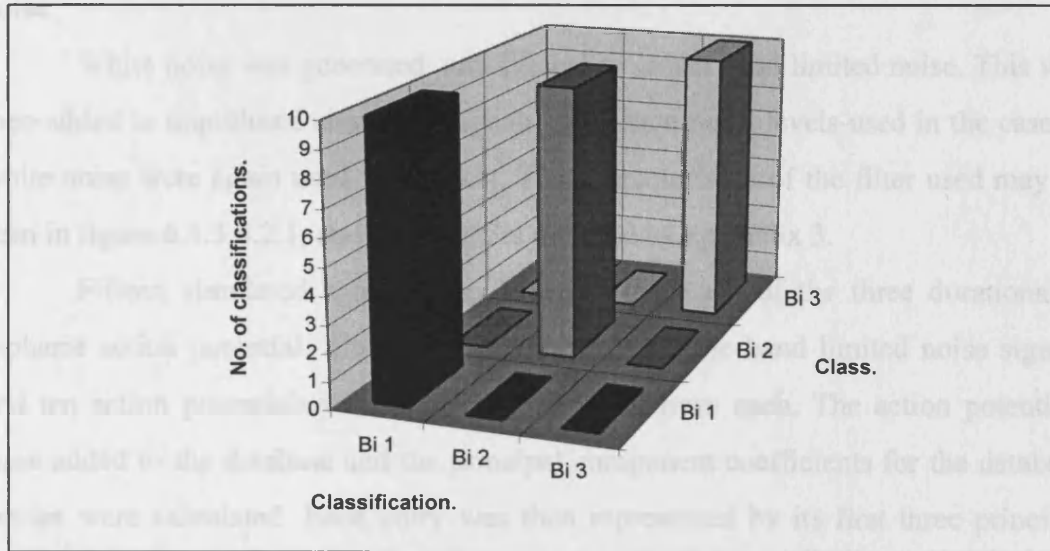
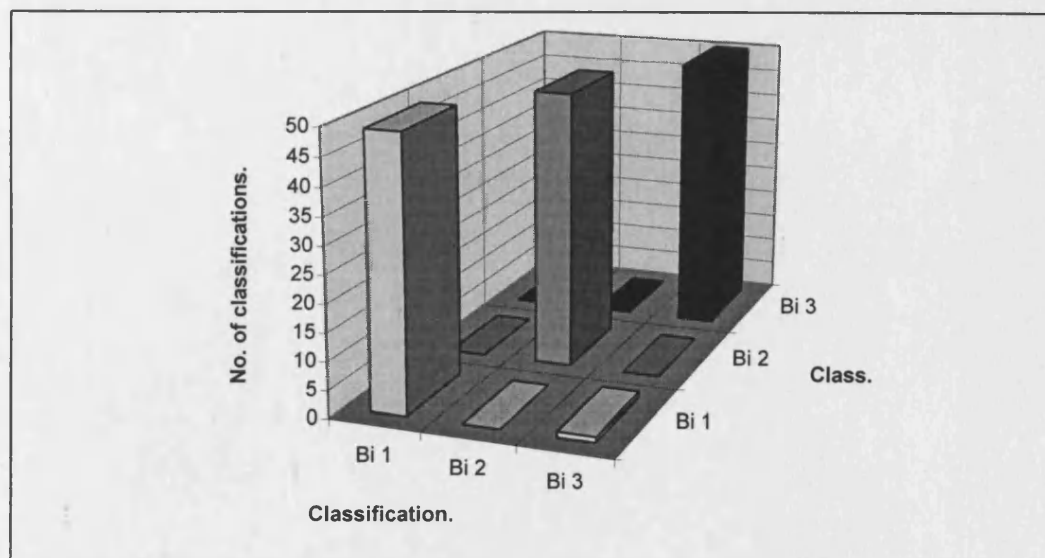


Figure 6.4.3.4.1.6 LVQ differentiation between noisy biphasics, noisy data.



6.4.3.4.2 MUAPs in band limited noise.

It is known that the noise present within the EMG signal is not in fact white in nature, it is band limited. The object of this test is to determine whether the neural network trained to group MUAPs into clusters using noise free data, and tested using data in white noise, will react any differently to data in the presence of band limited noise.

White noise was generated and filtered to create band limited noise. This was then added to unpolluted simulated signals. The same noise levels used in the case of white noise were again used in this test. The characteristics of the filter used may be seen in figure 6.4.3.4.2.1, and its design is outlined in Appendix 3.

Fifteen simulated signals were created: five each of the three durations of biphasic action potential. These were combined with the band limited noise signals and ten action potentials were extracted manually from each. The action potentials were added to the database and the principal component coefficients for the database entries were calculated. Each entry was then represented by its first three principal component coefficients. Test one from section 6.4.3.4.1 was repeated, the results of this test may be seen in figures 6.4.3.4.2.2 and 6.4.3.4.2.3. It is clear that there is little difference between the performance of the network in white and band limited noise.

Figure 6.4.3.4.2.1 The bandpass filter characteristics, ideal and real.

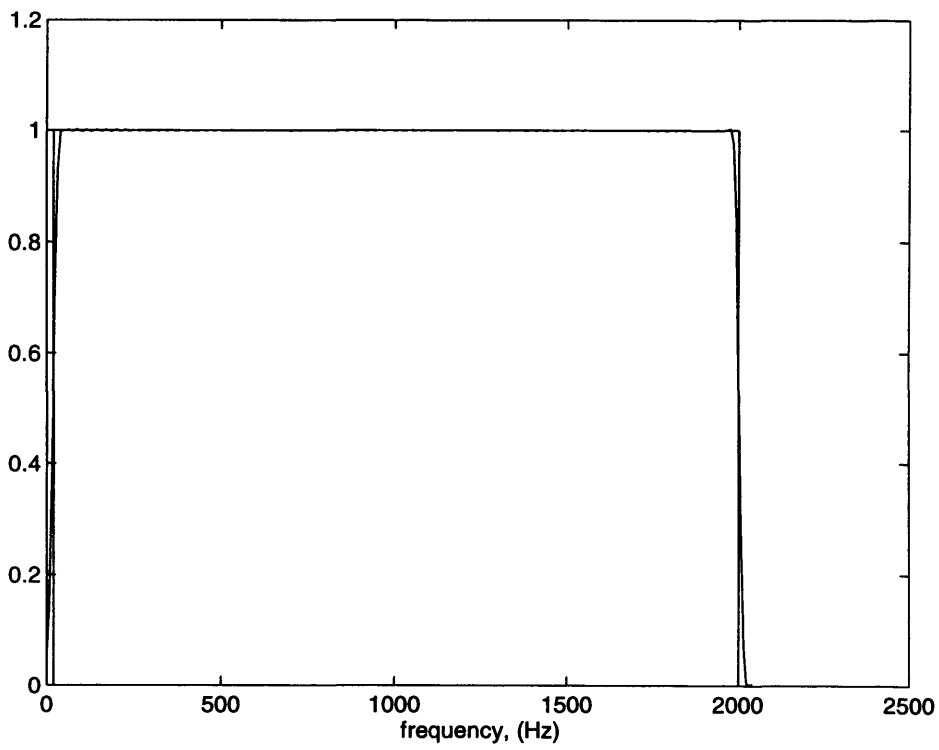


Figure 6.4.3.4.2.2 LVQ class determination in the presence of white noise, clean data.

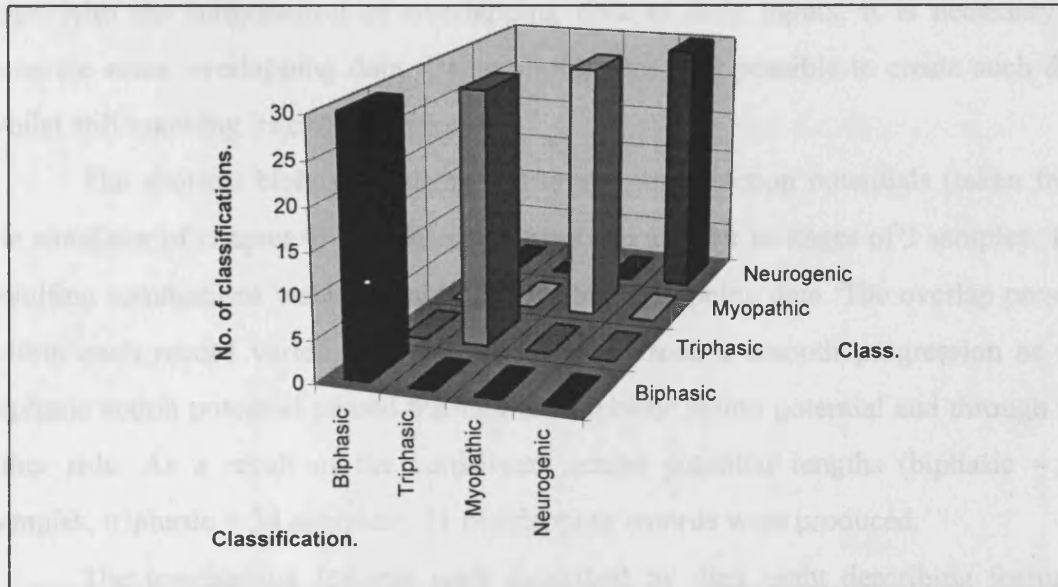
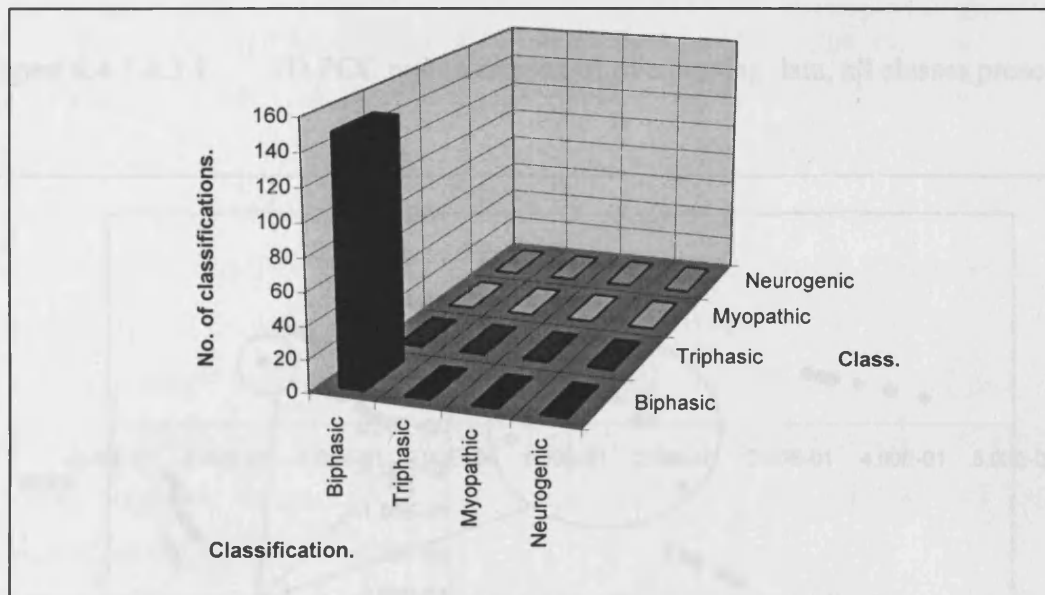


Figure 6.4.3.4.2.3 LVQ class determination in the presence of white noise, noisy data.



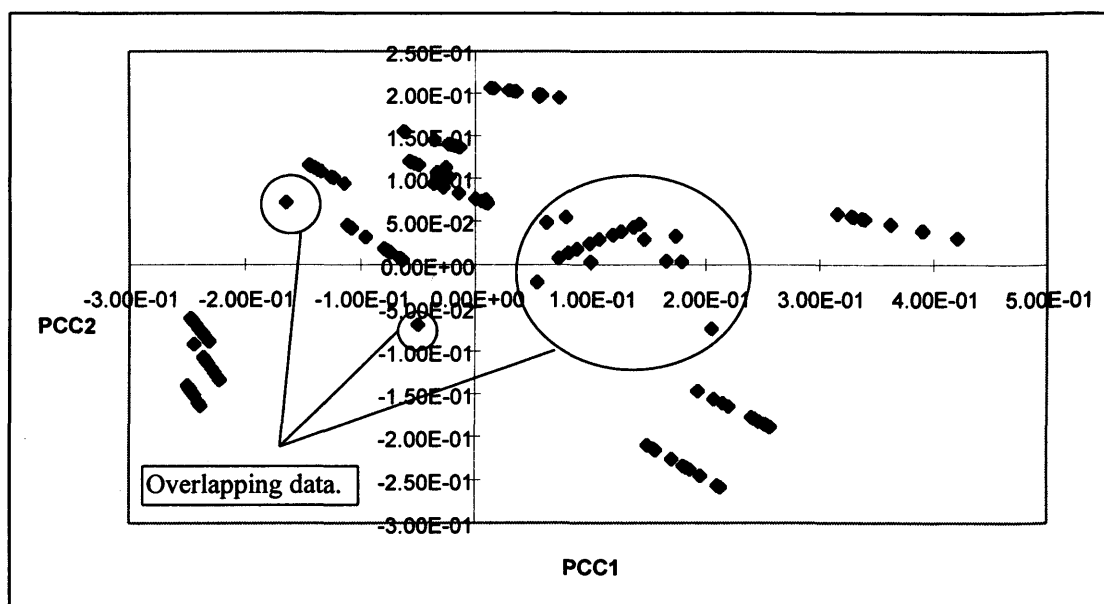
6.4.3.4.3 Identification of overlapping MUAPs.

In order to establish how neural networks trained upon non-overlapping data cope with the introduction of overlapping data at their inputs, it is necessary to generate some overlapping data. Using simulations it is possible to create such data whilst still knowing its characteristics.

The shortest biphasic and the shortest triphasic action potentials (taken from the simulator of chapter 4) were passed across one another in stages of 3 samples. The resulting summations were available for use as overlapping data. The overlap present within each record varied, and the whole set formed a smooth progression as the biphasic action potential passed through the triphasic action potential and through the other side. As a result of the constituent action potential lengths (biphasic = 33 samples, triphasic = 34 samples), 21 overlapping records were produced.

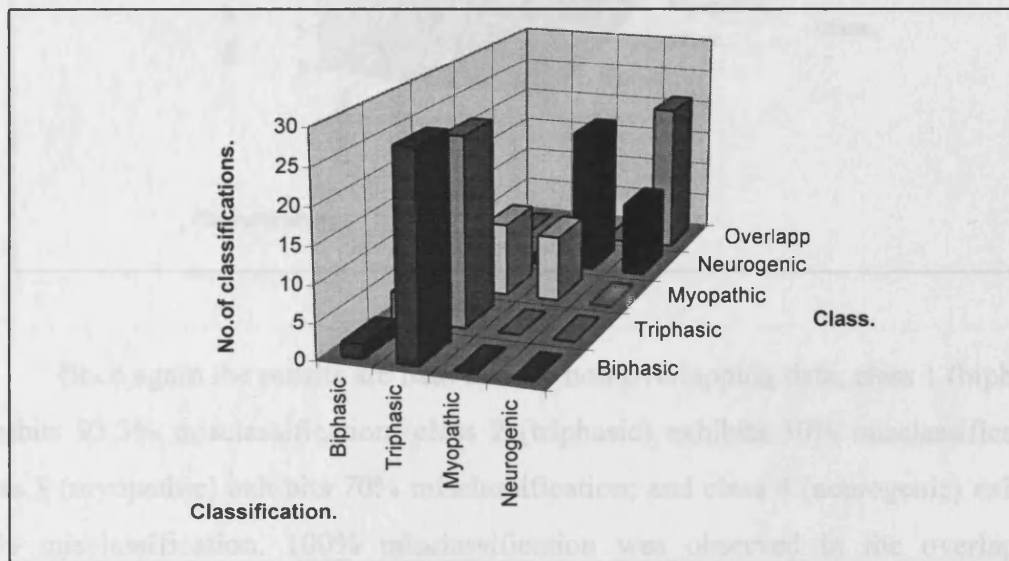
The overlapping features were described by their eight describing features. These were then analysed using principal component analysis in conjunction with the standard database used throughout this section. Each entry was again represented by its first three principal component coefficients. The principal component representation of the entire database in 2D may be seen in figure 6.4.3.4.3.1.

Figure 6.4.3.4.3.1 2D PCC representation of overlapping data, all classes present.



When presented for classification to the normal network trained to classify data into the four classes (normal biphasic, normal triphasic, myopathic and neurogenic), the following results were observed, figure 6.4.3.4.3.2:

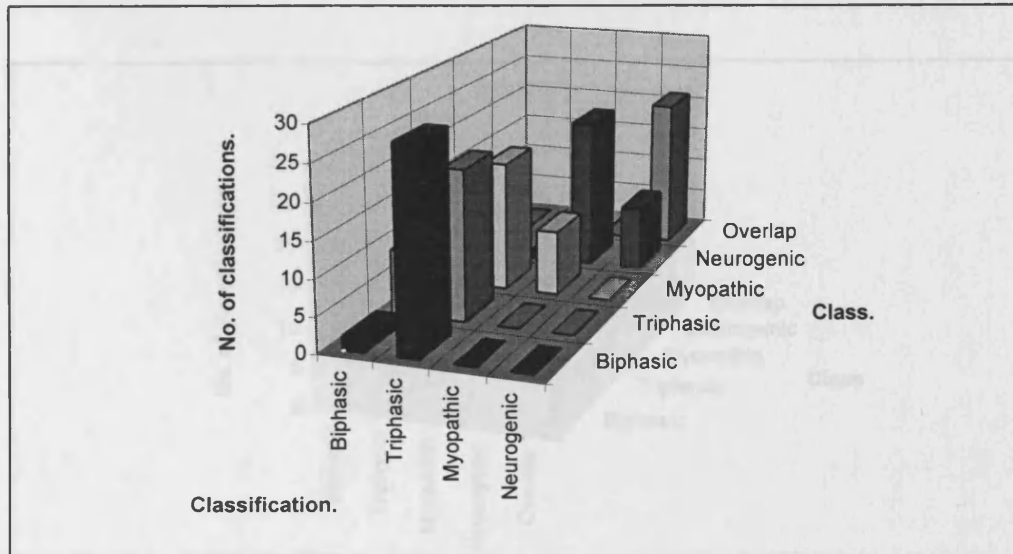
Figure 6.4.3.4.3.2 LVQ classification of overlapping data into four classes (1).



The actual misclassification rates are worse than the figure suggests. For the non-overlapping data, class 1 (biphasic) exhibits 93.3% misclassification; class 2 (triphasic) exhibits 13.3% misclassification; class 3 (myopathic) exhibits 70% misclassification; and class 4 (neurogenic) exhibits 70% misclassification. The overlapping data exhibits 100% misclassification. It is all classified as class 4 rather than class 1 or 2. Overall the misclassification rate is 70.9%.

The neural network was retrained, as before utilising non-overlapping data only, but this time with 12 neurons in the competitive layer. 5000 cycles were used for training purposes. The test set was once again presented and the following results were obtained, figure 6.4.3.4.3.3

Figure 6.4.3.4.3.3 LVQ classification of overlapping data into four classes (2).



Once again the results are bad. For the non-overlapping data, class 1 (biphasic) exhibits 93.3% misclassification; class 2 (triphasic) exhibits 30% misclassification; class 3 (myopathic) exhibits 70% misclassification; and class 4 (neurogenic) exhibits 70% misclassification. 100% misclassification was observed in the overlapping records, and as before, all overlapping data was misclassified as class 4. The overall misclassification rate was 70.9%

The next stage was to attempt the training of a network, and classification of the data set used in this section, to isolate overlapping data as a fifth class. This was attempted using 12, 20 and 25 neurons, each new network being trained for 5000 presentations of the training data. The entire database was used for the purpose of training, and upon its presentation for classification, the following results were obtained, figures 6.4.3.4.3.4 to figure 6.4.3.4.3.6.

For the 12 neuron network the misclassification rates stand as follows: class 1 (30%); class 2 (13.3%); class 3 (33%); class 4 (30%); and class 5 (0%). The overall misclassification rate was 22.7%.

For the 20 neuron network the misclassification rates stand as follows: class 1 (30%); class 2 (13.3%); class 3 (33%); class 4 (13.3%); and class 5 (4.7%). The overall misclassification rate was 16.3%.

Figure 6.4.3.4.3.4 LVQ classification of overlapping data into five classes (12 neurons).

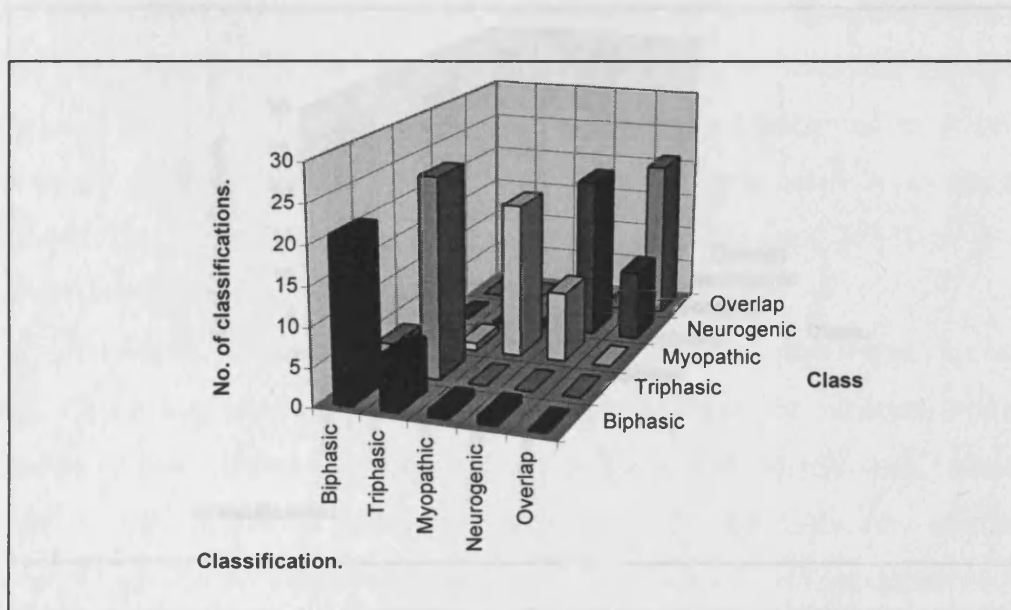
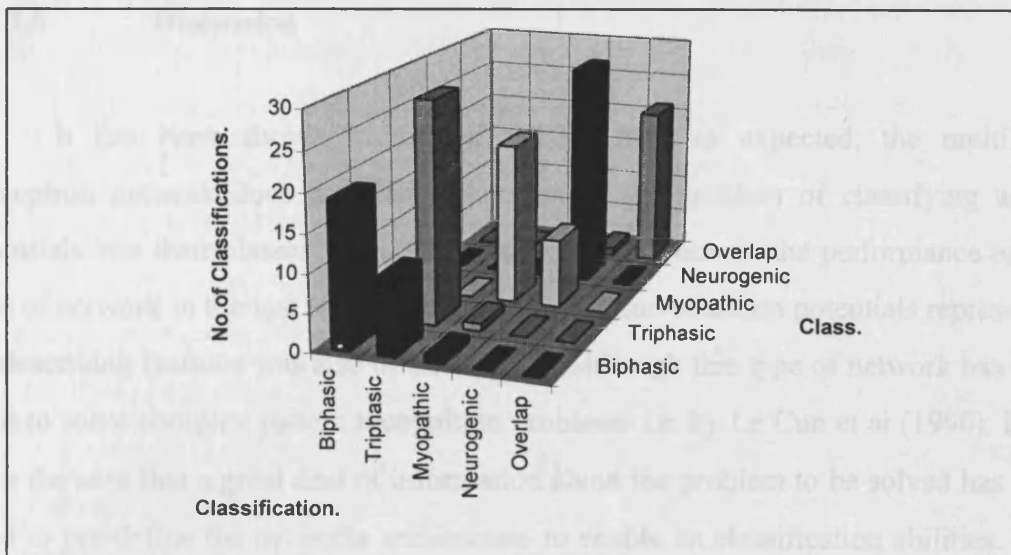
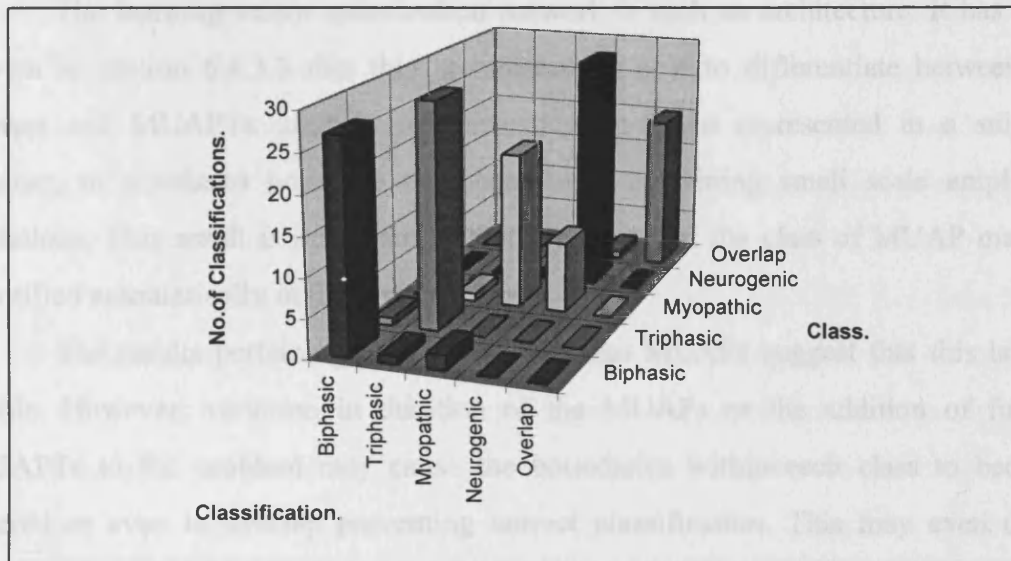


Figure 6.4.3.4.3.5 LVQ classification of overlapping data into four classes (20 neurons).



For the 20 neuron network the misclassification rates stand as follows: class 1 (37%); class 2 (3.3%); class 3 (30%); class 4 (3.3%); and class 5 (4.7%). The overall misclassification rate was 16.3%.

Figure 6.4.3.4.3.6 LVQ classification of overlapping data into four classes (3).



For the 25 neuron network the misclassification rates stand as follows: class 1 (10%); class 2 (3.3%); class 3 (33.3%); class 4 (0%); and class 5 (4.7%). The overall misclassification rate was 10.6%.

6.4.3.5 Discussion

It has been shown in section 6.4.3.2 that, as expected, the multilayer perceptron network does not find a solution to the problem of classifying action potentials into their classes. This result was expected because the performance of this type of network in the test relating to the classification of action potentials represented by describing features was also of this nature. Although this type of network has been used to solve complex pattern recognition problems i.e. by Le Cun et al (1990), it has been the case that a great deal of information about the problem to be solved has been used to pre-define the networks architecture to enable its classification abilities. That has not been the case here, because the multilayer perceptron network is not necessarily the most suited to pattern recognition, and backpropagation is not necessarily the most suited learning rule. There are other architectures and learning

methods, such as semi supervised methods, that are designed to perform in a more appropriate fashion.

The learning vector quantization network is such an architecture. It has been shown in section 6.4.3.3 that this architecture is able to differentiate between the classes and MUAPTs used in this investigation when represented in a suitable manner, in simulated noisefree data conditions containing small scale amplitude variations. This result is important in that it shows that the class of MUAP may be identified automatically in these conditions.

The results pertaining to classification into MUAPs suggest that this is also viable. However, variation in duration of the MUAPs or the addition of further MUAPTs to the problem may cause the boundaries within each class to become blurred or even to overlap preventing correct classification. This may even occur between the *normal biphasic* and *normal triphasic* classes. It would not however be a problem because the overall objective is to determine the performance of this method in clustering MUAP classes into *normal*, *myopathic* and *neurogenic*.

Section 6.4.3.4 shows how the LVQ networks trained on noisefree simulated data respond to the introduction of both white noise and band limited noise, to the problem. It is clear that the classification of these simulated action potentials represented by the first three principal component coefficients of their eight describing features may be separated into the desired classes with little misclassification for white noise and no misclassification for band limited noise. This result is of interest because the noise present within Real EMG signals is band limited in nature. Also, although the levels of noise used in these tests was low, that is in keeping with the conditions prevalent in the clinical environment.

When attempting to classify APs directly into the MUAP train from which they originate, in the presence of noise, large misclassification rates were observed. The reasons for these large rates are as follows: when many MUAPTs are present within the data set being analysed (in this case there were 12 MUAPTs present) the amount of input space allocated to each individual MUAPT cluster is small. This small allocation is due to many representations being present, and the spread in space between the different classes. The MUAPT clusters of one class are all represented in

one smallish section of the input space. Thus this is an effect of the method of representation of data, rather than a shortcoming of the network used.

The addition of noise to action potential trains moves the position of their MUAPs within and relative to their appropriate clusters. It is possible that the addition of noise will cause an action potential to be located closer to a cluster that is not its own, than to its own. This will cause the neurons of the wrong class to fire, resulting in an incorrect classification.

A second reason for misclassification is the effect of adding new data to the database causing the clusters within it to shift minutely. This problem is accentuated by the close proximity of small clusters and their corresponding neurons and may cause misclassifications. This problem is not a serious factor for the previous method of class identification, because the class clusters are so distinct. A method of countering this effect would be to calculate the PCCs of each action potential to be classified separately, with respect to the database. This would, however, significantly increase the processor time required and that is highly undesirable.

These results do not present a great setback. It is of great use to be able to classify data into the classes *normal*, *myopathic* and *neurogenic*. This ability could form the first stage of a decomposition routine, or be a tool in itself.

The third test in the section shows that the method of differentiating between MUAPs from trains of a like class performs well under noisy conditions for the simulated data used. This is not of as much interest as the method for differentiating classes, because the clusters are more likely to move within this input space, depending upon the characteristics of the MUAPs, than they are within the classes of the overall problem.

In section 6.4.3.4.3 the ability of the neural network trained for differentiation between classes to deal with overlapping data was assessed. As may be seen, the PCC representations of overlapping data do not fall within the bounds of the class clusters. This indicates that the neural network will be unable to classify the overlapping data correctly. This supposition is borne out by the results. Significant misclassifications occur. An attempt to train the network to classify overlaps into their own class also produces significant, if lower, misclassification rates. These results were to be expected when the position of overlapping data representations were compared with

those of non-overlapping data. The overlapping data representations tend to spread throughout the input space.

6.5 Summary.

It has been hypothesised in this chapter that the use of neural networks may provide a good method for clustering action potentials into their appropriate class groups. Some reasons for this hypothesis have been presented, along with a foundation for the subject of neural networks.

Attempts have been made to train various networks to cluster action potentials as dictated by the user with different levels of success. The performance of these networks has been assessed when classifying data polluted with white noise, with band limited noise, and with the superimposition of other action potentials.

Overall, these tests tell us that the method of principal component coefficient representation of non-overlapping, simulated MUAP data for classification with LVQ networks is suited to determining the class of that data. It is not suited to determining the MUAP from which it came. It is also not suited to operating with overlapping or superimposed data, though it is capable of dealing with realistic levels of noise.

Chapter 7 - Alternative applications in decomposition.

7.1 Introduction.

This chapter presents some further contributions to ongoing research in the decomposition of EMG signals. The first part of the chapter is used to describe some new ideas for helping to classify action potentials. The second part concerns the problem of how to deal with overlaps.

As a continuation of the work carried out in chapter 6 towards finding solutions to the problem of clustering MUAPs, this chapter looks at these two issues in the task of automatic decomposition. The first is that of multiple database principal component analysis. In section 7.2 this method is applied to the problem of MUAP class determination and tested in the presence of noise, amplitude variation and time dilation variation.

The second issue outlined in section 7.3 is a study in the resolution of overlapping MUAP templates. The feasibility of the method proposed by Loudon in 1991, is assessed with regard to required processor time. The same study is carried out for a proposed more thorough method of template resolution. All of these methods strive towards the creation of an automatic decomposition knowledge source to interact with a blackboard based MDSS.

7.2 Multiple database principal component analysis.

The concept of principal component analysis utilising more than one database as a method of EMG analysis was introduced briefly in chapter 1. In that case three databases were used to enable differentiation between normal, myopathic and neurogenic signals at force levels where interference was prevalent. The results obtained during the study were encouraging, providing good discrimination when using three dimensional representations of the signals in question, i.e. representing them by their first three

Simulation and analysis in electromyography.

principal component coefficients, (Jones et al, 1990). This success suggests that the method may be useful in discriminating between the classes of MUAPs in the time domain as well as interference EMGs in the frequency domain. The use of this method is also a logical progression from the use of single database PCA in chapter 6. However, the multiple database procedure is a discriminatory technique in itself. Here a more detailed description of the multiple database technique is made, with reference to the works of Jones, Lago and Parekh, (Jones et al, 1990)(Parekh 1986).

The idea of multiple database principal component analysis is that the number of databases corresponds to the number of classes into which the data is split. In the case of Jones *et al*, three databases were used to classify data into three distinct groups. Each database in multiple database PCA is made up from examples of signals corresponding to the class which it represents.

The basis of the method is that for each signal to be classified, principal component analysis is carried out with each of the databases present. The unknown vector representation of the signal is reconstructed in the following form, (Parekh, 1986);

$$X = G + p_1 \cdot c_1 + p_2 \cdot c_2 + p_3 \cdot c_3 + error \quad (1)$$

where X = new or unknown signal vector.

G = database or class mean.

p_n = principal component n of class.

c_n = principal component coefficient n
relating to unknown or new signal.

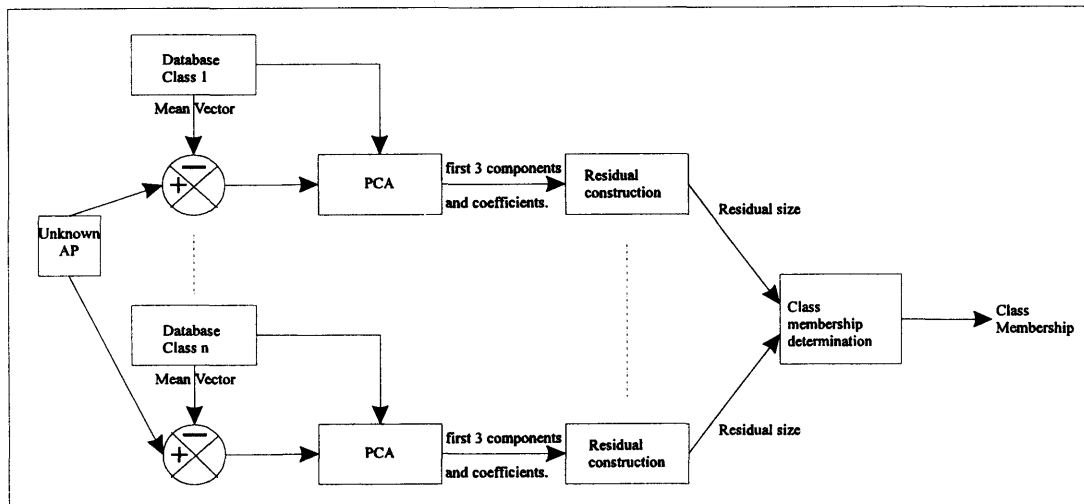
This process is carried out for each database or class. The schematic for this method may be seen in figure 7.2.1. The class to which the unknown vector belongs is identified as the one which has the smallest residual or error vector. This error vector is calculated by the following equation (2) and its magnitude is evaluated as the mean squared error, equation (3).

Simulation and analysis in electromyography.

$$E = X - G - p_1 \cdot c_1 - p_2 \cdot c_2 - p_3 \cdot c_3 \quad (2)$$

$$\sigma^2 = \frac{\sum (x_i - \bar{x})^2}{n} \quad (3)$$

Figure 7.2.1 The schematic diagram of multiple database PCA.



The following investigations are made in order to ascertain whether the method will be of use in differentiating between classes of MUAPs and between MUAPs from different trains within the same class. It is a pilot study to determine the method's suitability or lack of it.

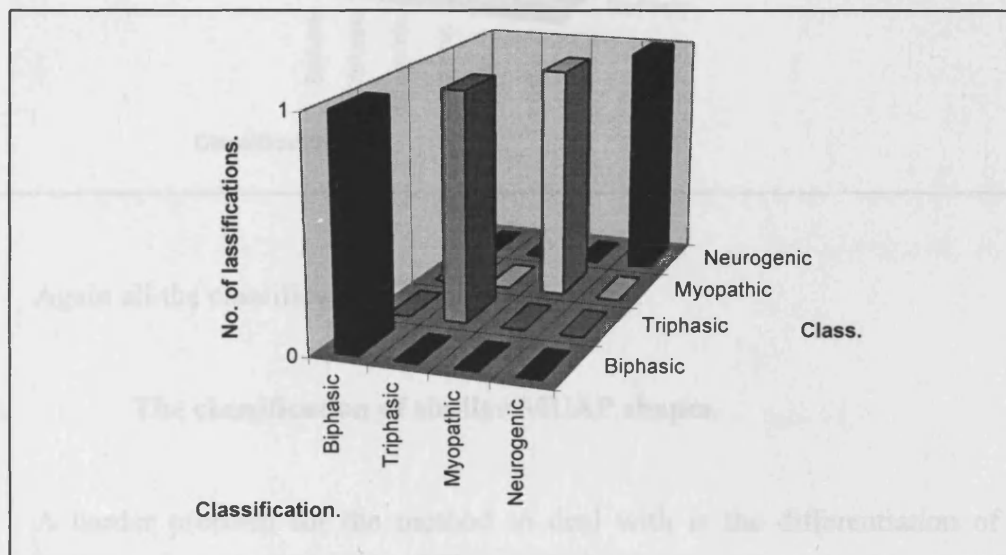
7.2.1 The classification of different MUAP shapes.

In order to see whether the multiple database PCA routine would be able to differentiate between the four MU classes, a database consisting of nine examples of the class was constructed for each class. The MUAPs in each class all came from the same MUAPT. All data was simulated. Principal component analysis was then carried out, using each database in turn, to identify one action potential from each class. The action

Simulation and analysis in electromyography.

potentials that were used for identification were not a part of the database though they came from the same MUAPT as those in the database. The results obtained may be seen in Figure 7.2.1.1. They consist of the sum of squared errors for each action potential being classified, calculated with each database. In each case, the smallest sum of squared errors is highlighted.

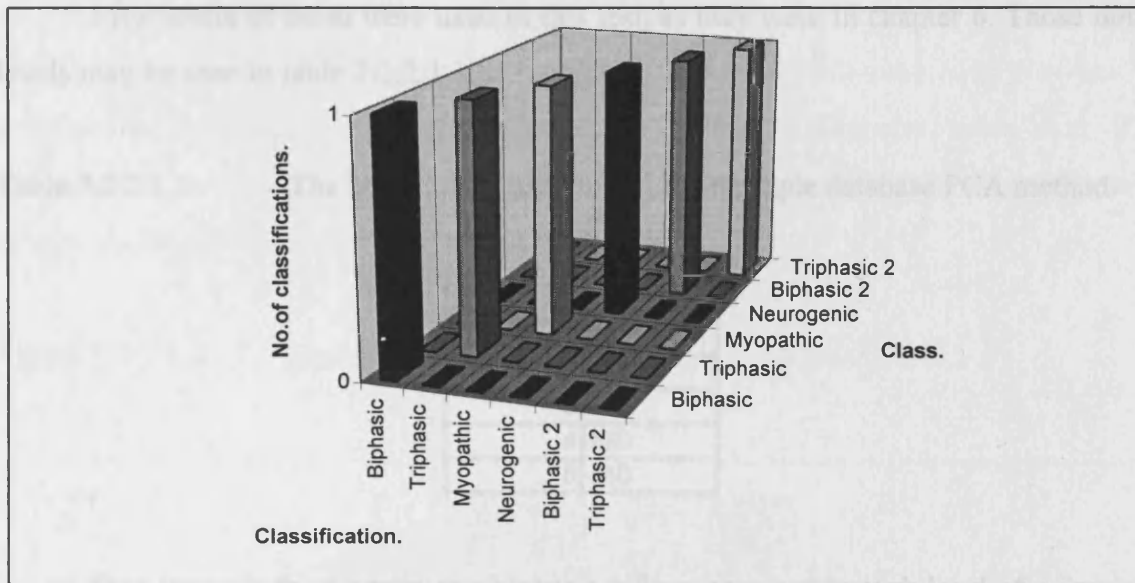
Figure 7.2.1.1 The results of class determination using multiple database PCA (1).



It may be seen that all the potentials in the above test were classified correctly. In order to further test the performance of the method tested under such circumstances, the experiment was repeated, this time using six databases representing two separate biphasic MUAP trains, two separate triphasic MUAP trains, a single myopathic MUAP train and a single neurogenic MUAP train. The results may be seen in Figure 7.2.1.2. Again, the lowest sum of squared errors for each attempted classification is highlighted.

Simulation and analysis in electromyography.

Figure 7.2.1.2 The results of class determination using multiple database PCA (2).



Again all the classifications made were correct.

7.2.2 The classification of similar MUAP shapes.

A harder problem for the method to deal with is the differentiation of action potentials from the same class but belonging to different trains of MUAPs within that class. It has already been seen that the method is capable of differentiating between two similar MUAPs, see section 7.2.1. It is the purpose of this investigation to assess the performance of the routine in classifying similar action potentials submerged in noise, or with amplitude or time dilation variation.

7.2.2.1 The classification of MUAP types in noise.

The databases utilised in the last test, six in number, were utilised to determine the performance of the method when classifying action potentials in the presence of noise. In

Simulation and analysis in electromyography.

this case white noise was used. The databases consist of nine examples of the class represented by the database, all of the examples were noise free.

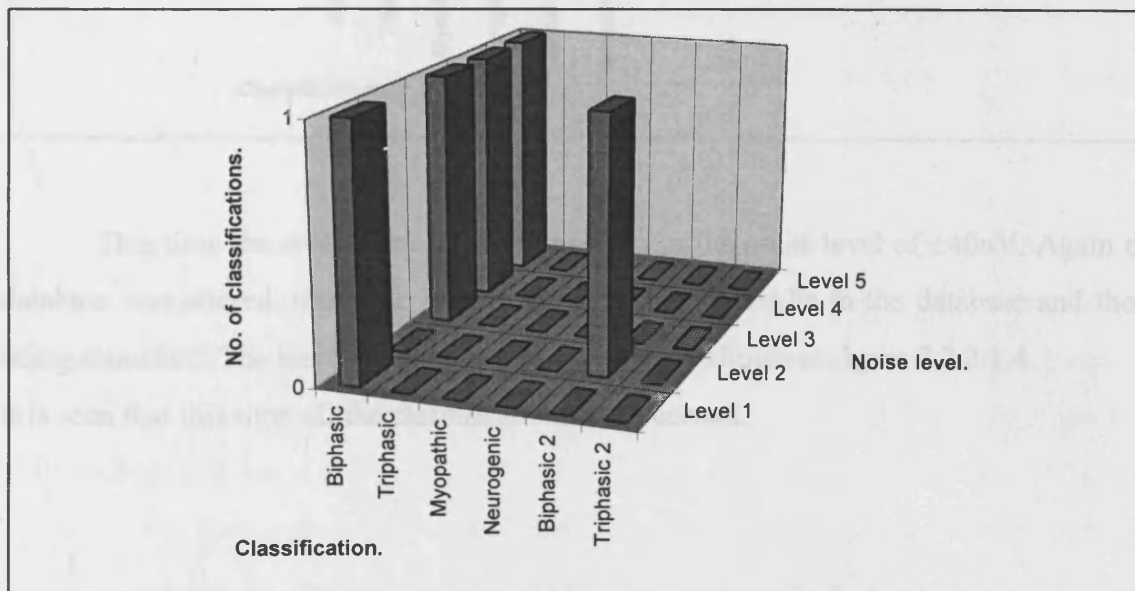
Five levels of noise were used in this test, as they were in chapter 6. Those noise levels may be seen in table 7.2.2.1.1.

Table 7.2.2.1.1 The noise levels used to test the multiple database PCA method.

Level	Range (uV)
1	± 5
2	± 10
3	± 20
4	± 30
5	± 40

One example from a type one biphasic train submerged in each level of noise was classified using the multiple database PCA method. The results are shown in figure 7.2.2.1.2.

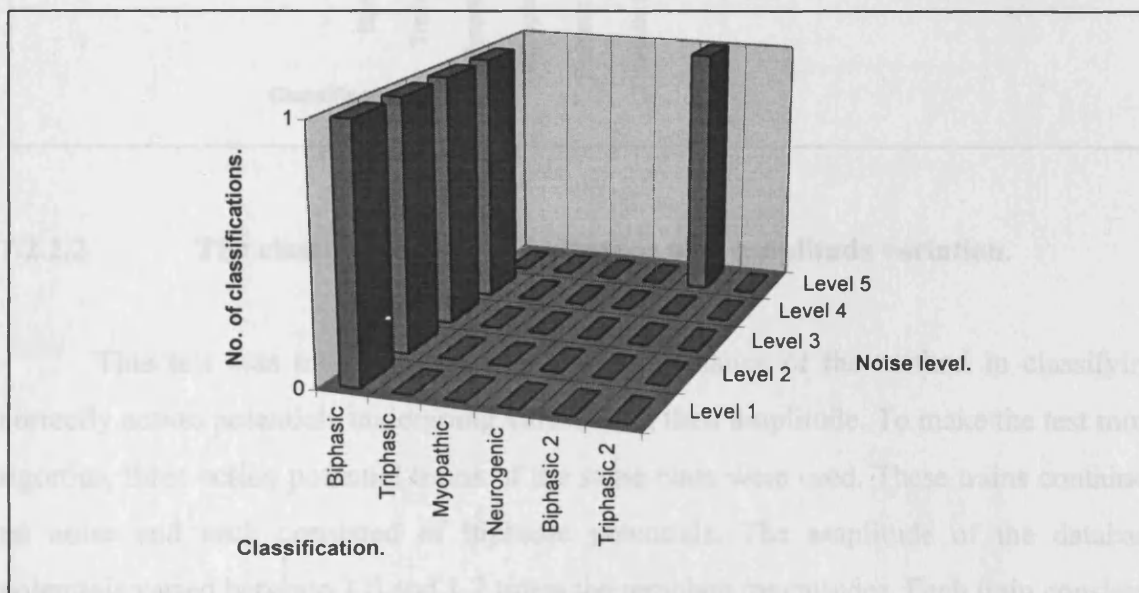
Figure 7.2.2.1.2 The results of MUAP determination in noise (1).



Simulation and analysis in electromyography.

As may be seen correct classification occurred at all levels with the exception of that containing $\pm 10\mu\text{V}$ noise. A new database was constructed for the 1st biphasic class. This database consisted of 15 examples, 5 of these examples were clean data, the other 10 consisted of 2 examples each of action potentials submerged in each noise level. The previous test was rerun replacing the original biphasic one class database with the newly constructed one. The results may be seen in figure 7.2.2.1.3

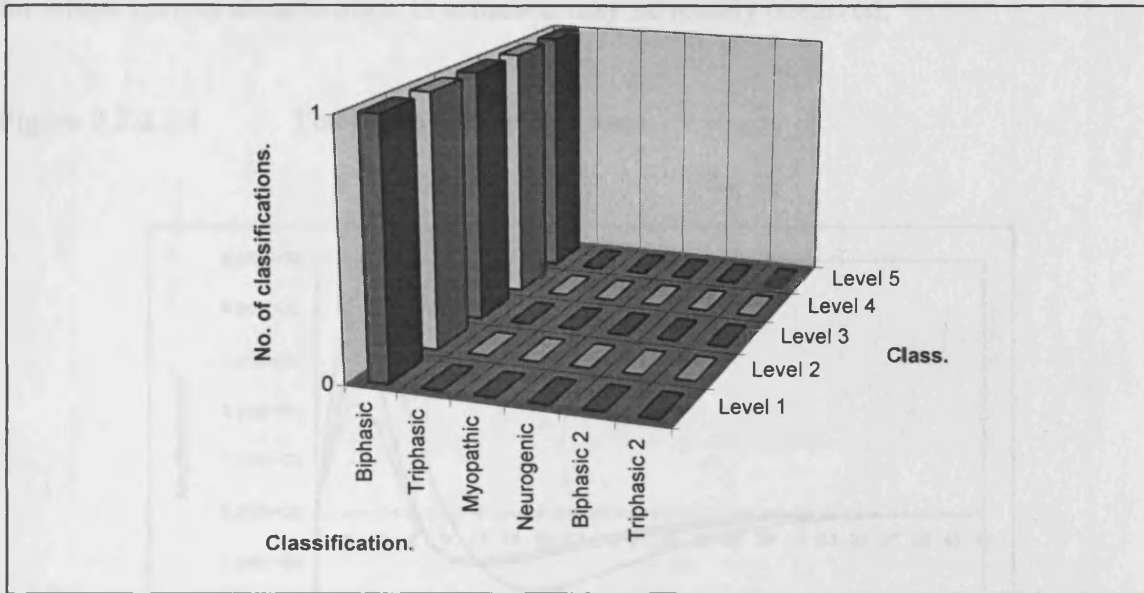
Figure 7.2.2.1.3 The results of MUAP determination in noise (2).



This time the error in classification occurs at the noise level of $\pm 40\mu\text{V}$. Again the database was altered, this time exchanging the noisy MUAPs in the database and those being classified. The test was rerun and the results are shown in figure 7.2.2.1.4.

It is seen that this time all the classifications were correct.

Figure 7.2.2.1.4 The results of MUAP determination in noise (3).



7.2.2.2 The classification of MUAP types with amplitude variation.

This test was intended to assess the performance of the method in classifying correctly action potentials undergoing variation in their amplitude. To make the test more rigorous, three action potential trains of the same class were used. These trains contained no noise and each consisted of biphasic potentials. The amplitude of the database potentials varied between 1.0 and 1.2 times the template magnitudes. Each train consisted of a different duration template.

Three databases each consisting of 10 examples were constructed, one corresponding to each of the three MUAP trains. Each train is a class in this test. For the first MUAP train, i.e. class 1, the template was varied in amplitude between 0.1 and 2.0 times its actual size. The variation was staged in steps of 0.1 times the original magnitude of the template. Each of these potentials was classified using multiple database PCA. The procedure was then repeated for class 2 and class 3. The templates may be seen in figure 7.2.2.2.1, and the results for each train at each amplitude may be seen in figures 7.2.2.2.2

Simulation and analysis in electromyography.

to 7.2.2.2.4. These figures depict the classification of each class of MUAP indicated by the multiple database PCA routine, as the amplitude was varied. The range of amplitude for which correct classification is achieved may be readily observed.

Figure 7.2.2.1 The MUAP templates used.

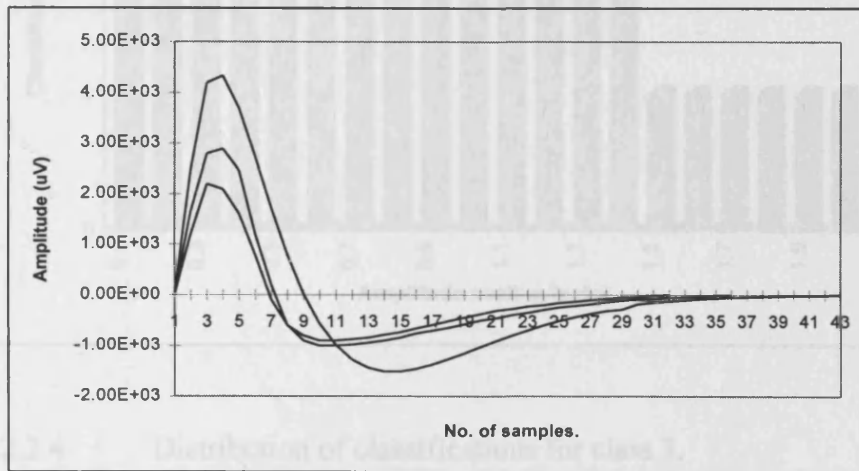


Figure 7.2.2.2 Distribution of classifications for class 1.

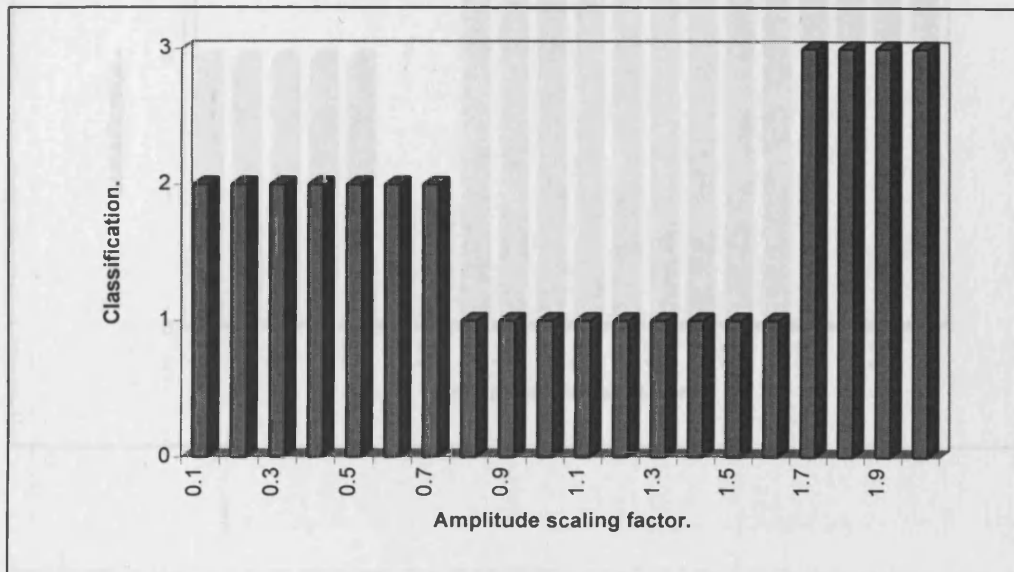


Figure 7.2.2.2.3 Distribution of classifications for class 2.

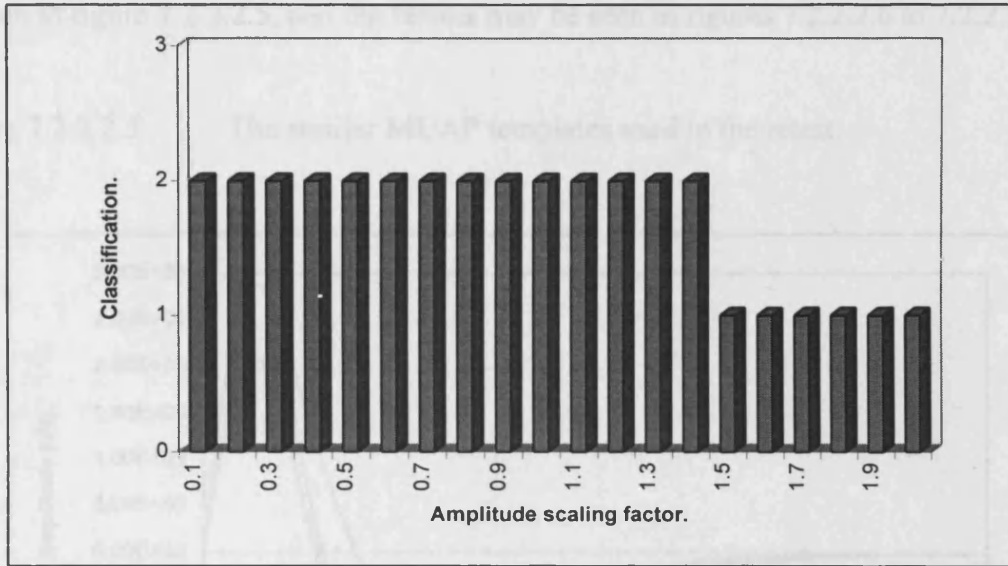
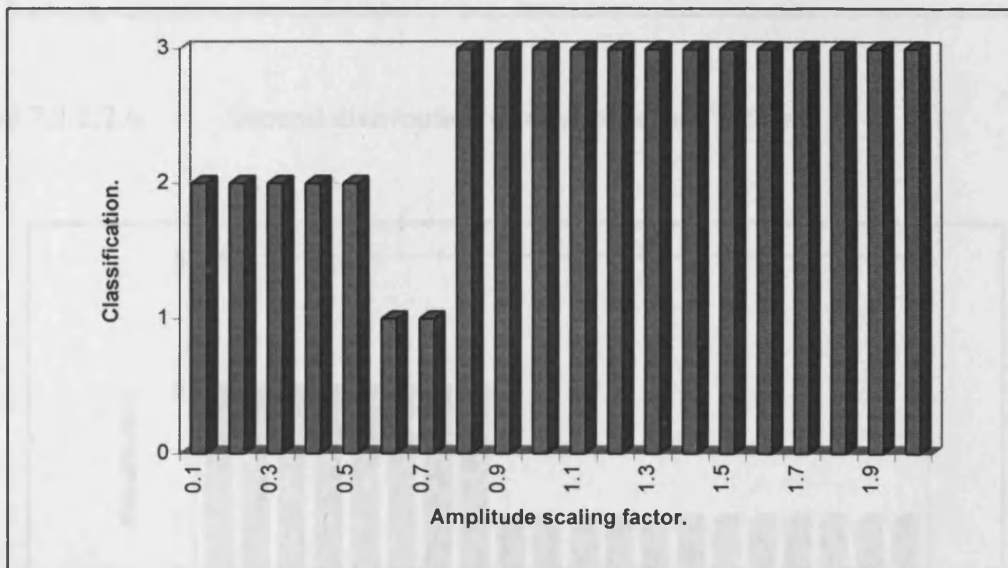


Figure 7.2.2.2.4 Distribution of classifications for class 3.



Simulation and analysis in electromyography.

A repeat of this test was made wherein two of the templates were more similar, i.e. a fourth class was used in preference of our existing class three. These templates may be seen in figure 7.2.2.2.5, and the results may be seen in figures 7.2.2.2.6 to 7.2.2.2.8.

Figure 7.2.2.2.5 The similar MUAP templates used in the retest.

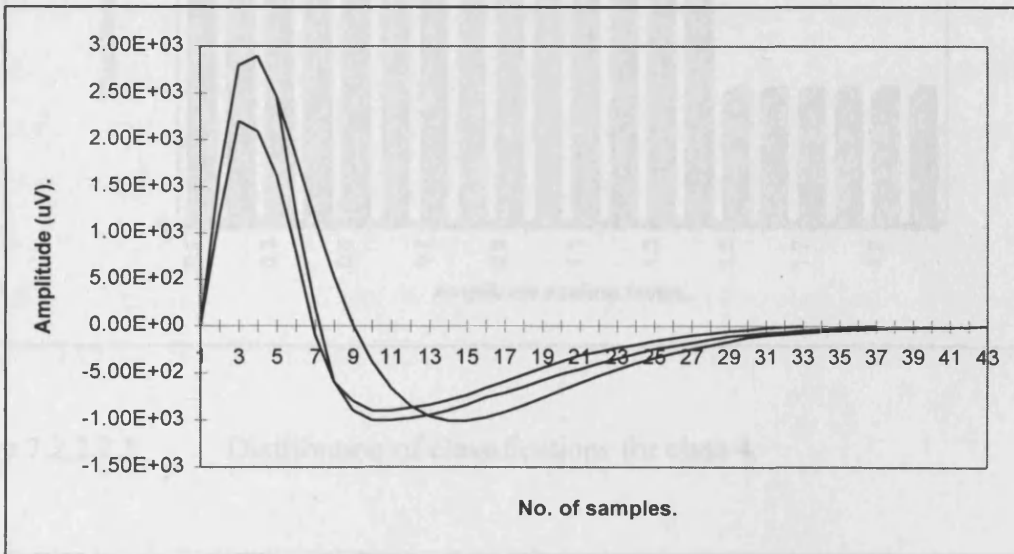
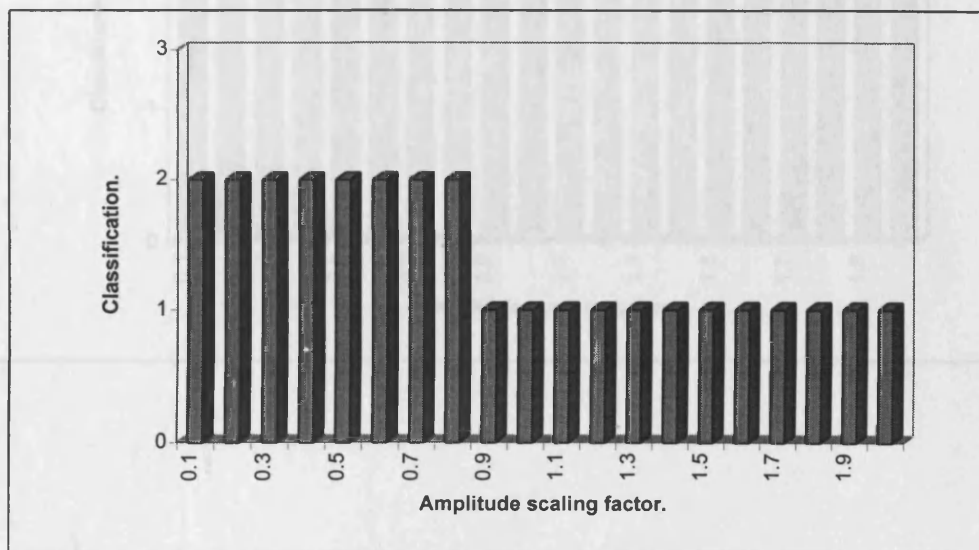


Figure 7.2.2.2.6 Second distribution of classifications for class 1.



Simulation and analysis in electromyography.

Figure 7.2.2.2.7 Second distribution of classifications for class 2.

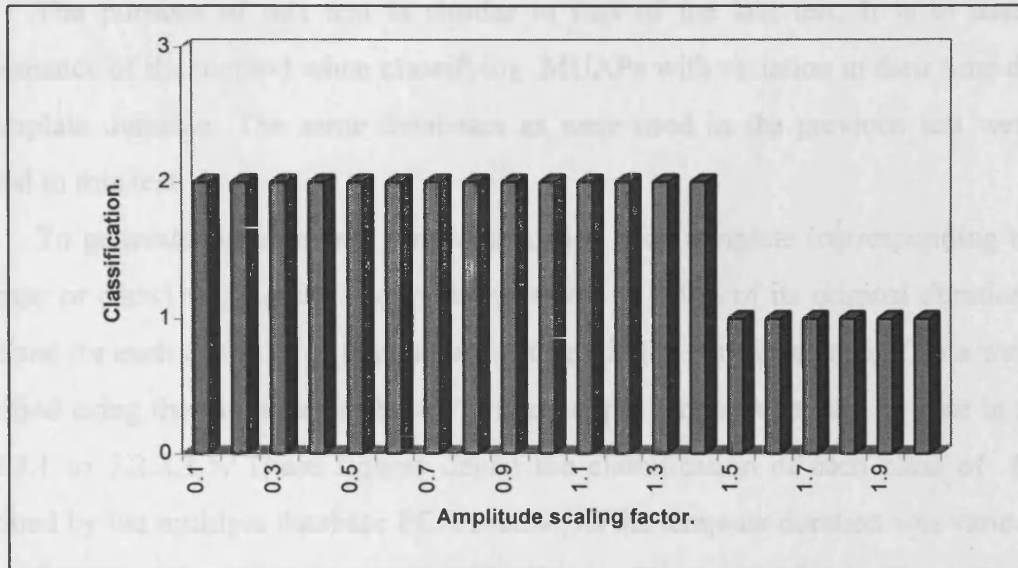
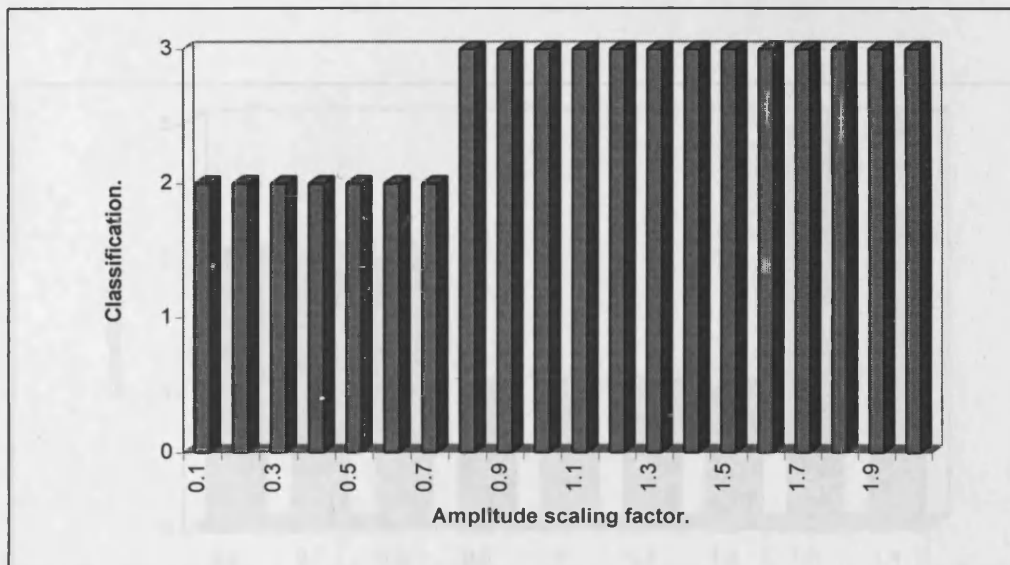


Figure 7.2.2.2.8 Distribution of classifications for class 4.



7.2.2.3 The classification of MUAP types with time dilation variation.

The purpose of this test is similar to that of the last test. It is to assess the performance of the method when classifying MUAPs with variation in their time dilation or template duration. The same databases as were used in the previous test were also utilised in this test.

To generate suitable data for classification each template (corresponding to each database or class) was varied in duration from 60 to 140% of its original duration. This was done for each of the three templates, in steps of 10%. The three sets of data were then classified using the multiple database PCA technique. The results may be seen in figures 7.2.2.3.1 to 7.2.2.3.5. These figures depict the classification of each class of MUAP indicated by the multiple database PCA routine, as the template duration was varied. The range of duration for which correct classification is achieved may be readily observed.

Figure 7.2.2.3.1 Distribution of classifications for class 1.

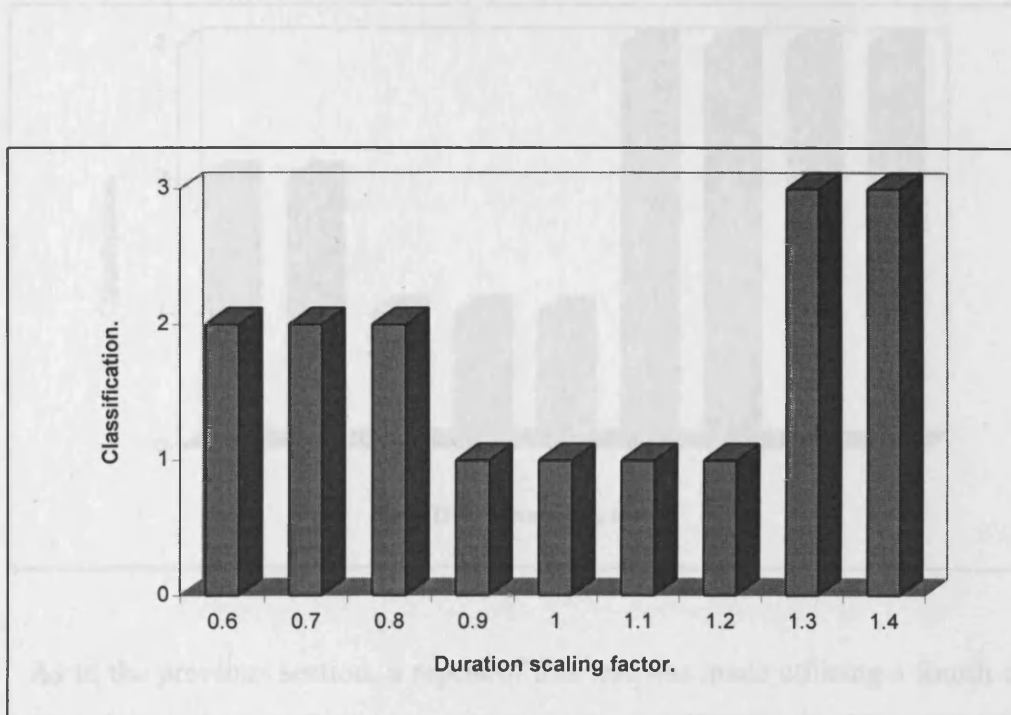


Figure 7.2.2.3.2 Distribution of classifications for class 2.

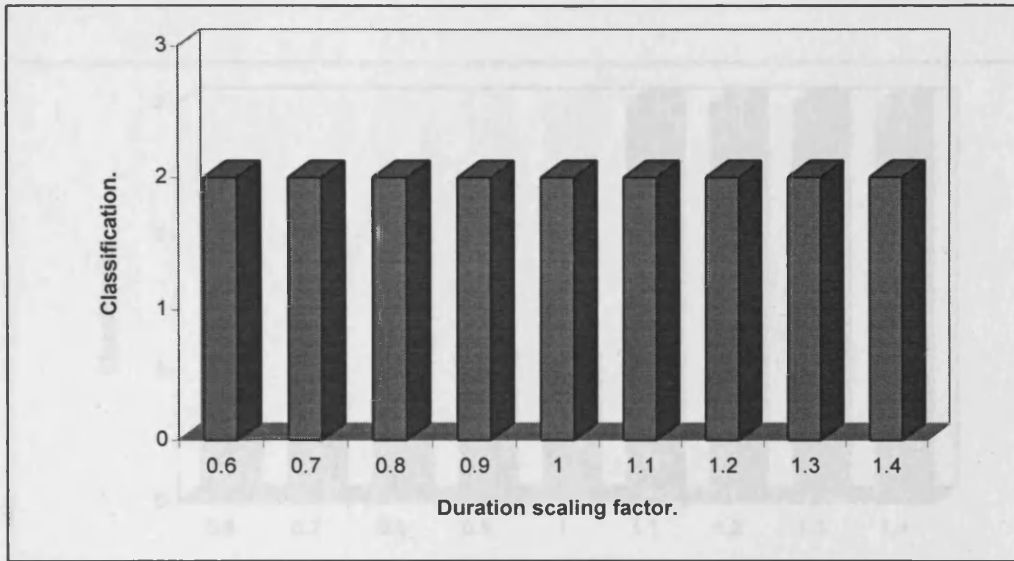
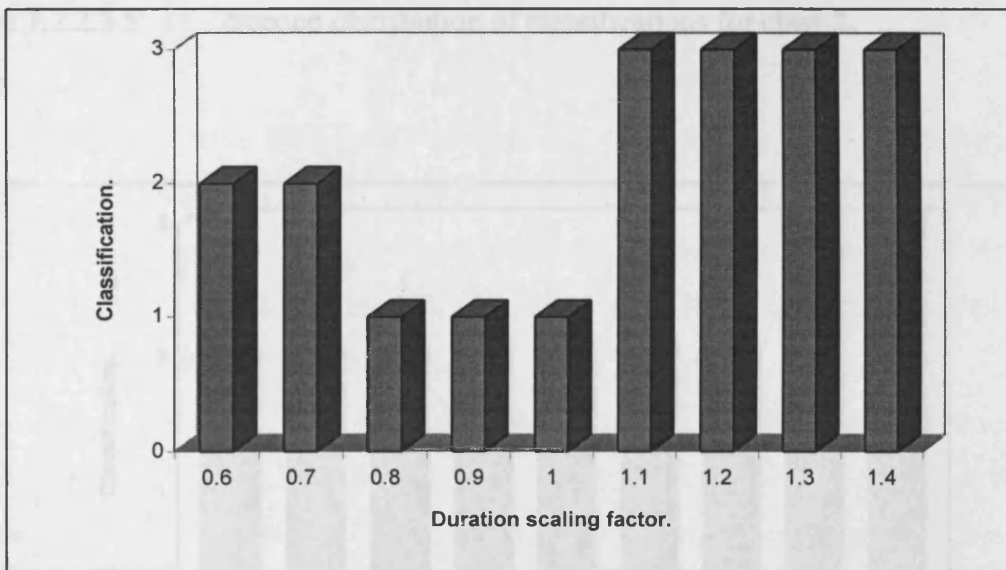


Figure 7.2.2.3.3 Distribution of classifications for class 3.



As in the previous section, a repeat of this test was made utilising a fourth class in preference of our existing class three. The results may be seen in figures 7.2.2.3.4 to 7.2.2.3.6.

Figure 7.2.2.3.4

Second distribution of classifications for class 1.

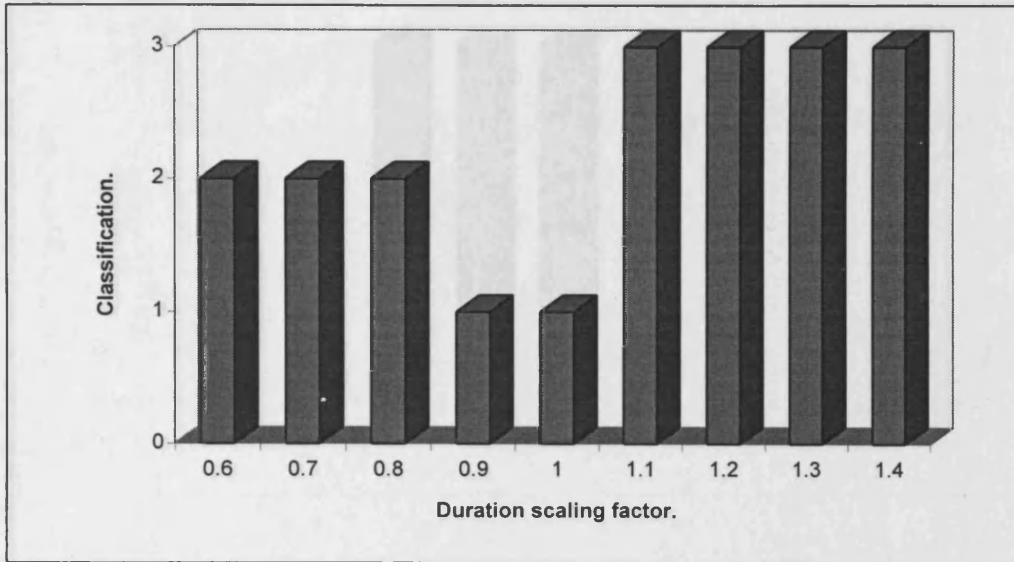


Figure 7.2.2.3.5

Second distribution of classifications for class 2.

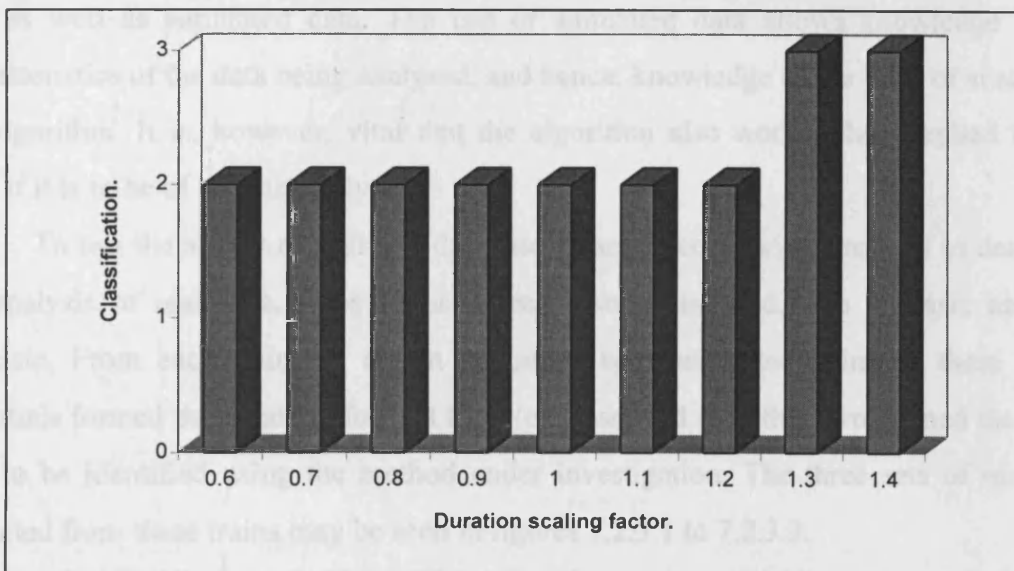
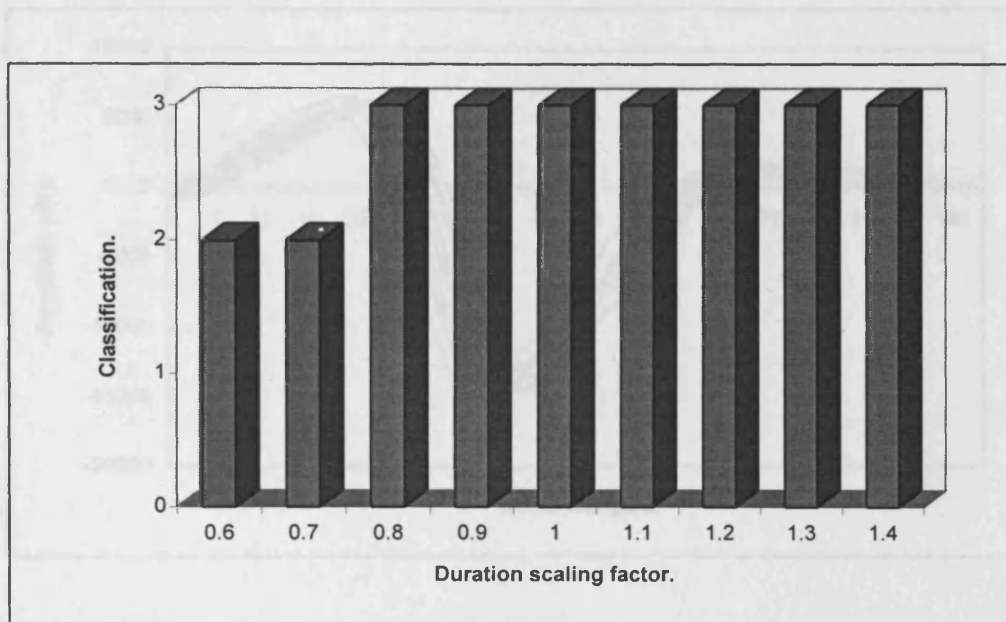


Figure 7.2.2.3.6 Distribution of classifications for class 4.



7.2.3 Tests with real data.

It is important to evaluate any method intended for analysis of the EMG upon real data as well as simulated data. The use of simulated data allows knowledge of the characteristics of the data being analysed, and hence, knowledge of the level of success of the algorithm. It is, however, vital that the algorithm also works when applied to real data, if it is to be of use clinically.

To test the ability of multiple database principal component analysis to deal with the analysis of real data, three trains of real data were used, two biphasic and one triphasic. From each train, 11 action potentials were extracted. Nine of these action potentials formed the database for that train (or class) and the other two formed the set of data to be identified using the method under investigation. The three sets of real data extracted from these trains may be seen in figures 7.2.3.1 to 7.2.3.3.

Simulation and analysis in electromyography.

Figure 7.2.3.1 - Real data set no. 1.

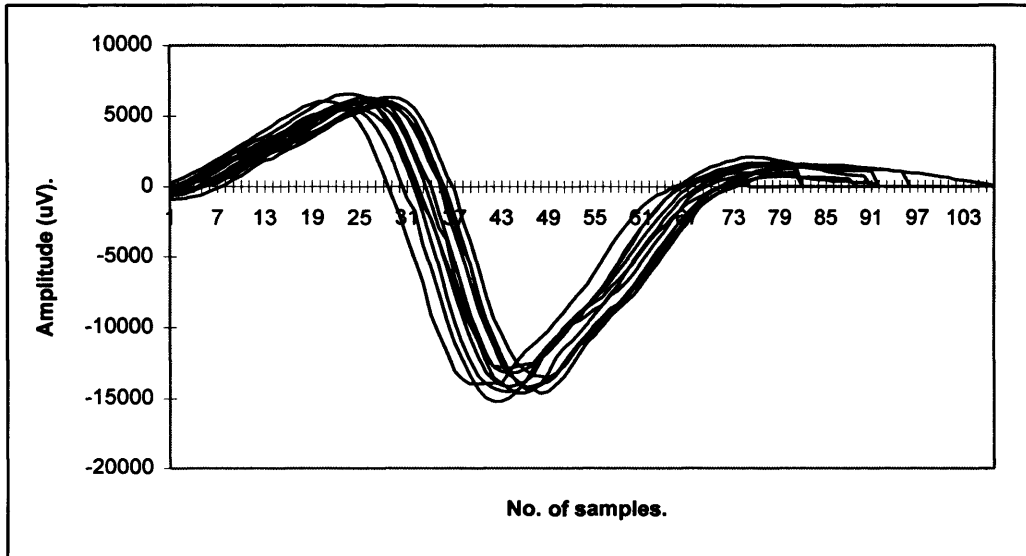
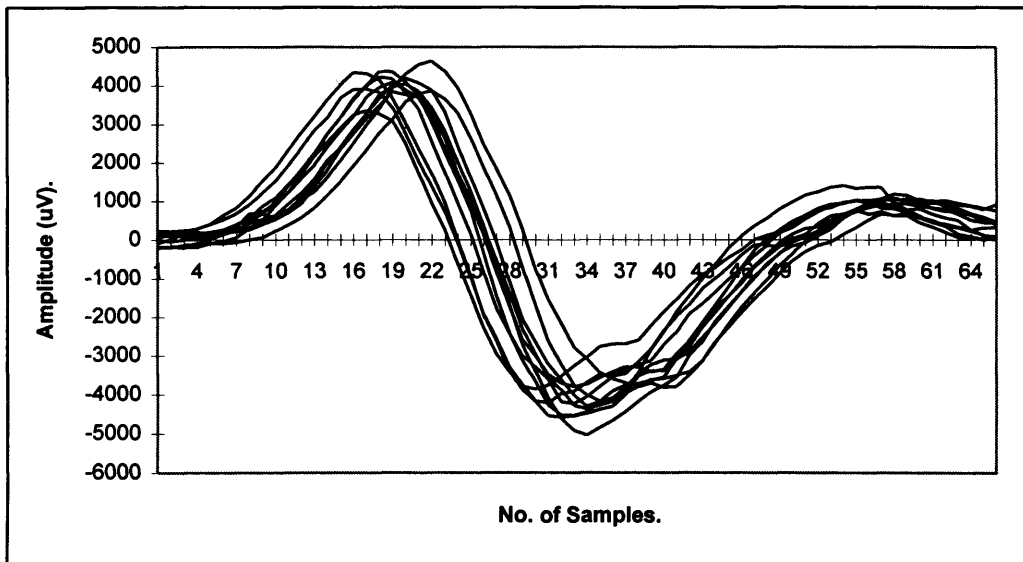
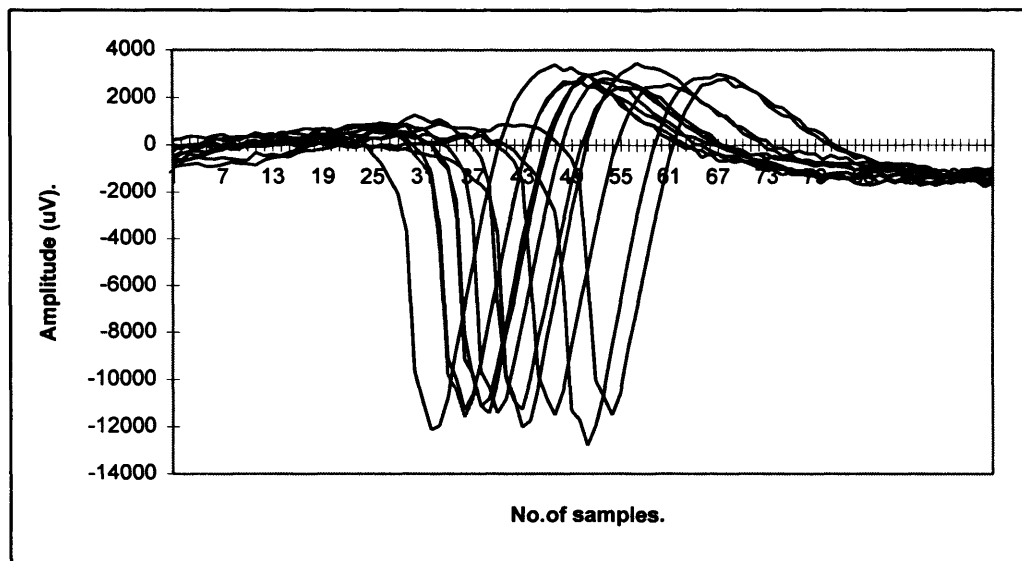


Figure 7.2.3.2 - Real data set no. 2.



Simulation and analysis in electromyography.

Figure 7.2.3.3 - Real data set no. 3.



Two tests were run to identify six action potentials, two each from each class of action potential. The classification was made between the three classes of action potential and each test was used to classify between three action potentials, one from each class.

As a result of these tests, the six action potentials were identified correctly. In each case the reconstruction of the action potential with the smallest mean squared error corresponded to the appropriate class. This may be seen in figures 7.2.3.4 and 7.2.3.5.

Simulation and analysis in electromyography.

Figure 7.2.3.4 - Smallest Mean squared errors, test 1.

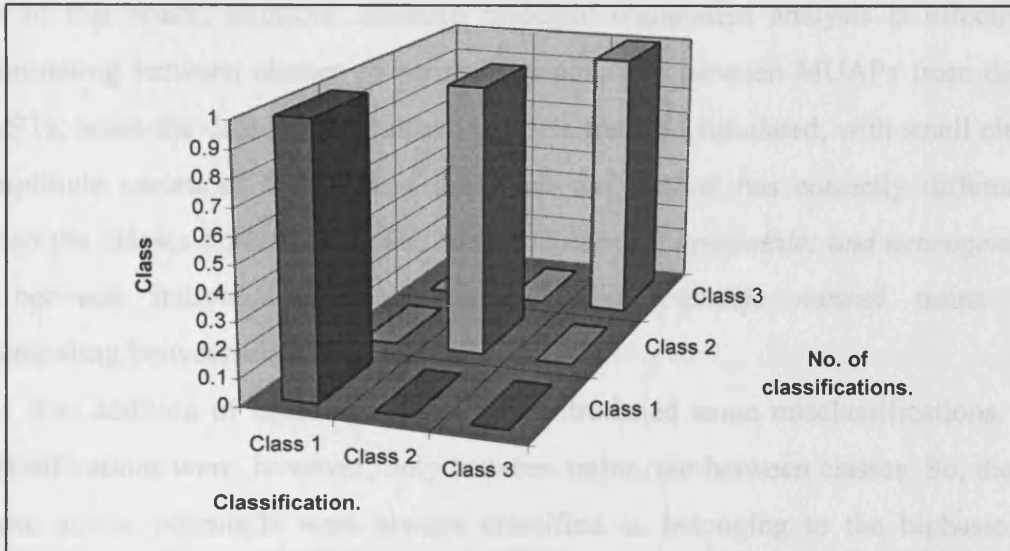
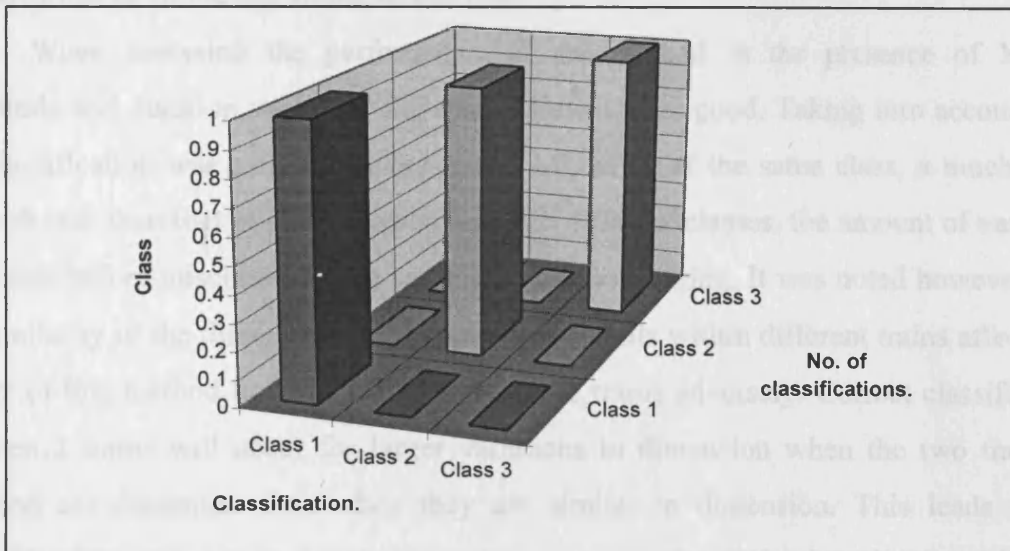


Figure 7.2.3.5 - Smallest Mean squared errors, test 2.



7.2.4 Discussion.

It may be seen from the results portrayed in the previous sections that, within the limits of this study, multiple database principal component analysis is effective in discriminating between classes of action potential, and between MUAPs from different MUAPTs, when the data being analysed is noise free and simulated, with small elements of amplitude variation. It has been seen that the method has correctly differentiated between the classes *biphasic normal*; *triphasic normal*; *myopathic*; and *neurogenic*, and also between individual *biphasic normal* and *triphasic normal* trains whilst discriminating between classes.

The addition of noise to the problem introduced some misclassifications. These misclassifications were, however, only between trains, not between classes. So, the noisy biphasic action potentials were always classified as belonging to the biphasic class, although they were not always classified as belonging to the correct train. This problem was alleviated by enlarging the appropriate databases to include noisy data as well as clean data. Increasing the size of the database and the variation of its content improved the performance of the algorithm, in this case.

When assessing the performance of the method in the presence of MUAP amplitude and duration variation, the results shown were good. Taking into account that the classification was carried out between 3 MUAPTs of the same class, a much more difficult task than that of classification between different classes, the amount of variation allowable before misclassification occurred was encouraging. It was noted however, that the similarity of the dimensions of the action potentials within different trains affects the ability of this method to distinguish between the trains adversely. Correct classification between 2 trains will occur for larger variations in dimension when the two trains in question are dissimilar than when they are similar in dimension. This leads to the suggestion that the method is better suited to class discrimination than to MUAPT discrimination, because there is less similarity between classes than there is between trains of MUAPs.

Simulation and analysis in electromyography.

The application of this method of classification to trains of real clinical data provided encouraging results. The correct classifications were made, even though the trains used all consisted of *normal* class action potentials.

It is obvious that the smallest mean squared error value in a classification may not be unequivocally accepted as corresponding to the correct MUAPT or class of MUAP. This is because the correct MUAPT may not be represented in the analysis. A dynamic threshold is required to ensure that only appropriate classifications are accepted. This would be necessary for the algorithm's use as a component of an automatic decomposition routine. A static threshold would be inappropriate because the magnitude of the mean squared errors produced with each database, for different action potentials, varies substantially.

Finally, this has been a pilot study for the application of this method to MUAP clustering, and although the results have been encouraging, a larger study is required to establish the feasibility of multiple database principal component analysis as a method of discriminating between MUAP classes.

7.3 Resolution of overlapping data.

In this section, 2 connected methods of resolving overlapping MUAP complexes are looked at with regard to their required processing times. The first method is that proposed by Loudon et al, (Loudon et al, 1992), and the second is an extension of this method devised to be more thorough in its operation.

7.3.1 Method 1.

The basis of this method for resolving superimposed MUAP waveforms is the fact that MUAPs forming a superimposed waveform will have a total area sum equal to that of the superimposed waveform (Loudon, 1991). In this method the above fact is used to limit the number of combinations assessed as the possible components of the complex, to those that are the closest in terms of the sum of areas. This analysis takes place after the

Simulation and analysis in electromyography.

analysis of non-overlapping waveforms, as such, the MUAPs contributing to the complex have already been identified. Only pairs and trios of MUAPs are considered.

The algorithm used to limit the number of possible combinations is as follows:

$$|T_{Amc} - T_{Asw}| < \text{threshold} \quad (4)$$

where T_{Amc} = total area of MUAP combination.

T_{Asw} = total area of superimposed waveform

The second stage of this method consists of a template matching routine. The combinations previously selected are utilised here. The MUAPs in a selected combination of MUAPs are subtracted one by one from the superimposed complex, in order that the residual error be found. This is achieved using maximum peak alignment prior to subtraction. The process is repeated for every possible order of MUAPs within the combination to ensure that the residual error selected is the smallest one available for that combination. The procedure is carried out for all the combinations selected in the first stage. If the residual is below a set threshold, that combination is selected for firing time analysis to check the availability of the component MUAPs at the firing time of the complex and assess the likelihood of the solution being correct.

7.3.2 Method 2.

There are shortcomings with method 1: the most appropriate residual may not be found in stage 2, thus a solution may not be found. If this is the case a more thorough examination of the selected combinations of MUAPs is required.

At this point instead of carrying out stage two of method one, it is necessary to evaluate the sum of squared differences between the superimposed complex and every time registration for the selected combinations. The combinations are limited to pairs and trios of MUAPs, as well as single MUAPs. The construction and evaluation of every

Simulation and analysis in electromyography.

combination of MUAPs within the selected combinations from previous sections is required. The minimum residual calculated corresponds to the correct combination as long as it is less than the selected threshold level.

7.3.3 Processing time requirements.

Processing time calculations for both of the introduced methods were carried out. These involve evaluating the number of operations required to resolve a superimposed complex and relating this figure to the running speed of a chosen machine. The basis for these calculations are that there are 6 separate MUAPs present within the scope of the problem, each with a length of 36 samples. The length of the overlap to be resolved, in samples, is 63. For the calculations see Appendix 4. To resolve this superimposed complex, the following number of operations were required:

Method 1 - 4482 Floating point operations (FLOPS)

Method 2 - 473084 FLOPS

For a machine running at 8 MFLOPS the required processor time for carrying out these operations is as follows:

$$\textit{Method 1} \quad - \quad T = \frac{4482}{8000000} = 0.00056s$$

$$\textit{Method 2} \quad - \quad T = \frac{473084}{8000000} = 0.059s$$

For a machine running at 10 MFLOPS the required processor time for carrying out these operations is as follows:

Simulation and analysis in electromyography.

$$\text{Method 1} \quad - \quad T = \frac{4482}{10000000} = 0.00045s$$

$$\text{Method 2} \quad - \quad T = \frac{473084}{10000000} = 0.047s$$

To resolve 100 overlaps, 10 each of 36, 46, 52, 56, 66, 72, 76, 86, 96 and 106 respectively, the required number of operations are:

$$\text{Method 1} \quad - \quad 437875 \text{ FLOPS}$$

$$\text{Method 2} \quad - \quad 66.483 \text{ MFLOPS}$$

Thus for a machine running at 8 MFLOPS the processing time would be:

$$\text{Method 1} \quad - \quad T = \frac{437875}{8000000} = 0.055s$$

$$\text{Method 2} \quad - \quad T = \frac{66483000}{8000000} = 8.31s$$

For a machine running at 10 MFLOPS the required processor time for carrying out these operations is as follows:

$$\text{Method 1} \quad - \quad T = \frac{437875}{10000000} = 0.044s$$

$$\text{Method 2} \quad - \quad T = \frac{66483000}{10000000} = 6.65s$$

7.3.4 Discussion.

The last section has given us some insight to the amount of processing time required to resolve overlapping MUAP complexes into their constituent MUAPs. The times were calculated using the required number of operations to carry out the procedure (an estimate) and the running speed of modern computers. The lower of the two running speeds used is based upon that of a Pentium 75Mhz processor.

The times indicated for the resolution of a single overlapping complex of 63 samples are small in duration. This is the case for both of the methods considered in this section. These times would be further reduced by the employment of a machine utilising a more speedy processing unit. However, the times given allow these methods to be considered as appropriate for inclusion in an automatic decomposition routine. They operate swiftly enough not to cause an unwanted delay in the overall processing time of such a routine.

Alterations to the time requirements of these methods would be caused by various factors. These factors include: the number of MUAPs present within the EMG under investigation; the lengths (number of samples) of the MUAPs within these MUAPs; the lengths (number of samples) of the superimposed complexes to be resolved; and the sampling frequency of the EMG under investigation.

The number of MUAPs in the investigation affects the number of possible combinations of MUAPs that could form the superimposed complex. This factor affects stage one of both methods. The other factors also affect both methods but they affect method 2 most severely because the calculations involved are more dependant upon MUAP lengths.

The sampling frequency used for the calculations was that of the simulator, 4096Hz. Were this to be increased, the lengths of both MUAPs and superimposed complexes would increase because the number of samples per unit time would increase. Along with this increase, the required processor time for these operations would increase too. This should not prove too detrimental when looking at the times for single resolutions. However, when resolving many complexes the second method could become

Simulation and analysis in electromyography.

unacceptably time consuming. As such, method two is better suited to isolating the most appropriate combination of MUAPs once method one has been implemented and if it has failed to find a solution below the acceptable threshold level. Method two serves better to complement method one than to replace it.

7.4 Summary.

In this chapter the idea of using multiple database principal component analysis as a method of discriminating between MUAP classes and MUAP trains has been considered. Using simulated data, in a limited experiment the effectiveness of this approach has been assessed and tested in the presence of noise, in the presence of MUAP amplitude variation and in the presence of MUAP duration variation. The method has been tried on real data as a precursor to a more in depth analysis, and results were found to be encouraging.

The time requirements of two similar methods of resolving superimposed MUAP complexes has also been assessed. It has been suggested that these methods are suitable for use as elements of an automatic decomposition routine, in a complementary rather than exclusive role.

Chapter 8 - Conclusions and future work.

8.1 - Conclusions.

As a result of the research undertaken within this thesis, conclusions may be drawn in several areas. These include methods of modelling electromyographic activity, simulation within the area of neurophysiology, and methods of discriminating between certain types of electromyographic activity. All of these studies aim to assist in the generation and operation of medical decision support system in the area of neuromuscular diagnosis.

When considering the type of system to be employed for the purpose of medical decision support is concerned, the discussion in chapter one demonstrates the suitability of the blackboard based system for this application. The diverse types of knowledge to be handled by the system make it an ideal choice.

As an aid in the design of this system, simulations of various aspects of the neurophysiological diagnosis procedure have been created. These simulations, limited for now to certain examples of specific disorders and normal conditions, have allowed a decision support system to be created and tested, where the real knowledge sources were not available at the time. The simulations also go part of the way towards the creation of a simulated patient for use in the target system. This acts as a source of reference of what test results are associated with particular types of disorder.

In order to further understanding in the difficult field of classifying interference EMGs for the purpose of the MDSS, an attempt was made to model these signals using chaos theory. It may be concluded from the results shown in chapter three that the dynamics of the interference EMG are not chaotic in nature. The construction of phase portraits shows looping trajectories rather than the “strange attractor” associated with chaotic behaviour. The correlation dimension shows behaviour indicating random dynamics for all cases except that of limb girdle muscular dystrophy, which shows some preliminary signs of chaotic behaviour. Lyapunov exponents also infer random behaviour

Simulation and analysis in electromyography.

rather than chaotic behaviour. The presence of chaotic dynamics for the case of limb girdle muscular dystrophy does not give enough grounds for assuming a general chaos based EMG model. However, the idea of chaotic dynamics behind the EMG should not be completely discarded. The future may bring new methods for determining the presence of chaos, that are more effective than those in use today. These should be utilised to further test the hypothesis that there are chaotic dynamics present within the clinical EMG.

At present it should be concluded that in general, a chaotic model for the firing of MUAPs within the EMG would seem inappropriate. A better suited model for simulation of the EMG remains banks of filters whose impulse responses are representative of various action potential templates, triggered by trains of pulses, whose firing is determined by statistical processes e.g. (Gaussian renewal), summed, to provide the EMG.

It may be concluded from this chapter that the number of chaotic parameters required to model specific disorder classes will not be useful in discriminating between those classes.

To further the simulations, already created, in enhancing the MDSS, a myoelectric activity simulator is made available. The simulator provides both spontaneous and voluntary activity to the MDSS in its role as a knowledge source. This KS will allow comparison of signals, clinician training and reference sources. When this simulation is added to the simulations of chapter two, the simulated patient reference source is highly enhanced and has already and has already proved useful in pilot trials of the MDSS (EPSRC Report GR/J47064).

Two new applications of known signal processing techniques are proposed and assessed. The use of neural networks to discriminate between MUAP classes and to discriminate between MUAP trains is investigated. The types of input required for success are also studied. From this work it may be concluded, as expected, that non-correlated inputs to the neural networks prove more efficient than correlated inputs, and that principal component coefficients are suitable non-correlated inputs. It is also concluded that, of the neural networks tried, the learning vector quantization network is

Simulation and analysis in electromyography.

the most useful, of the methods tried, for discrimination purposes using simulated data. The combined findings lead to the conclusions that the method using LVQ networks to cluster inputs represented by non-correlated factors is successful in discriminating between MUAP classes in clean and noisy conditions but not effective in discriminating between MUAP trains.

The second method assessed is that of multiple database principal component analysis. The results of chapter seven, section 2, allow the conclusion to be drawn that this method too is effective, within the limits of the investigation, in discriminating between action potential classes but not between action potential trains.

It may be seen from the results of the calculations in chapter seven, section 3, that rather than implementing separately the two methods of resolving overlapping action potential complexes within the decomposition knowledge source, the two methods should be implemented to complement one another. The more thorough method should only take effect when the more time efficient method fails. This is due to the relative processor time requirements for the separate methods.

The objectives stated in chapter one were met in the following ways. Various knowledge sources have been simulated (chapter two) and have enabled development of the MDSS. These simulations have also contributed to the creation of a simulated patient which is a useful addition to the MDSS. The created knowledge source simulating myoelectric activity (chapter four) also contributes to this simulated patient.

The hypothesis that the dynamics of the interference EMG are chaotic have been thoroughly investigated (chapter three) and discarded. Two methods of clustering MUAPs have been investigated (chapters six and seven), and the time requirements of two methods of overlapping MUAP resolution have been assessed. Overall the objectives originally set out for the research presented in this thesis have been met fully.

8.2 - Future Work.

Work should be done in the future in the area of simulation to help in the efficient operation and testing of the MDSS, and for the creation of a simulated patient. At present the simulation providing the results of nerve conduction velocity testing is only concerned with a selection of the nerves tested in the upper body. For completeness and to enable comparisons between upper and lower body conditions, this simulation should be expanded to include all the nerves present in the upper body that may need to be investigated and all the corresponding nerves in the lower body. Ultimately the MDSS needs to be provided with further real data knowledge sources as well as simulations of them, so it is required that more work be done to implement all the simulated knowledge sources as real working knowledge sources.

With regard to the method of discriminating between classes of MUAP using single database principal component analysis and learning vector quantization neural networks, so far all the investigations carried out have used simulated data. It is necessary to build a large database of low force, real, EMG signals, from which training and test data can be taken. The method then needs to be assessed using both a combination of real and simulated data, and purely real data. This is to verify that its performance is as good as results so far have suggested.

The tests carried out so far upon multiple database principal component analysis have been limited in scope, especially those carried out using real data. It is important that this study be widened in the future to include more tests upon simulated data and many more tests upon real data. This is required to validate those results already acquired and to add further confidence in the method.

Finally the major area for work in the future is the construction of a modular automatic decomposition routine for use as a knowledge source in the MDSS. A recent method of decomposing non-overlapping signals proposed by Stashuk (Stashuk & Paoli, 1998) utilises the combined results of various forms of EMG signal analysis to reach a solution to the problem. It is suggested that a similar method be utilised, combining the two methods of class discrimination proposed in this thesis with other methods such as

Simulation and analysis in electromyography.

firing time analysis. Also, it is suggested that such a scheme should utilise the methods of overlapping complex resolution as discussed in this thesis. The results of all these methods should be combined appropriately to produce a decomposed EMG signal from the raw data.

The quest for a useable MDSS in neurophysiology has proved difficult and much still needs to be done to achieve a satisfactory solution. This thesis, and the further works proposed, is a contribution to the international effort in this field.

Simulation and Analysis in Electromyography.

References.

Achari AN & Anderson MS, (1974), Myopathic changes in amyotrophic lateral sclerosis. *Neurology (Minneap)* 24: 477-481, 1974.

Argyropoulos CJ, Panayiatopoulos CP & Scarpalezos S, (1978), F and M wave conduction velocity in amyotrophic lateral sclerosis. *Muscle and Nerve*, 1978, 1: 479-485.

Babloyantz A & Destexhe A , (1988), Is the Normal Heart a Periodic Oscillator? *Biol. Cybern.* 58, 203-211,1988.

Basmajian J & De Luca CJ, (1985), *Muscles Alive - their functions revealed by Electromyography.* 5th Ed. 1985. Williams & Wilkins.

Bhullar HK, Loudon GH, Fothergill JC & Jones NB, (1990), Selective noninvasive electrode to study myoelectric signals., *Med. & Biol. Eng. & Comput.*, 1990, 28, 581-586.

Bortolan G & Casallegio A, (1995), Correlation dimension in rest ECG: A study in normal and arrhythmic patients., *Proceedings of the 1995 Conference on Computers in Cardiology*, Sept 1995, Vienna, Austria, 393-396.

Brody G, Scott RN & Balasubramanian R, (1974), A model for myoelectric signal generation., *Medical & Biological Engineering*, January 1974, PP29-41.

Broomhead DS & King GP, (1986a), Extracting qualitative dynamics from experimental data., *Physica* 20D, 1986, 217 -236.

Simulation and Analysis in Electromyography.

Broomhead DS & King GP, (1986b), On the qualitative analysis of experimental dynamical systems., *Nonlinear Phenomena and Chaos*, S. Sarkar, ed. (Adam Hilger, Bristol, 1986).

Buchthal F & Rosenfalck P, (1963), Electrophysiological aspects of myopathy with particular reference to progressive muscular dystrophy. In Bourne GH, Golarz MN (Eds) *Muscular dystrophy in man and animals* . Karger, Basel, 193-267 ,1963.

Casaleggio A, Pestelli S, Mela GS & Ridella S, (1988), Some results on a Fractal like behaviour of ECG signals, *Computers in Cardiology*, 1989, 421 - 424

Clamann HP, (1969), Statistical analysis of motor unit firing patterns in human skeletal muscle. *Biophysical Journal*, 9, 1233-1251, 1969.

Coatrieux JL, Toulouse P, Rouvrais B & Le Bars R, (1985), Automatic classification of electromyographic signals., *Electroenceph. & Clin. Neurophys.*, 1985, 55: 333-341.

Colston JR & Fearnley ME, (1967), Preliminary experience with an experimental action potential analyser on clinical electromyography. *Annals of Phys. Med.*, 1967, Vol. 9. PP 127-138.

Corkhill D, (1991), Blackboard systems, *AI Expert*, 41-47.

DeLisa JA, Lee HJ, Baran EM, Lai KS, Spielholz N, (1994), *Manual of nerve conduction velocity and clinical neurophysiology*, 3rd Ed., Raven Press, 1994.

DeLuca CJ, (1979), Physiology and mathematics of myoelectric signals., *IEEE Transactions on Biomedical Engineering*, Vol. **BME-26**, No. 6, June 1979, PP313-325.

Simulation and Analysis in Electromyography.

DeLuca CJ & Forrest WJ, (1973), Some properties of motor unit action potential trains recorded during constant force isometric contractions in man. *Kybernetic*, 12, 94-101, 1973.

Demuth H & Beale M, (1994), Neural Network toolbox for use with Matlab, The Mathworks Inc, Natick, Mass, US.

Desmedt JE & Borenstein S, (1976), Regeneration in Duchenne muscular dystrophy: electromyographic evidence. *Arch. Neurol.* 33(chic), 1976.

Eckmann JP, Oliffson Kamphorst S, Ruelle D & Ciliberto S, (1986), Liapunov exponents from time series., *Physical Review A*, Vol. 34, No. 6, December 1986.

Echternach JL, (1997), Introduction to electromyography and nerve conduction testing: A laboratory manual. SLACK Incorporated, NJ, USA, 1997.

Fausett L, (1994), Fundamentals of Neural Networks, Architectures, Algorithms and applications, Prentice Hall International, 156-195

Fuglsang-Frederikson A, Scheel U & Buchthal F, (1976), Diagnostic yield of analysis of the pattern of electrical activity and of individual motor unit potentials in myopathy. *J. Neurol. Neurosurg. Psychiat.*, 1976, Vol. 39, 742-750.

Fuglsang-Frederikson A, Scheel U & Buchthal F, (1977), Diagnostic yield of analysis of the pattern of electrical activity of muscle and of individual motor unit potentials in neurogenic involvement. *J. Neurol. Neurosurg. Psychiat.*, 1977, Vol. 40, 544-554.

Goodgold J & Eberstein A, (1977), Electrodiagnosis of neuromuscular diseases. 1977, 2nd Ed., Williams & Wilkins, Baltimore, 216-217.

Simulation and Analysis in Electromyography.

Grassberger P, Schreiber T & Schaffrath C, (1992), Nonlinear time sequence analysis, International journal of bifurcation and chaos, 1992, 1, 521-547.

Gurney K, (1997), An introduction to neural networks., UCL press, London.

Haykin S, (1994), Neural networks: a comprehensive foundation. Maxwell Macmillan International.

Hayward M & Willison RG, (1973), The recognition of myogenic and neurogenic lesions by quantitative EMG. New Developments in Electromyogr. and Clin. Neurophysiol. (Ed Desmedt JE) Vol. 2, PP 448-453, Karger, Basle, 1973.

Hayward M & Willison RG, (1977), Automatic analysis of the electromyogram in patients with chronic partial denervation. J. Neurol. Sci., 1977, Vol. 33, PP 415-423.

Hilborn RC, (1994), Chaos and nonlinear dynamics: an introduction for scientists and engineers. Oxford University Press, 1994.

Jones NB, & Lago PJA, (1977), Factors affecting the interpretation of EMG spectra. IEE Conf. Pub 159, 65-81, 1977.

Jones NB, & Lago PJA, (1982), Spectral Analysis and the Interference EMG, IEE PROC., VOL. 129, Pt A, No. 9, December 1982.

Jones NB, Lago PJA & Parekh A, (1987), Classification of point processes using principal component analysis. Mathematics in Signal Processing. PP 147-164, Clarendon Press, Oxford, 1987.

Simulation and Analysis in Electromyography.

Jones NB, Lago PJA & Parekh A, (1990), Principal component analysis of the spectra of point processes - An application in electromyography. *Mathematics in Signal Processing 2*. PP 369-384, Clarendon Press, Oxford, 1990.

Jones NB, Sehmi AS & Kabay S, (1992), Signal processing using combined methods, IFAC symposium on intelligent components and instruments, May 1992, 471-476, MALAGA.

Kangas J, Kohonen T & Laaksonen J, (1990), Variants of self organising maps, *IEEE transactions on neural networks 1*, 93-99.

Kearney MJ & Stark J, (1992), An Introduction to Chaotic Signal Processing, *GEC Journal of Research*, 1992, VOL. 10, NO. 1, 52-58.

Kosko B & Isaka S, (1993), Fuzzy Logic, *Scientific American*, July 1993, 76-81.

Lago PJA, (1979), Mathematical models of aspects of the electrical and mechanical activity of human muscle. PhD Thesis, University of Sussex, UK, 1979.

Lambert EH, (1982), Diagnostic value of electrical stimulation of motor nerves. *Electroencephalogr. Clin. Neurophysiol*, 1982, 22: 9-16.

Le Cun Y, Boser B, Denker JS, Henderson D, Howard RE & Hubbard W, (1990) Handwritten digit recognition with a backpropagation network., *Advances in neural information processing systems 2*., Morgan Kaufman, San Mateo, CA, 396-404, 1990.

Lefever RS & DeLuca CJ, (1982), A procedure for decomposing the myoelectric signal into its constituent action potentials. *IEEE Transactions on Biomedical Engineering*., Vol. **BME-29**, No. 3, March 1982.

Simulation and Analysis in Electromyography.

Lenman JAR & Ritchie AE, (1977), Clinical Electromyography, 2nd edition, Pitman Medical, 1977.

Liveson JA & Ma DM, (1992), Laboratory reference for clinical neurophysiology, FA Davis Company, Philadelphia, USA, 1992.

Loudon GH, (1991), Advances in Knowledge Based Signal Processing - A case study in Decomposition. Ph.D thesis, 1991. Submitted at the University of Leicester.

Loudon GH, Jones NB, & Sehmi AS, (1992), New signal processing techniques for the decomposition of EMG signals., Med. & Biol. Eng. & Comput.,1992, 30, 591-599.

Ludin HP, (1980), Electromyography in Practice, Georg Thiem Verlag, pp 48 - 101, 1980.

Maranzana Figini M & Fabbro M, (1981), A simulation model for the study of EMG signals in normal and pathological conditions., Electroencephalography and Clinical Neurophysiology, 1981, 52, 378-381.

McCulloch W & Pitts W, (1943), A logical calculus of the ideas immanent in nervous activity. Bulletin of Mathematical Biophysics, 7, 115-133.

McGill KC, Cummins KL & Dorfman LJ, (1985), Automatic decomposition of the clinical electromyogram., IEEE Transactions on Biomedical Engineering., Vol. BME-32, No. 7, July 1985.

Nii HP, (1994), Blackboard systems at the architecture level, Expert systems with applications, Vol. 7, 43-54, 1994.

Simulation and Analysis in Electromyography.

Ogo K & Nakagawa M, (1995), Chaos and fractal properties in EEG data., *Electronics and Communications in Japan, Part 3. Vol. 78, No. 10, 1995, 161 - 168.*

Parker PA & Scott RN, (1973), Statistics of the myoelectric signal from monopolar and bipolar electrodes., *Med. & Biol. Eng. & Comput.*, 11, 591-596, 1973.

Parekh A, (1986), Computer analysis of EMG turning points process. A thesis submitted for the degree of D.Phil at the University of Sussex, October 1986.

Person RS & Kudina LP, (1972), Discharge frequency and discharge pattern of human motor units during voluntary contraction of muscle., *Electroenceph. Clin. Neurophysiol.*, 32, 471-483, 1972.

Principe JC, Yu FS, Reid SA, (1990), Display of EEG Chaotic Dynamics, *Proc First Conf Visualisation Biomed Comput VBC 90.*, 1990, No. 1990., PP346-351.

Rapp P, Bashore T, Zimmerman I, Martinerie J, Albano A, Mees A, (1989), in *Chaos*, Ed Krasner, Amer. Assoc. Adv. Sci., 1989.

Richardson AT & Barwick DD, (1969), Clinical electromyography in disorders of voluntary muscles (Ed. Walton JN), 2nd Edition, Chap 27, 813-842, Churchill, London, 1969.

Rose AC & Willison RG, (1967), Quantitative electromyography using automatic analysis: studies in healthy subjects and patients with primary muscle disease. *J. Neurol. Neurosurg. Psychiat.*, 1967, Vol. 30, PP 403-410.

Rosenblatt F, (1962), *Principles of Neurodynamics*, Spartan Books.

Rosenfalck P & Masden A, (1954), *Acta. Physiol. Scand.*, 114 (Suppl. 31), 47, 1954.

Simulation and Analysis in Electromyography.

Sano M & Sawada Y, (1985), Measurement of the Lyapunov spectrum from chaotic time series. *Phys. Rev Lett.* 55, 1082, 1985.

Saranummi N, (1993), "The IFMBE and biosignal interpretation." *MBEC News.* No. 3, May 1993, 1-2.

Schwartz MS, Sargeant MK & Swash M, (1976), Longitudinal fibre splitting in neurogenic muscular disorders. Its relation to the pathogenesis of 'myopathic' change. *Brain* 99, 1976, 617-636.

Shiavi R & Negin M, (1975), Stochastic properties of motoneuron activity and the effect of muscular length., *Biol. Cybernetics.*, 19, 231-237, 1975.

Small GJ, Jones NB & Moreale E, (1997a), Simulation of knowledge sources for interaction with a blackboard based decision support system applied to neurophysiological diagnosis, Leicester University Engineering Department, Int. Rep. 97-19, Sept. 1997.

Small GJ, Jones NB & Fothergill JC, (1997b), Simulation of the clinical electromyogram, Proceedings of the World congress on Medical Physics and Biomedical Engineering, Nice, France, 14-19 Sept, 1997.

Small GJ, Jones NB, Fothergill JC & Mocroft AP, (1998), Chaos as a possible model of myoelectric activity., Proceedings of the IEE int. conf. Simulation 98. Innovation through simulation., University of York, Oct. 1998.

Stashuk D & Paoli GM, (1998), Robust supervised classification of motor unit action potentials., *Med. Biol. Eng. Comput.*, 1998, 36, 75-82.

Simulation and Analysis in Electromyography.

Swash M & Schwartz MS, (1981), Neuromuscular Diseases, A Practical Approach to Diagnosis and Management, Springer-Verlag, 1981.

Takens F, (1980), Detecting strange attractors in turbulence, Dynamical Systems and Turbulence, Warwick 1980. Springer-Verlag. PP366-381.

Trojaberg W & Buchthal F, (1965), Malignant and benign fasciculation. Acta Neurol. Scand 41: Suppl 13, 251-254 ,1965.

Wang S, (1995), A Framework for Medical Decision Support Systems - A case study in EMG Signal Processing. Ph.D thesis, 1995. Submitted at the University of Leicester.

Williams ER & Bruford A, (1970), Creatine Phosphokinase in motor neurone disease. Clin. Chim. Acta 27: 53-56, 1970.

Willison RG, (1964), Analysis of electrical activity in healthy and dystrophic muscle in man. J. Neurol. Neurosurg. Psychiat., 1964, Vol. 27. PP 386-394.

Wolf A, Swift JB, Swinney HL & Vastano JA, (1985), Determining Lyapunov exponents from a time series., Physica 16D, PP285-317, 1985.

Wolf A & Bessior T, (1991), Diagnosing chaos in the space circle, Physica 50D, 1991, Vol 50, 239 - 258.

Zimmerman H, (1990), Fuzzy set theory and its applications. Kluwer, Boston U.S.A, 1990.

Appendix 1.

Principal component analysis.

Principal component analysis.

Principal component analysis is a multivariate statistical analysis method in which the factors describing variability between members of a data set are calculated. This is achieved in the following manner: From the data set a mean vector and a variance-covariance matrix are calculated.

A set of new variables may be defined, made up from linear combinations of the measured variables, such that the first new variable contains the most variance, the second new variable contains the next greatest amount of variance, etc. The principal components of the data set are equal to the eigenvectors of the variance-covariance matrix formed above.

In effect, principal component analysis finds new variables which are linear combinations of the variables contained in the data set, so that they have maximum variation and are orthogonal. These new representations of our data set variables are made up from the mean vector plus weighted sums of the principal components.

This may be seen as:

$$F(x) = M(x) + a_1p_1 + a_2p_2 \dots\dots\dots$$

where $M(x)$ is the mean vector.

a_n is the n th principal component

p_n is the n th principal component coefficient corresponding to x .

or approximated by;

$$\sum_{n=0}^{N-1} a_n p_n(x)$$

Appendix 2.

Diagonal factor analysis.

Diagonal factor analysis.

Diagonal factor analysis, similarly to principal component analysis, is a method of describing a data set with non-correlated, orthogonal, factors. These factors are weighted sums of the original data set entries. The order and weights of these orthogonal data representations are calculated as follows:

Firstly the data set is standardised and the mean value of the data set is extracted from each entry within it. From this data set a correlation matrix is formed and the sum of squared correlations is calculated for each column in the correlation matrix. The sum of squared correlations serves as an indicator of how much of the total variance present in the original data set is described by each individual data entry represented by a column in the correlation matrix. The data entry associated with the column that has the highest sum of squared correlations is chosen to be the first diagonal factor. The weight given to this factor is the square root of the associated autocovariance.

For the second diagonal factor to be selected and its weight to be calculated, the effects of the first diagonal factor must be eliminated from the correlation matrix. Thus, the residual matrix is formed, each entry is determined using the equation:

$$R_{ij.A} = R_{ij} - P_i P_j$$

where $R_{ij.A}$ = ijth correlation value of residual matrix.

R_{ij} = ijth correlation value of correlation matrix.

P_i & P_j = weightings given to the ith and jth data entries.

the weightings are calculated as follows;

$$P_k = \frac{R_{vk}}{(R_{vv})^{\frac{1}{2}}}$$

where P_k = weighting of the kth data entry.

R_{vK} = kth value in row v of correlation matrix.

R_{vv} = value of selected weight for 1st diagonal factor.

The sum of squared correlations is then calculated for each column and the whole procedure is repeated until the weighting applied to the features is less than a chosen threshold. The number of factors chosen will be less than the original number of data set entries.

This information is based upon that in (Loudon, 1991).

Appendix 3.

Band pass filter construction.

Bandpass filter design.

It is known that the frequency components of the EMG below 20Hz are unstable and thus the EMG is recorded at frequencies above this level, i.e. the amplifiers bandwidth has a lower limit of 20Hz, (Basmajian & Deluca, 1985). The high frequency cut-off point of the amplifier is selected as being above the highest frequency of the wanted signal. The frequency limits imposed upon the signal also determine the frequency band of the noise too. For the case of our band limiting noise filter the band chosen was 20Hz - 2KHz. The 2KHz upper limit enables the routine to be tested thoroughly as some suggested upper limits were as low as 1KHz.

The filter used was designed using the MATLAB™ routine FIR2. An order of 256 was selected for the filter because this provided a good approximation to the ideal bandpass frequency band required. The characteristics of the filter have already been seen in chapter 6. The design is based upon the filter coefficients:

$$b(z) = b(1) + b(2)z^{-1} + \dots + B(n+1)z^{-n} .$$

Appendix 4.

Time intensive overlap resolution, calculations.

Time intensive method of resolving overlaps.

Assumptions: 1.) 6 MUAPs, each 36 samples in length.
2.) Machine running at 8 MFLOPS.

Calculations:

a.) Area of complex = $2n$ operations. n is no of samples in complex. must be odd as using simpsons approximation.

b.) Area of all candidate MUAPs.

$$= \sum_{i=1}^{i=m} 2n_i$$

c.) Discrimination using areas.

In this case there are single APs, double overlaps and triple overlaps to be considered. There are 6 singles, 15 possible double combinations and 20 possible triple combinations.

<i>Operations:</i>	Addition of areas	-	35 operations.
	discrimination	-	6 (single)
			29(double)
			39(triple)

The discrimination assumes selection of single AP with are nearest to complex, 2 nearest doubles and two nearest triples.

d.) Time registration possibilities for combinations selected in 1 -> 3.

For single chosen: align peak (n operations to find corresponding max. in complex, p operations to find max. in MUAP)

subtract AP from complex (n operations)

threshold residual (1 operation)

TOTAL OPERATIONS = $2n + p + 1$

For double combinations:

no of possible overlap positions = $p_1 + p_2 - 1$.

align peak 1 (n operations to find corresponding max. in complex, p operations to find max. in MUAP)

subtract AP 1 from complex (n operations)

align peak 2 (n operations to find corresponding max. in complex, p operations to find max. in MUAP)

subtract AP 2 from complex (n operations)

align peak 2 (n operations to find corresponding max. in complex)

subtract AP 2 from complex (n operations)

align peak 1 (n operations to find corresponding max. in complex)

subtract AP 1 from complex (n operations)

residual 1 < residual 2? (1 operation)

threshold residual (1 operation)

$$\underline{\text{TOTAL OPERATIONS} = 8n + 2p + 2}$$

For triple combinations:

$$\text{no. of possible overlap positions} = \sum_{n=a}^{n=b} (n_{ol}) + q - 1$$

n_{ol} = no. samples in double combination.

q = no. samples in single.

Must run APs through discrimination in all possible orders, thus 6 combinations.

$$\underline{\text{TOTAL OPERATIONS} = 18n + 3p + 12}$$

To resolve one overlap in this case of 63 samples.

a.) $2(63) = 126$.

b.) $6(2 \cdot 35) = 420$. (35 due to Simpson's approximation)

c.) $35 + 6 + 29 + 39 = 109$.

Short method

d.) $2(63) + 36 + 1 = 163$ (for single)

(double) ops. = $(8n + 2p + 2) \cdot 2 = (8(63) + 2(36) + 2) \cdot 2 = 1156$.

$$\text{(triple) ops} = (18n+3p=12)*2 = (18(63)+3(36)+12)*2 = 2508$$

$$\text{Total operations} = 126+420+109+163+1156+2508 = 4482$$

$$\text{Time to compute} = \frac{4482 \text{ FLOPS}}{8000000 \text{ FLOPS / S}} = 0.00056_s$$

Complete method

If previous method produces a residual that is too large, the following method should be employed. This method compares the sum of squared differences for the selected combinations at every time registration possible, with the complex being resolved.

$$\text{no. possibilities (double)} = n+p-1 = 36+36-1 = 71.$$

$$\text{no. possibilities (triple)} = \sum_{n=36}^{n=71} (n_{oi}) + q - 1 = 1296.$$

Operations: subtract possible combination from actual complex (n ops, n is longest of 2 waves)

square difference elements	(n ops)
sum squared elements	(n ops)
threshold	(1 op)
smallest?	(1 op)

thus $3n+2$ operations per combination.

$$\text{(single) ops} = 3n+2 = 3(63) + 2 = 191.$$

(double)

ops

$$=55(3(63)+2)+2(3(64)+2)+2(3(65)+2)+2(3(66)+2)+2(3(67)+2)+2(3(68)+2)+2(3(69)+2)+2(3(70)+2)+2(3(71)+2) = 13777.$$

(triple)

ops =no. ops*(3n+2) =

$$406(3(63)+2)+29(3(64)+2)+30(3(65)+2)+31(3(66)+2)+32(3(67)+2)+33(3(68)+2)+34(3(69)+2)+35(3(70)+2)+36(3(71)+2)+35(3(72)+2)+34(3(73)+2)+33(3(74)+2)+32(3(75)+2)+ \text{etc.....} = 222342.$$

for our 5 possible selections (1 single, 2 doubles and 2 triples)

No. Operations:

a.) $2(63)=126.$

b.) $6(2*35)=420.$ (35 due to simpson's approximation)

c.) $35+6+29+39=109.$

(single) = 191

(double) = $2(13777)$

(triple) = $2(222342)$

Total No. = 473084 FLOPS.

$$\text{Processing Time} = \frac{473084}{8000000} = \mathbf{0.059s}$$

For 100 Overlaps, 10 each of, 36, 46, 52, 56, 66, 72, 76, 86, 96, 106, respectively.

$$\text{a.)} = 20(36)+ 20(46)+ 20(52)+ 20(56)+ 20(66)+ 20(72)+ 20(76)+ 20(86)+ 20(96)+ 20(106) = 13840.$$

$$\text{b.)} = 420.$$

$$\text{c.)} = 35+[(6+29+39)*100] = 7435.$$

Short Method.

$$\begin{aligned} \text{(single)} &= [10(2(36)+36+1)] + [10(2(46)+36+1)] + [10(2(52)+36+1)] + [10(2(56)+36+1)] \\ &+ [10(2(66)+36+1)] + [10(2(72)+36+1)] + [10(2(76)+36+1)] + [10(2(86)+36+1)] + \\ &[10(2(96)+36+1)] + [10(2(106)+36+1)] = 17540. \end{aligned}$$

$$\begin{aligned} \text{(double)} &= [(10*2)(8(36)+2(36)+2)] + [(10*2)(8(46)+2(36)+2)] + \\ &[(10*2)(8(52)+2(36)+2)] + [(10*2)(8(56)+2(36)+2)] + [(10*2)(8(66)+2(36)+2)] + \\ &[(10*2)(8(72)+2(36)+2)] + [(10*2)(8(76)+2(36)+2)] + [(10*2)(8(86)+2(36)+2)] + \\ &[(10*2)(8(96)+2(36)+2)] + [(10*2)(8(106)+2(36)+2)] = 125520. \end{aligned}$$

$$\begin{aligned} \text{(triple)} &= [(10*2)(18(36)+3(36)+12)] + [(10*2)(18(36)+3(36)+12)] + \\ &[(10*2)(18(36)+3(36)+12)] + [(10*2)(18(36)+3(36)+12)] + [(10*2)(18(36)+3(36)+12)] + \\ &[(10*2)(18(36)+3(36)+12)] + [(10*2)(18(36)+3(36)+12)] + [(10*2)(18(36)+3(36)+12)] + \\ &[(10*2)(18(36)+3(36)+12)] + [(10*2)(18(36)+3(36)+12)] = 273120. \end{aligned}$$

$$\text{Total operations} = 13840 + 420 + 7435 + 17540 + 125520 + 273120 = \underline{\underline{437875}}.$$

$$\text{Time to compute} = \frac{437875 \text{ FLOPS}}{8000000 \text{ FLOPS/S}} = 0.0547_s$$

Complete Method.

$$\begin{aligned} \text{(single)} &= [10(3(36)+2)] + [10(3(46)+2)] + [10(3(52)+2)] + [10(3(56)+2)] + \\ &[10(3(66)+2)] + [10(3(72)+2)] + [10(3(76)+2)] + [10(3(86)+2)] + [10(3(96)+2)] + \\ &[10(3(106)+2)] = 20960. \end{aligned}$$

$$\begin{aligned} \text{(doubles)} &= \sum no.poss * no.ops = [(10*71)(3(36)+2)] + [(10*71)(3(46)+2)] + \\ &[(10*71)(3(52)+2)] + [(10*71)(3(56)+2)] + [(10*71)(3(66)+2)] + [(10*71)(3(72)+2)] + \\ &[(10*71)(3(76)+2)] + [(10*71)(3(86)+2)] + [(10*71)(3(96)+2)] + [(10*71)(3(106)+2)] = \\ &1564930. \end{aligned}$$

$$\text{(triples)} = \sum no.poss * no.ops = 31655130.$$

$$\begin{aligned} \text{Total operations} &= 13840 + 420 + 7435 + 20960 + (2*1564930) + (2*31655130) = \\ &66482775. \end{aligned}$$

$$\text{Total No.} = 66.483 \text{ MFLOPS.}$$

$$\text{Processing Time} = \frac{66.483 \text{ MFLOPS}}{8 \text{ MFLOPS / S}} = \mathbf{8.31s}$$

Appendix 5.

**Simulation of the clinical electromyogram, Proceedings of the World congress on
Medical Physics and Biomedical Engineering, Nice, France, 14-19 Sept, 1997.**

SIMULATION OF THE CLINICAL ELECTROMYOGRAM

G.J. Small, N.B. Jones & J.C. Fothergill

University of Leicester, Department of Engineering, Leicester LE1 7RH, UK

At present, the best model for determining the firing of motor units in the human muscle system, appears to consist of trains of impulses combined driving a bank of filters, the impulse responses of which are representative of the individual action potential shapes that appear in the EMG record. The most suitable distribution for the occurrence of each impulse in a train has received much attention over the years. Distributions such as the *Weibul*, *Poisson* and *Exponential* distribution have all been considered and shown not to be ideal. The Gaussian distribution has been settled upon as suitable for most purposes as it has been shown to explain some important properties of the EMG. However, the Gaussian distribution has deficiencies when determining the next firing of a motor unit, which are reason enough to search for new methods of determining the firing time of each motor unit that is active during a muscle contraction.

In all existing models the behaviour of the firing rate during muscle contraction has been assumed to be stochastic. However it is feasible that the next firing in a motor unit action potential train is determined by a chaotic deterministic process instead.

In an attempt to examine this idea investigations into the dynamics of the system driving the firing of motor unit during a contraction have been carried out. A numerical technique (correlation dimension analysis) was used, as the first step towards identifying the presence of chaos in the EMG record.

As a result of this analysis it is evident that the system driving motor unit firing during a contraction of the human muscle is not clearly chaotic in nature but indeed seems to have truly stochastic properties. Thus the original model consisting of filters triggered by trains of normally distributed impulses, remains the most suitable model available at present.

Appendix 6.

Chaos as a possible model of myoelectric activity., Proceedings of the IEE int. conf.

Simulation 98. Innovation through simulation., University of York, Oct. 1998.

CHAOS AS A POSSIBLE MODEL OF ELECTROMYOGRAPHIC ACTIVITY.

G J Small [†], N B Jones [†], J C Fothergill [†] & A P Mcroft [‡].

[†] University of Leicester, Department of Engineering, Leicester, LE1 7RH, England.

[‡] The Queen Elizabeth Hospital, Edgbaston, Birmingham, B15 2TH, England.

ABSTRACT.

Grounds for the hypothesis that chaotic dynamics may underly the EMG are established and discussed.

In order to test this hypothesis, investigations into the dynamics of the system driving the firing of motor units during a contraction have been carried out. They consist of: 1.) The construction of phase portraits. 2.) Correlation dimension analysis, and 3.) Calculation of dominant Lyapunov exponents.

The results obtained from analysing real EMG data recorded from both normal and disordered subjects do not support the hypothesis that the EMG arises for a system having chaotic dynamics.

As a result of this analysis it is evident that the system driving motor unit firing during a contraction of the human muscle may not be proven to be chaotic, at least not with the techniques presently available. Simulation may still be better achieved using a model based upon statistics.

INTRODUCTION.

This paper seeks to introduce and explain the existence of chaotic dynamics, especially in biomedical systems. A brief description of Chaos and the observable behaviour both causing and characterising it is given.

Evidence of the occurrence of chaos in biomedical systems is given, and along with details of pitfalls in current techniques for simulating electromyograms. This is used to form the hypothesis that the dynamics underlying the firing of MUAPs may be chaotic in nature, and as such, that a model based upon chaotic dynamics may be better suited to the purpose of EMG simulation than current techniques.

Methods used currently for identifying the presence of chaos in experimental and real time series are described, giving some insight as to how results should be interpreted.

What is Chaos.

Chaos may be defined as a deterministic dynamical process in which there is long term unpredictability arising from sensitive dependence on initial conditions.

Deterministic chaos is a natural occurrence in many non-linear systems, that 'until recent years has been believed to be totally unpredictable', Kearney & Stark (1). Chaotic systems are deterministic, although their output may be random in appearance.

In a chaotic system, any small differences in initial conditions grow exponentially with time, rather than decrease or grow linearly. It is therefore impossible to predict the long term behaviour of such systems, in spite of their being deterministic. However the short term behaviour of the system may be predicted successfully.

Chaotic behaviour is characterised by the divergence of nearby trajectories in state space. As a function of time, the separation between two initially close trajectories increases in an exponential way, at least for periods of short duration. The short duration is a necessary factor because in chaotic systems the trajectories remain within some bounded region by intertwining and wrapping around each other without intersecting and without repeating exactly. This forms a complex strange attractor in phase space, Hilborn (2). The presence of a strange attractor in the phase space of a system is usually a positive sign of chaos, although some non-chaotic strange attractors do exist.

Chaos in Biomedical Systems.

Evidence of chaotic behaviour has been found in biological signals, such as the Electrocardiogram (ECG). The ECG exhibits quasi-periodic behaviour, but with many irregularities in the record. Babloyantz & Destexhe found that the correlation dimension of recorded ECGs settled at values ranging from 3.6 ± 0.1 to 5.2 ± 0.1 , Babloyantz & Destexhe (3). These values suggested that the normal cardiac oscillations follow deterministic dynamics of a chaotic nature, characterised by an unusually high dimension. Babloyantz & Destexhe also suggested that any

mathematical model for the description of cardiac activity must contain at least five dimensions, to encompass the majority of the dimension range, and must show deterministic chaos in its output. These results were supported by Bortolan & Casallegio, who found that at rest, normal ECG had a correlation dimension value usually below 3, whilst for arrhythmic patients, the values were as large as 4.5, Bortolan & Casallegio (4). For the cardiac attractor, the largest Lyapunov exponent was found to be $\lambda = 0.38 \pm 0.08$ (3). This is a clear positive exponent and implies that the ECG exhibits chaotic dynamics.

Similar results have been obtained for the Electroencephalogram (EEG), where the EEG dimensionality varies according to the cognitive state, and also with some pathological brain conditions such as epileptic seizures, Rapp *et al* (5). Researchers have found that the EEG's correlation dimension falls within the range 3 to 8, Principe & Reid (6).

It has been reported, Ogo & Nakagawa (7), that the maximum Lyapunov index is positive for most of the EEG frequency components, for almost all subjects studied. In other words, it is estimated that the EEG is composed of a large number of frequency components with chaotic properties.

EMG Simulation.

The model upon which EMG simulation is currently based consists of banks of filters whose impulse responses are equivalent to individual MUAP templates, and trains of pulses determining the firing of each motor unit, thus determining the inter pulse interval (IPI) between each MUAP, Figure 1. The Model is derived conceptually from that presented by Parker & Scott (8), and others.

There has been much thought on the subject of determining the occurrence of motor unit firing. In 1979 DeLuca stated that only minimal (if any) dependence exists among the IPIs of a particular MUAP train. Therefore the MUAPT may be represented as a renewal pulse process, one in which each IPI is independent of all other IPIs, DeLuca (9).

This was supported by Jones *et al* in 1987, they reported that works carried out on different muscles had produced conflicting conclusions on the suitability of renewal procedures for modelling muscular behaviour. It was then suggested that the process of firing is almost certainly of the non-renewal type based on the biophysics of membrane recovery after firing. However, they concluded that the non-renewal characteristics exhibited were muscle dependant, and of less

importance than the distributions associated with the firings, Jones *et al* (10).

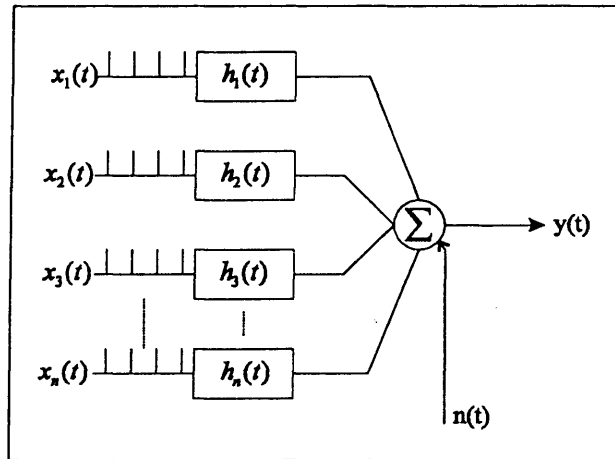


Figure 1 - The Current Model for EMG Simulation.

Various distributions have been suggested for this purpose. The Poisson distribution Brody & Scott (11) and the Weibull distribution Maranzana *et al* (12), Deluca & Forest (13), are two such distributions. None of these, however, would predict a peak in the EMG power spectrum at the appropriate firing frequencies, and the occurrence of this is, in fact, often observed, Jones & Lago (14). The use of a renewal process utilising Gaussianly distributed IPIs has been shown by Lago and Jones to predict the local peak in the EMG power spectrum, Lago and Jones (15), (10). So the Gaussian distribution has seemed to be the one most suited to modelling the EMG, to date.

Despite the success of the Gaussian distribution in modelling some key features of the EMG, it is deficient in determining the occurrence of each successive MU firing. The Gaussian distribution falls short of ideal because beyond a few standard deviations of the mean of the distribution, the probability of a firing occurring, although small, is not zero.

This cannot be ignored, because a model of motor unit firing based upon the Gaussian distribution could fire pulse $n+1$ at the same time as, or before pulse n , the previous pulse in the series of pulses making up the firing times of a MUAPT.

Models of the membrane.

The Hodgkin-Huxley membrane model is the analog circuit studied most in neurophysiology. Simplifications such as that by Fitzhugh & Nagumo, and others such as the Bonhoeffer-Van der Pol model show that there are

non-linear and positive and negative feedback processes in operation during neural discharge. These processes are prerequisite for the occurrence of chaos and so a chaotic model looks like an attractive alternative.

A Chaotic EMG Simulator?

It may be stated that the EMG is neither stochastic or deterministic. It is a highly structured signal, made up from a collection of signals that have elements of variation within them, and the contributions of other spontaneous factors. The fact that there are elements of variation within the signal, and that the firing of MUs appears to be difficult to predict, supports the suggestion that the EMG, at medium to high levels of force, may be better described by a chaotic model than by a model based on a random procedure such as Gaussian Renewal.

Other factors supporting this proposition are the problems inherent in the use of Gaussian renewal, the most suited statistical distribution, to determine the next firing of a MU, the presence of non-linear and positive and negative feedback processes in neural discharge, and the presence of chaotic dynamics in other biomedical systems, namely the heart and the brain.

METHODS OF IDENTIFYING CHAOS IN A TIME SERIES.

There are several different ways in which chaos may be identified in a time series. These include qualitative methods such as the construction of phase portraits. There are also quantitative methods such as correlation dimension analysis, and calculation of Lyapunov exponents. These three methods are employed in this investigation, and are described in this section.

Construction of Phase Planes/Portraits.

The phase plane/portrait is a representation of the state of a dynamical system in phase space. The instantaneous system state is represented by a point in this space. As time evolves, the system state changes forming a trajectory in the phase space, the ensemble of these forms the phase portrait, Cassaleggio *et al* (16), (3).

Phase portraits are constructed from a single measured system variable. A time delay is introduced between the

variables used to describe the system in m-dimensional phase space, leading to an m-dimensional vector;

$$X(t) = x(t), x(t + \tau), \dots, x(t + (m - 1)\tau)$$

The phase space spanned by the new variables, $x(t), \dots, x(t + (m - 1)\tau)$, has topological properties identical to the original phase portrait. Takens (17), Broomhead & King (18) & (19).

Two or three dimensional views of the phase portrait may be observed, these offer information about the dynamics of the system from which they are constructed. Stable systems have trajectories that approach a single point in phase space, an attractor, by describing a straight line or spiral. An example of chaotic behaviour, for the EEG the trajectories are much more complex because they attempt to approach a strange attractor, a sign of chaos, (3).

Correlation Dimension Analysis.

This quantitative method is based upon Takens Embedding Theorem, (17), which states that for all typical time series obtained from a finite degree of freedom dynamical system, there is some integer m and a function G such that:

$$x_{n+1} = G(x_n, x_{n-1}, \dots, x_{n-m+1})$$

where m is the embedding dimension, and $m \leq 2d + 1$, where d is the number of degrees of freedom of the underlying dynamical system.

The method of identification of chaos employed here requires the calculation of the correlation dimension for increasing values of m , (1). The correlation dimension seeks to measure the dimension of a finite data set extracted from a time series, in m-dimensional space, on which the points of the embedded data set lie. It is therefore a measure of the number of variables that are necessary to describe that data set.

The correlation dimension is defined as:

$$D_c = \lim_{E \rightarrow 0} \left\{ \frac{\log C(E)}{\log E} \right\}$$

that is, the gradient of the plot of $\log C(E)$ against $\log E$ as E , the separation of pairs of points, approaches zero. $C(E)$ is the proportion of pairs that are within a distance E of each other.

As the correct embedding dimension for a system is unknown and may not be calculated, a trial and error procedure must be followed to determine whether or not the system under scrutiny is chaotic. The correlation dimension must be calculated for increasing values of m , and the way in which it behaves determines the nature of the system.

If $D_c=0$ we have a regular periodic time series; if D_c continues to increase with m , then the series was generated by a truly random process, i.e. for white noise $D_c=\infty$; if however, the correlation dimension should stabilise at a non-integer value, then the system is said to contain a 'strange attractor'. This is usually a sign of chaos, although strange non-chaotic systems do occur.

There are certain factors which effect the computational accuracy of correlation dimension analysis, of which the two most pertinent are described. If insufficient data points are used in the analysis, a hard limit is set on the upper value of the correlation dimension, thus possibly preventing of a true result being reached, should the actual value of correlation dimension exceed the enforced upper limit, (2). A second effect of too few points is that, at higher levels of embedding the density of points in phase space is too low to yield useful information. The points appear to spread out in phase space giving the appearance that they are generated by a system dominated by random dynamics, and no correlation dimension will be settled upon.

Noise in the signal being analysed may effect accurate calculation of the correlation dimension. Whilst the average magnitude of the noise in the signal is greater than the separation of point pairs generated from the signal the noise will dominate the structure of the attractor and as such, effect the computed correlation dimension, (2).

Calculation of Lyapunov exponents.

The spectrum of Lyapunov exponents has proven to be the most useful dynamical diagnostic tool for chaotic systems, Wolf *et al* (20). Lyapunov exponents are a measure of the average exponential rates of either divergence or convergence of nearby trajectories in phase space. There are as many Lyapunov exponents as there are dimensions in the state space, however the largest or dominant Lyapunov exponent is considered to be of most interest.

Since nearby orbits in the system correspond to nearly identical states, exponential orbital divergence means that systems whose initial differences were irresolvable, will soon behave quite differently, (20).

Negative Lyapunov exponents are indicative of converging trajectories, positive exponents are indicative of diverging trajectories whilst zero exponents indicate the temporary continuous nature of a disturbance to the system. It is the presence of at least one positive Lyapunov exponent that indicates chaotic behaviour in a system. A positive exponent indicates that motion within the attractor is locally unstable and exhibits sensitive dependence to initial conditions, (19)

The Lyapunov exponent may be defined as follows. If two nearby trajectories on a chaotic attractor initially with separation d_0 at time $t=0$ diverge so that their separation becomes $d(t)$ at time t ,

$$d(t) = d_0 e^{\lambda t}$$

then λ is the Lyapunov exponent for the trajectories, (2).

ATTEMPTED IDENTIFICATION OF CHAOS IN THE EMG.

The three methods of identifying chaos, previously outlined in this paper are employed to determine whether the dynamics of MUAP firing exhibit any signs of chaotic behaviour. Authentic EMG signals, recorded using the TEAC R81 analogue recorder and digitised using an AT&T DSP32C 16Bit DSP board are analysed. The data was sampled at a rate of 8khz.

EMG Phase Portraits.

Phase portraits were constructed for EMG signals recorded from muscles considered to be in normal condition, and for signals recorded from muscles in various states of disorder. Different delays (τ) were employed, using signals of approximately 40000 samples.

The phase portraits observed, see fig 2, appear to consist of trajectories that loop as time passes and the state of the system driving MUAP firing changes. It is clear that the behaviour of the EMG is not periodic, periodicity being represented by a single closed curve. However the phase portraits of the EMG in no way proves that the underlying dynamics are Chaotic. It is, in fact, not possible to extract much useful information from these plots.

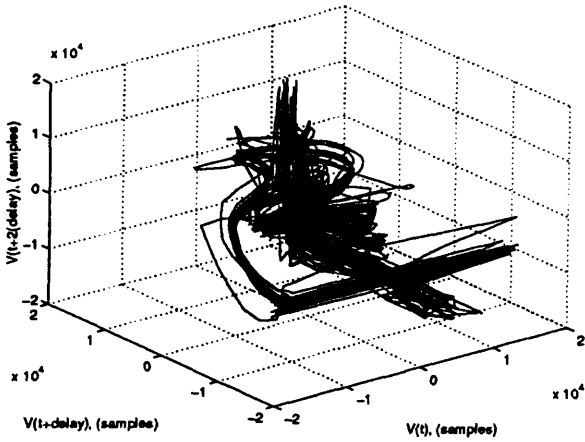


Figure 2 - A Phase Portrait of a signal recorded from a muscle with muscular dystrophy. Delay = 1mS.

The Behaviour of the correlation dimension (Dc).

Real signals of approximately 9000 samples, recorded from both normal and disordered muscle groups, were analysed using this technique.

Table 1 - The signals upon which correlation dimension analysis was performed.

Disorder	Signal No.	Subjects sex.	Samp freq. (KHz)	Duration. (S)
NORM	1	Male	8	1.12
	2			1.12
	3			1.12
	4			1.12
	5			1.12
MND.	1	Male	8	1.12
	2			1.12
LGMD	1	Male	8	1.12
	2			1.12
DMC	1	Male	8	1.12
	2			1.12
	3			1.12
	4			1.12
	5			1.12
PMA	1	Male	8	1.12
	2			1.12
	3			1.12
	4			1.12
	5			1.12

Where MND is Motor Neurone disease, LGMD is Limb girdle Muscular dystrophy, DMC is Dermatomyocytis and PMA is Primary muscle atrophy.

The correlation dimension was calculated for successive levels of embedding, 1 through 10, in order that the behaviour of Dc may be observed over the length of the progression.

The gradient of the log C(E)/log E plot is the correlation dimension, and this is calculated using regression analysis, with a 65% confidence level in the gradient of each regression line. This gives an indication of how accurate the estimate of the correlation dimension is, and provides a degree of assurance that the result is realistic.

Correlation dimension progressions were constructed for sets of signals exhibiting certain disorders, see table 1 and their behaviour was observed. See figures 3 and 4.

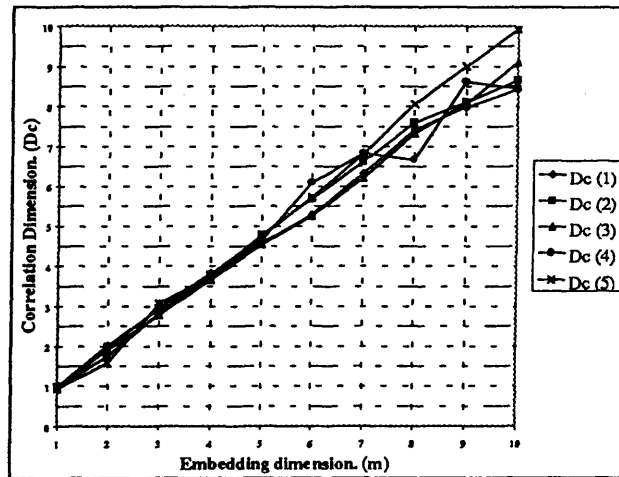


Figure 3 - Summary of correlation dimension progressions with increasing embedding dimension, for signals recorded from a muscle with no disorder.

The progression of the correlation dimension with increasing embedding dimension, for EMGs with no disorder, as seen in figure 3, indicates that the hypothesis of chaotic dynamics determining MUAP firing, is not a valid one.

It may be seen that the correlation dimension values, for all five signals in this class, continue to rise in an almost linear fashion. This does not match the standard behaviour for the correlation dimension of a chaotic system which will taper off and settle around some non-integer value. The non-integer value where the correlation dimension settles is an indication of chaos in this analysis, and the next integer above the correlation dimension is the minimum number of variables required to describe the system. If the value settled at was an integer, the system would not be chaotic. The non integer correlation dimension on its own, is not however, conclusive proof of the presence of chaos in a time signal. To obtain a definite affirmative,

further testing, such as calculation of Lyapunov exponents, must be carried out.

The progressions calculated from a muscle with an inherited motor sensory neuropathy and those from a muscle with chronic dermatomyocytis also have a prevailing tendency to increase almost linearly.

Figure 4 introduces some results which provide evidence in favour of chaos as a model for the EMG. The two progressions, in this case, for a muscle undergoing a severe form of myopathy, display a correlation dimension which appears to settle at values of 5.7 ± 0.3 in the case of signal one, and at 3.02 ± 0.1 in the case of signal two. However, the number of data points used for correlation dimension calculation, in this case ~ 9000 , is insufficient for accurate calculation at high levels of embedding. The number of data points necessary for accurate calculation of the correlation dimension is in the range 5^n to 10^n , where n is the embedding dimension.

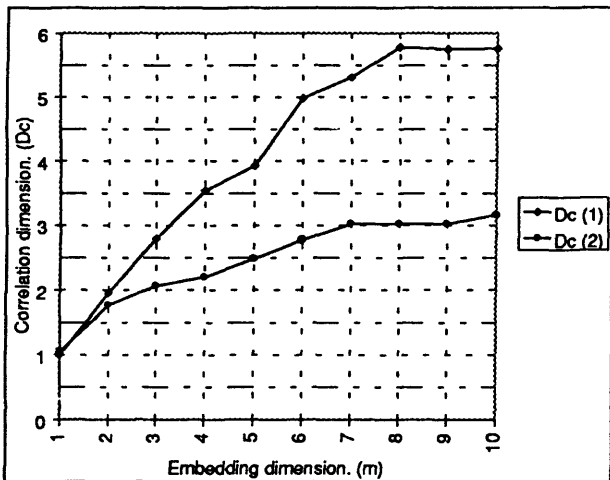


Figure 4 - Summary of correlation dimension progressions with increasing embedding dimension, for signals recorded from a muscle with limb girdle muscular dystrophy.

The number of points used here allows confidence in levels of embedding up to between 3 and 5. Thus, not much confidence can be placed in these apparent non-integer correlation dimensions, because they do not settle until the seventh or eighth level of embedding. It is also possible that this indication of chaotic behaviour is totally case specific. It does not, in itself, negate the general thesis that chaos theory will not provide an appropriate method for modelling the clinical electromyogram.

The progressions calculated from a muscle with a primary muscle atrophy are similar to the normals until the sixth level of embedding, but continue to increase at a much decreased rate after that. This could be attributed to a hard upper limit being set upon the

magnitude of the correlation dimension by a limited number of input data points. It does not however settle at a non-integer level.

3.5.3 Lyapunov exponents of the EMG.

Lyapunov exponents were estimated using the method previously described. The data upon which the analysis was performed, was the same data used for correlation dimension analysis, the sole difference being that the number of points used was raised from approximately 9000 to 32000.

In order to verify the stability of the resulting estimated dominant Lyapunov exponent it is necessary to repeat the calculation for varied embedding dimensions and evolution times etc.

The estimated values calculated for differing EMG signals varied in magnitude, but the amplitude was of the order of approximately 200 to 350 bits/second. This order of magnitude was estimated for various inputs to the estimation algorithm. See figure 5.

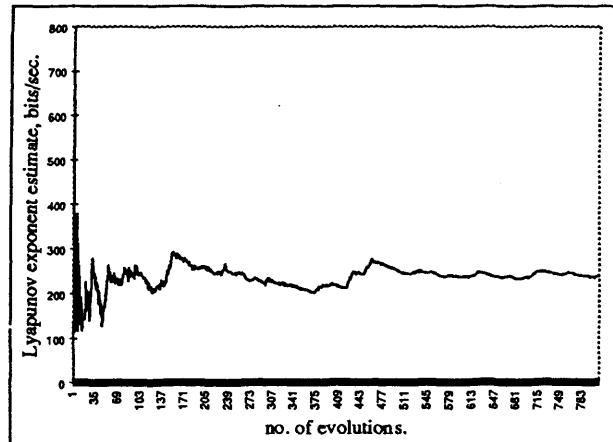


Figure 5 - Dominant Lyapunov exponent estimation for a normal signal.

An exponent falling within this range would lead to the belief that the data of interest was being drowned out by noise. There are two reasons for this not being so.

The analysis algorithm has been tested on data known to be chaotic in nature and in these instances has yielded the expected results. The algorithm is known to deal with some noise and the data being analysed has a very low noise content.

The second reason for believing that the unusually high exponent is not indicative of noise is more involved. A comparison between the dominant exponents yielded from real EMG signals and from synthetic signals

comprising MUAP templates firing randomly was made. The results for both types of signal were similar in that they exhibited exponents with amplitudes of the same order of magnitude, but more importantly numerically close to one another.

The dominant Lyapunov exponent estimated for a truly random time series whose dynamics were based upon the normal distribution, was an order of magnitude larger than those calculated for both the real EMG and synthetic signals.

The exponent then, leads us to believe that the dynamics displayed by our real signals are random. This is because the dominant exponent is large, suggesting noiselike random behaviour, but is not as large as that for a true random signal, also because the exponent is comparable with that of signals that do not contain a large proportion of noise, and whose dynamics are known.

These results, and their meaning, are in accordance with the information gained from correlation dimension analysis of real EMG signals. It is thus reasonable to believe that the dynamics behind the clinical electromyogram may be better described by a random procedure than a chaotic one.

CONCLUSIONS.

It may be concluded from the results yielded from construction of phase portraits, that the dynamics of the EMG appear not to be chaotic. With the results from correlation dimension analysis and dominant Lyapunov exponent analysis, it is even more likely that the underlying dynamics of the human muscular system are not chaotic, but are more random in nature.

In general, a chaotic model for the firing of MUAPs within the EMG would seem inappropriate. A better suited model for simulation of the EMG remains banks of filters whose impulse responses are representative of various action potential templates, triggered by trains of pulses, whose firing is determined by statistical methods e.g. (Gaussian renewal), summed, to provide a synthetic EMG.

REFERENCES.

- Kearney MJ & Stark J, (1992), An Introduction to Chaotic Signal Processing, GEC Journal of Research, 10, NO. 1, 52-58.
- Hilborn RC (1994), Chaos and nonlinear dynamics - an introduction for scientists and engineers., Oxford University Press, New York, USA.
- Babloyantz A & Destexhe A, (1988), Is the Normal Heart a Periodic Oscillator? Biol. Cybern. 58, 203-211.
- Bortolan G & Casallegio A (1995), Correlation dimension in rest ECG: A study in normal and arrhythmic patients., Proceedings of the 1995 Conference on Computers in Cardiology, Sept 1995, Vienna, Austria, 393-396.
- Rapp P, Bashore T, Zimmerman I, Martinerie J, Albano A, Mees A (1989), in Chaos, Ed Krasner, Amer. Assoc. Adv. Sci.
- Principe J C, Yu FS, Reid SA (1990), Display of EEG Chaotic Dynamics, Proc First Conf Visualisation Biomed Comput VBC 90., 1990, No. 1990., PP346-351.
- Ogo K & Nakagawa M (1995), Chaos and fractal properties in EEG data., Electronics and communications in Japan, Part 3. Vol. 78, No. 10, 1995, 161 - 168.
- Parker PA & Scott RN (1973), Statistics of the myoelectric signal from monopolar and bipolar electrodes. Med. Biol. Eng., 11, PP591-596.
- DeLuca CJ, (1979), Physiology and mathematics of myoelectric signals., IEEE Transactions on Biomedical Engineering, Vol. BME-26, No. 6, June 1979, PP313-325.
- Jones NB, Lago PJA & Parekh A, (1987), Classification of point processes using principal component analysis. Mathematics in Signal Processing. PP 147-164, Clarendon Press, Oxford, 1987.
- Brody G, Scott RN & Balasubramanian R, (1974), A model for myoelectric signal generation., Med. Biol. Eng., January 1974, PP29-41.
- Maranzana Figini M & Fabbro M, (1981), A simulation model for the study of EMG signals in normal and pathological conditions., Electroencephalography and Clinical Neurophysiology, 1981, 52, PP378-381.
- Deluca CJ & Forest WJ (1973), Some properties of motor unit action potential trains recorded during constant force isometric contractions in man., Kybernetik, 12, PP160-168.
- Jones NB, & Lago PJA, (1982), Spectral Analysis and the Interference EMG, IEE PROC., VOL. 129, Pt A, No. 9, December 1982.

15. Lago PJA & Jones NB (1977), Effect of motor unit firing time on EMG spectra., Med. Biol. Eng. & Comput., 15, PP648-655.
16. Casaleggio A, Pestelli S, Mela GS & Ridella S, (1988), Some results on a Fractal like behaviour of ECG signals, Computers in Cardiology, 1998, 421 - 424
17. Takens F (1980), Detecting strange attractors in turbulence, Dynamical Systems and Turbulence, Warwick 1980. Springer-Verlag. PP366-381.
18. Broomhead DS & King GP (1986), Extracting qualitative dynamics from experimental data., Physica 20D, 1986, 217 -236.
19. Broomhead DS & King GP (1986), On the qualitative analysis of experimental dynamical systems., Nonlinear Phenomena and Chaos, S. Sarkar, ed. Adam Hilger, Bristol, UK.
20. Wolf A, Swift JB, Swinney HL & Vastano JA, (1985), Determining Lyapunov exponents from a time series., Physica 16D, PP285-317.

Appendix 7.

The use of neural networks in the automatic extraction of firing time statistics in electromyography. Proceedings of the 8th international IMEKO conference on measurement in clinical medicine, September 16-19, 1998, Dubrovnik, Croatia.

THE USE OF NEURAL NETWORKS IN THE AUTOMATIC EXTRACTION OF FIRING TIME STATISTICS IN ELECTROMYOGRAPHY.

Gary J. Small* & N. Barrie Jones*.

*Dept. of Engineering, University of Leicester, University Road, Leicester, England, UK.

E-mail: nbj1@le.ac.uk

Abstract

This paper assesses the use and performance of some artificial neural networks (ANNs) in automatically decomposing the clinical electromyogram, with the aim of determining the intrinsic firing statistics.

Reasons for the need for automatic decomposition are given and one suggested method is highlighted.

In this method an attempt is made to train neural networks of different architectures to solve the problem of clustering action potentials into their constituent types using different inputs.

The performance of the most successful method is assessed in the presence of noise and overlapping data.

As a result of these tests, it is established that the method of action potential clustering into types, using learning vector quantization networks and principal component coefficients as inputs, is effective in clean data and in noisy data, but not in the presence of overlapping action potentials.

Keywords

Decomposition, electromyogram, neural network, principal component analysis.

Introduction

It is important for neurophysiological diagnosis that automatic analysis of the structure of the EMG is made possible. At present, the diagnostic procedure consists of visual recognition of action potentials within the signal observed from a contracting muscle. This procedure necessitates observation of only those potentials from motor units activated at low force. Visual identification of firing times to a good level of accuracy is not easy. An accurate automatic method of motor unit firing time determination would be of much use in diagnosis.

Previous methods for decomposing the EMG and thus determining firing time statistics have not been well received clinically. This is due to reasons varying from the procedure requiring too specialised equipment and time consuming expert interaction, to successful operation being limited to very low force levels.

A method of interest is that proposed by Loudon and Jones in 1992 [1]. This method of decomposition extracts segments of significant activity from the recorded EMG signal and represents them using a set of characteristic features. These features are then orthogonalised and clustered. The clustering is used to determine from which motor unit action potential train (MUAPT) the potentials came.

The clustering of features may be seen as a problem in pattern recognition. Neural networks of various architectures have been used, with various levels of success, to solve similar problems such as hand written character recognition, [2]. It is thus reasonable to hypothesise that the use of neural networks in grouping similar feature vectors will improve the performance of this method.

Another point in favour of this approach is the non-linear nature of the clustering problem. Neural networks can have the ability to solve non-linear problems. Thus their use may lead to better performance, providing more readily available and reliable firing time information than that presently used in the method of Loudon & Jones [1].

Feature methods

The initial consideration when trying to group data sets into distinct classes using neural networks, is how best to represent the data. Any representation must contain the majority of the information available about the data entry, or at least enough of this information to allow discrimination between similar but different entries. This is important because the distribution of inputs in the input space of the neural network determines the number of input units in the network and the ease of classification.

A suitable representation of data for input to neural networks, based upon that of [1], is outlined. The method consists of representing each input to the network by a set of eight features. These features are characteristic of certain aspects of action potentials that will vary between different MUAPTs. The features are listed below:

1. *The maximum peak to peak amplitude feature.*
2. *The maximum positive amplitude feature.*
3. *The positive area feature.*

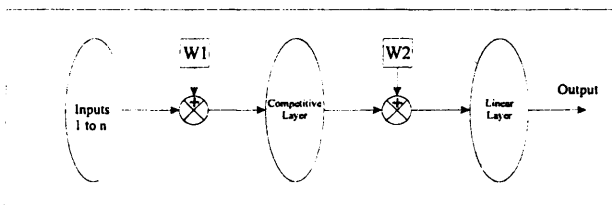
4. The negative area feature.
5. The maximum positive gradient feature.
6. The maximum negative gradient feature.
7. The number of turns feature.
8. The number of samples feature.

In the following investigation, these features will be used to create the input vectors presented to each neural network. The data used both for training and testing the neural networks is simulated and at this stage consists wholly of non-overlapping data. Each action potential within a data set is represented by its features for presentation to the neural networks.

The set of data used for training the networks consisted of *normal biphasic; normal triphasic; myopathic; and neurogenic* simulated action potentials. Within each of the four classes the duration of an action potential was fixed at five standards (those standards being different for each class, and representative of the limits of expectation for real data). For each class the amplitudes varied randomly. The training set consisted of five examples of each standard for each class. All data was simulated, noise free, and consisted solely of non-overlapping action potentials.

Various networks were trained to attempt classification of action potentials into the classes *normal biphasic; normal triphasic; myopathic; and neurogenic*. Single and multilayer perceptron networks were trained with different combinations of neurons for varied times using a selection of learning rates. Competitive and Learning vector quantisation networks, see figure 1, were also trained with different learning rates and different numbers of neurons, where appropriate.

Figure 1 - The learning vector quantization neural network.



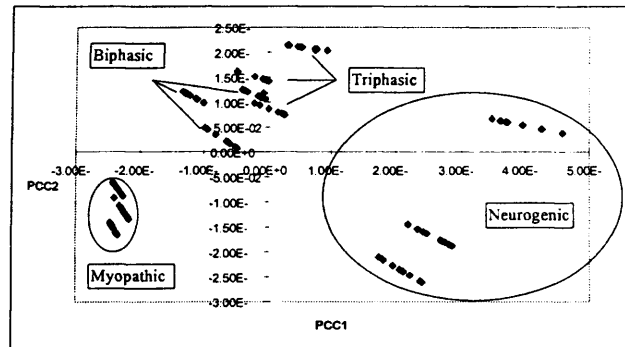
Feature results

It was found that the use of these eight correlated inputs to the ANN made correctly recognising individual inputs too difficult. Multilayer Perceptrons trained using backpropagation did not reach an acceptable level of error. Competitive networks yielded large scale errors, whilst networks trained using learning vector quantisation, though an improvement, also gave errors in classification.

Orthogonal factor methods

In order to decrease the complexity of each active segment's representation, the eight features were orthogonalised. Three factors accounting for the majority of variance in the original eight, the coefficients corresponding to the first three principal components, were used to represent each input. It was found that approximately 95% of the total variance was included in these factors. The distribution of inputs may be seen in figure 2.

Figure 2 - The orthogonalised data set.



The data set used in this investigation was similar in nature to that of the previous one. In this case the set consisted of 120 action potentials, 30 of each class. Three durations per class were present, which were representative of the typical range expected in the clinical environment. The data set was split into two sections, one for training and the other for testing.

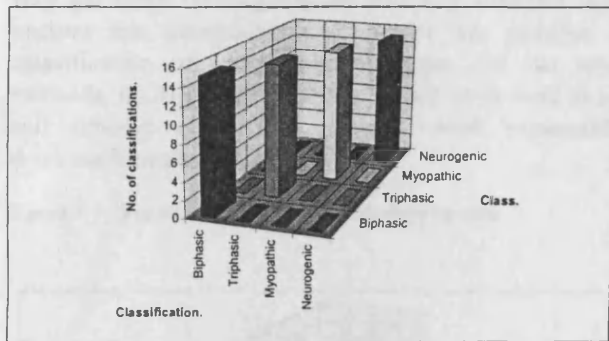
It was attempted to train multilayer perceptron networks and learning vector quantization networks to correctly classify the data. Various numbers of neurons and learning rates were employed during the training. Competitive networks were not used in this investigation because they are purely for observing the topographical characteristics of the data set [3], the learning vector quantization method is a semi-supervised hybrid of the competitive network and is used in its stead.

Factor results

The results obtained in this investigation for the use of multilayer perceptron networks were as before. The networks failed to reach an acceptable error level, no matter how the structure and learning of the network was altered.

The results for the learning vector quantization network when classifying both the training and test data sets were the same. 100% correct classification was achieved, see figure 3.

Figure 3 - The results of classification of training & test data.



Testing the method.

Real EMG signals are often polluted by the presence of noise and the potentials within them often obscure one another. What is seen by the clinician is the superposition of all such components. It is thus important to test the successful neural network from the previous section, to see how it will cope with the presence of noise and overlapping data.

The equipment used today to monitor and record EMG information is very sophisticated. As a result of this, the amount of noise present in the recorded signals is of a very low level.

Five different levels of noise were used to investigate the effect of noise upon the neural networks trained to classify clean simulated data. These noise levels are shown in table 1.

Table 1 Noise levels for simulated data.

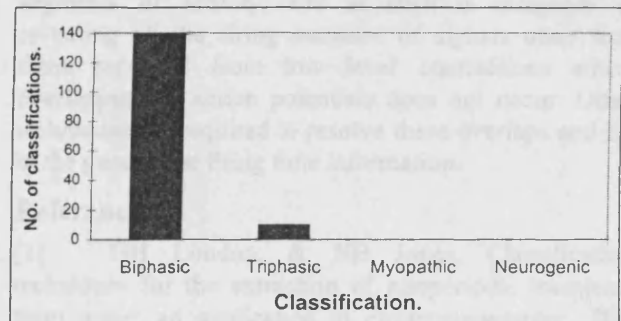
Level	Range (uV)
1	± 5
2	± 10
3	± 20
4	± 30
5	± 40

One EMG signal containing a single train of biphasic action potentials was simulated at each noise level. This was repeated for each standard duration of biphasic template present within the database used previously. The number of signals was 15. Action potentials were manually extracted, ten from each signal, and added to the general database. The database was then re-analysed using principal component analysis and the first three coefficients were again used to represent each data entry.

The purpose of this test was to assess the performance of the neural network trained to identify motor unit classes, in classifying action potential in the presence of noise. The entire database was presented to

the network and the following results were obtained: for the unpolluted data, 1 misclassification was recorded from the 120 presented inputs; for the noisy data, 10 misclassification were recorded for 150 presented inputs. Thus the misclassification rates were 0.83% and 6.67% respectively, see figure 4.

Figure 4 - Results for classification of noisy biphasic data.



In order to establish how neural networks trained upon non-overlapping data cope with the introduction of overlapping data at their inputs, it is necessary to generate some overlapping data. Using simulations it is possible to create such data whilst still knowing its characteristics.

The shortest biphasic and the shortest triphasic action potentials within the database were passed across one another in stages of 3 samples. The resulting summations were available for use as overlapping data. The overlap present within each record varied, and the whole set formed a smooth progression as the biphasic action potential passed through the triphasic action potential and out of the other side. As a result of the constituent action potential lengths (biphasic = 33 samples, triphasic = 34 samples), 21 overlapping records were produced.

The overlapping action potentials were described by their eight describing features. These were then analysed using principal component analysis in conjunction with the standard database used throughout this section. Each entry was again represented by its first three principal component coefficients.

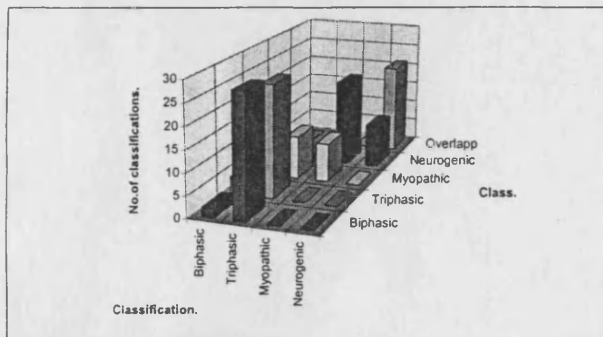
When presented for classification to the normal network trained to classify data into the four classes (normal biphasic, normal triphasic, myopathic and neurogenic), the following results were observed, figure 5.

Discussion

The results obtained during the feature investigation show that the combination of supervised and unsupervised learning methods present within learning vector quantization networks provide the best

way (of those investigated) of grouping together input vectors into identifiable clusters for the purpose of classification of action potential type. Of the other methods, multilayer perceptrons do not work well at all, and although competitive networks work reasonably, there are limitations with them.

Figure 5 - Results of classification of overlapping data



The results also indicate that a neural network is not capable of classifying any set of inputs in the way that the user would want them classified. Thus, the inputs to the network must be carefully selected to ensure that the problem may be solved.

It may be seen from the investigation using orthogonal features as inputs that the multilayer perceptron network is not capable of solving this problem without a great deal of pre-knowledge defining the architecture as in [2].

However, the learning vector quantization network is capable of accurately classifying both training and test data when that data is represented by orthogonal features. This is the case for the scope of this study using simulated action potentials.

The learning vector quantization method using orthogonal factors as inputs performs well in the presence of noise. The levels are low, though this is realistic because the levels of noise found in practice are also of low dimension.

When overlapping data is presented to the neural network, large scale misclassifications occur. This effect is due to the principal component coefficients of the overlapping data not falling within the designated class cluster areas. As such, the combined method of principal component coefficient representation and learning vector quantization classification is not suited to overlapping data, nor to data in the presence of overlapping data.

Conclusions

It is concluded that, within the limits of this study, the method outlined is capable of automatically

clustering action potentials into their type classes, for the purpose of determining firing statistics in clean, noise free, signals and also in signals containing low levels of noise. Low noise levels do in fact exist in real measurements due to the high performance of modern EMG data collection techniques. It may also be seen that this method is incapable of resolving overlapping segments of activity, and as such is incapable of revealing all the firing statistics of signals other than those recorded from low level contractions where overlapping of action potentials does not occur. Other techniques are required to resolve these overlaps and fill in the gaps in the firing time information.

References

- [1] GH Loudon, & NB Jones, Classification techniques for the extraction of nonperiodic transients from noise: an application in electromyography., IEE Proceedings-A, Vol. 139, No.2, March 1992.
- [2] Y Le Cun, B Boser, JS Denker, D Henderson, RE Howard, W Hubbard & LD Jackel, Handwritten digit recognition with a backpropagation network. In DS Touretsky, ed. Advances in neural information processing systems 2. San Mateo, CA: Morgan Kaufman, PP396-404.
- [3] J Kangas, T Kohonen & J Laaksonen, Variants of self organising maps, IEEE Transactions on neural networks 1, 93 - 99, 1990.